Extension and patterning of the vertebrate body

Roles of Gdf11 and Wnt3a signaling in the axial progenitors

Arnon Dias Jurberg

Dissertation presented to obtain the Ph.D degree in Developmental Biology

Instituto de Tecnologia Química e Biológica | Universidade Nova de Lisboa

Oeiras,
April, 2013

INSTITUTO
DE TECNOLOGIA
QUÍMICA E BIOLÓGICA
/UNL

Knowledge Creation

Extension and patterning of the vertebrate body

Roles of Gdf11 and Wnt3a signaling in the axial progenitors

Arnon Dias Jurberg

Dissertation presented to obtain the Ph.D degree in Developmental Biology

Instituto de Tecnologia Química e Biológica | Universidade Nova de Lisboa

Research work coordinated by:

FUNDAÇÃO CALOUSTE GULBENKIAN
Instituto Gulbenkian de Ciência

Oeiras,
April, 2013

INSTITUTO
DE TECNOLOGIA
QUÍMICA E BIOLÓGICA
/UNL

Knowledge Creation

To Raquel, Vania and
Henrique

FCT Fundação para a Ciência e a Tecnologia
MINISTÉRIO DA EDUCAÇÃO E CIÊNCIA

The work presented on this thesis was supported by the Fundação para a Ciência e a Tecnologia, grant SFRH/BD/33562/2008.

Apoio financeiro da FCT e do FSE no âmbito do Quadro Comunitário de apoio, BD nº SFRH/BD/33562/2008.

Table of contents

Acknowledgements

To Moisés Mallo, for the superb guidance throughout the many phases of my PhD training. I deeply appreciate the opportunity of working under your supervision and all your effort, support and encouragement.

To the former and present members of the Mallo laboratory, for the pleasant and stimulating environment during all these years. To Jennifer Rowland, Isabel Guerreiro and Tânia Vinagre, for teaching me many things during my initial steps in the laboratory, especially when I can pause a protocol to go home. Your innumerous advices and many scientific discussions were essential for shaping my scientific criticism over these years. To Ana Nóvoa, whose expertise in producing transgenics was indispensable to carry out this work. You make it seem easy and I deeply appreciate your dedication. To Özlem Aybüke, for your altruism and kindness. Thank you for giving me this example. To Rita Aires, that helped me countless times, since she was in a different laboratory until the last minute of this work. Many of our conversations turned to be fruitful and inspired the execution of some experiments or helped me organize some ideas. I am really grateful to you and Irma Varela for giving continuity to the projects I started and wish best of luck. To Rita Félix, for her incredible work with chicken embryos and great energy that made our laboratory environment more fun. To Ana Casaca, whose assistance with many experiences was of great help during a critical phase of my PhD. To Sofia Pereira, Vanessa Urbano and Andreia Nunes, for the encouragement and suggestions. To Inês Domingues, for making the laboratory a better place to work with your happiness and casualness. You made our life in the laboratory a great gastronomic experience. I am deeply grateful to you all for your kindness and friendship.

To our brother laboratory, the Rodríguez-León laboratory, for the countless times that you shared crucial and occasionally expensive reagents during desperate times. To Joaquín Rodríguez-León, for kindly making these loans become donations and all supportive comments. To Raquel Tomás, Joana Monteiro and Diana Pires, for making our laboratory environment yet more enjoyable and friendly.

To my thesis committee, Lars Jansen and Vasco Barreto, for spending your valuable time listening and also for sharing your experience with me. Your advices were greatly appreciated.

To the "Fundação para a Ciência e a Tecnologia", for the financial support (SFRH/BD/33562/2008).

To the "Programa Gulbenkian de Doutoramento", especially Henrique Teotónio and Thiago Carvalho, for making possible such magnificent and stimulating conditions for learning. To Thiago, my deepest gratitude for helping me whenever I needed. To Manuela Cordeiro, for your kindness and incredible administrative support.

To the Instituto Gulbenkian de Ciência (IGC), Fundação Calouste Gulbenkian and the IGC community, for the pleasant and motivating scientific environment. To Pedro Almada, for microscopes' training sections. To Joana Rodrigues, Marta Pinto and Tânia Carvalho, for the excellent histopathology assistance. To the Animal House team, especially Manuel Rebelo, Joana Bom, Sofia Leocádio, Graça Coelho and João Madureira, for the exceptional and laborious care spent daily to ensure proper animal welfare. To Ana Homem, for patiently ensuring the proper operation and maintenance of many equipments at the IGC. Without you many experiments would be delayed or interrupted. To many laboratories and their members, for having shared reagents and technical advices.

To Tiago Macêdo, Rômulo Areal, Rodrigo Oliveira, Gustavo Mello and Thiago Gouvêa, for bringing Brazil a little bit closer. Our many conversations about science, football, life in general and other subjects were essential for keeping my sanity. I deeply appreciate your encouragement and support during difficult moments and the many breaks with a couple of beers and good food. Many thanks for your friendship.

To Bernardo Pascarelli and Flávia Lamarão, for the friendly support overseas.

To Henrique Lenzi, my dear mentor and great source of inspiration, for showing me the beauty of science, music and arts. You are greatly missed.

Last but not least, to my family, whose great support was never absent, even when I crossed the Atlantic ocean to pursue my dreams. You all gave me the strength to handle these new challenges. To Raquel de Mendonça, my beloved soon-to-be wife, for showing me what really matters and staying by my side during all these years. To my mother Vania Dias, for everything possible and impossible you have made for me. No words are enough to acknowledge your efforts. To my father Pedro Jurberg, for giving me the right advices in the right moments. To my brother Igor, whose academic dedication and focus are an example for me. To all of you my deepest appreciation.

Abstract

Vertebrates exhibit an enormous diversity in body shapes. Despite this variability, they all develop by a common principle, in which new tissue is continuously added at the posterior embryonic end during development. Axial extension requires a tight balance between the maintenance of axial progenitors in an undifferentiated state and the production of cells fated to generate different body structures. Concurrently, newly formed tissues are endowed with patterning information that coordinates their differentiation. The interactions among all these processes are ultimately responsible for the generation of a properly organized body, divided into well-defined anatomical regions, and has a major impact in the morphological diversity of this taxon. A key event during posterior extension involves a switch in the mode of tissue production from the trunk to the tail. This switch is required to produce different types of tissue in each of these regions. In particular, while the trunk harbors many of the vital and reproductive organs, the tail is basically formed by vertebrae and associated muscles. Therefore, trunk formation requires the contribution of progenitors for neural tissue and paraxial mesoderm, as well as those for intermediate and lateral mesoderm. These latter progenitors are required to build a large part of the internal organs together with endodermal tissues. Conversely, tail tissues are mostly derived from the paraxial mesoderm and ectoderm with no contribution of the intermediate and lateral mesoderm. As a consequence, the trunk to tail transition includes the depletion of lateral and intermediate mesoderm progenitors. Progenitors for the neural tube and paraxial mesoderm also undergo a significant change, as they are reallocated from the anterior primitive streak and adjacent epiblast to the chordo-neural hinge (CNH) within the tail bud. The work described in

this thesis investigated these aspects and identified key mechanisms involved in the regulation of the trunk to tail transition.

The first part of this thesis shows that Gdf11 signaling is a major coordinator of this transition by regulating at least two different processes. First, the onset of Gdf11 activity in the epiblast promotes the formation of the hindlimbs and cloaca-associated mesoderm. This is achieved through activation of *Isl1* expression in progenitor cells of the lateral mesoderm by direct regulation of a relevant *Isl1* enhancer element. These findings suggest that the hindlimbs and cloaca arise as the product of the terminal differentiation of lateral mesoderm progenitors. Second, Gdf11 signaling regulates proper reallocation of bipotent neural and mesodermal progenitors into the CNH. In the absence of Gdf11, the tail bud is not properly organized and progenitor cells become segregated into distinct domains, eventually producing split tails. This ultimately results in tail truncation due to increased cell death. Gdf11 signaling participates in progenitor reallocation through a reduction in the levels of retinoic acid (RA) available to these cells. This is achieved by promoting an increase in the levels of the RA catabolizing enzyme Cyp26a1 at the posterior embryonic end. The results presented in this work reveal that *Gdf11* protects these bipotent progenitors from RA fluctuations during normal tail development. After the tail bud is formed, *Gdf11* also participates in the progressive termination of the main embryonic axis by modulating the expression of *Hox11* genes.

The second part of this thesis shows that Wnt3a is involved in the global coordination of axial elongation, regulating axial progenitor differentiation, mesoderm production and patterning. Wnt3a signaling in the epiblast seems to impair axial progenitor exit from the epiblast, affecting differentiation into mesoderm and neural tissue. Moreover,

Wnt3a levels seem to contribute to mesoderm compartmentalization into lateral (higher) and paraxial (lower) mesoderm. This observation is compatible with previously described fate-maps of the primitive streak. Wnt3a also upregulates some posterior Hox genes in the presomitic mesoderm, thus reinforcing the connection between mesoderm production and patterning. The more anterior induction of the hindlimbs and cloaca upon high levels of Wnt3a in the epiblast suggests that, similar to Gdf11 signaling, Wnt3a signaling may also be involved in triggering the trunk to tail transition by modulating the behavior of the axial progenitors. In turn, stabilization of β-catenin in the epiblast seems to be relevant for the proliferation and maintenance of axial progenitors. Altogether, the findings presented in this thesis shed light on the coordinated growth and patterning of the vertebrate embryo.

Sumário

Os vertebrados exibem uma grande diversidade de formas corporais. Apesar disso, eles são formados através de um princípio comum, no qual novos tecidos são continuamente adicionados à região posterior do embrião durante o desenvolvimento. Dessa forma, a extensão axial requer um estreito equilíbrio entre a manutenção de progenitores axiais em um estado indiferenciado e a produção de novas células, destinadas a gerar diferentes estruturas do corpo. Ao mesmo tempo, esses tecidos recém formados são providos de informações sobre padronização, que coordenam a sua diferenciação. Em última análise, a interação entre todos esses processos é reponsável pela geração de um corpo devidamente organizado, dividido em regiões anatômicas bem definidas, além de ter um profundo impacto na diversidade corporal desse táxon. Um evento importante durante a extensão posterior do corpo envolve a modificação no modo de produção dos tecidos do tronco para os tecidos da cauda. Essa mudança é necessária para a produção dos diferentes tipos de tecidos presentes nessas regiões. Em particular, enquanto o tronco contém os órgãos vitais e reprodutivos, a cauda é basicamente constituída por vértebras e músculos associados. Dessa forma, a geração do tronco necessita da contribuição de vários tipos de progenitores, que são responsáveis pelos tecido nervoso e mesoderma paraxial, assim como pelos mesoderma lateral e intermediário, além do endoderma. Em conjunto com o endoderma, os progenitores de mesoderma lateral e intermediário estão envolvidos em grande parte da formação dos órgãos internos. Por outro lado, os tecidos da cauda derivam principalmente do mesoderma paraxial e do ectoderma, sem qualquer contribuição dos mesodermas lateral e intermediário. Consequentemente, a transição do tronco para a cauda envolve o esgotamento de progenitores para

mesoderma lateral e intermediário, enquanto os progenitores para o tubo neural e mesoderma paraxial são reposicionados da região anterior da linha primitiva e do epiblasto adjacente para a região de articulação cordoneural (do inglês, *chordoneural hinge*) no primórdio da cauda. Usando murganhos como modelo experimental, o trabalho descrito nessa tese investigou esses aspectos e identificou importantes mecanismos envolvidos na regulação da transição do tronco para a cauda.

A primeira parte desta tese mostra que a sinalização por Gdf11 coordena essa transição ao regular pelo menos dois processos distintos. Em primeiro lugar, o início da atividade de Gdf11 no epiblasto promove a formação dos membros posteriores e do mesoderma associado à cloaca. Esse processo ocorre através da ativação da expressão de *Isl1* nas células progenitoras para mesoderma lateral, via a regulação direta de um elemento regulatório específico. Esses resultados sugerem que os membros posteriores e a cloaca surgem a partir da diferenciação terminal dos progenitores para mesoderma lateral. Em segundo lugar, a sinalização por Gdf11 regula o reposicionamento de progenitores bipotentes neural-mesoderma para a zona de articulação cordoneural. Na ausência de Gdf11, o primórdio da cauda é incapaz de manter-se organizado e as células progenitoras segregam-se em domínios distintos, eventualmente causando uma divisão da cauda e seu truncamento devido ao aumento de morte celular. Os nossos resultados sugerem que a sinalização por Gdf11 participa no reposicionamento desses progenitores através da redução dos níveis de ácido retinóico (AR) disponível. Isso ocorre pelo aumento dos níveis de expressão da enzima catabolizante *Cyp26a1* na região posterior do embrião. Esses resultados revelam que a sinalização por Gdf11 protege esses progenitores bipotentes de flutuações nos níveis de AR durante o desenvolvimento normal da cauda.

Após a formação do primórdio da cauda, Gdf11 ainda participa na terminação progressiva do eixo embrionário principal ao modular a expressão de genes *Hox11*.

A segunda parte desta tese mostra que Wnt3a está envolvido na coordenação global da extensão axial, regulando a diferenciação dos progenitores axiais, a produção de mesoderma e a padronização de novos tecidos. A sinalização por Wnt3a parece comprometer a saída dos progenitores axiais do epiblasto, afetando a diferenciação em mesoderma e tecido nervoso. Além disso, os níveis de Wnt3a parecem contribuir para a compartimentalização do mesoderma em mesoderma lateral (alto) e mesoderma paraxial (baixo). Essa observação é compatível com descrições anteriores dos destinos das células que provém da linha primitiva. Além disso, Wnt3a induz alguns genes Hox no mesoderma presomítico, reforçando a relação entre a produção de mesoderma e a padronização do corpo. A anteriorização dos membros posteriores e da cloaca causada pelos altos níveis de Wnt3a no epiblasto sugere que, similarmente à sinalização por Gdf11, a sinalização por Wnt3a também pode estar envolvida com a transição do tronco para cauda ao regular o comportamento dos progenitores axiais. Por sua vez, a estabilização de β-catenina no epiblasto parece ser importante para a proliferação e a manutenção desses progenitores. Assim, os resultados apresentados nesta tese esclarecem importantes aspectos envolvidos na coordenação entre o crescimento e a padronização do embrião de murganho.

List of Abbreviations

Acvr1b	*activin A receptor, type 1B*
AHP	anterior head process
Alk	activin-like kinase
AP	anterior-posterior
AVE	anterior visceral endoderm
Bmp	bone morphogenetic protein
Bmpr1a	*bone morphogenetic protein receptor, type 1A*
Cdh1	E-cadherin
Cdx	Caudal-type homeobox
Cer1	*cerberus 1 homolog* (*Xenopus laevis*)
CNH	chordoneural hinge
DIG	digoxigenin
Dkk1	*dickkopf homolog 1* (*Xenopus laevis*)
Dll1	*delta-like 1 (Drosophila)*
DMSO	dimethyl sulfoxide
DNA	deoxyribonucleic acid
dpTB	dorso-posterior tail bud tail bud
DV	dorso-ventral
DVE	distal visceral endoderm
e.g.	*exempli gratia*
EDTA	ethylenediaminetetraacetic acid
EGTA	ethylene glycol tetraacetic acid
EMT	epithelial-mesenchymal transition
En1	*engrailed 1*
ENU	*N*-ethyl-*N*-nitrosurea
Eomes	*eomesodermin homolog* (*Xenopus laevis*)
Erk	Extracellular signal-regulated kinase
Errβ	*Estrogen-related receptor, beta*
Fgf	Fibroblast growth factor
Fgfr	Fibroblast growth factor receptor
Fox	forkhead box
Gata	GATA binding protein
Gdf	growth and differentiation factor
Grb2	*growth factor receptor bound protein 2*
Hand2	*heart and neural crest derivatives expressed transcript 2*
HCl	hydrogen chloride/hydrochloric acid
Her1	*hairy and Enhancer of Split 1*
Her7	*hairy and Enhancer of Split 7*
Hesx1	*homeobox gene expressed in ES cells*

Hex/Hhex	*hematopoietically expressed homeobox*
ICM	inner cell mass
Isl1	*Islet1*
$K_3Fe(CN)_6$	potassium ferricyanide
$K_4Fe(CN)_6.3H_2O$	potassium ferrocyanide trihydrate
kb	kilobase
kg	kilogram
Klf2	*Kruppel-like factor 2* (*lung*)
KOH	potassium hydroxide
Lef1	*lymphoid enhancer binding factor 1*
Lefty1	*left right determination factor 1*
Lfng	*Lunatic fringe*
LiCl	lithium chloride
Lim1/*Lhx1*	*LIM homeobox protein 1*
LPM	lateral plate mesoderm
LR	left-right
Lrp	low density lipoprotein receptor-related protein
LTAP	long-term axial progenitors
Maml3	*Mastermind like 3 (Drosophila)*
Map4k4	mitogen-activated protein kinase kinase kinase kinase 4
MAPK	mitogen-activated protein kinase
Mesp2	*Mesoderm posterior 2*
mg	milligram
$MgCl_2$	magnesium chloride
Mixl1	*Mix1 homeobox-like 1 (Xenopus laevis)*
ml	milliliter
Msgn1	*Mesogenin1*
NaCl	Sodium chloride
$NaHCO_3$	sodium bicarbonate
Nanog	*Nanog homeobox*
NC	notochord
NSB	node-streak border
NT	neural tube
º C	degrees Celsius
Oct4/*Pou5f1*	octamer-binding transcription factor 4/*POU domain, class 5, transcription factor 1*
Otx2	*orthodenticle homolog 2* (*Drosophila*)
p38IP	p38-interacting protein
PBS	phosphate buffered saline
PBT	phosphate buffered saline, containing 0.1% Tween-20

PCR	polymerase chain reaction
Pcsk	proprotein convertase subtilisin/kexin
PD	proximal-distal
Pdgfra	*platelet derived growth factor receptor, alpha polypeptide*
PFA	paraformaldehyde
PGCs	primordial germ cells
PS	primitive streak
PSM	presomitic mesoderm
P-Smad2/3	phosphorylated Smad2/3
RA	retinoic acid
Raldh2/Aldh1a2	*aldehyde dehydrogenase family 1, subfamily A2*
RAR	retinoic acid receptor
RBPJ*κ*	recombination signal binding protein for immunoglobulin kappa J region
RNA	ribonucleic acid
RNAi	RNA interference
Shh	*sonic hedgehog*
Snai1	snail homolog 1 (Drosophila)
Sox	SRY-box containing gene
STAP	short-term axial progenitors
T	*brachyury*
TBM	tail bud mesenchyme
Tbx6	*T-box 6*
Tcf1	*transcription factor 1, T cell specific*
TE	trophectoderm
TE buffer	Tris-EDTA buffer
VE	visceral endoderm
vTB	ventral tail bud
X-gal	5-bromo-4-chloro-indolyl-β-D-galactopyranoside
ZPA	zone of polarizing activity
µl	microliter
µm	micrometer

List of Figures

List of Tables

Chapter I – Introduction

"Nothing in biology makes sense except in the light of Evolution"

Theodosius G. Dobzhansky

Introduction

The relative broad observation that complex organisms derive from single cells has intrigued several generations of researchers over the years. Adult phenotypes result from a specific hierarchical sequence of developmental stages. The comprehensive understanding of these multiple steps will help to explain how distinct cell identities are generated and maintained during development through the modulation of the activity of the same, single genome. Indirectly, it may also help in Translational Medicine for the *in vitro* development of tissues or even organs for transplants and other aspects of human healthcare. Moreover, it may shed light on how phenotypic diversity has arisen and is being propagated during evolution. Indeed, how changes in embryonic development provide the grounds for adaptation and ultimately to evolution still remain largely elusive.

Taking vertebrates as an example, they display a large diversity of body shapes and sizes usually as a result from adaptation to the most varied environments. However, an overall similar organization into regional domains along their primary (anterior-posterior, AP) body axis is easily recognized when comparing different groups. Quantitative and qualitative differences in the formation of these regions are the basis of their morphological diversity. Curiously, limbs are always located at the level of anatomical transitions and animals with extended trunks, as diverse as snakes and whales, frequently present loss of the hindlimbs (Bejder and Hall, 2002; Burke et al., 1995; Cohn and Tickle, 1999; Greene and Cundall, 2000; Richardson et al., 1998; Thewissen et al., 2006; Wiens and Slingluff, 2001; Woltering, 2012). These observations, therefore, may imply that extension of the trunk and limb specification along the AP axis may be related. Elucidating the

mechanisms that control the organization of the vertebrate body is thus essential to understand their evolution. The thesis work described herein aimed to investigate some of the mechanisms involved in the production of the vertebrate body, focusing more specifically on axial extension, maintenance of progenitors and AP patterning of the mouse embryo.

I - Making a mouse embryo

The complex vertebrate body arises from a series of tightly regulated and interdependent morphogenetic events. Since early development, crucial decisions are made to properly allocate cells into lineages as they proliferate and differentiate. Intricate cell movements and specific patterning programs ultimately reorganize the body into interdependent modular functional structures. In mammals, following fertilization of the oocyte by the sperm cell, a set of rapid cell divisions give rise to a solid mass of cells called morula. These cells then undergo the first lineage decision during development as they form a fluid-filled cellular sphere, known as blastocyst. In particular, the blastocyst comprises two distinct cell populations: (1) a pluripotent inner cell mass (ICM) that gives rise to the embryo proper, and (2) an outer epithelial layer, known as the trophoectoderm, which mediates implantation and expand to form the placenta and other extraembryonic tissues (reviewed by Arnold and Robertson, 2009). Early development, however, is not in the scope of this work and will be only briefly discussed herein. Further description of such stages can be found elsewhere (Arnold and Robertson, 2009; Chen et al., 2010; Nowotschin and Hadjantonakis, 2010; Rossant and Tam, 2009).

I.1 - Early patterning: formation of the two-layered embryo

At E3.5, some individual cells within the ICM start to express epiblast-specific genes (*e.g. Nanog*, *Klf2* and *Fgf4*), whereas others express endoderm-specific genes (*e.g. Gata4*, *Gata6*, *Sox17* and *Pdgfra*) in a "salt and pepper", mutually exclusive mosaic and seemingly stochastic pattern (Artus et al., 2012; Chambers et al., 2003; Chazaud et al., 2006; Frankenberg et al., 2011; Fujikura et al., 2002; Gerbe et al., 2008; Guo et al., 2010; Kurimoto et al., 2006; Mitsui et al., 2003; Niswander and Martin, 1992; Plusa et al., 2008; Rossant et al., 2003). In addition, some molecules that play patterning roles at later developmental stages, such as *Lefty1*, *β*-catenin and *Cer1*, were also reported to be differentially distributed already in pre-implantation embryos (Chazaud and Rossant, 2006; Takaoka et al., 2006; Torres-Padilla et al., 2007), raising the possibility that the inner cell mass is already more patterned than initially thought. How such mosaicism arises in the ICM is still ill-defined, but seems to depend on Fgf4/Erk signaling (Arman et al., 1998; Chazaud et al., 2006; Cheng et al., 1998; Feldman et al., 1995; Goldin and Papaioannou, 2003; Wilder et al., 1997).

Cells expressing epiblast and endoderm-specific genes eventually segregate to produce two layers (Fig. 1A). The visceral endoderm layer becomes in contact with the blastocelic cavity and eventually expands to cover the entire surface of the mural trophectoderm (TE) and epiblast (Arnold and Robertson, 2009; Kaufman, 1992; Plusa et al., 2005, 2008; Rossant and Tam, 2009). Such endodermal lining of the mural TE and the epiblast comprises the extraembryonic parietal endoderm (Kaufman, 1992). The ICM cells between the visceral endoderm and trophectoderm generate the epiblast, an epithelial sheet of columnar cells that gives rise to the

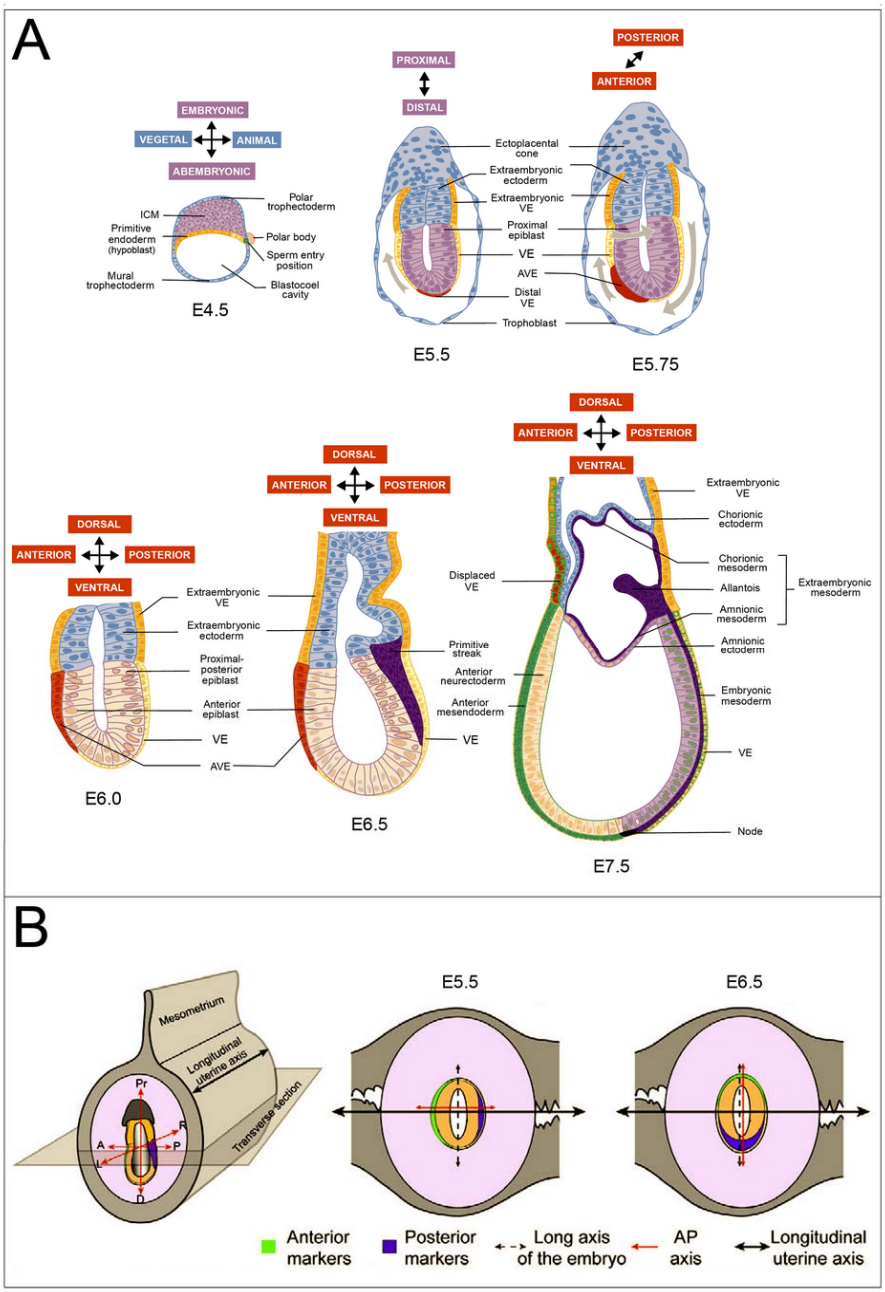

Figure 1. Axis formation in the mouse embryo. A Overview of the morphological events that establish the main embryonic axes. Lateral view. **B** Rotation of the AP axis in relation to the long axis of the embryo occurs prior to gastrulation (adapted from Guo and Li, 2007; Lu et al., 2001).

embryo proper. The segregation of these two ICM layers produces the first evidence of dorso-ventral (DV) polarity in the embryo, determined

as the epiblast-primitive endoderm (hypoblast) axis (Fig. 1A). At this stage (around E4.5), the embryo undergoes implantation in the uterine wall, which occurs through the ICM side of the embryo and produces the ectoplacental cone (Fig. 1A). This structure gradually penetrates the endometrial tissue and grows in size, eventually resulting in the formation of a large part of the extraembryonic tissues that support the development of the embryo proper. In the mouse, this is associated with a concave bending at the center of the epiblast, which produces a radially symmetric cup-shaped structure pointing outwards (the "egg cylinder" stage, which occurs by E5.5 in the mouse). Together, these events determine the formation of a proximal-distal (PD) axis (Fig. 1A).

I.1.a - Establishment of the anterior-posterior axis

The first event leading to the establishment of the AP axis is the induction of the distal visceral endoderm (DVE) at the distal end of the egg cylinder (Fig. 1A) (Beddington and Robertson, 1999; Mesnard et al., 2004; Perea-Gomez et al., 2004; Takaoka et al., 2011; Thomas and Beddington, 1996; Thomas et al., 1998). The DVE arises from a group of *Lefty1*$^{+/}$*Gata6*$^{+}$ cells in the blastocyst as result from complex interactions between the visceral endoderm (VE), the epiblast and the extraembryonic ectoderm (Cai et al., 2008; Takaoka et al., 2011). Its formation seems to require the input from several signaling pathways, including BMP, Nodal/Activin and Wnt/β-catenin. Complex interactions between these pathways produce a restricted area at the distal part of the egg cylinder prone for DVE differentiation (Arnold and Robertson, 2009; Norris and Robertson, 1999; Varlet et al., 1997; Yamamoto et al., 2009). These molecular interactions include a BMP

signal from the extraembryonic ectoderm that promotes both the formation of the VE and the restriction of the DVE to the distal end of the embryo by blocking their development in the proximal region (Yamamoto et al., 2009). On the other hand, a PD gradient of Nodal/Activin forms in the epiblast and induces FoxH1 to initiate the transcription of *Lefty1* in the distal end of the embryo (Beck et al., 2002; Brennan et al., 2001; Granier et al., 2011; Takaoka et al., 2006). In turn, Bmp4 induces the expression of *Wnt3* in the epiblast, which sustains *Nodal* expression in the vicinity of the extraembryonic ectoderm (Ben-Haim et al., 2006; Liu et al., 1999; Miura et al., 2010; Norris and Robertson, 1999; Vincent et al., 2003).

Once established, DVE cells migrate toward the future anterior side of the embryo (Hermesz et al., 1996; Takaoka et al., 2011; Thomas and Beddington, 1996; Thomas et al., 1998). This event produces directional movements in the VE layer, which culminate in the asymmetrical positioning of a group of cells with patterning properties in the proximal region of the embryo (Fig. 1A) (Chu and Shen, 2010; Miura et al., 2010; Takaoka et al., 2011). These cells are known as the anterior visceral endoderm (AVE). Contrary to previously thought, the AVE does not derive from the DVE. Instead, the AVE originates independently at the distal end of the embryo from a different subset of VE cells that start to express *Lefty1* and *Cer1* after E5.5 (Fig. 1A) (Takaoka et al., 2011). Genetic ablation of DVE cells did not impair AVE differentiation, but its cells remained at the distal end of the embryo, indicating that the DVE is essential for AVE migration but not for its induction (Takaoka et al., 2011). The subsequent repositioning of AVE cells within the post-implantation embryo rotates the AP axis, aligning it parallel to the long axis of the embryo and perpendicular to

the longitudinal axis of the uterine horn (Fig. 1B) (Guo and Li, 2007; Mesnard et al., 2004; Perea-Gomez et al., 2004).

Rotation of the AP axis depends on Wnt/*β*-catenin and FGF signaling (Barrow et al., 2007; Guo and Li, 2007; Kimura-Yoshida et al., 2005). Loss of *Wnt3* blocks the alignment of the AP axis to the long axis of the embryo (Fig. 1B) (Barrow et al., 2007; Tortelote et al., 2012). Conversely, deletion of the Fgf8 spliceform *Fgf8b* reveals that FGF signaling does not affect proper positioning of the AVE, but it is required for correctly orienting the embryo in the uterine horn (Guo and Li, 2007). The precise mechanisms underlying *Wnt3* and *Fgf8b* roles in the rotation of the AP axis remain to be scrutinized.

The mechanisms controlling the polarity of AVE movement are also not fully understood. *β*-catenin seems to play a role in this process because genetic ablation of this molecule blocks AVE migration (Morkel et al., 2003). The role of *β*-catenin in this process is mediated by activation of the Nodal co-receptor *Cripto* (Morkel et al., 2003). Interestingly, inactivation of *Wnt3* or of all Wnt signaling activity through the inactivation of the common essential Wnt co-receptors Lrp5/6 has no negative effects on AVE formation (Kelly et al., 2004), suggesting that *β*-catenin also participates in Wnt-independent processes despite its essential role in canonical Wnt activity. An additional connection between Wnt/*β*-catenin signaling and AVE migration was provided by the finding that the Wnt antagonist Dkk1 in the anterior region functions as an attractive cue for AVE cells, whereas Wnt3a repels these cells from the posterior side (Kimura-Yoshida et al., 2005). Other factors involved in AVE migration are *Bmpr1a*-mediated BMP signaling and the homeobox-containing transcription factor *Otx2* (Acampora et al., 1995; Kimura et al., 2000;

Matsuo et al., 1995; Miura et al., 2010). Otx2 activity seems to be mediated by Dkk1, since the expression of this Wnt antagonist is able to rescue the *Otx2* mutant phenotype (Acampora et al., 2009; Kimura-Yoshida et al., 2005; Zakin et al., 2000). Likewise, conditional inactivation of *Bmpr1a* in the epiblast also affects *Dkk1* expression (Miura et al., 2010). However, the absence of an AVE migration phenotype in *Dkk1* mutants indicates that other Wnt inhibitors might also participate in this process (Mukhopadhyay et al., 2001). Indeed, other Wnt antagonists such as *Sfrp1* and *Sfrp5* are expressed in the AVE (Finley et al., 2003; Kemp et al., 2005).

After positioned in the future anterior end of the embryo, the AVE acts as a signaling center with two main functions. First, the AVE is required to produce anterior structures, most particularly those rostral to the hindbrain. Second, it coordinates the formation of a midline structure in the opposite side of the embryo, named the primitive streak (PS), which appears as a local deformation in the posterior epiblast by E6.5 in the mouse (Perea-Gomez et al., 2004; Rivera-Pérez and Magnuson, 2005; Thomas and Beddington, 1996).

Genetic analyses demonstrated that both Nodal/Activin and Wnt/*β*-catenin signaling are crucial for the establishment of a proper PS, since inactivation of *Nodal* or *Wnt3* blocks its formation (Barrow et al., 2007; Conlon et al., 1994; Liu et al., 1999; Tortelote et al., 2012). The AVE assists proper PS formation by secreting Nodal and Wnt inhibitors, thus restricting the activity of these pathways to the posterior epiblast (Belo et al., 1997; Conlon et al., 1994; Finley et al., 2003; Kemp et al., 2005; Kimura et al., 2000, 2001; Meno et al., 1999; Norris and Robertson, 1999; Oulad-Abdelghani et al., 1998; Perea-Gomez et al., 2002, 2004, 2001; Piccolo et al., 1999). For instance, inactivation of

both Nodal antagonists *Cer1* or *Lefty1* results in the formation of multiple ectopic PS throughout the epiblast (Perea-Gomez et al., 2002). Posterior restriction of Nodal activity seems to require Smad5-dependent BMP signaling, as mutant embryos for *Smad5* show expanded expression of *Nodal* and an ectopic PS (Pereira et al., 2012). Likewise, restriction of Wnt3 activity to the posterior embryonic tissues also depends on antagonists in the AVE, as previously mentioned (Finley et al., 2003; Kemp et al., 2005; Mukhopadhyay et al., 2001).

These signaling pathways, however, exhibit distinct roles in the initiation of the PS. Whereas Nodal signaling is critical for determining the site of the PS (Gu et al., 1998; Perea-Gomez et al., 2002; Pereira et al., 2012), Wnt/*β*-catenin signaling is involved in the production of mesoderm (Barrow et al., 2007; Huelsken et al., 2000; Kelly et al., 2004; Liu et al., 1999; Tortelote et al., 2012). This activity is initially mediated by Wnt3, as its inactivation reproduces the phenotype of *Lrp5;Lrp6* double mutants or of *β*-catenin null embryos (Huelsken et al., 2000; Kelly et al., 2004; Liu et al., 1999). *Wnt3* is sequentially expressed in the posterior VE and in the posterior epiblast as a result of an autoregulatory feedback loop (Tortelote et al., 2012). Curiously, initiation of the PS seems to depend on the expression of Wnt3 in the VE, as this structure is still formed following the conditional inactivation of this gene in the epiblast (Tortelote et al., 2012). Absence of *Wnt3* expression in the epiblast, however, impairs the maintenance of gastrulation (Tortelote et al., 2012).

I.2 - Gastrulation: formation of the embryonic germ layers

Formation of the PS marks the onset of the gastrulation process, which comprises a series of extensive and coordinated cell movements that

ultimately rearrange the embryo in three germ layers. These layers eventually produce all tissues and organs in the body (reviewed by Gilbert, 2003). The PS coordinates gastrulation by modulating functional changes of epiblast cells. Cells located anterior to the PS are not affected by its activity and remain in the epiblast to give rise to ectoderm. Eventually, these Sox3-expressing cells form the surface ectoderm and neural tissues (Acloque et al., 2011; Burdsal et al., 1993; Mikawa et al., 2004; Quinlan et al., 1995; Tam and Loebel, 2007; Wilson et al., 2009). Conversely, epiblast cells at the level of the PS move towards the midline and leave the epithelial layer through the PS, giving rise to both mesoderm and definitive endoderm (Fig. 2A,B, D) (Voiculescu et al., 2007; Williams et al., 2012). Thus, the PS defines the site of ingression, in which epiblast cells change their characteristics to a mesenchymal phenotype and migrate towards the anterior region of the embryo as two bilateral wings (Fig. 2B,C) (Kinder et al., 1999; Lawson et al., 1991; Parameswaran and Tam, 1995). The production of mesoderm, therefore, involves an epithelial-mesenchymal transition (EMT).

FGF signaling is a key regulator of EMT during gastrulation. In particular, loss of *Fgf8* or *Fgfr1* does not affect PS and mesoderm induction, but results in an accumulation of cells in the epiblast, protruding into the proamniotic cavity (Ciruna and Rossant, 2001; Ciruna et al., 1997; Deng et al., 1994; Guo and Li, 2007; Sun et al., 1999; Yamaguchi et al., 1994). Interestingly, a similar phenotype is observed following the conditional inactivation of *Wnt3* in the epiblast, which may have resulted from the downregulation in the expression of *Fgf8* (Tortelote et al., 2012).

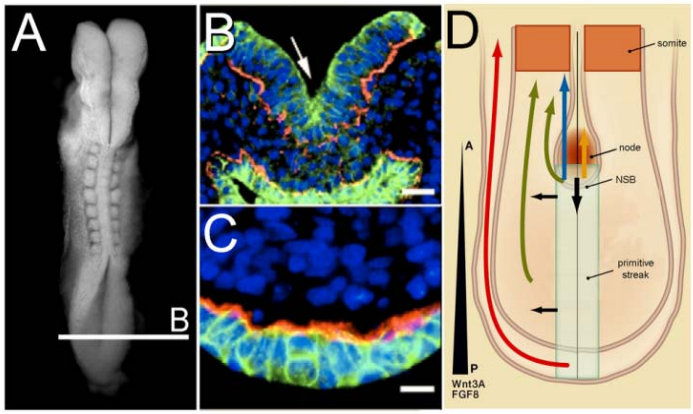

Figure 2. Gastrulation in the mouse embryo. A Gross morphology of a mouse embryo at E8.5. Dorsal view (Jurberg et al., unpublished). **B,C** Basal membrane integrity during gastrulation. *red* laminin, *green* E-cadherin, *blue* nuclei (from Ohta et al., 2007). **B** Epithelial-mesenchymal transition at E8.5. *Arrow* marks the primitive groove. **C** Tail ventral mesoderm at E10.5 shows cessation of gastrulation. **D** Cell fates during PS ingression. *red arrow* lateral mesoderm, *green arrow* paraxial mesoderm, *blue arrow* neural ectoderm, *yellow arrow* axial mesoderm. *NSB* node-streak border (adapted from Ramkumar and Anderson, 2011).

The activity of FGF signaling during EMT relies on the activation of the zinc finger transcription factor Snai1 (Ciruna and Rossant, 2001; Ciruna et al., 1997; Schlueter and Brand, 2009). Snai1 downregulates expression of several cell adhesion molecules characteristic of epithelial cells. In particular, Snai1 binds the promoter of the E-cadherin gene (*Cdh1*) and shuts down its expression (Batlle et al., 2000; Cano et al., 2000). Similarly, Snai1 also represses the expression of tight junction components, such as claudins and occludins (Ikenouchi et al., 2003). Inactivation of *Snai1* is lethal because of abnormal formation of extraembryonic mesoderm due to the maintenance of epithelial characteristics (Carver et al., 2001; Ciruna and Rossant, 2001). Curiously, conditional inactivation of *Snai1* in the epiblast does not affect gastrulation to a large extent, but embryos exhibit alterations in left-right (LR) asymmetry, vascular abnormalities and increased apoptosis, dying by E9.5 (Murray and Gridley, 2006). This finding indicates that Snai1 is probably not the only regulator of

EMT during mouse gastrulation and other factors might exist to compensate its activity.

Protein stability of E-cadherin is also regulated at the cell junctions during EMT in the PS. This regulation requires the activity of the NCK-interacting kinase (NIK)/Map4k4 pathway, which activates p38 MAPK through the p38-interacting protein (p38IP) (Zohn et al., 2006). In the absence of p38IP, E-cadherin is retained in the nascent mesoderm, ultimately impairing cell migration away from the PS (Zohn et al., 2006). However, expression of *Fgf8* and *Snai1* are not affected in these mutant embryos, indicating that p38IP does not modulate E-cadherin through their regulation (Zohn et al., 2006). Whether FGF signaling regulates p38 activity during EMT in the PS remains to be evaluated.

I.2.a - Cell fates during primitive streak ingression

Transplantation experiments have shown that epiblast cells are multipotent prior to ingression through the PS. In particular, grafted cells into a different area of the epiblast are able to contribute to tissues normally produced by the recipient area (Carey et al., 1995; Lawson et al., 1991; Tam et al., 1997). In addition, this indicates that epiblast cells do not have a pre-specified fate. Instead, the fate they assume during gastrulation largely depends on their position relative to the PS (Fig. 2D) (Beddington, 1982, 1981; Kinder et al., 1999; Lawson and Pedersen, 1992; Lawson et al., 1991; Parameswaran and Tam, 1995; Quinlan et al., 1995; Ramkumar and Anderson, 2011; Smith et al., 1994; Tam and Beddington, 1987; Tam et al., 1997, 2001; Tam, 1989; Watson and Tam, 2001; Wilson and Beddington, 1996). Cells located close to the PS ingress at earlier developmental times and contribute to

more anterior embryonic tissues along the AP axis, whereas cells located farther from the PS gastrulate later and contribute to more posterior structures (reviewed by Tam and Behringer, 1997). Differently from the chick (Voiculescu et al., 2007), however, the mouse epiblast exhibits reduced cell intermingling and the PS elongates through the gradual ingression of cells toward the distal region of the embryo (Williams et al., 2012).

During early stages of gastrulation, cells that leave the epiblast give rise almost exclusively to extraembryonic mesoderm, producing predominantly the yolk sac mesoderm and the allantois (Fig. 3A). The allantois forms the umbilical cord and the mesodermal components of the fetal placenta (reviewed by Rossant and Cross, 2001). In addition to the extraembryonic mesoderm, cells ingressing at these early stages in the anterior PS form the anterior mesoderm (prechordal plate and anterior head process) and cardiac mesoderm (Fig. 3A). Some of these cells also contribute for the production of definitive endoderm, which eventually develops into the embryonic fore- and midgut (Lawson and Pedersen, 1987; Lawson et al., 1991; Tam and Beddington, 1987).

Concomitant to these early gastrulation events, the PS extends anteriorly, reaching its longest length around E7.5. At this stage, the most posterior region of the PS still organizes the production of extraembryonic mesoderm. However, by this time, production of cardiac mesoderm is mostly complete and more anterior areas of PS now organize the paraxial, intermediate and lateral components of the embryonic mesoderm. Fate mapping experiments have revealed that the paraxial mesoderm is formed from cells ingressing through the anterior PS and the intermediate and lateral mesoderm are organized by progressively more posterior areas of the PS (Figs. 2D and 3B). Thus,

there is a correlation between the mediolateral (also represented as DV) position of the mesodermal derivatives and the AP position of the PS at which those mesodermal structures are produced (Fig. 3). As the embryo continues growing, the PS reduces in length and eventually folds, ceasing its contribution to extraembryonic mesoderm. The anterior region of the PS at E8.5 now produces mostly paraxial mesoderm and endoderm, whereas more posterior areas of the PS still contribute to LPM.

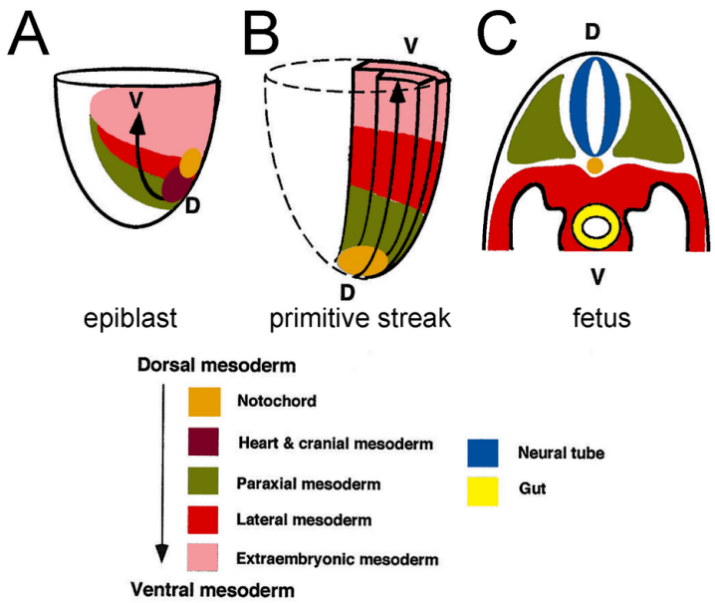

Figure 3. Fate map of the gastrulating mouse embryo. A Epiblast of early-streak stage embryo is regionalized in a dorso-ventral (DV) fashion before germ layer formation. **B** Late-streak stage embryo maintains the early DV relationship during cell ingression. The heart mesoderm has already ingressed through the PS and is no longer represented. **C** Distribution of different types of tissues in the fetus. Cross-section of the trunk region (adapted from Tam & Behringer 1997).

A shallow depression on the ventral side of the embryo forms at the most anterior end of the PS, giving rise to a characteristic transient structure known as the node (Fig. 2D) (Kinder et al., 2001; Sulik et al., 1994; Yamanaka et al., 2007). Similar to equivalent structures in other

vertebrates, the mouse node exhibits organizing activity, since it can induce secondary axis formation other than head structures when transplanted ectopically (Beddington, 1994; Tam and Steiner, 1999; Tam et al., 1997). However, the precise contribution of this organizing activity during normal development in the mouse is still unclear.

Fate mapping experiments indicate that the mouse node contributes mostly to axial tissues, including the prechordal mesoderm, the notochord and the floor plate of the neuroectoderm, as well as it also provides cells to the definitive endoderm (Fig. 2D) (Kinder et al., 2001; Lawson et al., 1991; Yamanaka et al., 2007). In addition to its role in gastrulation, the node is also responsible for generating an unidirectional flow of extraembryonic fluid, which triggers the initial events that establish LR asymmetry in the embryo (reviewed by Lee and Anderson, 2008).

The mouse notochord arises from three distinct processes. Its anterior region is formed from the anterior head process (AHP), which condenses on the midline of the embryo without crossing the node (Yamanaka et al., 2007). Axial mesoderm cells that enter the node produce the trunk notochord through mediolateral intercalation, while the tail notochord arises from node-derived cells that migrate caudally (Kinder et al., 2001; Sulik et al., 1994; Yamanaka et al., 2007). Despite their different modes of formation and genetic requirements, the notochord gather together as a continuous rod-like structure (Fig. 4) (Yamanaka et al., 2007). The notochord has an important role in patterning either the DV axis of the neural tube and the LR axis of the developing embryo (reviewed by Lee and Anderson, 2008).

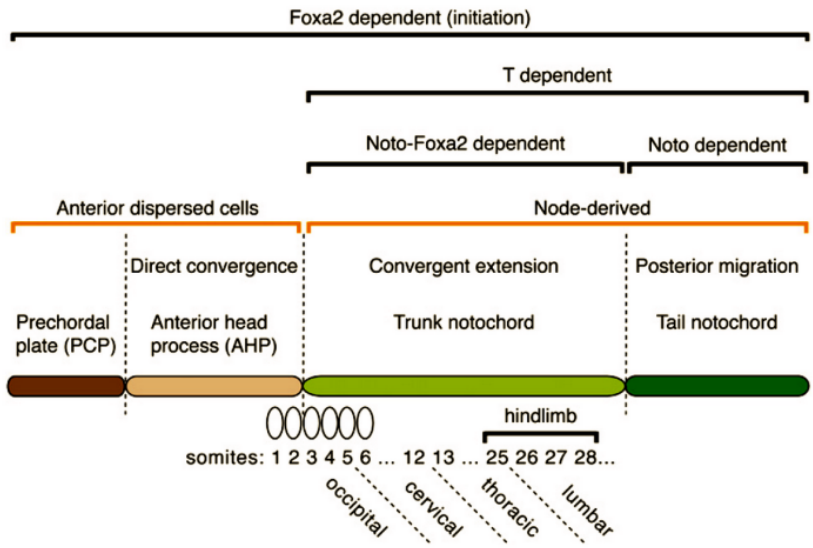

Figure 4. Notochord morphogenesis. Schematic representation summarizes the distinct modes of notochord formation during mouse development, from anterior (*left*) to posterior (*right*) The black brackets at the top indicate the genetic dependence of each region on different transcription factors. The orange brackets in the middle refer to the cell types that originate these regions of the notochord. Distinct morphogenetic mechanisms are involved in the formation of each region. Anatomical regions are represented at the *bottom* (from Yamanaka et al. 2007).

I.2.b - Mesoderm production

Gastrulation is closely linked to the production of mesoderm. This tight relationship makes it difficult to discern between direct and indirect effects on mesoderm formation. Despite this caveat, the induction of mesoderm is usually associated with the expression of *T* (*Brachyury*). This link was established from the observation that a spontaneous mutation in this gene resulted in the complete block in the production of mesoderm posterior to the forelimb bud in the mouse, affecting also the formation of the notochord and the allantois (Chesley, 1935; Herrmann et al., 1990). Extensive studies of a variety of mutant alleles for this gene have revealed that distinct levels of *T* are required at each axial level (Chesley, 1935; Gruneberg, 1958; Herrmann, 1991; Herrmann et al., 1990; MacMurray and Shin, 1988; Stott et al., 1993; Yanagisawa, 1990). Mutant or chimeric embryos harboring mutated

cells for *T* exhibit deficient morphogenetic cell movements with reduced cell migration away from the PS (Hashimoto et al., 1987; Wilson and Beddington, 1997; Wilson et al., 1993, 1995; Yanagisawa et al., 1981).

Wnt signaling is a major regulator of mesoderm development. Loss of *Wnt3* impairs the expression of *T* and blocks mesoderm production (Barrow et al., 2007; Liu et al., 1999; Tortelote et al., 2012). The same phenotype is observed in *Lrp5;Lrp6* double mutants or in *β*-catenin null embryos (Huelsken et al., 2000; Kelly et al., 2004), thus reinforcing the requirement for Wnt/*β*-catenin signaling for mesoderm induction. However, it is not clear if this is a direct effect or an indirect consequence of the absence of PS in these mutants. Regardless of this aspect, mesoderm formation depends initially on Wnt3 and it is subsequently maintained by Wnt3a as Wnt3 levels decrease (Arnold et al., 2000; Cambray and Wilson, 2007; Galceran et al., 1999; Liu et al., 1999; Takada et al., 1994; Yamaguchi et al., 1999). Accordingly, mice mutant for *Wnt3a* fail to produce mesodermal structures posterior to the forelimb bud, which leads to a strong axial truncation (Takada et al., 1994).

After the initial stimulation by Wnt3, *T* establishes a feedback loop to sustain *Wnt3a* expression by directly binding to its promoter (Evans et al., 2012; Martin and Kimelman, 2008). Intriguingly, the *β*-catenin/Lef1/Tcf1 transcription complex is essential for sustaining *T* expression, but seems to be dispensable for its initiation (Galceran et al., 2001). This suggests that Wnt3 and Wnt3a may use a different set of effector complexes to regulate *T* expression. However, the identity of such potential effectors is still not known as the epiblast of E8.5 embryos seems to be negative for the expression of other members of

the Lef1/Tcf family (Galceran et al., 1999), although earlier expression of these genes still needs to be determined.

Alternatively, it is possible that *T* expression in the PS is initiated by a mechanism that does not involve Wnt/*β*-catenin signaling. Indeed, *T* is activated in the notochord by a Wnt/*β*-catenin-independent mechanism (Galceran et al., 2001; Haegel et al., 1995; Wilkinson et al., 1990). Recently, Fletcher et al. (2006) have shown that the *Fgf8* splice form Fgf8b, but not Fgf8a, is able to induce *T* expression in *Xenopus*. Accordingly, *T* expression is lost in the extraembryonic ectoderm and greatly impaired in the epiblast of *Fgf8b* mutants at E6.5, with no evident effect on the expression of *Nodal* and *Wnt3* (Guo and Li, 2007). In addition, double conditional inactivation of *Fgf4* and *Fgf8* in the PS reduces *T* expression in the caudal end, but not in the notochord domain (Boulet and Capecchi, 2012). Therefore, it is possible that *T* expression is first induced by FGF signaling in the posterior epiblast as well as the underlying PS and later sustained by Wnt/*β*-catenin signaling, initially through Wnt3 and then through Wnt3a by a positive autoregulatory loop (Hierholzer and Kemler, 2010). The mechanism controlling *T* expression in the notochord still remains to be elucidated.

Intriguingly, the head mesoderm and the first seven or eight somites, which give rise to the cervical area, are not affected in *T* mutants. A similar observation was reported for other mouse mutants, including those for *Wnt3a*, *Tbx6* and *Raldh2* single mutants or *Cdx* compound mutants (Chapman and Papaioannou, 1998; Herrmann et al., 1990; Mic et al., 2002; Niederreither et al., 1999; van Rooijen et al., 2012; Takada et al., 1994; Wilson and Beddington, 1997; Yoshikawa et al., 1997). This suggests that formation of the head and cervical region of the vertebrate body is controlled by a different mechanism than the

one operating in more posterior axial regions. Whether other members of the T box family would be able to compensate the absence of *T* activity at early embryonic stages remains to be determined.

I.3 - Axis extension

During gastrulation, the vertebrate body grows by the progressive addition of new tissue at the caudal end of the embryo (Fig. 2). Initially, axial growth is driven by the PS, which organizes the continuous production of the different mesodermal compartments and of endoderm for the formation of the trunk. By E9.0, the mouse embryo inverts the position of its germ layers, reallocating the ectoderm to the outside and the endoderm to the inside, while mesoderm remains in the middle (Fig. 3C) (Tam and Behringer, 1997). This event is called turning (or axial rotation) and usually occurs by E9.0, giving to the embryo the characteristic "fetal" position (see Kaufman, 1992).

A major switch in the mode of tissue production occurs after embryo turning. Around E9.5, the ingression of epiblast cells through the PS ceases and the cells responsible for sustaining the axial growth are relocated to the tail bud, which further sustains the growth of the tail (Figs. 2C and 5) (Cambray and Wilson, 2002, 2007; Ohta et al., 2007; Wilson and Beddington, 1996). Such switch also reflects in the mode of neural tube formation, which changes from folding of the neural plate (primary neurulation, during trunk formation) to the cavitation of a rod-like structure into a tube (secondary neurulation, during tail elongation) (Gofflot et al., 1997; Handrigan, 2003; Nievelstein et al., 1993).

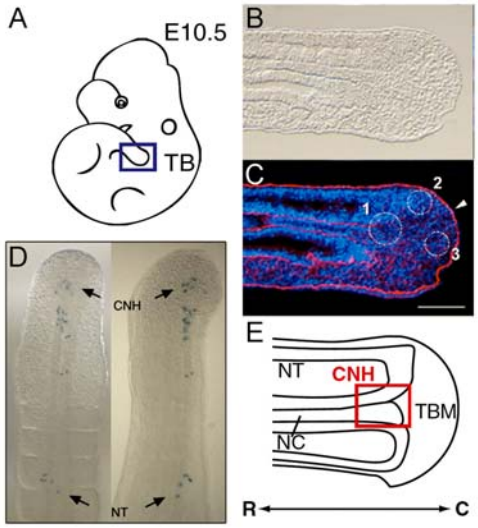

Figure 5. Organization of the mouse tail bud. A Schematic representation of a mouse embryo at E10.5, highlighting the tail bud (blue box) (from Wilson et al. 2009). **B-E** Mouse tail bud at E10.5. **B, C** The tail bud mesenchyme (*TBM*) can be divided into three regions. *1* chordoneural hinge (CNH), *2* dorsal posterior tail bud mesoderm, *3* ventral tail bud mesoderm. In **C**, *red* laminin, *blue* nuclei. Arrowhead indicates the posterior surface ectoderm. Sagittal section, scale bar 100 µm (from McGrew et al. 2008). **D** Cell lineage tracing using a R26nlaacZ mouse line reveals resident cells in the CNH with bipotent neural and mesodermal potency. *NT* neural tube (from Tzouanacou et al. 2009). **E** Schematic representation of the tail bud, highlighting the CNH (*red box*). *NC* notochord (from Wilson et al. 2009).

The tail bud comprises the caudal extremities of the neural tube, the notochord and the hindgut, in addition to a group of morphologically homogeneous mesenchymal cells encased by surface ectoderm (Fig. 5). The surface ectoderm derives from the posterior region of the ectodermal surface overlying the late PS (Tam and Beddington, 1987; Wilson and Beddington, 1996). A thickening of the ectoderm at the ventral side of the tail bud, known as ventral ectodermal ridge (VER), is the lattermost site of cell ingression (Fig. 2C) (Gajović and Kostović-Knezević, 1995; Ohta et al., 2007; Tam and Beddington, 1987; Wilson and Beddington, 1996). The VER is required for the upregulation of *Noggin* in the ventral mesoderm of the tail, which results in the inhibition of BMP signaling and in the termination of the PS-derived EMT (Fig. 2C) (Ohta et al., 2007). In

addition, ablation of the VER in tail bud explants at E10.5 blocked somitogenesis and impaired further tail elongation (Gofflot et al., 1997, 1998; Goldman et al., 2000). These later contributions of the VER during tail elongation remain poorly characterized.

I.3.a - Axial progenitors

Independently of the mode of tissue production, extension of the body is thought to rely on populations of axial progenitors. The existence of axial progenitors was proposed after cell tracing and grafting experiments because a population of resident cells in between the node and the rostral region of the PS (now known as the node-streak border, NSB) was able to contribute to different axial compartments during body extension, such as neural tube, notochord and somites (Fig. 2D) (Cambray and Wilson, 2002, 2007; Forlani, 2003; Lawson et al., 1991; Mathis and Nicolas, 2000a, 2000b; Nicolas et al., 1996; Selleck and Stern, 1991; Smith et al., 1994; Snow, 1981; Tam and Beddington, 1987; Tam and Tan, 1992; Tzouanacou et al., 2009; Wilson and Beddington, 1996). Later in development, these cells are reallocated into a region of the tail bud just caudal to the posterior end of the notochord and the overlying neural tube, which was termed as the chordoneural hinge (CNH) (Cambray and Wilson, 2002; Pasteels, 1942, 1939, 1943). Within the tail bud, these progenitors are still able to sustain axial growth through accretion (Fig. 5) (Cambray and Wilson, 2002; Sausedo and Schoenwolf, 1993, 1994).

Some authors called these progenitors "axial stem cells" (Kondoh and Takemoto, 2012; Olivera-Martinez et al., 2012; Takemoto et al., 2011; Wilson et al., 2009), but there is no evidence so far that they strictly self-renew, especially because their expression profile

seems to change as development proceeds (Cambray and Wilson, 2007; Iimura and Pourquié, 2006). Thus, McGrew et al. (2008) have proposed to name resident cells in the PS or in the tail bud as "long-term axial progenitors" (LTAP). Cells that do not persist for longer periods in these regions and contribute only to limited areas of axial tissue were termed "short-term axial progenitors" (STAP) (McGrew et al., 2008). In this context, one of the major barriers for the study of LTAPs is the lack of specific and reliable cell markers. Most genes that have been shown to be expressed in the NSB or in the tail bud are also present elsewhere, often in nearby regions of the embryo (Cambray and Wilson, 2007; Wilson et al., 2009). However, the simultaneous use of multiple markers has started to help in the identification of these cells. For instance, Martin and Kimelman (2012) have shown that axial progenitors in zebrafish express both the neural marker *Sox2* and the mesodermal marker *T*. The same pattern was also observed in chicken and human embryos (Olivera-Martinez et al., 2012). Whether this pattern is evolutionary conserved in the mouse remains to be confirmed.

In the absence of specific cells markers, most information about the properties and behavior of the axial progenitors derive from grafting and cell tracing experiments. Transplantation of CNH cells to the NSB region of younger embryos have revealed that they are not committed to a specific fate, although they exhibit a reduced ability to populate more anterior embryonic regions (Cambray and Wilson, 2002; McGrew et al., 2008). Whereas cell potency seems to depend on the specific area of the tail bud used as source, grafted cells are able to change their Hox gene expression profile to suit the new environment, in a process that seems to depend on cell-cell interactions (McGrew et

al., 2008). Indeed, these authors described three regions in the tail bud mesenchyme, with distinct cell properties (Fig. 5C). The CNH harbors resident LTAP, which have the ability to generate both neural and mesodermal descendants. Dorsal and ventral regions in the tail bud contain STAPs, which may have been derived from the CNH. In particular, cells in the dorsal posterior region of the tail bud (dpTB) have a reduced capacity to persist and contribute only to mesoderm, whereas ventral tail bud (vTB) cells do not remain in the tail bud and give rise to small areas of paraxial mesoderm (Fig. 5).

Genetic experiments have also provided indirect evidence of the mechanisms controlling the biology of the axial progenitors. For instance, *Tbx6* drives axial progenitors into a mesodermal fate at the expense of neural tissue through the downregulation of *Sox2* (Takemoto et al., 2011). When *Tbx6* is genetically inactivated, ectopic neural tube-like structures flank the axial neural tube (Chapman and Papaioannou, 1998). In the resulting mesoderm, high levels of Wnt/*β*-catenin signaling further specifies paraxial mesoderm, while low levels drive mesoderm differentiation to vascular endothelium in the zebrafish (Martin and Kimelman, 2012). Blood formation depends on *Cdx* genes, which are downstream targets of Wnt/*β*-catenin signaling (reviewed by Lengerke and Daley, 2012).

In the mouse, however, loss of *Cdx* genes causes severe axial truncations and has revealed redundant functions between family members in the formation of the axial skeleton, neural tube and the cloacal derivatives (Van den Akker et al., 2002; Chawengsaksophak et al., 1997, 2004; van Nes et al., 2006; Savory et al., 2009; Subramanian et al., 1995; van de Ven et al., 2011; Young et al., 2009). Among them, *Cdx2* has the most prominent role. Whereas inactivation of *Cdx1* or

Cdx4 produces mild anterior homeotic transformations, the conditional inactivation of *Cdx2* in the epiblast results in the block of axial growth at the level of the hindlimbs (Savory et al., 2009). In turn, the *Cdx2*$^{+/-}$*;Cdx4*$^{-/-}$ allelic combination (*Cdx2/4* mutants) exhibits an intermediate phenotype (Van Nes et al., 2006; Young et al., 2009). Intriguingly, *Cdx2/4* deletion does not affect the behavior and self-renew capacity of the axial progenitors when they are grafted into a wild type environment (Bialecka et al., 2010), suggesting that *Cdx* genes may act non-cell autonomously to maintain a progenitor niche in the tail bud (Bialecka et al., 2010; Young et al., 2009).

Conversely, axial progenitors seem to be highly sensitive to retinoic acid (RA). Administration of RA to pregnant females results in anterior homeotic transformations, ectopic formation of neural tissue and truncation of the caudal region of the embryos due to widespread apoptosis (Alles and Sulik, 1990; Kessel, 1992; Shum et al., 1999). RA activity in the tail bud seems to be regulated by the RARγ, since its inactivation is able to rescue the tail phenotype caused by exogenous administration of RA or by loss of *Cyp26a1* (Abu-Abed et al., 2003; Iulianella et al., 1999). Analyses of gene expression upon increased levels of RA have revealed that many genes, such as *Cdx4*, *T*, *Wnt3a*, and *Fgf8*, were also downregulated in the tail bud (Abu-Abed et al., 2003; Iulianella et al., 1999; Olivera-Martinez et al., 2012). Of particular interest, FGF signaling seems to have a central role on the axial progenitors by promoting the expression of both *Sox2* and *T* in the tail bud of chicken embryos (Olivera-Martinez et al., 2012).

I.4 - From progenitors to body structures

Elongation of the embryonic main body axis requires a tight balance between the maintenance of axial progenitors in an undifferentiated state and the production of new cells. The organized deposition of tissue precursors endowed with patterning information ultimately generates the different body structures. Although all these processes are interconnected during development, they will be discussed herein in separate for simplification.

I.4.a - Somitogenesis

The structures that best characterize vertebrates are associated with their muscle-skeletal system. The largest part of this system derives from the paraxial mesoderm (reviewed by Brent and Tabin, 2002; Christ et al., 2007), although other embryonic tissues also participate in its formation. For instance, neural crest cells generate most of the craniofacial skeleton and the lateral mesoderm gives rise to the limb skeleton (reviewed by Capdevila and Izpisúa Belmonte, 2001; Cordero et al., 2011).

During the posterior growth of the embryo, the paraxial mesoderm forms through the progressive addition of precursors derived initially from the PS and then from the tail bud (reviewed by Wilson et al., 2009). The addition of such new tissue in the caudal end of the embryo is accompanied by the periodical formation of pairs of symmetrical segments of mesoderm, known as somites, at both sides of the neural tube (Fig. 6). This determines two major domains in the paraxial mesoderm: a segmented region composed of an AP succession of somite pairs and the non-segmented presomitic mesoderm (PSM) located more posteriorly (Fig. 6). Somites are produced at the anterior

end of the PSM through the combined activity of two dynamic variables: the "determination front", which marks the region of the PSM where a new inter-somitic border is formed, and the "segmentation clock", which establishes the pace of somitogenesis.

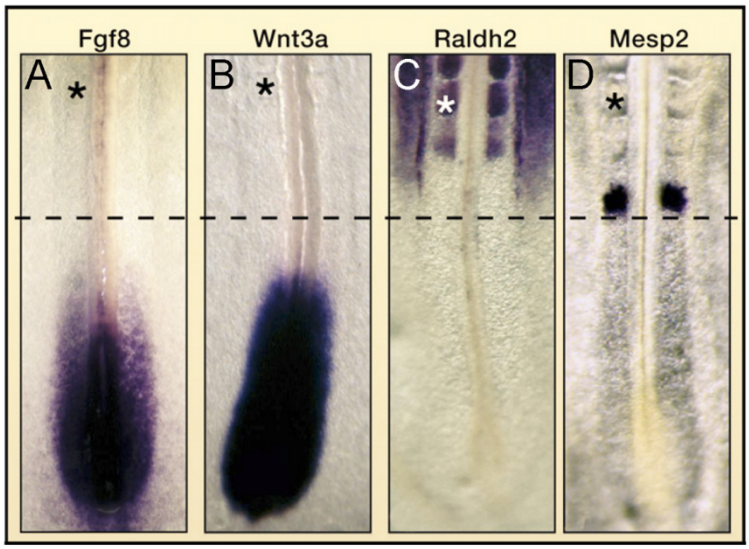

Figure 6. The determination front. A-D Whole-mount *in situ* hybridization of chicken embryos for key components of the segmentation program. Expression of *Fgf8* (**A**), *Wnt3a* (**B**), *Raldh2* (**C**), and *Mesp2* (**D**). * marks the last formed somite (from Pourquié 2011).

The determination front is thought to arise from the combination of two opposite gradients, an anterior to posterior gradient of RA and a posterior to anterior gradient of Wnt3a and Fgf8 (Fig. 6A-D) (Diez del Corral et al., 2003; Dubrulle and Pourquié, 2004a; Dubrulle et al., 2001; Moreno and Kintner, 2004; Sirbu and Duester, 2006). The relevance of the FGF and Wnt/*β*-catenin activities for setting the determination front has been extensively investigated in many animal models. In particular, increased FGF levels in the PSM of chicken or zebrafish embryos resulted in a more anterior position of the new inter-somitic border and smaller somites (Dubrulle et al., 2001; Sawada et

al., 2001). On the other hand, the determination front was displaced caudally and larger somites were formed when FGF activity was blocked by chemical inhibitors (Dubrulle et al., 2001; Sawada et al., 2001). However, the most compelling evidence for a role of FGF signaling in somitogenesis was provided by genetic experiments in mice (Naiche et al., 2011; Niwa et al., 2007; Wahl et al., 2007). In particular, the conditional inactivation of both *Fgf4* and *Fgf8* in the PS resulted in axial truncation due to the premature differentiation of PSM cells (Naiche et al., 2011).

Similarly, high levels of Wnt/*β*-catenin signaling also maintain PSM cells in an undifferentiated state. Although the phenotypes resulting from the inactivation of *Wnt3*, *Wnt3a*, *Lrp5;Lrp6* or *β*-catenin did not allow analysis of the role of these molecules in somite formation in mice (Huelsken et al., 2000; Kelly et al., 2004; Liu et al., 1999; Takada et al., 1994), the inhibitory properties of this pathway in the PSM were demonstrated by the constitutive activation of *β*-catenin, which resulted in embryos with an extended PSM that failed to produce new somites (Aulehla et al., 2008; Dunty et al., 2008). On the other hand, the conditional inactivation of *β*-catenin in the PS produced small, misshapen somites as a result of the abnormal PSM (Dunty et al., 2008).

Mutant mice for the RA-synthesizing enzyme *Raldh2* have revealed that RA has an indirect effect on the determination front and somite size by antagonizing FGF signaling in the ectoderm (Diez del Corral et al., 2003; Sirbu and Duester, 2006; Vermot and Pourquié, 2005; Vermot et al., 2005). RA seems to be also involved in the maintenance of somite symmetry by protecting the paraxial mesoderm from the asymmetric stimulus produced by the LR genetic program

(Diez del Corral et al., 2003; Sirbu and Duester, 2006; Vermot and Pourquié, 2005; Vermot et al., 2005).

The second component of somitogenesis involves the so-called segmentation clock. The first evidence for its existence was found in chicken embryos from the observation of dynamic expression of *Hairy1* in the PSM (Fig. 7A-I) (Palmeirim et al., 1997). Its expression oscillated as a wave sweeping the PSM in a posterior to anterior direction, with a periodicity roughly matching the time required for the formation of a new somite (Palmeirim et al., 1997). A large number of genes have been further described with cycling behavior in the PSM in chicken, mouse and zebrafish embryos (Aulehla et al., 2003; Dale et al., 2006; Dequéant et al., 2006, 2008; Krol et al., 2011; Niwa et al., 2007). In general, they mostly belong to the Notch, FGF and Wnt/*β*-catenin signaling pathways. Both FGF and Notch signaling modulate genes that cycle in synchrony with each other, whereas Wnt/*β*-catenin signaling regulates genes that oscillate in the complementary phase (Aulehla et al., 2003; Dequéant et al., 2006, 2008; Krol et al., 2011; Niwa et al., 2007). Interestingly, the identity of cycling genes differed between those three species, suggesting the existence of a non-conserved mechanism controlling these oscillations (Krol et al., 2011).

The role of oscillating genes from the FGF and Wnt/*β*-catenin pathways is still not clear. However, Wnt/*β*-catenin signaling activates the cyclic expression of many Notch signaling members through the induction of *Msgn1* expression in the rostral part of the PSM (Chalamalasetty et al., 2011). *Msgn1* expression is also affected by the conditional inactivation of *Fgfr1* in the PS, whereas the expression of *Wnt3a* was only slightly expanded in the PSM (Wahl et al., 2007). Indeed, perturbations in FGF signaling affect the expression of multiple

genes, including members of the Wnt/*β*-catenin and Notch pathways (Niwa et al., 2007; Wahl et al., 2007). Oscillations in Notch members have a better defined role in somitogenesis. They synchronize cyclic gene expression among neighboring PSM cells, in addition to initiate *Mesp2* expression by E7.5 (Conlon et al., 1995; Evrard et al., 1998; Hrabě de Angelis et al., 1997; Oginuma et al., 2008).

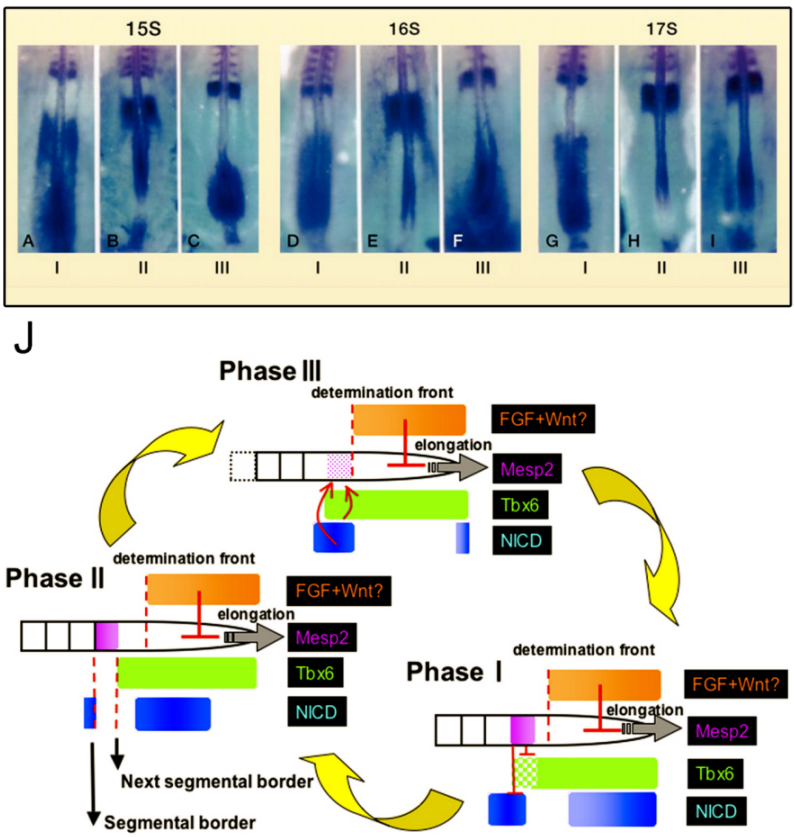

Figure 7. Somitogenesis. A-I Whole-mount *in situ* hybridization of chicken embryos for *cHairy1* shows oscillation in gene expression (from Pourquié 2011). **J** A model for periodic segmentation. Schematic representation of the temporal and spatial changes in the expression patterns and relationships among *Mesp2* (*pink*), *Tbx6* (*green*), NICD (*blue*) and FGF signaling (*orange*) during a single cycle of somitogenesis. See text for further information. *NICD* Notch intracellular domain (from Oginuma et al. 2008).

Mesp2 is a key effector in the formation of inter-somitic boundaries. Its expression results from the interaction between the

molecular activities associated to the clock and the determination front. The combined activity of Wnt/*β*-catenin and Notch signaling sustain the expression of *Tbx6* in the entire PSM through the regulation of *T* and *RBPJκ*, respectively (Chapman et al., 1996; White et al., 2005; Yamaguchi et al., 1999). Tbx6 induces the activation of *Mesp2*, determining its anterior border of expression (Oginuma et al., 2008; Yasuhiko et al., 2006). In turn, the posterior border of the *Mesp2* domain is defined by active repression through the FGF gradient in the PSM (Oginuma et al., 2008; Sasaki et al., 2011; Yasuhiko et al., 2006, 2008). Consistent with this, conditional inactivation of both *Fgf4* and *Fgf8* in the PS resulted in the expansion of the *Mesp2* expression domain (Naiche et al., 2011). Mesp2 suppresses Notch activity through the induction of *Lfng*, as well as downregulates Tbx6 protein through proteasome-dependent degradation just before a new segment is established in the rostral region of the PSM (Fig. 7J) (Morimoto et al., 2005; Oginuma et al., 2008).

These findings have led to a model in which the new segment border is produced at the AP level of the PSM where the inhibitory activity of FGF and Wnt/*β*-catenin signaling falls below the threshold required to block the molecular mechanisms of segmentation. The inhibitory gradients result from the restricted production of the relevant molecules at the most posterior end of the PSM, which are then progressively degraded as they occupy more anterior areas of the PSM (Aulehla et al., 2008; Dubrulle and Pourquié, 2004a; Dubrulle et al., 2001; Dunty et al., 2008; Sawada et al., 2001). The increasing growth of the embryo thus produces the concomitant displacement of the source of signals. This results in a constant posterior shift of the

determination front at the same pace as the growth of the PSM (Fig. 7J) (reviewed by Pourquié, 2011).

I.4.b - Trunk formation and organ specification

The vertebrate body is made of many other different structures in addition to the muscle-skeletal system. Each of them differentiates under the control of unique morphogenetic programs, usually involving tightly regulated sequential steps and multiple tissue interactions. A comprehensive discussion of the mechanisms involved in organogenesis is not in the scope of this thesis. This section briefly describes how some of these structures are correctly specified within the mouse trunk as the embryo elongates. Detailed description of those processes can be found elsewhere (heart, Abu-Issa and Kirby, 2007; Lin et al., 2012; Srivastava, 2006; Stennard and Harvey, 2005; hematopoietic system, Medvinsky et al., 2011; thymus, Gordon and Manley, 2011; gut, Lewis and Tam, 2006; Zorn and Wells, 2009; lungs, Morrisey and Hogan, 2010; liver, Si-Tayeb et al., 2010; Tremblay, 2011; pancreas, Puri and Hebrok, 2010; Gittes, 2009; Oliver-Krasinski and Stoffers, 2008; spleen, Burn et al., 2008; urogenital system and kidneys, Bowles and Koopman, 2013; Costantini and Kopan, 2010; Dressler, 2009; Quaggin and Kreidberg, 2008; Shah et al., 2004; Suzuki et al., 2009; Yamada et al., 2006).

The trunk can be defined as a region of the body encompassing major organs and further divided into thorax and abdomen. The first organ to be induced during development is the heart, resulting from the combined action of BMP, FGF, Shh, Notch, RA and Wnt signaling in the most anterior region of the lateral mesoderm, underneath the cephalic neural plate (Duester, 2008; Srivastava, 2006). Correct

morphogenesis and positioning of the heart depends on the inductive activity of the anterior visceral endoderm through the secretion of Bmp2 over the splanchnic mesoderm, in conjunction to head and foregut morphogenesis (Fig. 8A,B) (Madabhushi and Lacy, 2011; Schultheiss et al., 1997). The invagination of the endodermal sheet initiates foregut formation at the same time as broad AP regional patterning through a Nodal gradient. High Nodal levels promote anterior endoderm together with Foxa2 and Mixl1 transcription factors, whereas posterior endoderm differentiates under low levels of Nodal and a Sox17-dependent mechanism (reviewed by Zorn and Wells, 2009).

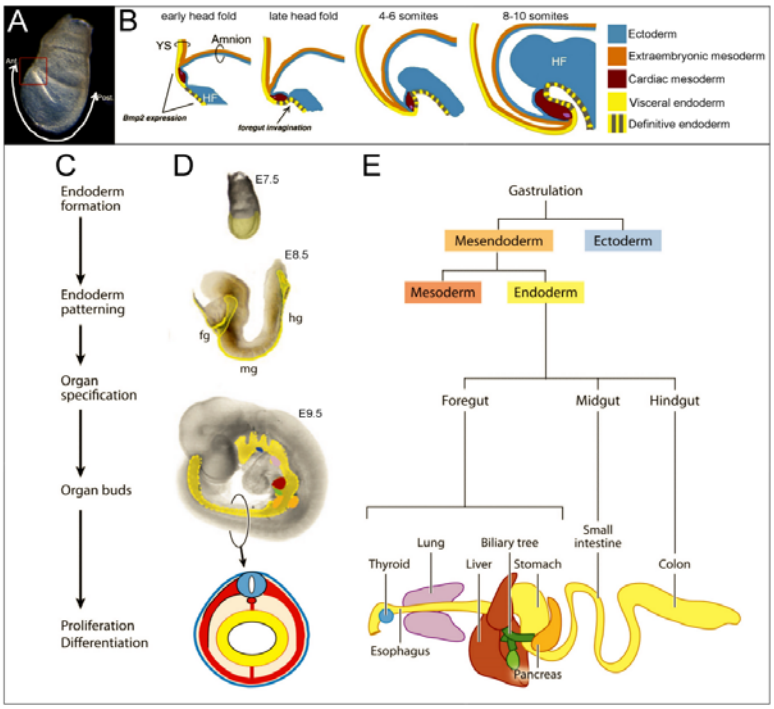

Figure 8. Organ specification during mouse development. A,B Head and heart formation occur concomitantly to foregut invagination. **A** Early head fold stage embryo. Lateral view. *Red box* highlights the anterior embryonic/extraembryonic junction. **B** Schematic representation of the highlighted region in **A**, showing foregut invagination through time. **C-E** Overview of endoderm organ formation (adapted from Zorn & Wells 2009). **C** Major events are listed in chronological order. D Mouse stages highlighting the endoderm (*yellow*) matches the events in **C**. A schematic cross section of a E9.5 embryo illustrates the germ layer arrangement. *red* mesoderm, *blue* neural tube, *fg* foregut, *mg* midgut, *hg* hindgut. E Endoderm cell lineages projected on to a schematic of the gastrointestinal tract (adapted from Madabhushi and Lacy, 2011).

Other trunk-associated organs originate from endodermal and mesodermal tissues laid down during the axial extension of the body. The epithelial components of the gastrointestinal and respiratory systems derive from the definitive endoderm, which generates the mature organs upon interactions with the lateral mesoderm (reviewed by Zorn and Wells, 2009). The classical view of endoderm formation implied that epiblast-derived cells invade and displace the VE layer (Lawson and Pedersen, 1987; Lawson et al., 1986). However, a recent study suggested that the VE is not completely displaced to extraembryonic regions, but some VE cells intermingle with the definitive endoderm to produce the embryonic gut (Kwon et al., 2008). At E8.0, the endoderm starts a sequence of regional specification processes along the DV and AP axes that generate the primordia of the lungs, the gastrointestinal tract and its associated organs. These primordia interact with the mesenchyme of the lateral plate, which provides several other organ components such as the muscular layers of the intestine and the vasculature, while neural crest cells provide autonomic innervation (Fig. 8C-E) (reviewed by Zorn and Wells, 2009). Kidney specification occurs in three steps from the intermediate mesoderm at the level of the prospective hindlimbs, resulting from the concerted activity of RA signaling along the AP axis and the BMP and Activin signaling along the medio-lateral axis (reviewed by Costantini and Kopan, 2010). The gonads are formed from paired rudiments of intermediate mesoderm that bud off near the developing kidney. However, the gametes originate from primordial germ cells (PGCs) that are set aside early in development during gastrulation. These cells arise from the extraembryonic mesoderm in close proximity to the posterior

region of the PS and the allantois by E6.5 (Ginsburg et al., 1990). Around E9.5-E11.5, the PGCs migrate through the hindgut toward the genital ridges, where they develop in testis cords or become the ova depending on the sex of the animal (reviewed by Bendel-Stenzel et al., 1998; Molyneaux and Wylie, 2004). A transient compartment at the caudal end of the hindgut, the cloaca, gives rise to the exit of the genitourinary system and to the anorectal sinus (Seifert et al., 2008). In mammals, this occurs through its septation into distinct openings by a *Shh*-dependent mechanism (Mo et al., 2001). Concomitantly, the cloacal membrane gives rise to the genital tubercle through the concerted activity of Shh, FGF, BMP and Wnt/*β*-catenin signaling (reviewed by Suzuki et al., 2009). The genital tubercle is the last structure to develop along the AP axis (Haraguchi et al., 2000; Perriton et al., 2002).

I.5 - Anterior-posterior patterning of the body

At the same time the embryo grows, tissue precursors at particular axial levels acquire positional information, ultimately resulting in the production of a properly organized body divided in well-defined anatomical regions (*e.g*. neck, trunk and tail). Such distribution also has functional relevance, since most of the internal organs involved in vital and reproductive processes are associated with the trunk. *Per se*, this reveals distinctive requirements for the development of each region of the body, usually involving tightly regulated sequential steps and multiple tissue interactions.

I.5.a- Anterior-posterior patterning of the axial skeleton

The axial skeleton is a major derivative of the paraxial mesoderm, emerging from the sclerotome of the differentiating somites (reviewed by Christ et al., 2000). Overall, the axial skeleton is divided into five major anatomical regions, from anterior to posterior: 1) cervical, 2) thoracic, 3) lumbar, 4) sacral, and 5) caudal. The length of each of these regions is at the base of the diversity observed in the vertebrate body. Whereas a high degree of variability occurs among species, a given species exhibits an invariable distribution, which is termed vertebral formula. For instance, the mouse, the focus of this thesis work, presents seven cervical, thirteen thoracic, six lumbar, four sacral and a variable number of caudal vertebrae (C7T13L6S4Cd24-30) (reviewed by Mallo et al., 2009).

A wealth of genetic experiments performed during the last three decades helped to identify many of the players involved in patterning of the axial skeleton. They are part of a variety of signaling pathways and include many transcription factors. The current paradigm considers Hox genes as major players in this process and different signaling pathways eventually converge in the regulation of their activity.

Hox genes

Initially identified in mutant flies with altered segment identity, homeotic genes (Hox) proved to be highly conserved during animal evolution (reviewed by Gehring, 1987; Lewis, 1978; Wellik, 2007). They encode transcription factors with a specific 60-amino acid DNA-binding domain (homeodomain), determining regional identities along the AP and proximo-distal axes (Kissinger et al., 1990; McGinnis et al., 1984; Otting et al., 1990; Scott and Weinert, 1984). Mammals have 39

Hox genes distributed in four clusters (A to D), which were originated from two duplication events of an original single cluster, followed by secondary losses of some genes (Asrar et al., 2012; Bailey et al., 1997; Duboule and Dollé, 1989; Garcia-Fernàndez, 2005; Hart et al., 1987; Holland et al., 1994; Kappen et al., 1989; Krumlauf, 1994; Pearson et al., 2005; Schughart et al., 1989). Each cluster harbors 13 paralogous groups, classified on the basis of their distribution within the cluster and sequence similarity (Fig. 9) (reviewed by Alexander et al., 2009).

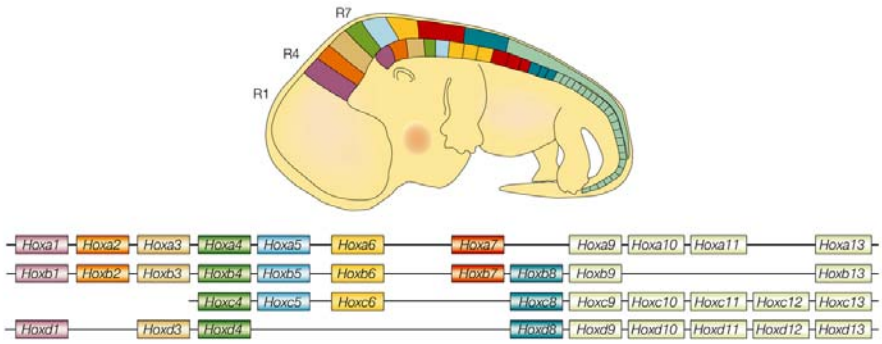

Figure 9. Hox clusters in the mouse. Top Schematic representation of Hox expression in the mouse embryo at E12.5. Approximate domains of expression are color-coded to the genes in the cluster diagram. **Bottom** Schematic representation of Hox genomic distribution (adapted from Pearson et al. 2005).

The clustered organization of Hox genes raised interesting functional properties, in which gene activation follows the order they are distributed along the chromosome. In particular, genes located at more 3' regions of the cluster are expressed earlier in development than genes at more 5' regions (Dollé et al., 1989; Duboule and Dollé, 1989; Gaunt and Strachan, 1996; van der Hoeven et al., 1996; Izpisúa-Belmonte et al., 1991; Kondo and Duboule, 1999). In addition, gene distribution within the cluster correlates with their sequence of activation along the AP axis. Thereby, Hox genes at the 3' end of the cluster are activated at more rostral regions than those occupying more

5' locations within the cluster (Dollé et al., 1989; Gaunt et al., 1988). These temporal and spatial colinearities determine well-defined anterior boundaries of expression at distinct axial levels as the embryo grows, but overlapping gradients towards the tail (Burke et al., 1995; Duboule and Dollé, 1989; Graham et al., 1989). Such patterns of expression led to propose the concept of posterior prevalence, according to which Hox proteins activated at more caudal regions are able to override the effects of more anterior Hox genes (Bachiller et al., 1994; Duboule, 1991; Duboule and Morata, 1994; González-Reyes and Morata, 1990). However, a mechanistic explanation for this phenomenon still remains elusive.

The role of Hox genes in patterning the axial skeleton has been extensively studied, mostly using genetic approaches in the mouse. The current paradigm states that the first step in Hox-mediated patterning of the axial skeleton involves the definition of global anatomical regions (McIntyre et al., 2007; Vinagre et al., 2010; Wellik and Capecchi, 2003). For instance, formation of the thoracic region, typically defined by the presence of rib-bearing vertebrae, is first induced by the activation of *Hox6* genes in the paraxial mesoderm (Vinagre et al., 2010). The first indication for this was obtained from the comparison of Hox gene expression patterns between species with different vertebral formulas, showing that the anterior expression limit of genes from this paralog group correlates with the cervical to thoracic transition and not with absolute somite levels (Burke et al., 1995). The role of *Hox6* genes in promoting thoracic characteristics was later supported by transgenic experiments in the mouse, which revealed that *Hoxb6* is able to induce rib formation along the whole AP axis (Vinagre et al., 2010). Conversely, the lumbar region is produced by the activation of *Hox10*

genes, which block rib formation (Carapuço et al., 2005; Vinagre et al., 2010). Such activity was initially revealed by the analysis of mutant mice with complete inactivation of all *Hox10* genes, which resulted in the ectopic growth of ribs in the lumbar region (Wellik and Capecchi, 2003). The ability of *Hox10* genes to block rib formation was later confirmed by transgenic experiments in which *Hoxa10* was precociously expressed in the PSM, resulting in totally rib-less embryos (Carapuço et al., 2005). The sacrum results from the activity of the next Hox paralog group, Hox11, as demonstrated by the absence of the sacral region in mice lacking the whole Hox11 group, which acquired lumbar morphology (Wellik and Capecchi, 2003). The finding that the different vertebral regions are specified in an AP sequence and that this is controlled by the sequential activity of Hox genes in the 3' to 5' direction, together with the observation that determination of a particular anatomical region somehow implies overriding the characteristics of the immediately anterior region, provide good experimental evidence for the concept of posterior prevalence in vertebrates.

Global patterning of the axial skeleton seems to be determined in the PSM prior to somite formation. This was initially shown by classical transplantation experiments in chicken embryos (Fomenou et al., 2005; Kant and Goldstein, 1999; Kieny et al., 1972; Nowicki and Burke, 2000). In particular, when the PSM of the prospective thoracic region was heterotopically transplanted into the PSM of the prospective cervical region, the resulting somites developed according to its donor characteristics, producing embryos with ribs associated to the cervical vertebrae (Nowicki and Burke, 2000). More recently, genetic manipulations in the mouse indicate that Hox genes seem to produce

their patterning effects also in the PSM and not in the differentiating somites. For instance, precocious overexpression of *Hoxa10* in the PSM resulted in the absence of ribs in the thorax. Conversely, overexpression of this gene in the somites caused only milder phenotypes (Carapuço et al., 2005; Vinagre et al., 2010). Similar experiments performed with *Hoxb6* and *Hoxa11* suggested that the activity of these genes in promoting, respectively, thoracic and sacral characteristics is also mostly relevant in the PSM (Carapuço et al., 2005; Vinagre et al., 2010).

In addition to defining the global anatomical regions of the body, Hox genes are also involved in providing positional identity to the individual vertebrae that compose each of the different areas. Consistent with this, mutations in many different Hox genes produce distinct types of milder homeotic transformations that affect a limited set of vertebrae (Van den Akker et al., 2001; Chen et al., 1998; Condie and Capecchi, 1993, 1994; Horan et al., 1994, 1995; Manley and Capecchi, 1997). However, how the identity of each vertebra is determined remains poorly understood and it is not easily interpreted from the analysis of existing mutants. Kessel and Gruss (1991) have proposed the existence of a "Hox code", in which such identities are provided by the combination of the activity of several Hox genes acting at the different AP levels. However, the complexity of the possible combinations makes it almost virtually impossible to test this hypothesis in a conclusive way.

Retinoic acid signaling

This was the first pathway associated with alterations in the patterning of the axial skeleton (Shenefelt, 1972). In particular, treatment of

pregnant females with exogenous RA resulted in both anterior and posterior transformations of vertebral identity, depending on the specific time of administration (Kessel, 1992; Kessel and Gruss, 1991). Compatible with this, inactivation of RARs produced cervical transformations resembling those observed in *Hoxb4* and *Hoxb5* single mutants (Jeannotte et al., 1993; Lohnes et al., 1994; Ramírez-Solis et al., 1993). Such similarity raised the possibility that the AP patterning activity of RA results from the control of Hox gene expression. The first indication that RA might control Hox gene activation was provided by *in vitro* experiments showing that treatment of teratocarcinoma cells with RA resulted in the collinear activation of Hox genes of the B cluster (Simeone et al., 1990). In the mouse, changes in vertebral identity upon RA treatment correlated with anterior shifts of Hox expression domains (Kessel, 1992; Kessel and Gruss, 1991). How RA modulates Hox gene expression is still not clear. However, some Hox genes harbor RAREs in their regulatory regions (Dupé et al., 1997; Gould et al., 1998; Langston and Gudas, 1992; Langston et al., 1997; Oosterveen et al., 2003a, 2003b; Pöpperl and Featherstone, 1993; Studer et al., 1998; Zhang et al., 1997). The existence of such elements suggest that at least part of Hox regulation involves the direct interaction between RA receptors and Hox regulatory regions.

Wnt/β-catenin signaling

This pathway also influences segmental identity along the AP axis. Although mutants for *Wnt3a* exhibit a strong truncation posterior to the forelimbs, which precludes the assessment of patterning effects (Takada et al., 1994), homeotic transformations were observed in the

cervical area of Wnt3a null mutants, with fusions between the axis (C2) and the atlas (C1) (Ikeya and Takada, 2001). Analysis of *Wnt3a*$^{vt/vt}$ hypomorphs confirmed this transformation and also revealed posterior identity changes in the thoracic region, as well as lumbar to sacral transformations (Ikeya and Takada, 2001). As for RA, it is possible that Wnt3a affects AP patterning through activation of Hox gene expression. Consistent with this, Wnt3a was able to induce posterior Hox (*e.g. Hoxa9* and *Hoxa10*) genes in embryoid bodies or in human fibroblasts (Klapholz-Brown et al., 2007; Lengerke et al., 2008). Similarly, *β*-catenin was shown to directly induce *Hoxa10* expression in myeloid progenitor cells (Bei et al., 2012). However, how this regulation is produced in the developing embryo is still far from being understood.

FGF signaling

The FGF pathway is also involved in AP patterning processes. A series of defects in the axial skeleton resulted from genetic perturbations in the activity of Fgfr1 (Partanen et al., 1998). A gain-of-function allele resulted in posteriorization of the axial skeleton, with transformation of the last cervical vertebra into a thoracic identity and the last thoracic vertebra adopting a lumbar character (Partanen et al., 1998). Conversely, some hypomorphic alleles produced posterior truncations at the lumbosacral level or in the tail, in addition to homeotic transformations in both anterior and posterior directions (Partanen et al., 1998).

The observation of subtle alterations of the Hox expression domains at earlier developmental stages in embryos carrying these hypomorphic phenotypes suggested that the AP patterning activity of

Fgfr1 also relies on the modulation of Hox gene expression (Partanen et al., 1998). Other experimental observations also support this hypothesis. In particular, incubation of *Xenopus* cap explants with Fgf ligands resulted in activation of posterior Hox genes (Cho and De Robertis, 1990; Cox and Hemmati-Brivanlou, 1995; Kolm and Sive, 1995; Lamb and Harland, 1995; Pownall et al., 1996). Similarly, implantation of Fgf8-soaked beads adjacent to the caudal PSM of chicken embryos shifted anteriorly the rostral boundaries of *Hoxb9* and *Hoxa10* without provoking abnormal cell movement along the AP axis (Dubrulle et al., 2001). A dose-dependent effect on the activation of Hox genes by Fgf8 is also observed in tissue explants (Liu et al., 2001). However, the molecular mechanisms controlling Hox expression through Fgf stimulation are still largely unknown.

GDF11 signaling

Gdf11 activates another signaling pathway that strongly impacts axial patterning. Mutants for this gene exhibit a minor alteration in the seventh cervical vertebra, but have strong effects in more posterior parts of the skeleton, with four or five extra rib pairs and seven to nine lumbar vertebrae, as well as variable degrees of tail truncation. The extension of the trunk (thorax and lumbar region) displace the hindlimbs posteriorly in relation to the forelimbs, without an apparent increase in total body length at earlier stages (McPherron et al., 1999).

The similarity in the phenotype of other mutants has revealed many members of this pathway that were further confirmed by biochemical approaches, such as the proprotein convertase Pcsk5, the Activin type IIA (*Acvr2a*) and IIB (*Acvr2b*) receptors and the Tgf-β type I receptor Alk5 (*Tgfbr1*) (Andersson et al., 2006; Essalmani et al.,

2008; McPherron et al., 1999; Oh and Li, 1997; Oh et al., 2002; Szumska et al., 2008). However, it is possible that Gdf11 is not the only ligand that can activate this pathway because compound mutants between *Gdf11* and its close relative *Mstn* had enhanced skeletal abnormalities, suggesting that these genes share redundant functions in axial patterning (McPherron et al., 2009).

Perturbations in Gdf11 signaling produced shifts in the expression of some Hox genes both in mouse and in chicken (Liu, 2006; McPherron et al., 1999; Szumska et al., 2008). This suggests that Hox genes could be involved downstream of Gdf11 in the control of AP patterning processes during vertebrate development. Accordingly, loss of Gdf11 resulted in the activation of Hox genes of posterior groups (Hox9 to 13) at more caudal positions, whereas gain-of-function experiments resulted in the opposite effect (Liu, 2006; McPherron et al., 1999; Szumska et al., 2008). Interestingly, Gdf11 seems to exert its function by enhancing Fgf8 ability to induce posterior Hox genes in tissue explants (Liu et al., 2001). Whether this is the case in the mouse remains to be determined.

I.5.b- Anterior-posterior patterning of non-axial structures

In addition to the axial skeleton, other anatomical properties of the vertebrate body present defined patterns along the AP axis. Of particular relevance for this thesis is the position of the limbs or equivalent structures. Similar to the axial formula, limb position is variable among species, but constant within a given species. In fact, limbs are positioned at the level of regional transitions along the body. Whereas forelimbs are located at the transition from the cervical region to the trunk, the hindlimbs are positioned at the transition from the

trunk to the tail region (Fig. 10) (Burke et al., 1995). This suggests the existence of conserved mechanisms coupling patterning of the axial skeleton with non-axial structures.

Limbs arise from specific areas of the LPM, called limb fields, in which directional cell behaviors, such as migration, intercalation and division, drive their outgrowth (Boehm et al., 2010). In the mouse, the forelimb bud arises at E9.0 at the level of somites 8-9 to 13-14, whereas the hindlimb buds are formed around E10.0, at the level of somites 23-24 to 28-29. However, as the embryo grows, the hindlimb position shifts from the initial level to somites 34-35 (Burke et al., 1995). The molecular mechanisms responsible for limb induction and morphogenesis are relatively well known (Bénazet and Zeller, 2009; Capdevila and Izpisúa Belmonte, 2001; Fernandez-Teran and Ros, 2008; Rabinowitz and Vokes, 2012; Zeller et al., 2009). Interestingly, while many of the growth and patterning mechanisms seem to be conserved to a large extent between the forelimb and hindlimb buds, the key regulators for the initial induction and patterning seem to differ. In particular, forelimb bud induction requires *Tbx5* activity and *Hox9* genes for initial patterning events. Whereas Tbx5 activates the crucial expression of *Fgf10* in limb mesenchyme (Agarwal et al., 2003; Ng et al., 2002; Ohuchi et al., 1997), *Hox9* genes activate the *Hand2*-*Shh* pathway in the zone of polarizing activity (ZPA) (Fig. 10D) (Xu and Wellik, 2011). On the other hand, induction of the hindlimbs depends on *Tbx4* and the LIM-homeodomain protein *Isl1*. *Tbx4* has an equivalent role of *Tbx5*, activating *Fgf10* in the hindlimbs, but it is not exclusively required for its expression (Naiche and Papaioannou, 2003, 2007). Similarly to *Hox9* genes in the forelimbs, *Isl1* activates the

Hand2-Shh pathway in the ZPA of the hindlimbs (Fig. 10D) (Itou et al., 2012).

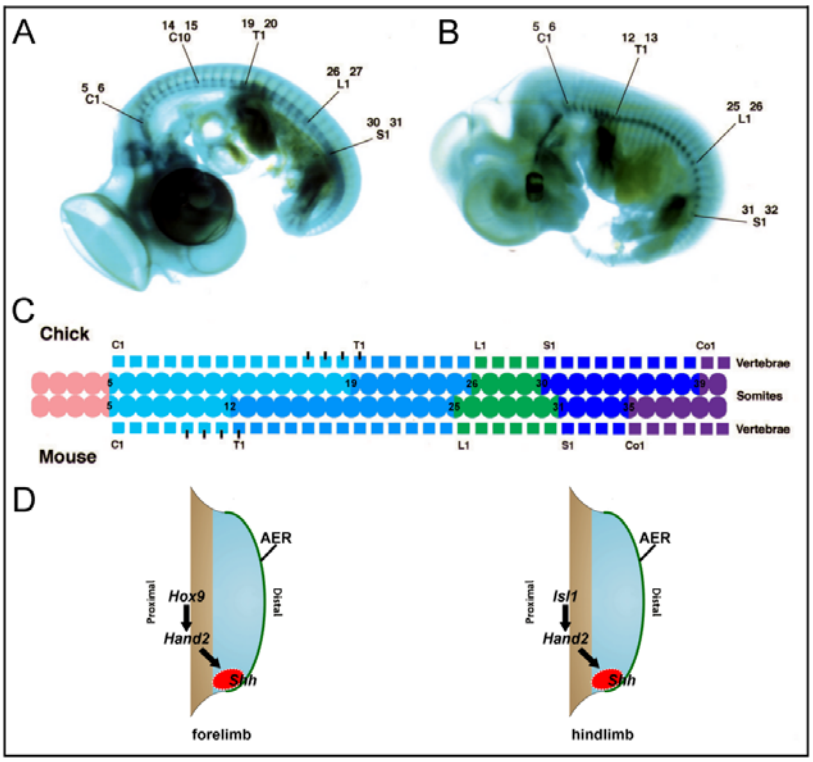

Figure 10. Regional transitions along the AP axis. A-C Axial formulae of chicken and mouse (adapted from Burke et al. 1995). **A** A HH25-26 chick embryo and **B** a E13.5 mouse embryo stained with alcian green and cleared in methyl salycilate. Vertebral numbers are indicated. **C** Schematic representation comparing the axial formulae of chicken and mouse. Black bars represents spinal nerves contributing to the brachial plexus. **D** Schematic representation of limb initiation, summarizing distinct regulatory mechanisms between forelimb and hindlimb (modified from Zeller et al. 2009 after Itou et al. 2012).

Given the importance of Hox genes in AP patterning, these genes have been considered major candidates to control the position of the limbs (reviewed by Capdevila and Izpisúa Belmonte, 2001). However, genetic experiments in the mouse do not seem to support this hypothesis entirely (Van den Akker et al., 2001; Chen et al., 1998; Cohn and Bright, 1999; McIntyre et al., 2007; Rancourt et al., 1995; Wellik and Capecchi, 2003). This raises the possibility that Hox genes

are not major players in setting the position of the limbs along the AP axis. Alternatively, the limb fields could be specified through a combination of Hox genes in the LPM that so far escaped identification (reviewed by Capdevila and Izpisúa Belmonte, 2001).

Specification of the forelimb field seems to be connected with the posterior restriction of the heart field through the activity of RA, which downregulates *Fgf8* expression in the LPM of the zebrafish (Waxman et al., 2008; Zhao et al., 2009). In the mouse, RA produced in the paraxial mesoderm activates *Tbx5* and *Hand2* in the LPM, in addition to upregulating *Hox9* genes in the forelimb field (Mic et al., 2004; Niederreither et al., 2002). Interestingly, the *Tbx5* gene contains regulatory regions that respond to Hox proteins of the paralog groups 4 and 5 (Minguillon et al., 2012). Likewise, the induction of the pectoral fin in zebrafish by RA signaling is mediated by *Hoxb5b* (Grandel and Brand, 2011; Waxman et al., 2008; Zhao et al., 2009). These observations bring back the possibility that Hox genes could be implicated in determining the position of the forelimb bud.

The observation that vertebrates with extended trunks usually exhibit loss of the hindlimbs raises the possibility that the transition from trunk to tail may share a common regulation with the specification of the hindlimbs and cloaca. Indeed, Hox genes have also been suggested to play a role in the positioning of the trunk to tail transition (Burke et al., 1995). Expression analyses in vertebrates with long trunks, such as snakes and caecilians, revealed that activation of Hox genes from paralog groups 10 to 13 was delayed when compared to other vertebrates with shorter trunks (Di-Poï et al., 2010; Woltering et al., 2009). Similar to vertebrates bearing shorter trunks, but not necessarily short bodies (e.g. some lizards), the activation of these

genes first occurred at the axial level corresponding to the end of the trunk (Di-Poï et al., 2010; Woltering et al., 2009). This suggests that Hox genes of these posterior groups, particularly those of the groups 10 and 11, could be involved in setting the position of the trunk to tail transition and, consequently, the hindlimb bud. However, genetic studies in the mouse do not support this hypothesis, since total inactivation of either *Hox10* or *Hox11* genes had no apparent effect on the position of the hindlimbs, despite their strong phenotypic consequences on the axial skeleton (Wellik and Capecchi, 2003). Likewise, ectopic expression of members of these paralog groups or of the *Hox6* group produced major alterations in the axial skeleton without obvious effects on the position of the hindlimbs (Carapuço et al., 2005; Vinagre et al., 2010; Young et al., 2009).

Together, the aforementioned findings raise the question on the role of Hox genes in specifying non-axial structures along the AP axis. The study of Hox function, however, is hampered by the redundancy within members of a paralogous group (Van den Akker et al., 2001; McIntyre et al., 2007; Wellik and Capecchi, 2003). It is still possible, therefore, that alterations in the trunk to tail transition level and in limb position resulting from loss-of-function approaches can only be observed upon the concerted inactivation of all Hox genes involved in such processes, similar to what is observed in the patterning of the axial and limb skeleton. The mechanisms responsible for these changes during mouse development are the focus of this thesis. The existence of mutants in the Gdf11 pathway that exhibit simultaneous alterations in several aspects of axial and non-axial patterning opens the possibility to investigate these mechanisms in conjunction. Moreover, the key

importance of Wnt/*β*-catenin signaling in the posterior growth of the vertebrate embryo is also addressed in this thesis.

Thesis Aims

General Aim

To investigate molecular mechanisms controlling vertebrate axial extension and trunk to tail transition.

Specific Aims

1. To determine the role of Gdf11 signaling on the regional transition from trunk to tail in the mouse;

2. To address the role of Wnt/*β*-catenin signaling during the formation of distinct mesodermal compartments during axial extension;

3. To investigate the mechanisms controlling tail elongation.

Chapter II

GDF11 controls trunk to tail transition by modulating the activity of axial progenitors

adapted from

Jurberg AD, Aires R, Nóvoa A, Mallo M. Switching axial progenitors from producing trunk to tail tissues in vertebrate embryos. *Submitted*

II.1 - Summary

The vertebrate body is made by progressive addition of new tissue from progenitors at the posterior embryonic end. Although this process is continuous, extension through the trunk and tail regions involves different mechanisms, ultimately resulting in the production of internal organs associated with the trunk but not the tail. The transition from trunk to tail is a complex process that combines controlled depletion of the progenitors for intermediate and lateral mesoderm, switch from primitive streak (PS) to tail bud-mediated axial extension and induction of the hindlimbs and cloaca. We show that Gdf11 signaling is a major coordinator of this transition. In the absence of Gdf11 the switch from trunk to tail formation is substantially delayed and precocious activation of this signaling anticipates the trunk to tail transition, bringing the hindlimbs and cloaca next to the forelimbs and leaving extremely shortened trunks. During this process Gdf11 signaling activates *Isl1* in the progenitor cells of the lateral mesoderm, promoting the formation of the hindlimbs and cloaca-associated mesoderm as the product of the terminal differentiation of these progenitors. *Gdf11* also coordinates the repositioning of the bipotent neuromesodermal (N-M) progenitors from the anterior PS and adjacent epiblast to the tail bud, in part by reducing the retinoic acid available to the progenitors. Later, Gdf11 activity is required in the tail bud for the progressive and regulated termination of the main embryonic axis, an activity that might be mediated by *Hox* genes.

II.2 - Background

Vertebrates display a large diversity of body shapes and sizes. Despite such morphological variations, their primary body axis is always

generated from head to tail through a similar principle, consisting of the progressive addition of new tissue at the posterior end of the embryo (reviewed in Stern et al., 2006; Wilson et al., 2009). This process requires a fine balance between the maintenance of progenitor pools and the continuous production of cells that form the different body structures. Cells leaving the axial progenitor pools at different stages during the elongation process execute patterning and differentiation programs that are specific to each particular axial level. This ultimately results in the formation of a properly structured body. Quantitative and qualitative differences in these general processes are the basis of vertebrate body shape diversity. One of the most important components of anterior-posterior (AP) regional variation is the portion of the postcranial body occupied by the neck, trunk, and tail. For instance, the prototypical snake's body has a very long trunk and rather short neck and tail. In contrast, birds exhibit long necks and reduced tails, whereas some lizards have fairly short necks and trunks, but very long tails. Thus, elucidating the mechanisms that control this regional organization is essential to understand the evolution of the vertebrate body plan.

The transition from trunk to tail is one of the key elements in AP organization of the vertebrate body. While the trunk holds most of the vital and reproductive organs, the tail is basically composed of vertebrae and its associated muscles. These differences reflect major changes in developmental mechanisms during axial extension. From an embryological perspective, trunk tissues require an extensive contribution from all three germ layers, including the lateral and intermediate components of the mesoderm, which in concert with the endoderm originate the trunk-associated organs (Carlson, 1999).

Conversely, tail tissues are mostly derived from the paraxial mesoderm and ectoderm. This means that the trunk to tail transition marks the posterior end of the endoderm, as well as of the lateral and intermediate mesoderm. Interestingly, this is associated with the induction of the hindlimb buds from the lateral mesoderm and with the activation of particular molecular programs in the ectoderm, hindgut endoderm, and ventral lateral mesoderm, which result in the production of the embryonic cloaca (Suzuki et al., 2009). The consequences of this embryological feature are still patent in the adult animal as the end of the trunk typically correlates with the position of the cloaca and its derivatives (mostly represented by the caudal end of the digestive, reproductive and excretory systems), and of the hindlimbs, if the animal has them.

The trunk to tail transition is also associated with a switch in the mechanism guiding embryonic axial growth. Trunk formation is driven by a midline structure called the primitive streak (PS), in which ingressing cells from the epiblast generate the embryonic mesoderm and definitive endoderm (Psychoyos and Stern, 1996; Wilson and Beddington, 1996). Conversely, caudal growth during tail formation is associated with the activity of the tail bud (Kanki and Ho, 1997; Schoenwolf, 1977). This change in the mode of axial growth involves the relocation of axial progenitors from the PS and adjacent areas of the epiblast to the caudal neural hinge (CNH) at the posterior end of the tail bud (Cambray and Wilson, 2002, 2007; Wilson and Beddington, 1996). In addition, it reflects the way in which new tissues are formed at the posterior embryonic end. The best documented example is that of neural tube formation (Gofflot et al., 1997; Schoenwolf, 1984). In the trunk, neural tube development relies on primary neurulation, whereby

the neural tube results from the folding of the neural plate. In contrast, spinal cord formation in the tail is made by secondary neurulation, characterized by the formation of a rod-like structure that then hollows to create a tube (Gofflot et al., 1997; Schoenwolf, 1984).

The mechanisms controlling the trunk to tail transition are largely unknown, despite their importance. As for other aspects of AP regional patterning, most of the studies involving differences between the trunk and the tail have focused on their associated skeleton (reviewed by Mallo et al., 2009, 2010; Wellik, 2007). In the adult animal, the trunk typically expands through the thoracic and lumbar segments of the vertebral column, whereas the transition to the tail occurs through the sacrum and the tail itself is comprised by caudal vertebrae. Regional specification of these skeletal segments results from the execution of distinct patterning programs during differentiation of the somitic mesoderm (reviewed by Mallo et al., 2009, 2010; Wellik, 2007). Although coordinated with the networks controlling other aspects of trunk and tail development, these mechanisms mostly operate within the paraxial mesoderm and cannot account for such transition. Indeed, a variety of genetic experiments in the mouse indicate that the embryo can undergo major patterning changes in their axial skeletons with very little or no obvious effects on hallmarks of the trunk to tail transition, such as the position of the hindlimbs (Carapuço et al., 2005; McIntyre et al., 2007; Vinagre et al., 2010; Wellik and Capecchi, 2003). There are a few mutant phenotypes, however, that are suggestive of a simultaneous alteration in several aspects of the trunk to tail transition. Those associated with the inactivation of Gdf11 signaling in mice are particularly interesting, as they produce a global anteriorization of the axial skeleton (Andersson

et al., 2006; Essalmani et al., 2008; McPherron et al., 1999; Oh et al., 2002; Szumska et al., 2008). Mutants for members of this pathway generally present 16-18 thoracic and 7-8 lumbar segments instead of the wild type 13 and 6 vertebrae, respectively. In these mutants, transformations in the axial skeleton are associated with a posterior displacement of the hindlimbs by about 6-8 vertebral units, as well as several abnormalities in the urogenital system (Andersson et al., 2006; Esquela and Lee, 2003; McPherron et al., 1999; Oh et al., 2002; Szumska et al., 2008).

Here, we show that Gdf11 signaling is a major regulator of the trunk to tail transition during vertebrate development. Whereas loss of *Gdf11* delays the specification of the cloaca and the induction of the hindlimbs, precocious activation of Gdf11 signaling in the epiblast using a constitutively active form of its receptor, $Alk5^{CA}$, produces a remarkable anteriorization of these structures, with a concomitant reduction in trunk length. Strikingly, by using different promoters, we show that this activity is required in the axial progenitors of the epiblast and not in the derived mesoderm. We present evidence that the switch from trunk to tail progenitors requires a combination of several processes. These include activation of *Isl1* in the progenitors for the lateral mesoderm, which results in the induction of the hindlimb buds and cloacal tissues. The regulation of *Isl1* expression by Gdf11 signaling seems to be mediated by direct control of a relevant enhancer of *Isl1* that is specifically active during this transition. In addition, Gdf11 signaling is involved in the orderly relocation of the bipotent N-M progenitors from the PS to the tail bud, a process that requires inactivation of retinoic acid signaling. Finally, Gdf11 signaling seems

to be involved in the progressive termination of the tail, an activity likely mediated to some extent by the activation of *Hox11* genes.

II.3 - Results

Loss of Gdf11 delays trunk to tail transition in mice

Gdf11 mutant newborn animals present anterior homeotic transformations along the axial skeleton, with posterior displacement of the hindlimbs by 6 to 8 vertebrae (McPherron et al., 1999). Analysis of these mutants at embryonic day (E)11.5 revealed that the hindlimb buds were indeed more posteriorly located, producing an increased interlimb (trunk) region by 5 or 6 somites when compared to wild type embryos (Fig. 11A,B). At this stage, *Gdf11* mutant hindlimbs were visibly smaller than those of their wild type littermates (Fig. 11A,B), which contrasted with their normal morphology at E18.5 (Fig. 11C,D). Embryonic staging based on hindlimb morphology (Boehm et al., 2011) revealed that the hindlimbs of E10.5 and E11.5 *Gdf11* mutant embryos corresponded to those of younger wild type embryos by about 6 and 17 hours, respectively (Fig. 11E). This observation raised the possibility that hindlimb specification is delayed in *Gdf11* mutant embryos. Consistent with this hypothesis, analysis of *Tbx4* expression, an early hindlimb marker (Gibson-Brown et al., 1996), revealed that the hindlimb fields were first identified at an axial level 5-6 somites more posterior in *Gdf11* mutants than in wild type embryos (Fig. 11F,G). These results suggest that *Gdf11* is involved in establishing the position at which the hindlimb is induced along the AP axis.

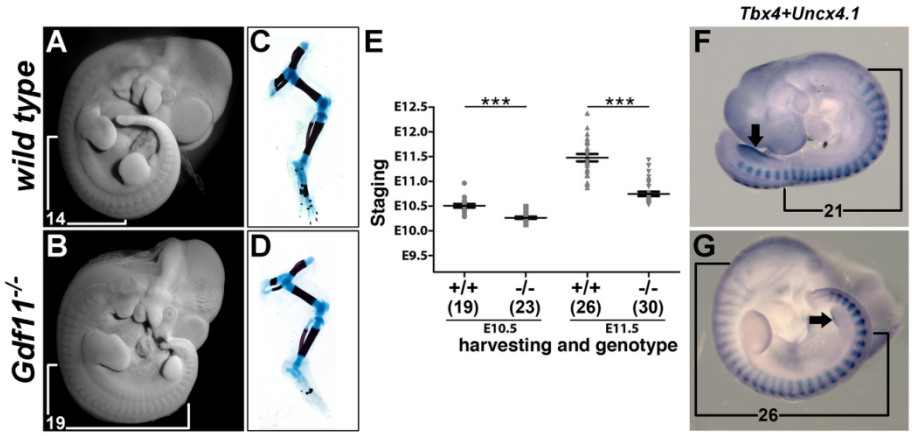

Figure 11. Delayed hindlimd development in *Gdf11* mutants. A,B Gross morphology of representative wild type and *Gdf11* mutant embryos at E11.5. The smaller size of the hindlimb was evident in the mutants. Somite counting in the interlimb region is indicated. **C,D** Hindlimb skeletons of E18.5 wild type and *Gdf11* mutant fetuses revealed normal morphology in the mutants. **E** Estimation of embryonic age of E10.5 and E11.5 wild type and *Gdf11*$^{-/-}$ embryos according to the size of the hindlimbs. The data are reported as mean ± SEM. ***, P<0.0001. **F,G** Identification of hindlimb induction (evidenced by *Tbx4*, *arrows*) with respect to somite number (evidenced by *Uncx4.1*) at E10.0. Hindlimbs are induced at the level of somite 21 and 26, respectively.

Given the correlation between the hindlimbs and the trunk to tail transition, the above results raise the possibility that Gdf11 signaling plays a fundamental role in setting this transition. Consistent with this, other hallmarks of the trunk to tail transition were also posteriorly displaced in *Gdf11* mutants, compared with wild type littermates. In particular, we examined both endodermal (*Shh* and *Fgf8* expression) (Fig. 12A-D) and mesodermal (*Isl1* and *Raldh2* expression) (Fig. 12E-H) components of the developing cloaca. In *Gdf11* mutants, these markers were expressed next to the posterior end of the hindlimb buds, similar to what was observed in wild type embryos, revealing that the primordium of the cloaca was also located at a more posterior absolute axial level. In addition to the posterior displacement of the hindlimb buds and the cloaca, formation of other tissues and structures typically associated with the trunk was caudally extended in *Gdf11* mutant embryos. For instance, expression of *Raldh2* and *Pax2* revealed

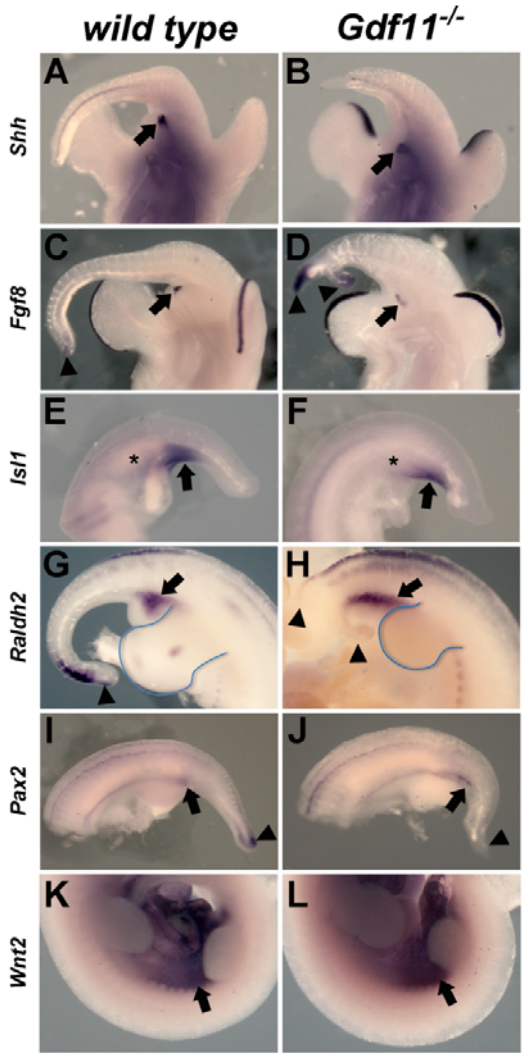

Figure 12. Posterior displacement of the trunk to tail transition in *Gdf11* mutants. Whole-mount *in situ* hybridization of wild type (A,C,E,G,I,K) and *Gdf11* mutant embryos (B,D,F,H,J,L). **A,B** Endodermal component of the cloaca (*arrows*) evidenced by *Shh* expression at E11.5. **C,D** Cloacal and urethral epithelium is revealed by *Fgf8* expression (*arrows*) at E11.5. *Gdf11* mutants exhibited increased expression of *Fgf8* in the tail bud (*arrowheads*). **E,F** Mesodermal component of the cloaca evidenced by *Isl1* expression at E10.0. * marks the site of hindlimb outgrowth. **G,H** *Raldh2* expression revealed an extended mesodermal component of the developing cloaca (*arrows*) at E11.5. Mutants also exhibited altered expression in the tail (*arrowheads*). **I,J** Extended formation of intermediate mesoderm as identified by *Pax2* expression (*arrows*) at E10.5. Downregulation of *Pax2* expression was also observed in the tail of the mutants (*arrowheads*). **K,L** Visceral lateral mesoderm revealed by *Wnt2* expression (*arrows*) at E11.5.

a posterior elongation of the intermediate mesoderm, which is the precursor of the urogenital tract (Fig. 12G-J). Similarly, the visceral

lateral mesoderm extended to more caudal levels, as evidenced by the expression of *Wnt2* (Fig. 12K,L). Altogether, these results show that the trunk to tail transition was posteriorly displaced in *Gdf11* mutants and that this was associated with a concomitant extension of trunk-associated tissues to cover the body up to the cloacal level. They also indicate that the alterations observed in the axial skeleton of these mutants (McPherron et al., 1999) are just one manifestation of a more global deregulation of AP patterning processes.

Alk5 activation in the epiblast anteriorizes the trunk to tail transition

To explore whether *Gdf11* signaling is able to dominantly control the trunk to tail transition, we took a gain of function approach in mouse embryos. Genetic and biochemical experiments revealed that Gdf11 first binds Acvr2b to form a complex that then activates Alk5 (also known as Tgfbr1) to initiate a signaling cascade mediated by Smad2 (Andersson et al., 2006; Ho et al., 2010; Liu, 2006; Oh et al., 2002). Accordingly, it has been suggested that the start of *Gdf11* functional activity is determined by Alk5 availability, which in axial tissues seems to start at around E9.0 (Andersson et al., 2006). Therefore, for our gain of function experiments we produced transgenic embryos expressing a constitutively active version of *Alk5* (*Alk5*^{CA}), which signals independently of the ligand (Charng et al., 1996; Wieser et al., 1995).

We first expressed *Alk5*^{CA} using an enhancer element of the *Cdx2* gene (*Cdx2P-Alk5*^{CA} transgenics), which is active from E7.5 in the posterior part of the embryo, including the caudal lateral epiblast (CLE) and the PS (Benahmed et al., 2008; Gaunt et al., 2005). *Cdx2P-Alk5*^{CA} embryos exhibited strong phenotypes affecting posterior embryonic growth, which could be classified in two groups. The most

severe phenotypes included a drastic axial truncation leaving very little tissue posterior to the forelimbs (see below). This phenotype did not permit the analysis of patterning processes in the trunk region of these embryos. Another group of *Cdx2P-Alk5*^{CA} embryos, however, exhibited milder phenotypes, extending their AP axis beyond the forelimb bud level. These embryos had short bodies but contained clearly recognizable hindlimbs and tails, and preserved fairly normal overall regional organization (Fig. 13). Interestingly, their hindlimbs were located very close to the forelimbs, leaving extremely short trunks spanning 0-6 misshapen somites in contrast to the typical 12-13 somites observed in wild type E10.5 embryos (Fig. 13). The position of the anteriorized hindlimbs was often asymmetric and in one transgenic embryo the hindlimb buds were duplicated. In these embryos the cloaca also developed in a more anterior location, maintaining its relative anatomical position with respect to the hindlimbs (Fig. 13). Globally, these phenotypes were essentially the opposite to those observed in *Gdf11* mutant embryos, thus reinforcing the important role of Gdf11/Alk5 signaling in establishing the position of the trunk to tail transition. However, we were not able to recover any affected *Cdx2P-Alk5*^{CA} transgenic at a stage that allowed direct evaluation of AP patterns in the axial skeleton. The anterior expression boundaries of *Hoxa9* and *Hoxc10* at E10.5 were anteriorized to maintain their position relative to the hindlimb bud, indicating altered AP patterns in the paraxial mesoderm and neural tube (Fig. 13I-L). This observation is consistent with previous Gdf11 gain of function experiments in chicken embryos (Liu, 2006). Altogether, these results indicate the existence of a global and coordinated posteriorization of the body plan of *Cdx2P-Alk5*^{CA} transgenic embryos that involves tissues from all germ layers.

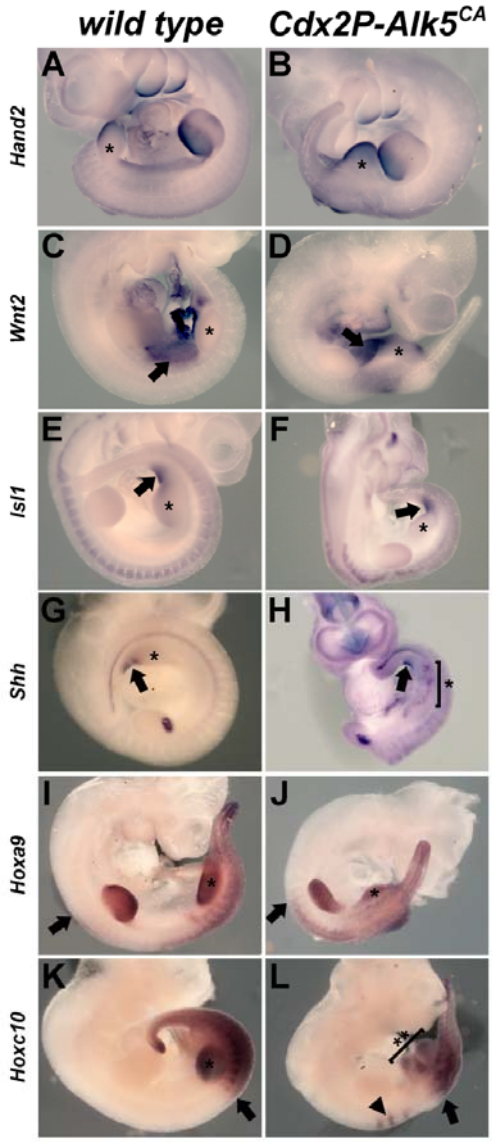

Figure 13. Anteriorization of the trunk to tail transition in *Cdx2P-Alk5^{CA}* transgenic embryos. Analysis of different aspects of AP patterning in E10.5 wild type (A,C,E,G,I,K) and *Cdx2P-Alk5^{CA}* (B,D,F,H,J,L) embryos. * indicates the hindlimbs. **A,B** Lateral mesoderm and hindlimbs evidenced by *Hand2* expression. **C,D** Visceral lateral mesoderm evidenced by *Wnt2* expression (*arrows*). **E,F** Mesodermal component of the cloaca evidenced by *Isl1* expression (*arrows*). **G,H** Endodermal component of the cloaca by *Shh* expression (*arrows*). Trangenics exhibited diffused expression of *Shh* in the hindlimbs (*bracket*). **I,J** Expression of *Hoxa9*. *Arrows* mark the anterior limit of expression in the neural tube. **K,L** Expression of *Hoxc10*. *Arrows* mark the anterior limit of expression. *Arrowhead* indicates ectopic expression in the neural tube in the transgenics. The *bracket* indicates a duplicated hindlimb.

It has been reported that the *Cdx2* enhancer used in these experiments is active in both the axial progenitor-containing posterior epiblast and in the underlying mesodermal compartments (Benahmed et al., 2008). To evaluate if the phenotypes observed in the *Cdx2P-Alk5*^{CA} transgenics derived from Alk5 activity in the epiblast or in the mesodermal compartments, we overexpressed *Alk5*^{CA} in the paraxial mesoderm using the *Dll1*-msd enhancer (Beckers et al., 2000) and in the lateral mesoderm using a *Hoxb6* enhancer (Becker et al., 1996). We could not identify any abnormality in any of these transgenics (n=21 and n=22, respectively), indicating that the phenotypes observed in *Cdx2P-Alk5*^{CA} transgenics are most probably derived from the activation of Alk5 signaling in the epiblast and not in the derived mesodermal compartments.

Taken together, our results indicate that Gdf11/Alk5 signaling is a key modulator of the transition from trunk to tail in the mouse. In addition, they show that this signaling is required in the epiblast and it is therefore very probable that it primarily acts on the axial progenitors. This suggests that Gdf11 signaling might be involved in the modulation of the different functional changes in these progenitors driving their switch from making trunk to tail tissues.

Altered tail bud organization in Gdf11 mutant embryos

A typical characteristic of *Gdf11* mutant skeletons is their truncation at the sacral/caudal level (McPherron et al., 1999). In midgestation embryos, we found that the tails of *Gdf11* mutant embryos exhibited variable phenotypes, typically being distally thinner than in wild type embryos and duplicated in a proportion of them (Fig. 14). The presence of somites in both dorsal an ventral regions of the duplicated tails led us

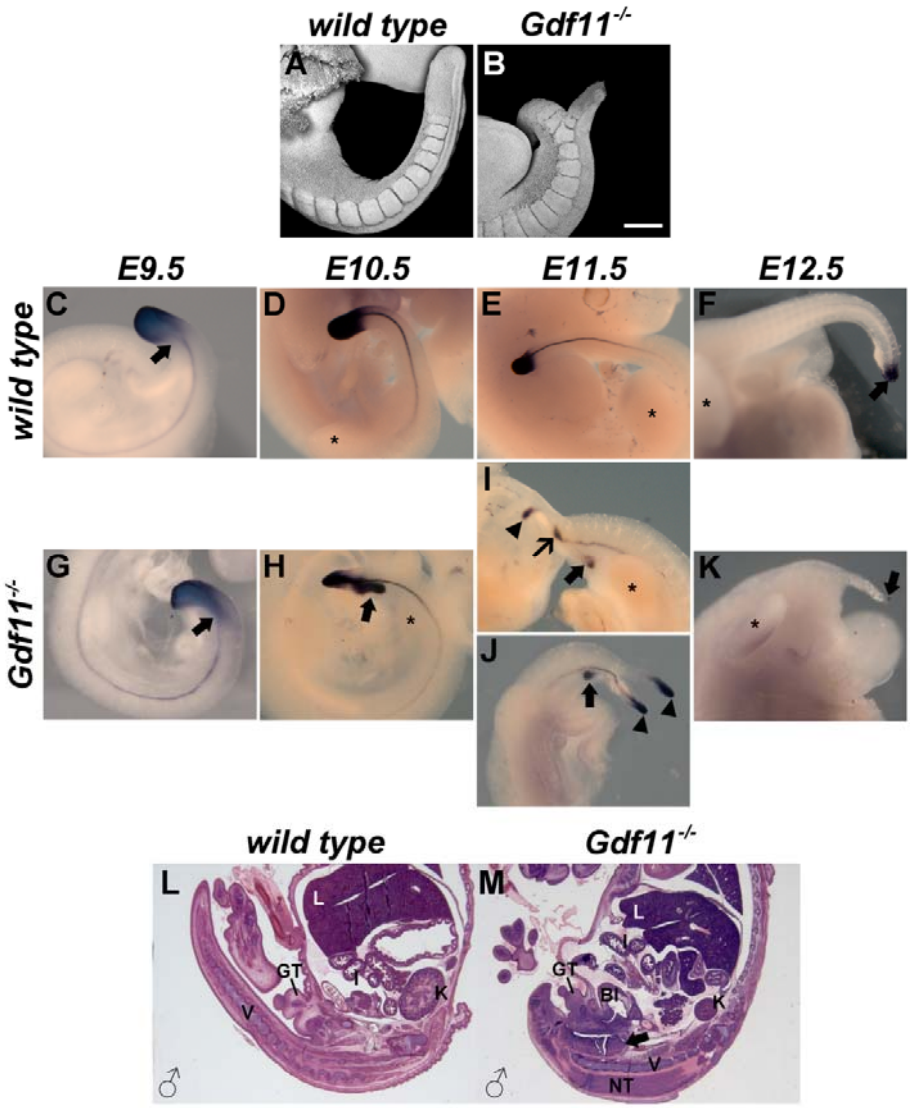

Figure 14. Abnormal tail growth in *Gdf11* mutants. A,B Tail morphology of E10.5 embryos observed by confocal microscopy. Note the somites in both sides of the split tail in mutants. *scale bar* = 200 µm. **C-K** Whole-mount *in situ* hybridization for *T* (Brachyury) in wild type (**C-F**) and *Gdf11* mutant embryos (**G-K**). *Arrows* and *arrowheads* indicate abnormal *T* expression in mutant tails. * marks hindlimb position. **L,M** Sagittal sections of the posterior region of wild type and *Gdf11* mutant fetuses at E15.5. The *arrow* indicates the ectopic neural tissue ventral to the vertebral column in the mutants. *V* vertebral column; *NT* neural tube; *Bl* bladder; *K* kidney; *L* liver; *I* intestine; *GT* genital tubercle.

to further examine tail growth in *Gdf11* mutants. Expression of the nascent mesoderm marker *T* (Brachyury) revealed deviations from the normal expression pattern already at E9.5, during the trunk to tail

transition when the mutant phenotype was still not morphologically evident. Transcripts for this gene were distributed in a broader domain that extended anteriorly through the prospective tail tip of *Gdf11*$^{-/-}$ embryos (Fig. 14C,G). This broadening was progressively resolved into a distinct domain, which appeared to segregate by E10.5 (Fig. 14D,H). In these embryos, distal thinning of the tail bud started to become evident. At E11.5 we could observe two or three distinct *T*-positive domains along the ventral side of the tails of *Gdf11* mutants, from their tip to the posterior border of the hindlimb buds, even in embryos without split tails (Fig. 14E,I). In embryos with split tails, *T* was expressed at both tail tips (Fig. 14J). Interestingly, in all *Gdf11*$^{-/-}$ embryos analyzed at E11.5 we found an ectopic *T*-expression domain located next to the hindlimbs, regardless of whether or not their tails were split (Fig. 14E,I,J). Surprisingly, although these cells were positive for *T*, we could not identify ectopic formation of mesodermal tissues in the caudal end of the *Gdf11* mutants. At E12.5, mutant tails were very thin and *T* expression was very weak in the tail tip(s). The ventral pool of *T*-positive cells was no longer observed (Fig. 14F,K). Instead, we observed ectopic neural tissue ventrally located outside the vertebral column at later stages (Fig. 14L,M), which is consistent with previous analysis of both *Gdf11* and *Pcsk5* mutant embryos (Szumska et al., 2008). These findings led us to hypothesize that the *T*-positive cells that failed to become incorporated into the CNH may comprise bipotent N-M axial progenitors that subsequently differentiated into neural tissue. Accordingly, it has been recently established that the bipotent N-M progenitors in the tail bud take a neural fate in the absence of Wnt3a activity (Martin and Kimelman, 2012; Takemoto et al., 2011).

To address this hypothesis, we examined a number of other genes that have been previously associated with the posterior growth of the tail. In general, the expression patterns observed in *Gdf11* mutant tails suggest a splitting of the posterior organizing area (Fig. 12C,D,G,H, 14 and 15). In particular, we found ventral expression of the neural progenitor marker *Sox2* (Fig. 15A-D) and expanded expression of *Foxa2* in the tails of the mutants (Fig. 15E-H). *Fgf8* expression was upregulated in the tail tip(s) and in the AER of the hindlimbs, which could also be consequence of the growth delay of mutant hindlimbs (Fig. 12C,D). Conversely, *Wnt3a* and *Mesp2* expression were downregulated in the mutants (Fig. 15I-P). Their levels of expression were higher in the ventral region than in the dorsal part in mutants bearing split tails (Fig. 15I-P). In turn, *Uncx4.1* expression seemed unaltered, except by a condensed ectopic domain at the tail tip of the mutants (Fig. 15Q-T). *Cdx2* expression exhibited a ventral compact domain in the mutants at E10.5 (Fig. 16A-D), which seemed to correlate with the abnormal accumulation of blood from E10.5 onwards (Fig. 16E-H). As a consequence, the dorsal region of mutant tails became gradually deprived of blood vessels and tails truncate due to increased apoptosis at later stages (Fig. 16I-L). No other tested marker labeled the *T*-positive cells that lagged behind during tail growth of *Gdf11* mutants (Fig. 15).

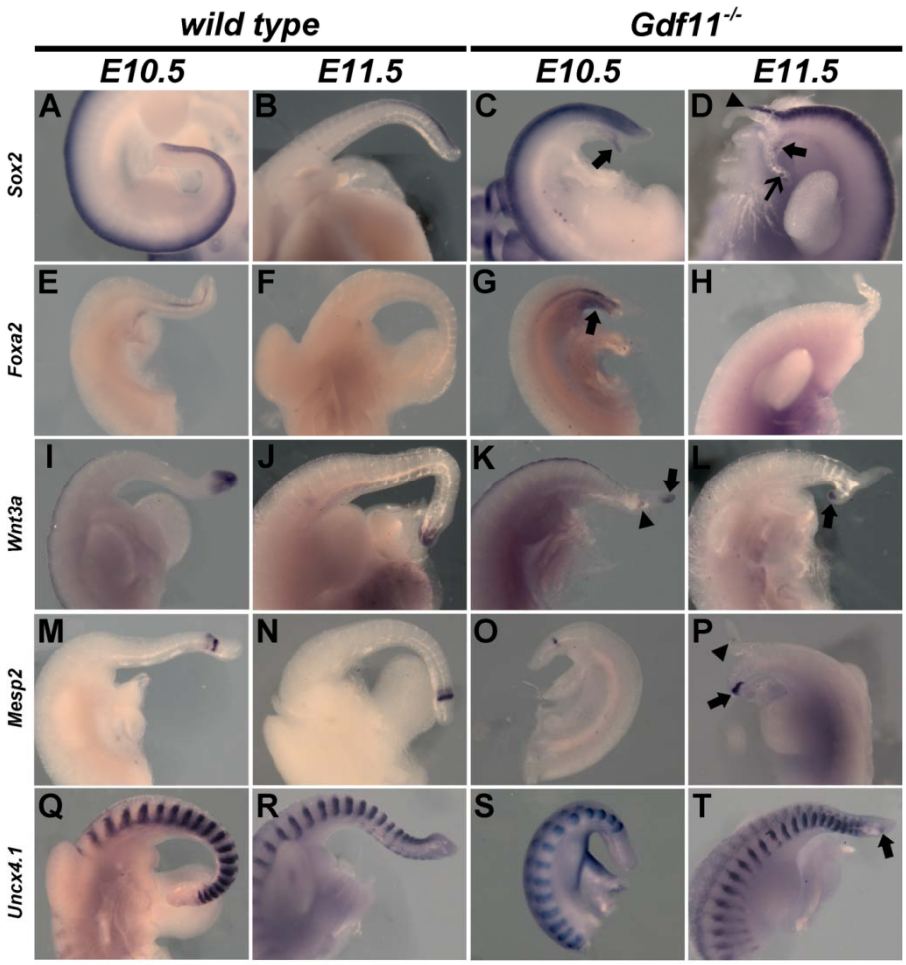

Figure 15. Abnormal tail bud organization in *Gdf11* mutants. Whole-mount *in situ* hybridization of wild type (A,B,E,F,I,J,M,N,Q,R) and *Gdf11* mutant embryos (C,D,G,H,K,L,O,P,S,T). **A-D** *Sox2* expression revealed ectopic neural progenitors in the ventral region of mutant tails (*arrows*). *Arrowhead* indicates anteriorization of the dorsal domain of expression. **E-H** Expansion of the *Foxa2* expression domain in *Gdf11* mutants at E10.5 (*arrow*). **I-L** Downregulation of *Wnt3a* expression in *Gdf11* mutants (*arrows*). *Arrowhead* indicates an ectopic domain. **M-P** Altered *Mesp2* expression in *Gdf11* mutants. *Arrowhead* indicates a faint domain in the dorsal split tail, whereas the ventral split tail exhibits fairly normal expression (*arrow*). Compare with *Wnt3a in situ* hybridization. **Q-T** *Uncx4.1* expression revealed unaltered somites, except by an ectopic expression domain in the tail tip of mutants at E11.5 (*arrow*).

Altogether, our findings are consistent with an abnormal transition from the PS to CNH in the absence of Gdf11 activity. Loss of *Gdf11* seems to affect the behavior of axial progenitors during the establishment of the CNH. Thus, cells that are normally fated to take part of the tail bud becomes split into several domains along the tail.

This results in ectopic expression of various genes involved in tail growth and we hypothesize that the split might result from the number (or specific characteristics) of progenitors trapped halfway through the tail. If the number is large enough, a ventral budding generates another tail. In turn, ectopic expression of *Cdx2* at E10.5 may underlie the abnormal formation of blood vessels, that ultimately results in tail truncation due to increased cell death. This finding is in agreement with the observation that *Cdx* genes induce posterior lateral plate mesoderm for hematopoietic differentiation (reviewed by Lengerke and Daley, 2012).

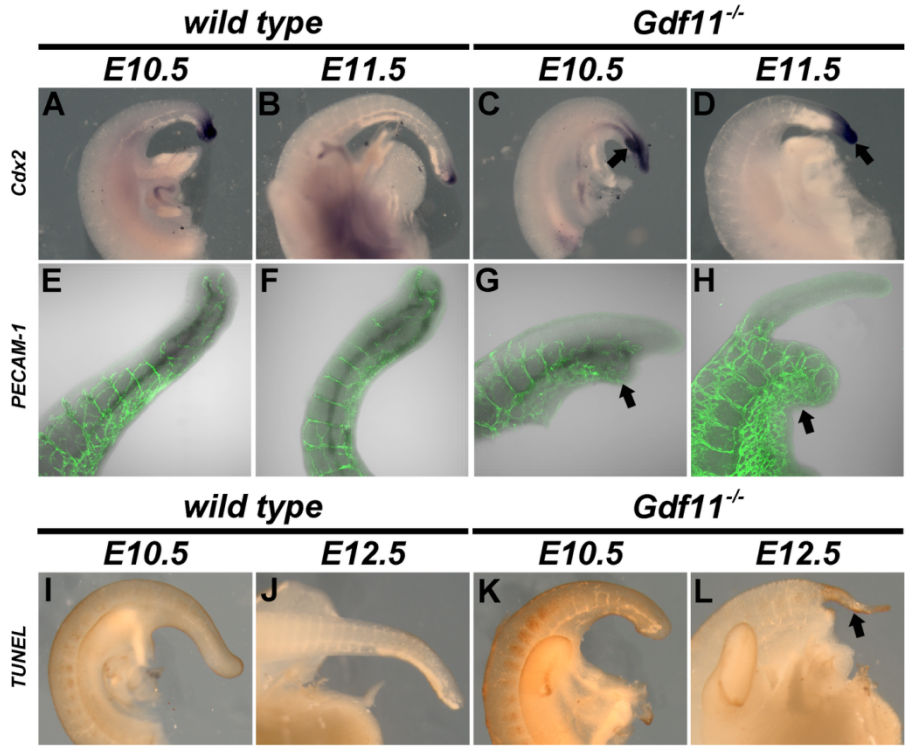

Figure 16. Abnormal blood vessel formation and tail truncation in *Gdf11* mutants. A-D Whole-mount *in situ* hybridization for *Cdx2* in wild type (A,B) and *Gdf11* mutant embryos (C,D) revealed an ectopic domain of expression in mutant tails at E10.5, that disappeared at E11.5 (*arrows*). Note upregulation of *Cdx2* expression in the mutants. **E-H** Whole-mount immunostaining for PECAM-1 evidenced a ventral increase in blood vessels at the ventral region and an impairment in vascularization at the dorsal region of mutant tails (*arrows*). **I-L** Increased cell death in *Gdf11* mutants at E12.5 as evidenced by TUNEL reactions (*arrow*).

Gdf11 is required to reduce RA levels during the transition from PS to CNH

It has been reported that the tail truncation of *Gdf11*$^{-/-}$ fetuses can be partially rescued by pharmacological inhibition of retinoic acid (RA) signaling at E8.5 and E9.5 (Lee et al., 2010). This timing of treatment fits with the PS to CNH transition, which raises the possibility that the tail rescue may have resulted from the recovery of this process. To test this possibility, we analyzed how treatment with the RA inhibitor AGN193109 affects tail bud development in *Gdf11* mutants. We found that increasing the treatment period in one day by starting at E7.5 improved tail morphology (Fig. 17A,B,D), but affected head development in the mutants (not shown). Notwithstanding some degree of variability (probably resulting from different efficiencies of the treatment), the tails of these embryos at E10.5 were consistently longer and thicker than those of untreated *Gdf11*$^{-/-}$ embryos, some of them resembling the tails of wild type embryos (Fig. 17A,B,D). In addition, we did not find any embryo with a split tail. *T* expression in the caudal end of these embryos also showed some variability but in most embryos it was restricted to the tail tip without ectopic *T*-expressing domains (Fig. 17D). Consistent with these results, we found that wild type embryos expressed the RARγ in a condensed domain in the tail, which seemed to localize with the CNH region within the tail bud. Conversely, *Gdf11* mutants exhibited spread expression of RARγ in the tail bud (Fig. 17E-H), suggesting that CNH cells were disorganized. Together, these findings indicate that inhibition of RA signaling produces a significant reversion of the abnormalities observed in the PS to CNH transition typically observed in *Gdf11* mutants, placing RA

signaling as a key element causing the abnormal behavior of axial progenitors in *Gdf11* mutant embryos.

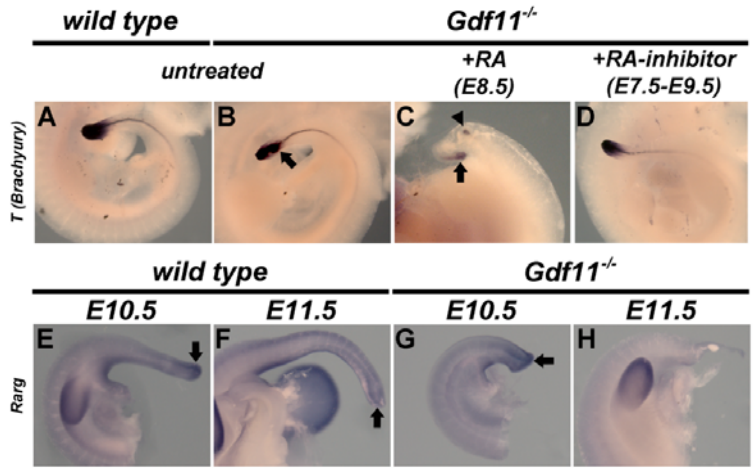

Figure 17. Impact of RA signaling on *Gdf11* mutant tails. Whole-mount *in situ* hybridization of wild type (A,E,F) and *Gdf11* mutant embryos (B-D,G,H). **A-D** Expression of *T* in untreated wild type (**A**) and *Gdf11* mutant (**B**) embryos, as well as in RA-treated (**C**) and RA-inhibitor-treated (**D**) *Gdf11* mutant embryos. *Arrows* and *arrowhead* show ectopic *T* domains. Note the rescue of *T* expression in **D**. **E-H** *Rarg* expression in the tail bud of wild type embryos (**E,F**) revealed a condensed domain in the CNH (*arrows*). Mutant embryos exhibited an enlarged domain of expression at E10.5 (*arrow* in **G**) and absence expression at E11.5 (**H**) due to tail truncation.

To further explore this hypothesis, we performed the complementary experiment and analyzed the effect of increased RA levels on the axial progenitors of *Gdf11*$^{-/-}$ embryos at the time of the PS to CNH transition. At E11.5, RA-treated mutant embryos had variable tail malformations that were always stronger than those observed in non-treated *Gdf11* mutant embryos (Fig. 17C). Tail morphologies varied from hair-like shapes to the complete absence of the tail posterior to the hindlimbs, which fit with the stronger skeletal truncations described for *Gdf11* mutants after similar treatments (Lee et al., 2010). *T* expression in the posterior part of these embryos was mostly restricted to the ectopic ventral domain, while expression in the remaining tail tip was severely reduced (Fig. 17C). It should be noted

that the low RA concentrations used in these experiments had no detectable effect on wild type embryos. Only higher concentrations of RA produce a similar effect on these embryos (Kessel, 1992). This indicates that *Gdf11* mutants exhibit an increased sensitivity to RA. The effects that exogenous modulation of RA signaling has on the axial progenitors of *Gdf11* mutants are consistent with the idea that the distribution of progenitors between the tail tip and the ectopic domains depends on RA signaling. Furthermore, these effects suggest that appropriate PS to CNH transition requires complete block of RA signaling in these progenitors. These results reinforce the interpretation that the truncated tail phenotypes observed in *Gdf11* mutants are, at least to some extent, the result of a failure to undergo proper PS to CNH transition.

Because the strength of the *Gdf11*$^{-/-}$ axial progenitor phenotype can be altered by exogenous modulation of RA levels, it is probable that Gdf11 signaling is required to adjust the amount of available RA at the posterior embryonic end. Considering the essential role of *Cyp26a1* in RA degradation (Abu-Abed et al., 2001; Sakai et al., 2001), a possible mechanism for RA signaling control by Gdf11 activity is to regulate the expression levels of *Cyp26a1* during the trunk to tail transition. Consistent with this, at the time of the PS to CNH transition, *Cyp26a1* expression levels were reduced in the posterior end of *Gdf11* mutant embryos (Fig. 18A,B). This could be the origin of an uneven RA distribution along the AP axis, which would eventually result in the exposure of progenitor pools to critical levels of RA during the PS to CNH relocation. At later stages, however, *Cyp26a1* expression levels were higher in the mutants, mainly in the dorsal region of the tail (Fig. 18C-F). Since *Cyp26a1* expression is induced by RA (White et al.,

1996), this later upregulation may represent a response to compensate high levels of RA and protect the bipotent N-M progenitors in the tail bud.

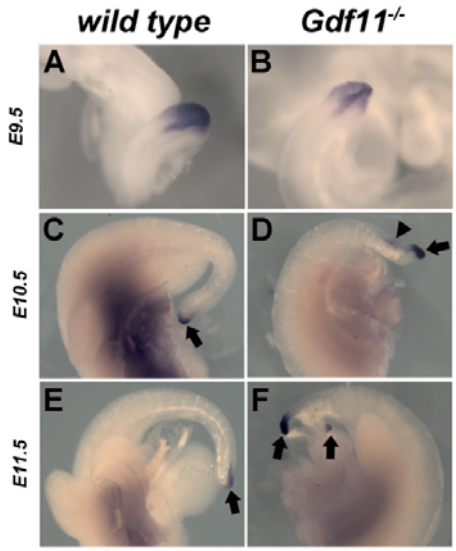

Figure 18. *Cyp26a1* expression in *Gdf11* mutants. Whole-mount *in situ* hybridization of wild type (A,C,E) and *Gdf11* mutant embryos (B,D,F). **A,B** Decreased *Cyp26a1* expression at equivalent stages of the trunk to tail transition (21 somites for wild type, 27 somites for *Gdf11*$^{-/-}$ embryos). **C,D** Partial retention of *Cyp26a1*-positive cells in the dorsal region of mutant tails at E10.5 (*arrowhead*). Cells that remain in the tip seem to increase *Cyp26a1* expression (*arrow*). **E,F** Splitting of the tail in the mutants segregates the *Cyp26a1* domain (*arrows*). Note increased levels of *Cyp26a1* expression in comparison with the wild type littermate.

Hox genes do not play a major role in establishing the AP position of the hindlimb

The above results show that RA plays a role in *Gdf11* function controlling the PS to CNH transition. However, inhibition of RA signaling had no or only minor effects on other aspects of the *Gdf11* mutant phenotype, including the axial formula and the hindlimb position (not shown) (Lee et al., 2010). This indicates that Gdf11 signaling controls the axial position of the trunk to tail transition and the proper formation of the CNH through different mechanisms.

The alterations in the axial formula can be explained by abnormal Hox gene expression in the paraxial mesoderm (Fig. 19A-F) (McPherron et al., 1999; Szumska et al., 2008). It is not clear, however, how Gdf11 signaling controls the changes related to the lateral mesoderm during trunk to tail transition that lead to the induction of structures such as the hindlimb buds. Analysis of *Hoxa9* and *Hoxc10* expression in both *Gdf11* mutant and *Cdx2P-Alk5*^{CA} transgenic embryos showed that their activation followed the altered position of the hindlimbs (Figs. 13I-L and 19A-F), suggesting that Hox genes could control AP patterning in the lateral mesoderm during the trunk to tail transition. A few mutant phenotypes including genes of the *Hox9*, *Hox10* and *Hox11* groups have been reported to include a slight posterior displacement of their hindlimbs (Favier et al., 1996; McIntyre et al., 2007), but they seem too mild to support a major role for Hox genes in this process. To understand if the absence of stronger phenotypes resulted from functional redundancies (as observed for other Hox-dependent processes) we took a gain of function approach by precociously expressing the Hox genes of these paralogs in transgenic embryos. Only transgenics expressing a gene of the *Hox9* group (*Hoxb9*) in the epiblast showed a slight, yet consistent, anterior displacement of the hindlimbs by one segmental unit (1 somite at E10.5, which was translated into 5 instead of 6 lumbar vertebra at E18.5) (Fig. 19G-J). However, no obvious alterations in the hindlimb position were detected when *Hoxa10, Hoxc10*, or *Hoxa11* were used in similar experiments. Also, combined expression of different Hox genes did not change the phenotypes obtained with individual Hox genes (not shown). Therefore, the results from both gain and loss of function approaches are not supportive of a major role of Hox genes in

specifying the hindlimb position along the AP axis during trunk to tail transition.

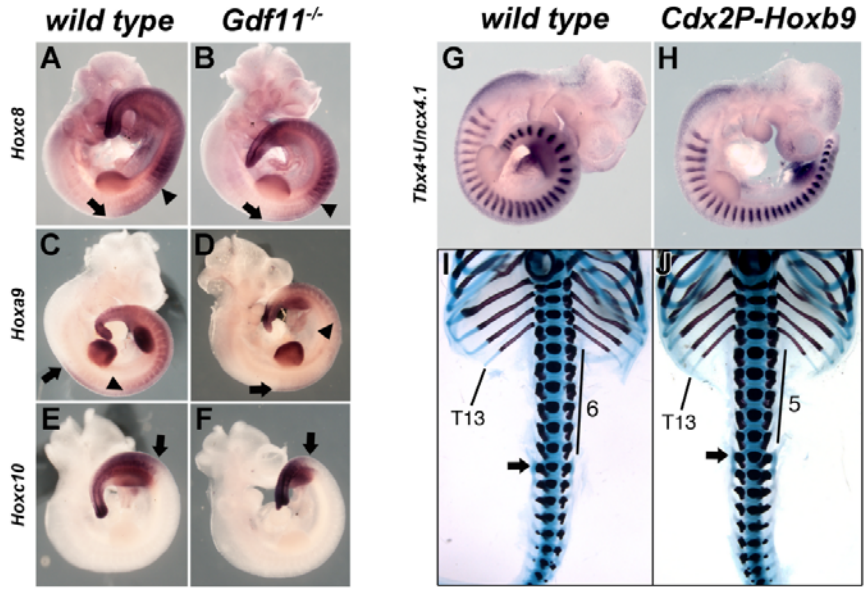

Figure 19. Positioning of the hindlimbs is not strongly affected by Hox genes. Whole-mount *in situ* hybridization of wild type (A,C,E,G) and *Gdf11* mutant embryos (B,D,F) or *Cdx2P-Hoxb9* transgenics (H). **A-F** Analysis of Hox gene expression at E10.5. **A,B** *Hoxc8*. **C,D** *Hoxa9* **E,F** *Hoxc10*. *Arrows* and *arrowheads* mark the anterior border of expression in the neural tube and paraxial mesoderm, respectively. In (E,F) they are coincident. **G-J** Effect of *Hoxb9* on the trunk to tail transition. **G,H** The position of the hindlimb (evidenced by *Tbx4*) was analyzed in relation to somite number (evidenced by *Uncx4.1*) in E10.5 wild type (**G**) and *Cdx2P-Hoxb9* (**H**) embryos. Representative wild type and transgenic embryos exhibited interlimb regions with 12 and 11 somites, respectively. **I,J** Skeletal analysis of wild type (**I**) and *Cdx2P-Hoxb9* (**J**) fetuses at E18.5. The number of the last rib-containing vertebra (T13), the number of lumbar vertebra and the position of the first sacral vertebra (*arrow*) are indicated.

Isl1 *organizes the terminal differentiation of lateral mesoderm progenitors during trunk to tail transition*

Given the relatively minor effect of Hox genes on positioning the hindlimb, we investigated other factors that could mediate hindlimb induction by Gdf11 during the trunk to tail transition. We noticed that both *Hand2* and *Shh* expression in the hindlimbs of *Cdx2P-Alk5*^{CA} transgenics was not restricted to the posterior mesenchyme, but extended into more anterior areas of the hindlimb bud (Figs. 13A,B,G,H and 20A,B). *Isl1* has been shown to control a *Shh/Hand2*

network associated with hindlimb induction (Itou et al., 2012). This observation, together with cell tracing studies showing that this gene is specifically activated in the lateral mesoderm associated with the hindlimb and ventral lateral mesoderm (Yang et al., 2006), in addition to genetic experiments indicating that it is involved in early stages of hindlimb induction (Itou et al., 2012; Kawakami et al., 2011), suggest a possible role for *Isl1* in patterning the lateral mesoderm during trunk to tail transition downstream of Gdf11 signaling. To test this possibility we first expressed this gene using the *Cdx2P* enhancer in transgenic embryos (*Cdx2P-Isl1* transgenics). Although the observed phenotypes varied in intensity, these transgenics typically exhibited a more anterior position of the hindlimbs (Figs. 20C-H and 21A,B), which at E10.5 could reach a position up to 6-8 somites away from the forelimb buds (Fig. 20E-F). In contrast to what we observed in *Cdx2P-Alk5*^{CA} transgenics, the anteriorized position of the hindlimbs in *Cdx2P-Isl1* transgenics was associated with a truncation of the tail bud already evident at E10.5 (Fig. 20G-H'). At E18.5, this was reflected in the complete truncation after the 8th thoracic vertebra affecting both the axial skeleton and the neural tube (Fig. 21A-C,F). However, these fetuses had hindlimbs with strikingly normal skeletal morphology, which were "floating" within the soft tissue adjacent to the caudal end of the truncated axial skeleton (Fig. 21A,B). In addition, the digestive and excretory systems of *Cdx2P-Isl1* transgenics had an organized opening to the exterior (Fig. 21D,G), although the urethra and rectum shared a common end (Fig. 21D,G). They also had recognizable external genitalia (Fig. 21D,G) and fully developed kidneys (Fig. 21E,H). In contrast, we could not identify any sign of the gonads. These results indicate that the structures derived from the areas that are

normally associated with *Isl1*-positive tissues (*e.g.* the most caudal parts of the lateral and of the intermediate mesoderm) were largely not affected by the precocious activation of *Isl1* in the epiblast. Areas that are normally not in contact with *Isl1* activity, however, like the paraxial mesoderm, neural tube, and more anterior areas of the intermediate mesoderm (*e.g.* those forming the gonads) were strongly affected by expression of *Isl1*.

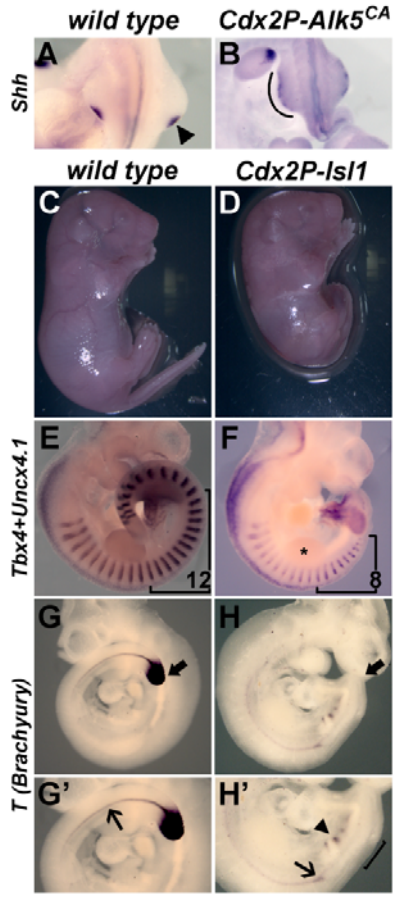

Figure 20. Overexpression of *Isl1* in the epiblast affects the trunk to tail transition. A,B Whole-mount *in situ* hybridization for *Shh* expression in wild type (A) and *Cdx2P-Alk5*^{CA} transgenic (B) embryos at E10.5. **C,D** Gross morphology of wild type (**C**) and *Cdx2P-Isl1* transgenic (**D**) fetuses at E18.5 revealed shortening of the AP axis with eventual truncation of the tail. **E-H'** Whole-mount *in situ* hybridization of wild type (E,G,G') and *Cdx2P-Isl1* transgenic embryos (F,H,H') at E10.5. **E,F** Identification of hindlimb induction (evidenced by *Tbx4*) with respect to somite number (evidenced by *Uncx4.1*). Interlimb somite numbers are indicated in representative wild type and *Cdx2P-Isl1* embryos. * marks the position of the forelimb in the transgenics. **G,H'** Disruption of posterior notochord (*thin arrow*) and abnormal tail bud organization (*thick arrow*) in the transgenics as revealed by *T* expression. *Bracket* marks hindlimb position, which is located 6 somites posterior to the forelimb bud in this embryo. *Arrowhead* indicates ectopic *T* expression.

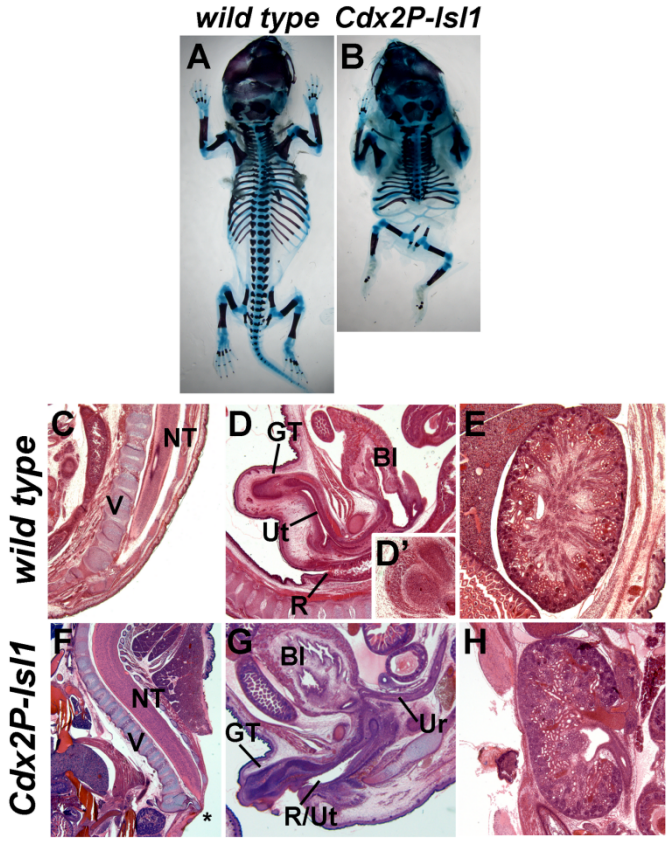

Figure 21. ***Isl1*** **is involved in the terminal differentiation of the lateral mesoderm. A,B** Skeletal analysis of wild type (**A**) and *Cdx2P-Isl1* transgenics (**B**) at E18.5 revealed axial truncation posterior to the thoracic region, without impairment of hindlimb morphology. Dorsal view. **C-H** Sagittal sections of the posterior region of wild type and *Cdx2P-Isl1* transgenic fetuses at E18.5. **C,F** Precocious neural tube termination and truncation of the vertebral column at the level of lumbar region in *Cdx2P-Isl1* transgenics (marked by an *). **D,G** Urogenital region of wild type (**D**) and *Cdx2P-Isl1* (**G**) embryos revealed fused rectum and urethra (*R/Ut*) in the transgenics. Gonads (**D'** in the wild type) were not observed in *Cdx2P-Isl1* embryos. **E,H** Normal morphology of the kidneys in the transgenics. *V* vertebral column; *NT* neural tube; *Bl* bladder; *Ur* ureter; *GT* genital tubercle.

Unlike *Cdx2P-Isl1* embryos, we could not observe any abnormal phenotype when *Isl1* was expressed in the paraxial or lateral mesoderm (*Dll1P-Isl1* and *Hoxb6P-Isl1* transgenics, respectively). This indicated that, similar to Gdf11/Alk5 signaling, *Isl1* may affect mesodermal AP patterning when activated in the axial progenitors of the epiblast but not in the mesodermal tissues after their ingression through the PS. Given that *Isl1* expression is associated with the induction of the most posterior derivatives of the lateral mesoderm, we

hypothesized that this gene might trigger the terminal differentiation of the trunk progenitors. In the progenitors for the lateral mesoderm this would be associated with specific physiological programs (like those resulting in hindlimb induction), but in axial progenitors for tissues normally not in contact with *Isl1* activity, it would simply result in their depletion. To test if this could indeed be the case, we analyzed *T* expression in *Cdx2P-Isl1* transgenics at E10.5. We found that in these embryos *T* was expressed in the notochord associated with the anterior part of the embryo up to the hindlimb level, but posterior to this region we could only detect a few ectopic spots and no expression in the tail bud (Fig. 20E,F). This is consistent with the idea of a complete loss of progenitors forming neural and paraxial mesodermal structures of the tail bud. Altogether, these data support the incompatibility between *Isl1* expression and the maintenance of axial progenitors and suggest a developmental role for *Isl1* in the programmed termination of the lateral mesoderm progenitors as part of the trunk to tail transition.

The observation that *Isl1* and Gdf11 signaling are both required in the axial progenitors to modulate AP patterning of the lateral mesoderm led us to explore if *Isl1* is a direct target of Gdf11/Alk5 signaling. Kang et al. (2009) have recently characterized enhancer elements involved in the activation the *Isl1* gene in the cardiac progenitors and in the posterior part of the embryo. We found several putative Smad2 binding sites within one of the most conserved regions of this enhancer (CR2 in Kang et al. 2009) (Figs. 22A,B), suggesting that *Isl1* could be a target of the Gdf11 pathway. In transgenic embryos, CR2 was able to drive expression of a reporter gene specifically in the caudal end of the lateral mesoderm (Fig. 22D), thus mimicking the normal expression domain of *Isl1* in this area (Fig. 22C) (Yang et al.,

2006). Inactivation of all potential Smad sites in this enhancer rendered it inactive (Fig. 22E), indicating that they are required for its activity. To confirm binding, we performed chromatin immunoprecipitation experiments on the posterior region of E9.0 mouse embryos and detected the *Isl1* CR2 enhancer using an antibody for phosphorylated Smad2/3 (Fig. 22F). Taken together, our results identify *Isl1* as a direct physiological target of *Gdf11* in its activity to modulate the trunk to tail transition during mouse axial elongation.

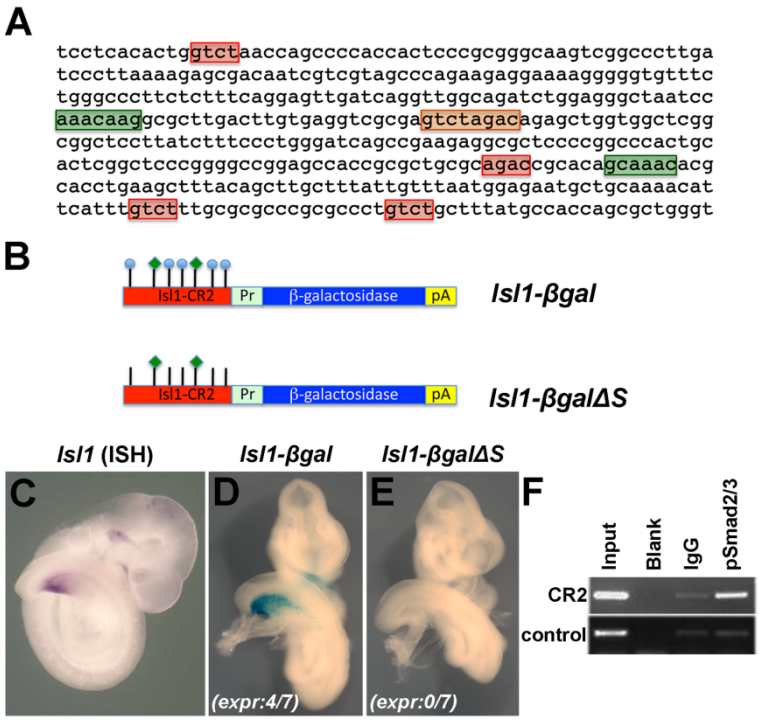

Figure 22. *Isl1* is a direct target of Smad2. A Sequence of the CR2 enhancer of the *Isl1* gene. Fox binding sites are highlighted in green and the Smad binding sites in red and in orange (the palindromic site). **B** Schematic representation of reporter constructs for the *Isl1-CR2* enhancer. The Fox and Smad binding sites are represented by green diamonds and blue circles, respectively. In the mutant construct (*Isl1-βgalΔS*), the Smad binding sites were mutated. *Pr* adenovirus 2 minimal late promoter; *pA* SV40 polyadenylation signal. **C** Whole-mount *in situ* hybridization for *Isl1* in wild type embryo at E9.25. **D,E** Whole-mount *β*-galactosidase staining of transgenic reporter embryos at E9.25. **D** Reporter expression mimics the endogenous expression of *Isl1* (compare with **C**). **E** Lack of reporter expression in *Isl1-βgalΔS* transgenics revealed that putative Smad binding sites are crucial for *Isl1* activation in the ventral-lateral mesoderm during the trunk to tail transition. Numbers of positive cases in relation to the total number of harvested embryos is indicated between brackets. **F** Chromatin immunoprecipitation from the posterior region of E9.25 wild type embryos using antibodies for IgG (unspecific control) and phosphorylated Smad2/3 (pSmad2/3) and PCR amplification of the CR2 enhancer.

Gdf11 signaling participates in the termination of the AP axis

In addition to the extended thoracic and lumbar domains, the skeletons of *Gdf11* mutants demonstrate additional characteristics that differ from those observed in wild type animals. In wild type mice, the tail vertebrae progressively lose complexity in an AP sequence. Whereas the first 4 or 5 caudal segments still contain neural arches surrounding the end of the spinal cord, those in more posterior positions are essentially reduced to small vertebral bodies (Fig. 23A,E). In *Gdf11* mutants with longer tails (including those treated with RA inhibitor (Lee et al., 2010) and a few untreated that were less truncated than the average mutant) all caudal vertebrae look rather similar with neural arches that enclose a neural tube extending into more posterior areas than in wild type embryos (Fig. 23C,F).

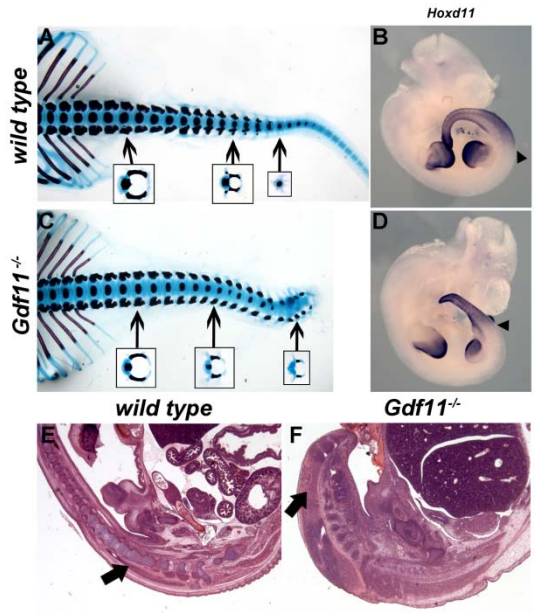

Figure 23. *Gdf11* affects the termination of the tail. A,C Skeletal analysis of wild type (**A**) and *Gdf11* mutant (**C**) fetuses at E18.5. Dorsal view. Vertebral elements at selected axial levels are highlighted. **B,D** Whole-mount *in situ* hybridization for *Hoxd11* revealed that the anterior limit of expression (*arrowheads*) is shifted posteriorly in mutant embryos at E11.5. **E,F** Sagittal sections of the posterior region of wild type (**E**) and AGN193109-treated *Gdf11* mutant (**F**) fetuses at E15.5 revealed an enlarged neural tube filling the whole extent of the vertebral column of treated mutants. *Arrows* indicate the neural tube.

In other systems, *Gdf11* and its close relative *Gdf8* have been reported to act as "chalones" to negatively regulate tissue growth (Gamer et al., 2003; Gokoffski et al., 2011; McPherron et al., 1997; Wu et al., 2003). The phenotype we have observed in the tails of *Gdf11* mutants also fits this interpretation, as the neural and mesodermal derivatives are larger in the mutant tails, yet keeping a high degree of histological organization. If this is the case, we would predict that over-stimulation of Gdf11 signaling would result in increased depletion of progenitors. The truncation observed in a subset of *Cdx2P-Alk5*^{CA} transgenics could thus be the consequence of such effect. Consistent with this hypothesis, we found strongly reduced or absent expression of *Wnt3a*, *Fgf8* and *T* in the remaining tissue posterior to the forelimbs (Fig. 24A-C'), which helped to identify this region as a small tail-tip-like structure. We could observe a similar structure in most of these transgenic embryos. The presence of such a reduced tail bud is compatible with an extreme deregulation of axial progenitor differentiation in these *Cdx2P-Alk5*^{CA} transgenics, ultimately resulting in increased cell death (Fig. 24E-E') and truncation of the AP axis.

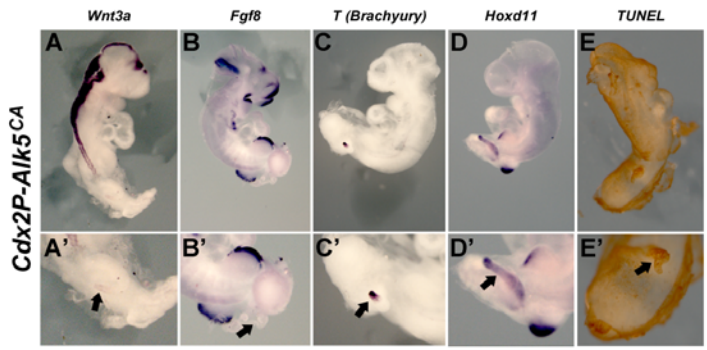

Figure 24. Truncation of *Cdx2P-Alk5*^{CA} transgenics. A-D' Whole-mount *in situ* hybridization in E10.5 transgenic embryos. **A-D'** Expression of *Wnt3a* (**A,A'**), *Fgf8* (**B,B'**), *T* (**C,C'**) expression is downregulated, while *Hoxd11* expression is precociously activated in the posterior region of the transgenics. See Figs. 9, 11, 12 and 20 for wild type embryos. **E,E'** Increased cell death in the tail tip of transgenic embryos as revealed by TUNEL reaction. **A'-E'** show amplification of the posterior region. *Arrows* mark the tail-like tip.

Interestingly, the tails of *Gdf11*$^{-/-}$ fetuses resemble to some extent those observed in total *Hox11* mutants (Wellik and Capecchi, 2003). In particular, the presence of vertebrae with fully developed neural arches extending considerably beyond the fifth caudal vertebra and the very reduced or completely absent sacral structures of *Gdf11*$^{-/-}$ skeletons (Fig. 23C) are features of the *Hox11* mutants (Wellik and Capecchi, 2003). This suggests that the abnormal morphology of the *Gdf11*$^{-/-}$ caudal vertebrae might result from down-regulation of *Hox11* gene expression. In *Gdf11* mutants, *Hoxd11* transcripts were detected at more absolute caudal levels than in wild type embryos, similar to what we observed for other posterior Hox genes. However, when the expression domain was assessed relative to the hindlimb, *Hoxd11* activation did not follow the same morphological landmarks as in wild type embryos. Instead, it was activated in even more caudal areas, closer to the area where the tail becomes thinner in these embryos (Fig. 23B,D). Analysis of truncated *Cdx2P-Alk5*^{CA} embryos for *Hoxd11* expression revealed that this gene is precociously activated in the tissue caudal to the forelimb buds, most particularly in the tail-tip-like structure (Fig. 24D,D'). Therefore, the absence of *Hoxd11* expression seems to correlate with tail growth, whereas tail termination seems to be connected to the presence of *Hoxd11* transcripts. This is compatible with the hypothesis that down-regulation of *Hox11* genes plays a role in the tail phenotype observed in *Gdf11* mutants.

II.4 - Discussion

In this work, we have shown that *Gdf11* is a central modulator of the processes involved in the trunk to tail transition in the mouse embryo. This was supported by both loss and gain of function experiments. In

Gdf11 mutant embryos the trunk to tail transition (which can be conveniently identified by the position of the hindlimb and cloaca-related tissues) was posteriorly displaced, leading to the formation of a longer trunk. Conversely, precocious activation of Gdf11 signaling using a constitutively activated form of its receptor Alk5 produced a strong anterior displacement in the hindlimb position, which resulted in dramatically shortened trunks. It should be noted that although delayed, the trunk to tail transition still occurs in *Gdf11* mutant embryos. One possible explanation is that Gdf11 activity is partially compensated by other molecules that activate the same signaling pathway. A candidate for such molecule is *Gdf8* (*Myostatin*) as inactivation of this gene intensifies the *Gdf11* mutant phenotype in the axial skeleton (McPherron et al., 2009). An analysis of the trunk to tail transition in *Gdf11/Gdf8* double mutants has not been reported. However, the longer rib cages observed in these embryos, together with the more anterior axial truncation at the lumbar level, and the presence of strongly reduced hindlimbs (McPherron et al., 2009) are compatible with a largely incomplete or absent trunk to tail transition. Alternatively (or in addition), other signaling pathways can act in parallel during this process, protecting *Gdf11* mutant embryos from a complete block in the switch from making trunk to tail tissues.

The hindlimb and ventral lateral mesoderm as a product of terminal differentiation of the lateral mesoderm progenitors

During the trunk to tail transition the axial progenitors relocate from a position in the PS and adjacent epiblast to the CNH (Cambray and Wilson, 2002, 2007; Wilson and Beddington, 1996). This relocation does not include all progenitors. In particular, those for the lateral and

intermediate mesoderm, involved in the genesis of the trunk associated organs, are not incorporated into the CNH. Instead, specific differentiation programs are activated in these progenitors to generate the hindlimbs and the ventral lateral mesoderm, which interacts with the hindgut endoderm to organize the posterior end of several trunk associated organ systems. Indeed, even in some snakes, a small hindlimb primordium is produced in this position that later fails to produce a full grown member (Cohn and Tickle, 1999). Gdf11 signaling seems to play an essential role in this process through a mechanism that includes activation of *Isl1* in the progenitors for the lateral mesoderm. This is in keeping with lineage tracing experiments showing that in wild type embryos, *Isl1* becomes specifically activated in the progenitors of the hindlimb and ventral lateral mesoderm (Yang et al., 2006). It is also consistent with genetic experiments showing that hindlimbs are not formed in the absence of this gene (Itou et al., 2012; Kawakami et al., 2011). In addition, we showed here that precocious activation of *Isl1* in axial progenitors of the epiblast was able to induce the hindlimbs and cloacal tissues at more anterior axial levels, thus mimicking to some extent the *Cdx2P-Alk5*^{CA} phenotypes (see below). Importantly, a conserved enhancer for the *Isl1* gene that activates expression in the most caudal part of the lateral mesoderm, contains several Smad binding sites that are essential for its activity, thus establishing a direct connection between Gdf11 signaling and *Isl1* activation. In this context, it should be noted that activation of this enhancer requires other factors in addition to Gdf11 signaling. Indeed, this regulatory element is inactive in the progenitors for the neural tube or paraxial mesoderm, although Gdf11 signaling is active in this area. Fox genes are among the best candidates to cooperate with Gdf11

signaling in activating this enhancer because it also contains Forkhead binding sites that are essential for enhancer activity (Kang et al., 2009). *FoxF1* is one of the prime candidates to play a physiological role in this process because its expression is detected in the lateral mesoderm but not in the neural tube and paraxial mesoderm (Mahlapuu et al., 2001).

One of the most striking characteristics of the *Cdx2P-Isl1* transgenics was the totally different effects that *Isl1* expression had on the various axial progenitors. In the progenitors of the lateral mesoderm, precocious *Isl1* activation had surprisingly little effect on the morphogenesis of the posterior lateral mesoderm derivatives, other than their induction at a more anterior axial level. However, *Isl1* activation had strong deleterious effects on the progenitors of more medial tissues, like the notochord, the neural tube, and paraxial mesoderm, which normally do not express *Isl1*. Therefore, the phenotype that we observed in the *Cdx2P-Isl1* transgenics might indicate that *Isl1* activity has negative effects on progenitor maintenance, bringing them into terminal differentiation pathways. In the progenitors of the lateral mesoderm, the cessation of progenitor renewal is combined with activation of the genetic programs resulting in the formation of structures like the hindlimb or the ventral lateral mesoderm. From this perspective, the hindlimb and cloacal tissues represent the product of terminal differentiation of the progenitors for the lateral mesoderm associated with the trunk to tail transition. In *Cdx2P-Isl1* transgenics, axial progenitors were precociously exposed to *Isl1*. In the progenitors for the lateral mesoderm, this triggered the physiological program at an earlier developmental stage. However, activation of *Isl1* in the precursors of neural tube and paraxial mesoderm led to a block in progenitor maintenance that was not

associated with an organized differentiation program, thus producing the morphological truncation of axial structures.

It should be noted that we never found *Cdx2P-Isl1* transgenics with hindlimbs closer than 6 somites to the forelimb buds or with axial truncations anterior to the 8th thoracic segment, indicating that the competence of the axial progenitors to respond to *Isl1* was not uniform along the AP axis. Considering that *Alk5* can induce hindlimb buds at more anterior levels than *Isl1* when prematurely activated in the epiblast, it is probable that the competence of the axial progenitors to respond to *Isl1* was also provided by Gdf11. Whether this is indeed the case as well as the mechanisms mediating this gain of competence remains to be determined.

Intriguingly, the skeletal phenotype that we observed in *Cdx2P-Isl1* transgenics is remarkably similar to the clinical characteristics found in patients with severe cases of spinal segmental dysgenesis (Mahomed and Naidoo, 2009), which raises the possibility that deregulation of *Isl1* expression during trunk to tail transition could be in the origin of this human syndrome.

Setting the PS to CNH transition

Another of the major processes associated with the trunk to tail transition is the relocation of the N-M progenitors from the anterior PS and adjacent epiblast to the CNH to form the tail bud (Cambray and Wilson, 2002, 2007; Wilson and Beddington, 1996). Our results indicate that Gdf11 signaling was also involved in this process and that this activity was mediated by modulation of RA availability at the posterior embryonic end. In addition, our data suggest that proper PS to CNH transition requires a complete block of RA signaling because its

pharmacological inhibition produced a significant recovery of the PS to CNH reorganization in *Gdf11*$^{-/-}$ embryos. This is consistent with the phenotype of *Cyp26a1* mutant embryos (Abu-Abed et al., 2001, 2003; Sakai et al., 2001). Indeed, it has been shown that in the absence of this RA-catabolyzing enzyme, embryos are exposed to an excess of RA that produces axial truncations at the lumbo-sacral level, which coincides with the stage when the PS to tail bud transition is taking place. The expression patterns reported for markers like *T* or *Cdx4* in *Cyp26a1* mutant embryos are compatible with strong alterations in the PS to tail bud transition (Abu-Abed et al., 2003). Our data also suggest that Gdf11 signaling modulates RA availability by regulating *Cyp26a1* expression. Accordingly, *Cyp26a1* levels were lower in *Gdf11* mutants than in wild type embryos during trunk to tail transition. Interestingly, the observation that *Cyp26a1* expression was reduced but not completely inactivated in *Gdf11* mutants at this developmental stage may explain the segregation of the axial progenitors into several domains. In particular, progenitors closer to the tail tip would be surrounded by sufficient *Cyp26a1* to protect them from RA. However, the levels of *Cyp26a1* in more anterior areas would fall below the threshold level required for effective RA clearance, leaving progenitors in this area exposed to RA. A reduction in *Cyp26a1* expression in the tail of *Gdf11* mutants has been previously reported at later developmental stages, associated with other developmental processes (Lee et al., 2010), further reinforcing the connection between Gdf11 signaling and the RA catabolic pathway.

The apparent separation between RA-responding and RA-non-responding progenitors observed in *Gdf11* mutants suggest that the PS to CNH transition might require activation of stage-specific

characteristics in the axial progenitors (e.g. adhesion properties) that would target them to specific regions (a progenitor niche?) of the posterior embryonic end, eventually generating a tail-bud primordium that organizes posterior embryonic growth. According to this hypothesis, acquisition of those properties would require complete downregulation of RA signaling in these progenitors. Activated RA signaling during the PS to CNH transition would impair colonization of the tail bud primordium niche. When the majority of progenitors respond to RA (like *Cyp26a1* mutants, *Gdf11* mutants treated with low doses of RA, or wild type embryos treated with high RA doses), the tail bud does not form and severe axial truncations occur at the level of the trunk to tail transition (Abu-Abed et al., 2001, 2003; Kessel, 1992; Lee et al., 2010; Sakai et al., 2001).

Gdf11 signaling is required to control the behavior of axial progenitors in the tail bud

After the trunk to tail transition, the CNH generates neural tissue and paraxial mesoderm from common bipotent progenitors (Tzouanacou et al., 2009). As development proceeds, the production of these tissues is gradually reduced, resulting in the formation of progressively smaller vertebrae and, in the absence of neural tube, posterior to the 4^{th} or 5^{th} caudal vertebra. The phenotype of *Gdf11* mutants suggests that Gdf11 signaling plays an essential role in the progressive termination of the main embryonic axis. In particular, the vertebrae posterior to the hindlimbs of *Gdf11*$^{-/-}$ fetuses are all larger than in wild type embryos, with neural arches accommodating an enlarged neural tube that extends until the posterior end of their vertebral column. This tail characteristic is shared by RA inhibitor-treated and -untreated *Gdf11* mutants,

although tails were longer in the former. This might reflect the increased progenitor number populating the tail bud upon RA inhibition, as evidenced by the expression of *T*. From an embryological perspective, the *Gdf11*$^{-/-}$ tail phenotype suggests that the number of cells produced per embryonic AP length unit during tail formation was higher in *Gdf11* mutants than in wild type embryos. This is compatible with the interpretation that Gdf11 acts as a "chalone" in the tail bud by negatively controlling its growth (Gamer et al., 2003). Interestingly, several members of the Tgfβ superfamily have been shown to present chalone activity in other biological contexts (Gamer et al., 2003; McPherron et al., 1997; Wu et al., 2003), including *Gdf11* itself in the olfactory epithelium (OE), where it controls tissue size by preventing overproduction of neural progenitors (Gokoffski et al., 2011; Wu et al., 2003). According to this idea, Gdf11 signaling would exert negative control on the production of the bipotent N-M progenitors in the tail bud, eventually leading to the progressive and regulated termination of tail growth. This interpretation is consistent with the strong phenotype observed in some *Cdx2P-Alk5*^{CA} transgenics, in which the truncation could be the consequence of precocious depletion of progenitors.

It will be important to understand the cellular and molecular basis of the chalone activity of Gdf11. It has been recently reported that the combination of low Smad2/3 levels together with high Akt signaling (which can be stimulated by FGFs) promotes expansion of pluripotent progenitors in cultured human ES cells (Singh et al., 2012). In chicken embryos, Fgf4-soaked beads induced ectopic expression of *T* and *Sox2* in the tail bud, which raised the possibility that high levels of FGF signaling may promote a N-M bipotent state (Olivera-Martinez et al., 2012). A similar phenomenon might be occurring in *Gdf11*

mutant tails as their *Fgf8* expression levels seem to be higher than in wild type embryos (Fig. 12C,D). This would indicate the existence of an equivalent mechanism in the tail bud to coordinate maintenance of a progenitor pool with the production of differentiated cells that contribute to the new tissues in the growing tail. Interestingly, it has been hypothesized that the chalone activity of *Gdf8* in muscle cells and of *Gdf11* in OE progenitors involves blocking the growth promoting activity of FGF signaling (Gamer et al., 2003; Wu et al., 2003). Moreover, it has been suggested that tail-bud growth relies on the dynamic activity of long-term axial progenitors within the CNH together with other progenitors with more restricted differentiation capacities located in more dorsal and ventral areas of the tail bud (McGrew et al., 2008). Our results suggest that Gdf11 signaling may be involved in regulating the relative equilibrium among these progenitor groups and/or in their ability to generate downstream derivatives.

Finally, it is possible that posterior Hox genes could play a role in the control of tail growth downstream of Gdf11 signaling. In particular, the sacral and caudal phenotypes of *Gdf11* mutants resemble those of the global *Hox11* mutants (Wellik and Capecchi, 2003), suggesting that *Hox11* genes could act downstream of Gdf11 in this process. Expression of *Hoxd11* upon inactivation or hyper-activation of Gdf11 signaling is compatible with this view. If *Hox11* genes are indeed involved in these processes, they would be a further addition to the list of Hox genes regulating the physiology of the axial progenitors. Indeed, a role for *Hoxa5* and *Hoxb8* genes in promoting axial growth and for *Hox13* genes in restricting posterior extension in the mouse has already been demonstrated (Young et al., 2009). Involvement of *Hox* genes in the control of organ size has also been described in *Drosophila*

(Crickmore and Mann, 2006), indicating that this might be a more general characteristic of *Hox* genes.

II.5 - Material and Methods

Transgenic constructs, mice and embryos

The *Gdf11* mutant strain used in this work has been described previously (McPherron et al., 1999). The constructs for the production of transgenic embryos were generated using standard molecular cloning techniques. The enhancers used for these constructs were a 9.5 kb fragment upstream of the *Cdx2* gene (*Cdx2P*) (Benahmed et al., 2008), the msd enhancer of the *Dll1* gene (Beckers et al., 2000), and the lateral mesoderm enhancer of the *Hoxb6* gene (Becker et al., 1996). The *Isl1* CR2 enhancer (Kang et al., 2009) was amplified by PCR from mouse genomic DNA using primers 5'-TCCTCACACTGGTCTAACCAG-3' and 5'-GGACATCCCCACCCAGCGCTG-3'. To produce an enhancer without Smad binding sites, the different Smad targets (Fig. 22) were modified to CACA, except for the palindromic target GTCTAGAC that was changed to CATGCAGG. All these modifications were performed using a PCR-based mutagenesis strategy and verified by direct sequencing. The wild type and mutant *Isl1* enhancers were cloned upstream of the adenovirus 2 minimal late promoter (Conaway and Conaway, 1988) and the resulting regulatory elements were inserted upstream the *β-galactosidase* cDNA. The *Isl1* cDNA was IMAGE clone 40130540. To produce the $Alk5^{CA}$ cDNA, we used IMAGE clone 7098473, corresponding to the rat gene, and changed the threonine 204 for an aspartic acid (Charng et al., 1996; Wieser et al., 1995) using a PCR-based mutagenesis strategy. The mutation was confirmed by

direct sequencing of the cDNA clones. All transgenic constructs contained the SV40 polyadenylation signal in addition to the regulatory regions and relevant cDNAs.

Transgenic embryos were generated by pronuclear injection of the relevant constructs according to standard methods (Hogan et al., 1994). To obtain *Gdf11* mutant embryos of specific stages, matings were set up using $Gdf11^{+/-}$ animals and plugs checked in the morning of the following day. The day that plugs were found was considered E0.5. In the case of transgenic embryos, E0.5 was considered the day after the transfer of injected oocytes. Embryos were collected from pregnant females by cesarean section and fixed with 4% paraformaldehyde (PFA) in PBS for *in situ* studies or with Mirsky's fixative (National Diagnostics) for *β*-galactosidase staining.

Genotyping

Embryos at different stages were genotyped by PCR from genomic DNA extracted from the yolk sacs. Yolk sacs were incubated overnight at 50º C in yolk sac lysis buffer containing proteinase K (50 mM KCl, 10 mM Tris-HCl pH8.3, 2 mM $MgCl_2$, 0.45% Tween-20, 0.45% NP40, with 200 μg/mL of proteinase K). Heat inactivation of the lysates was performed at 95º C for 30 minutes. Fetuses were also genotyped by PCR from genomic DNA extracted from the intestines or the skin. Samples were incubated overnight at 50º C under agitation in Laird's buffer containing proteinase K (100 mM Tris-HCl pH8.5, 5 mM EDTA, 0.2% SDS, 200 mM NaCl, with 100 μg/mL of proteinase K). Pups were similarly genotyped from tail biopsies using Laird's buffer. Genomic DNA was precipitated in isopropanol and transferred to TE buffer (1 mM EDTA, 10 mM Tris-HCl pH8.0). PCR was performed

using 1 µl of the genomic DNA solution. Primers used for genotyping are summarized in Table 1.

Table 1. Primer information for genotyping.

Gene	Forward	Reverse
Gdf11	GAGTCCCGCTGCTGCCGATATCC	TAGAGCATGTTGATTGGGGACAT
	GGATCGGCCATTGAACAAGATG	GAGCAAGGTGAGATGACAGGAG
rat *Alk5*	ACGTTCATGGTTCCGAGAGGC	ATCATGTCTCACAGCAAGTCC
Hoxc8	AGCTGCCACGGAGACGCCTCC	GGCGTGAGAGACTTCAATCCG
Hoxb9	AACTGGCTGCACGCTCGCTCTTCC	GGGAAGAGCTAGGGAGGACTG
Hoxc9	GGCAGCAAGCACAAAGAGGAG	GGGCAGGGCTTAGGATTGTTC
Hoxd9	CTCAGCTTGCAGCGATCACC	CGGTTCTGGAACCAGATTTTGAC
Hoxa10	AGCGAGTCCTAGACTCCACGC	GTCCGTGAGGTGGACGCTACG
Hoxc10	CCTCGGAGAGCGAGAAGGAAC	CAGTTCCCGGATCCGATTCTC
Hoxd10	CAGAATTCGACCCACGCGTCCGCCCAC	CATCTAGATCCTGGCCTCACATGGGCC
Hoxa11	AACTTCAAGTTCGGACAGCGG	TCAGTGAGGTTGAGCATGCGG
Hoxc13	ACTTCGCTGCTCCTGCATCCA	CAGCTGCACCTTAGTGTAGGG
Isl1	ACCGCACGTCCACAAGCAG	AGCTGCGAGGACATTGATGC

Morphometric staging and statistics

Comparison of hindlimb development between wild type and *Gdf11* mutant embryos was performed using the morphometric system developed by Boehm et al. (2011). Data were presented as mean ± SEM and compared using the Student's t test ($P<0.05$ was considered significant).

Carmine staining for confocal analysis

Embryos were stained in hydrochloric carmine using a modified protocol from Machado-Silva et al. (1998). Briefly, PFA-fixed embryos were washed in PBT and then brought to 100% methanol through a methanol/PBT (PBS containing 0.1% Tween-20) series. Then, embryos were brought back to 75% methanol in PBT and stained overnight in a carmine solution (2% w/v carmine powder in 70% ethanol, 2% chlorine

acid) under agitation, in the dark. Embryos were then washed quickly in 5% acid ethanol and dehydrated again in 100% methanol. At this stage, images were taken with a Zeiss StereroLumar scope. Subsequently, embryos were transferred to methyl salicylate through a graded series of methyl salicylate in methanol and imaged by laser scanning confocal microscopy (Zeiss LSM-510 Meta).

In situ hybridization

In situ hybridization on whole embryos was performed using DIG-labeled antisense RNA probes as previously described (Kanzler et al., 1998). Probe information is summarized in Table 2.

Table 2. Probe information for *in situ* hybridization.

Gene	Plasmid backbone	Endonuclease	RNA polymerase	Size [bp]
Cdx2	pKS	SalI	T7	
Cyp26a1	pKS	NotI	T3	560
Fgf8	pKS	ClaI	T3	785
Foxa2		Asp700	T7	
Hand2	pSKII$^+$	NotI	T7	1900
Hoxa9	pCMV-Sport6	EcoRV	T7	2053
Hoxc10	pKS	EcoRI	T3	1091
Hoxc8	pKS	EcoRI	T7	1313
Hoxd11		EcoRI	T7	
Isl1	pT7T 3D	EcoRI	T3	459
Mesp2	pKS	BamHI	T7	
Pax2	pKS	NotI	T3	1200
Raldh2	pCMV-Sport6	SalI	T7	2242
Rarg	pCRII-TOPO	SpeI	T7	400
Shh	pSKII	HindIII	T3	642
Sox2	pSKII	XhoI	T3	700
T	pKS	NotI	T3	1800
Tbx4		XbaI	SP6	
Tbx5		SpeI	T7	
Uncx4.1	pSV-Sport	SalI	T7	1500
Wnt2	pGEM7Zf	HindIII	T7	1606
Wnt3a	pKXM	MluI	T3	1400

β-galactosidase staining

Fixed embryos were processed in accordance with Carvajal et al. (2001). In brief, they were washed three times in the washing buffer (0.02% Tween-20 and 0.02% NP40 in PBS) and stained in the staining solution (5 mM $K_3Fe(CN)_6$, 5 mM $K_4Fe(CN)_6.3H_2O$, 2 mM $MgCl_2$, 0.4 mg/mL X-gal, diluted in the washing buffer) for variable periods at 37º C in the dark. Embryos were post-fixed overnight at 4º C in Mirsky's fixative and stored in the washing buffer at 4º C.

Retinoic acid inhibitor and retinoic acid treatments

Treatment with RA inhibitor and RA were performed as in Lee et al. (2010) with slight modifications. Briefly, the stock solution of RA inhibitor AGN193109 (1 mg/ml in DMSO) was dissolved in corn oil and administered to pregnant females in three doses of 2 mg/kg of body weight between E7.5 and E9.5. For RA treatments, a 25 mg/ml solution of all-trans RA in DMSO was diluted in corn oil and was administered at E8.5 by oral gavage at a final concentration of 10 mg/kg of body weight.

Skeletal analysis

Skeletal analyses were performed using the Alcian blue/alizarin red staining method as previously described (Mallo and Brändlin, 1997). In brief, fetuses were eviscerated and skinned prior to being fixed overnight in 100% ethanol. Samples were stained overnight in Alcian blue solution for cartilage and then fixed overnight, again in 100% ethanol. Then, fetuses were incubated for about six hours in 2% KOH for digestion of soft tissues and stained for three hours in alizarin red solution for bone. Finally, they were incubated overnight again in 2%

KOH for washing excess of staining and removing remaining soft tissues. Skeletons were stored in 25% glycerol in PBS.

Histology

For histological analyses, fetuses were fixed in Bouin's fixative and embedded in paraffin; 10 μm thick sections were then stained with haematoxylin/eosin using standard histological methods.

Chromatin immunoprecipitation

Assays were carried out in accordance with Kutejova et al. (2008), with slightly modifications. In brief, the posterior region of E9.0 embryos was dissected in PBS and fixed in 1% formaldehyde for 15 minutes at room temperature, under agitation. Tissues were then disintegrated with a 25G needle and incubated in a lysis buffer (0.2% SDS, 1 mM EDTA, 0.5 mM EGTA, 10 mM Tris-HCl pH8.0, 0.1% sodium deoxycholate) containing protease inhibitors for 20 minutes at 4º C, under agitation. Samples were sonicated to 200bp-1kb fragments and centrifuged at maximum speed for 10 minutes at 8º C. Supernatants were diluted (1:10) with ChIP dilution buffer (1% Triton X-100, 2 mM EDTA, 150 mM NaCl, 20 mM Tris-HCl pH8.1) and immunoprecipitated overnight using antibodies anti-phosphorylated Smad2/3 (#8685, Cell Signaling Technology) and control rabbit IgG (#2729, Cell Signaling Technology) pre-bound to Dynabeads Protein A (Invitrogen) in ChIP dilution buffer at 4º C, under agitation. Bound chromatin to the Dynabeads was repeatedly washed with RIPA buffer (50 mM Hepes, 1 mM EDTA, 0.7% sodium deoxycholate, 1% NP-40, 0.5% LiCl) and then in TE buffer pH8.0. Between every wash, beads were collected with a magnetic concentrator. The DNA was eluted from the beads by

the addition of an elution buffer (1% SDS, 10 mM $NaHCO_3$) and incubated for 6 to 16 hours at 65º C. The immunoprecipitated DNA was purified using the Qiaquick PCR kit (Qiagen) and amplified by PCR using primers Isl1-enh-ChIP-F, 5'-GCGACAATCGTCGTAGCCCAG-3' and Isl1-enh-ChIP-R, 5'-GAGCGCCTCTTCGGCTGATCC-3' for the CR2 enhancer and primers P95enh_ChIP_F, 5'-CGGCTAGGATGAGGTGAAGGCA-3' and P95enh_ChIP_R, 5'-CGGATGCATAGCCTGCATAATGC-3' for a negative control region.

II.6 - Acknowledgments

We would like to thank Alexandra McPherron and Se-Jin Lee for providing the *Gdf11* mutant strain, José Belo, Jacqueline Deschamps, Denis Duboule, Achim Gossler, Bernhard Herrmann, Andreas Kispert, Malcolm Logan, Andrew McMahon and Erik Olson for sending plasmids containing regulatory elements and probes for *in situ* hybridization, Deneen Wellik for sharing unpublished data and Élio Sucena, Inês Domingues and Jennifer Rowland for reading the manuscript. This work was supported by grants PTDC/BIA-BCM/110638/2009 and PTDC/SAU-BID/110640/2009 to M.M. and by PhD fellowships SFRH/BD/33562/2008 to A.D.J. and SFRH/BD/51876/2012 to R.A.

Author contributions: A.D.J. and M.M. designed research; A.D.J., R.A. and M.M. performed research; A.N. performed pronuclear microinjection of DNA constructs; A.D.J. and M.M. analyzed data; and A.D.J. and M.M. wrote the paper.

Chapter III

Hunting down axial progenitors: generation of a transgenic mouse line with tamoxifen-inducible Cre recombinase activity in the primitive streak

adapted from

Jurberg AD, Nóvoa A, Mallo M. A transgenic mouse line with tamoxifen-inducible Cre recombinase activity in both the primitive streak and axial progenitors. *In preparation*

III.1 - Summary

We generated transgenic mouse lines expressing an inducible Cre recombinase driven by a primitive streak (PS) *T* (Brachyury) regulatory element. Crossing this line to "floxed" reporter lines revealed that Cre activity was tightly regulated upon tamoxifen administration. Early treatment resulted in the most widespread recombinant territory along the AP axis, while induction at later time-points caused recombination in progressively more restricted territories to the caudal region. Recombinant cells were observed in all three germ layers derivatives at E9.5 embryos, despite the time of treatment. This suggests that the promoter used in this line is active not only in the PS, but also in a population of axial progenitors. The time-controlled component of this line should prove valuable to study gene function during mouse gastrulation.

III.2 - Background

During gastrulation mesoderm and definitive endoderm are formed from epiblast cells that leave this epithelial layer by ingression through the PS (reviewed by Mikawa et al., 2004; Tam and Loebel, 2007; Wilson et al., 2009). This process occurs during an extended time period of development, associated with embryo growth in the anterior-posterior axis. The fate of the cells that transverse the PS depends of a variety of factors, including the specific developmental stage at which they cross this structure. At early stages, cells form extraembryonic, cardiac and cranial mesoderm, as well as definitive endoderm. Cells that cross the streak at later times in development produce mostly paraxial and lateral plate mesoderm (reviewed by Arnold and Robertson, 2009). The genetic control of gastrulation is complex. This

is reflected in the transcriptomic profile of the chicken PS, in which about 40% of the entire genome is expressed (Alev et al., 2010). As a result, many genes involved in mesodermal development are also required for PS formation or gastrulation movements. Indeed, inactivation of a number of these genes using conventional loss-of-function approaches proved to be embryonic lethal resulting in abnormal embryo implantation or gastrulation (*e.g.* Gu et al., 1998; Larue et al., 1994). To circumvent early lethality and address gene function at later embryonic stages, conditional mouse lines and tissue-specific Cre deleters have been used with considerable success (*e.g.* Lewandoski, 2001). Transgenic lines expressing a Cre recombinase driven by a PS-specific element were generated to study the genetic networks controlling mesoderm development (Feller et al., 2008; Perantoni et al., 2005). In these lines Cre-dependent recombination occurs in all cells that arise from the PS and does not allow temporal control on the recombination process. However, considering that PS activity changes spatially and temporarily throughout development, such temporal control might be useful for the understanding of the molecular mechanisms underlying gastrulation.

III.3 - Results and discussion

Line characterization

We generated five transgenic founder lines expressing a tamoxifen-inducible Cre recombinase ($CreER^T$) (Hayashi & McMahon 2002) under the control of the PS-specific promoter of the *Brachyury* (*T*) gene (Clements et al., 1996; Stott et al., 1993). This element was reported to be inactive in the node or notochord (Clements et al., 1996). Three of

the lines produced strong reporter fluorescence signal when crossed to Rosa26R-YFP$^{+/+}$ females (Srinivas et al., 2001) after a single intraperitoneal injection of tamoxifen at E7.5 (Fig. 25). The line #47 gave the strongest signal and was chosen for further characterization.

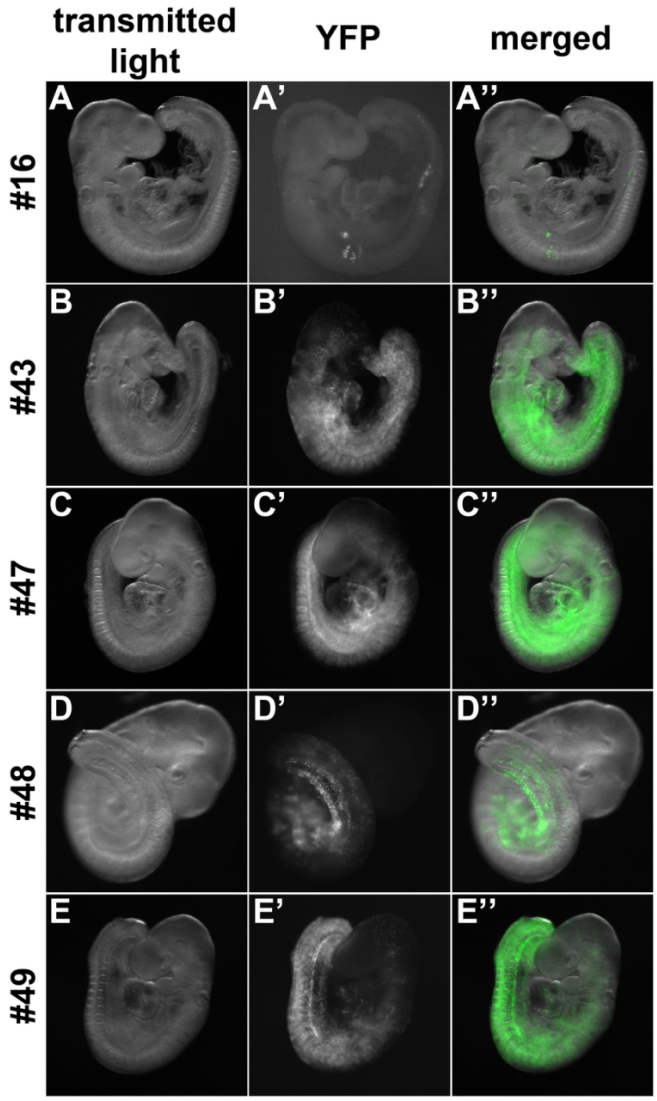

Figure 25. Founder lines induced variable degree of recombination. Rosa26R-YFP$^{+/+}$ pregnant females were treated with tamoxifen at E7.5 and embryos were harvested at E9.5. Lines #16 (**A-A''**) and #48 (**D-D''**) exhibited a reduced recombinant territory and were not characterized. Lines #43 (**B-B''**), #47 (**C-C''**) and #49 (**E-E''**) showed extensive recombination. Line #47 was chosen for further characterization. Lines #43 and #49 were cryopreserved.

To perform a more detailed characterization of CreER^T induction in this line, transgenic males and *Rosa26R-YFP*$^{+/+}$ females were put together and mating was checked in two-hour intervals. When a vaginal plug was detected the mid-point of the mating interval was considered as embryonic stage (E) 0.0. We then administered a single dose of tamoxifen to pregnant females from E7.5 to E8.5 in two-hour intervals, which corresponds to the time required for the formation of a new somite pair in the mouse (Tam, 1981). Corn oil injected at E7.5 served as a negative control for induction. Embryos were harvested at E9.5 and examined under a fluorescence stereoscope (SteREO Lumar.V12, Zeiss). In addition to the *Rosa26R-YFP* strain, we also used the *Rosa26R-β-galactosidase* reporter line (Soriano, 1999) to obtain better detail on the recombinant tissues. In this case, transgenic males were crossed to *Rosa26R-β-galactosidase*$^{+/+}$ females and a single dose of tamoxifen was administered at E7.5, E8.0 or E8.5. The analysis of these embryos was performed by staining for β-galactosidase activity (Carvajal et al., 2001) at E9.5, and sectioning the stained embryos with a vibratome. The same recombination patterns were visualized in both reporter strains for the matching time-points of treatment and will be described here simultaneously.

Some variability in somite numbers was observed and only the embryos containing 24-27 somite pairs were considered for CreER^T characterization. Scarce spontaneous recombination eventually occurred in the absence of tamoxifen treatment, suggesting a minor leakage in CreER^T activity (Fig. 26A-A''). When non-induced CreER^T activity was detected, it always produced only a very small number of recombinant cells, generally grouped together, indicating that they had probably resulted from a rare, single-cell recombination event.

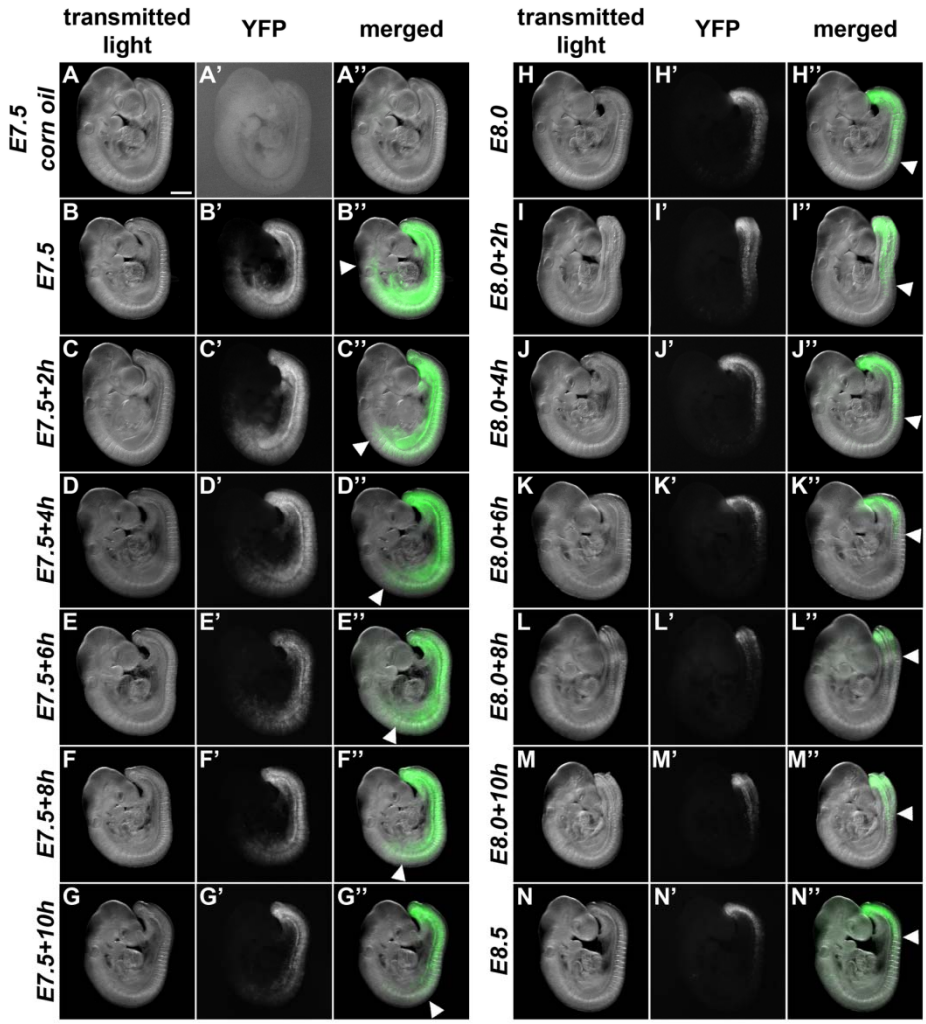

Figure 26. Time-dependent recombination in *T*-streak-CreER^{T}::Rosa26R-YFP embryos. While non-treated embryos showed only rare events of spontaneous recombination (**A-A''**), administration of tamoxifen at early stages induced extensive recombined territories that got progressively restricted to the caudal region as tamoxifen was being administered at later time-points (**B-N''**). See text for more information. Left labels adjacent to images show the exact time tamoxifen administration. *Arrowheads* indicate the approximate anterior boundary of recombination.

We observed that the time of tamoxifen administration directly correlated with a gradual change in the domains of recombinant cells along the AP axis (Fig. 26). Early administration of tamoxifen at E7.5 produced the most widespread recombinant territory at E9.5, up to the level of the branchial arches (Figs. 26B-B" and 27A-A'"). In particular, streak derivatives such as the forelimb buds and more posterior lateral plate mesoderm, the somites, the hindgut, the notochord and the allantois underwent extensive recombination. We only detected a few positive cells in the heart (Figs. 26B-B" and 27A-A'"). As tamoxifen was being administered at later time-points, the territories positive for recombination became progressively restricted to more caudal regions (Figs. 26 and 27), indicating that $CreER^T$ activity was indeed properly controlled. The number of recombinant cells within a mesodermal derivative also decreased following later induction. For instance, while recombination was observed in the majority of cells in the forelimb buds and the lateral plate mesoderm of E9.5 embryos upon tamoxifen administration at E7.5, only a few scattered recombinant cells were observed in those tissues when tamoxifen was administered at E8.0 (Figs. 26 and 27A-B'"). Administration at E8.5 resulted in the presence of recombinant cells mostly at the level of the presomitic mesoderm of E9.5 embryos (Figs. 26N-N" and 27C-C'"). In these embryos, very few scattered recombinant cells were observed at the forelimb or interlimb levels, mostly in the paraxial mesoderm (Fig. 27C-C'"). Surprisingly, close analysis of sections of β-galactosidase-stained embryos revealed several recombinant cells in non-PS derivatives at all three time-points analyzed, mostly particularly the neural tube (Fig. 27). This is consistent with recent reports that have shown the existence of an axial

progenitor population in the node-streak border at E8.5 and later in the CNH (Cambray and Wilson, 2002, 2007; Tzouanacou et al., 2009).

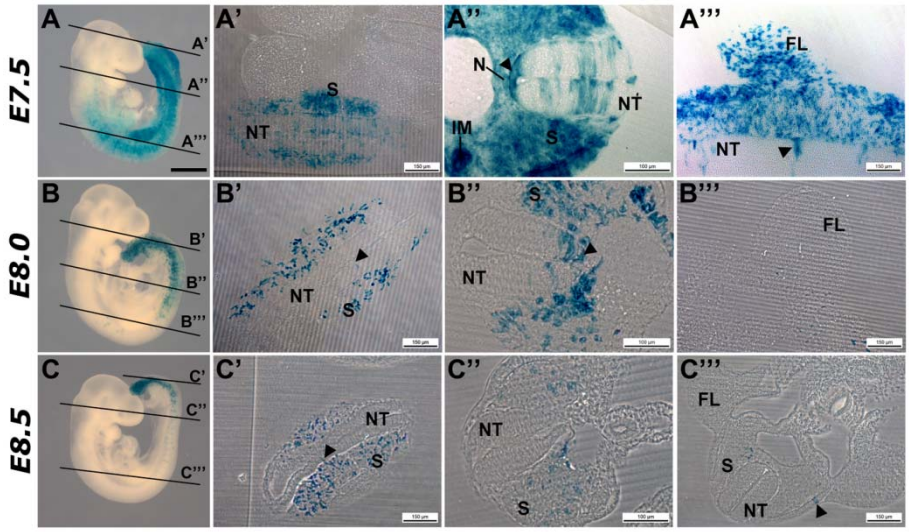

Figure 27. Histological assessment of recombination in *T*-streak-CreER^{T}::Rosa26R-*β*-galactosidase embryos. A-C Whole-mount *β*-galactosidase staining of embryos at E9.5. Left labels adjacent to images indicate the time of tamoxifen administration. **A'-C'''** Cross-sections at the indicated levels in **A-C**. **A-A'''** Early treatment caused an extensive recombination territory up to the level of the branchial arches. Note recombination in the neural tube, especially in the floor plate. **B-B'''** Treatment at E8.0 produced recombination in a lesser extension, not affecting the forelimb buds. *Arrowheads* indicate recombination in nervous cells. **C-C'''** Late induction induced recombination restricted to the presomitic mesoderm region, with a few scattered cells in the trunk somites. The number of recombinant cells within a mesodermal derivative decreased as induction occurred at later moments (**A'-C'''**). Recombination was observed in all three germ layers despite the time of tamoxifen administration. *Arrowhead* in **C'''** indicates recombination in the surface ectoderm. *NT* neural tube; *S* somite; *N* notochord; *IM* intermediate mesoderm; *FL* forelimb.

To determine the delay between tamoxifen administration and the onset of CreER^{T} activity, *Rosa26-YFP*$^{+/+}$ females that had been crossed with *T-streak-CreER*^{T} males were treated at E8.5 and embryos harvested at 2, 4, 6, 8, and 10 hours after injection. We could not find signs of recombination up to 6 hours. Some cells could be identified 8 hours after injection but clear induction of recombination was only observed in embryos analyzed 10 hours after tamoxifen administration (Fig. 28).

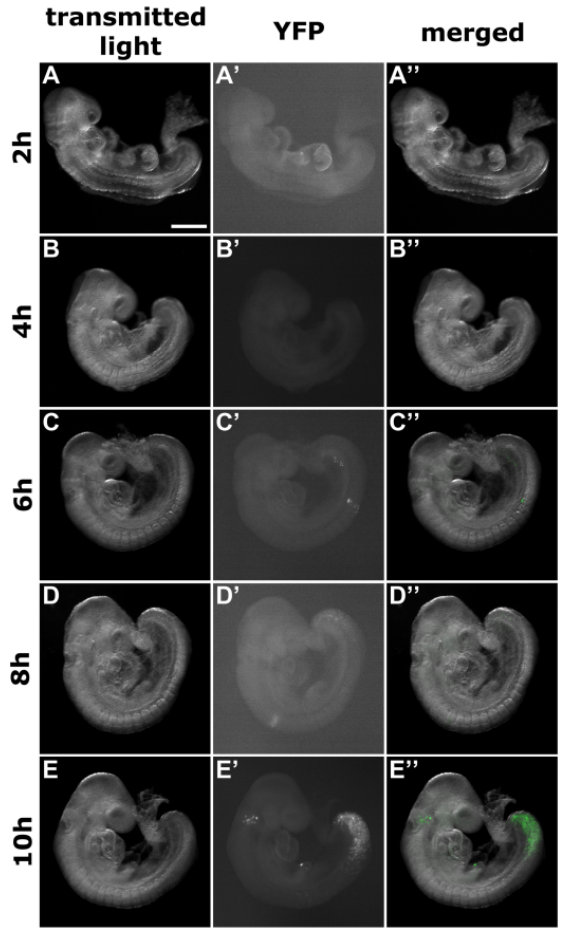

Figure 28. Induction of recombination in *T*-streak-CreER^T::Rosa26R-YFP embryos. No evident sign of recombination was observed after up to six hours of treatment (**A-C''**), only a few scarce spontaneous events. Embryos harvested eight hours after tamoxifen administration exhibited early signs of recombination (**D-D''**) and clear induction was observed ten hours after treatment (**E-E''**).

Dosage effects of tamoxifen treatment on mouse development and CreER^T activity were also addressed by intraperitoneal administration of other two tamoxifen concentrations at E8.0 and E8.5. Embryos were also harvested at E9.5. Administration of 4 mg of tamoxifen per 20 grams of body weight produced no obvious differences in the activation patterns when compared to their matching time-points treated with 2 mg per 20 grams of body weight (not shown). However, administration of 6 mg of tamoxifen per 20 grams of

body weight seemed to be toxic, as no embryos were recovered for any of the two administration time-points after three independent rounds of treatment (not shown).

Clonal analysis of PS progeny produced an unexpected finding in Gdf11 mutants

Next, we used the inducible property of this transgene to evaluate the behavior of axial progenitors during mouse posterior extension. Low frequency recombination was achieved by administering 0.2 mg or 50 µg of tamoxifen per 20 grams of body weight. We reasoned that if a recombination event occurs in a long term axial progenitor at early developmental stages, this cell would remain in the CNH at later stages, while still producing descendents in both the neural tube and mesodermal compartments at different axial levels. Conversely, if such long term axial progenitors are not targeted by recombination upon early induction, positive cells would be restricted to a particular axial level and would not be found in the tail bud at later stages.

In the first set of experiments, we crossed *T-streak-CreER*$^{T+/+}$ males with *Rosa26R-β-galactosidase*$^{+/+}$ females and administered a low tamoxifen dose at E7.5 or at E8.5. Embryos were then harvested at E10.5 or E11.5. We found embryos representative of both situations. In particular, some embryos showed no labelled cells in the tail posterior to the hindlimbs and contained positive clones only in more anterior areas of the body (Fig. 29A). However, a few embryos exhibited a reduced number of cells in the CNH two-three days after the pulse of tamoxifen. These cells also produced descendents in both the neural and mesodermal compartments in a wide AP domain (Fig. 29B-D). These findings suggest that recombination occurred in long term axial

progenitors and confirm that the *T* enhancer used in this construct in active in these cells.

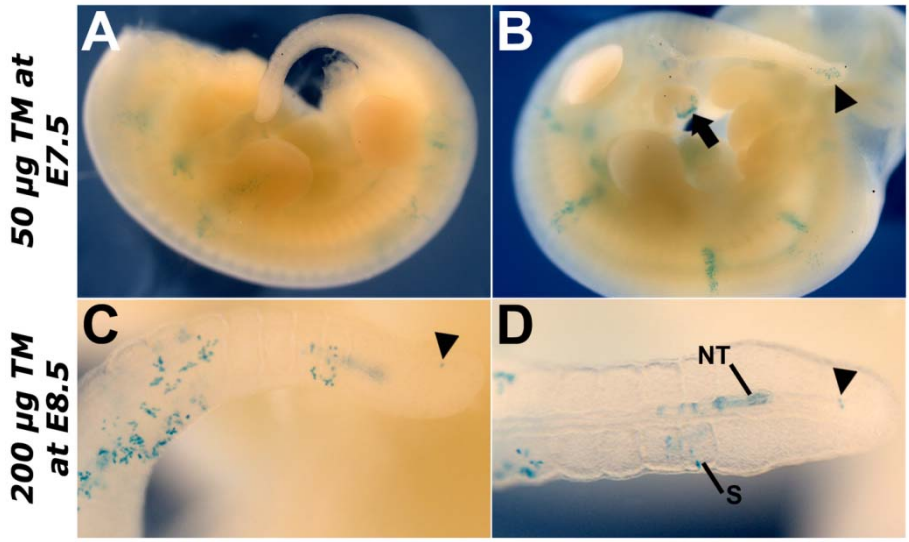

Figure 29. Low dose of tamoxifen induces reduced recombination. Whole-mount *β*-galactosidase staining of *T*-streak-CreER$^{T\,+/0}$::Rosa26R-*β-gal*$^{+/0}$ embryos. **A,B** Treatment with 50 µg of tamoxifen at E7.5 basically induced two patterns of recombination. **A** Dispersed clones along the AP axis anterior to the hindlimbs. **B** Interspaced clones along the AP axis, also posterior to the hindlimbs. *Arrowhead* indicates a group of recombined cells in the tail bud. Note recombination also in the hindgut (*arrow*). **C,D** Treatment with 200 µg of tamoxifen at E8.5. The same tail is shown in lateral (**C**) and dorsal (**D**) views. *Arrowheads* indicate a single event of recombination in the CNH region. Note positive cells in both the neural tube (*NT*) and the somites (*S*).

Then, we decided to take advantage of this system to investigate the long term axial progenitors in *Gdf11* mutant embryos. We observed that these mutants exhibit segregation of *T*-positive populations during tail growth (see chapter 2). We thus introduced the *Gdf11* mutant allele into the *T-streak-CreER*$^{T+/+}$ and *Rosa26R-β-galactosidase* backgrounds (*Gdf11*$^{+/-}$*;T-streak-CreER*$^{T+/+}$ and *Gdf11*$^{+/-}$*;R26R-β-gal*$^{+/+}$ mice, respectively). Surprisingly, we were not able to harvest any *Gdf11*$^{-/-}$*;R26R-β-gal*$^{+/0}$*;T-streak-CreER*$^{T+/0}$ embryos at any stage, regardless of whether they were treated or not with tamoxifen. Indeed, we found that the genotypes for the *Gdf11* alleles significantly deviated from the

expected Mendelian (1:2:1) ratio (Table 3), which suggests early lethality of *Gdf11*$^{-/-}$ embryos in the *T-streak-CreER*$^{T+/0}$ background. These findings raise the intriguing possibility that in the mouse line #47, the *T-streak-CreER*^{T} transgene had affected the expression of a gene that is essential for embryonic development in the absence of *Gdf11*, but it is dispensable when *Gdf11* is present. Interestingly, in the *Gdf11* mutant background, the presence of one single allele of *T-streak-CreER*^{T} was already lethal very early in development. Alternatively, expression of the *CreER*^{T} molecule in the PS is not compatible with development in the absence of *Gdf11*. To discern between these two possibilities, we are now testing the compatibility of a different *T-CreER*^{T} mouse line (#49) with the absence of *Gdf11*.

Table 3. Gdf11 genotyping in the *R26R-β-gal*$^{+/0}$*;T-streak-CreER*$^{T+/0}$ #47 background[1].

Genotype	*Number of embryos obtained*	*Frequency (%)*	
		Observed	**Expected**
Gdf11$^{+/+}$	68	44.2	25
Gdf11$^{+/-}$	86	55.8	50
Gdf11$^{-/-}$	0	0	25
Total	154	100	100

[1]The fit to Mendelian expectation was tested with a chi-square test: $\chi^2 = 62.16$, degrees of freedom = 2, $P<0.0001$.

Identification of the integration locus

At the same time we started the experiments with the transgenic line #49, we determined the locus of transgene integration in the *T-streak-CreER*^{T} line #47 using the method described by Liang et al. (2008) (Fig. 30). We found that the transgene inserted as multiple copies into an intergenic region on chromosome 14, between an uncharacterized putative protein named Gm6999 and the protocadherin-8 isoform 2

precursor gene (*Pcdh8*) at the 5' side and the olfactomedin-4 precursor gene (*Olfm4*) at the 3' side (Fig. 30A). The site of integration was confirmed by multiplex PCR using two primers for the endogenous chromosome and a primer for the transgene (Fig. 30C) (see materials and methods). Based on evolutionary conservation (Siepel et al., 2005), it is possible that integration has disrupted a regulatory region (Fig. 30). Current efforts are being made to further examine this genetic interaction.

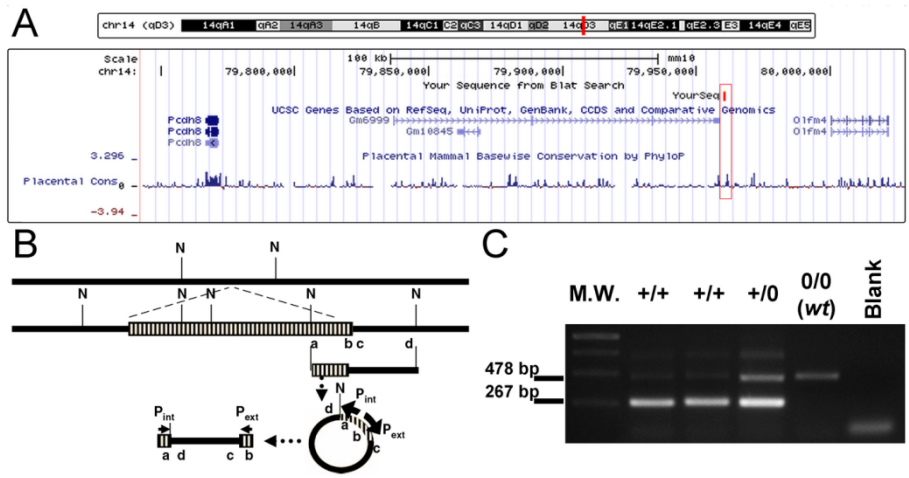

Figure 30. Integration locus of the *T*-streak-CreER^T transgene in mouse line #47. A Schematic representation of the integration locus on mouse chromosome 14. Two known genes and a putative protein localize nearby the site of integration. The proximity to a conserved region suggest that the transgene has disrupted a regulatory element. **B** Schematic representation of the identification strategy described by Liang et al. (2008). See Liang et al. (2008) for further information. **C** Genotyping of homozygous (+/+), heterozygous (+/0) and wild type (0/0, *wt*) mice for the *T*-streak-CreER^T transgene using primers designed after the determination of the integration locus.

III.4 - Material and Methods

Transgenesis, genotyping and mice

The *R26R-β-galactosidase*$^{+/+}$ and *R26R-YFP*$^{+/+}$ reporter lines (Soriano, 1999; Srinivas et al., 2001) were purchased from Jackson laboratories. The *T*-streak-CreER^T construct for the production of transgenic lines

was kindly provided by A. Gossler and B. Herrmann. We generated transgenic mice in a FVB/N genetic background by pronuclear injection using standard procedures (*e.g.* Nagy et al., 2003). Genotyping was carried out by polymerase chain reaction (PCR) from genomic DNA obtained from tail tip biopsies, using primers CreF, 5'-CGAGTGATGAGGTTCGCAAG-3' and CreR, 5'-CACCAGCTTGCATGATCT-3', which produce a 885 bp product. Amplification conditions were: initial denaturation at 95º C for 5 minutes, followed by 35 cycles of (1) 95º C for 45 seconds, (2) 62º C for 45 seconds, (3) 72º C for 45 seconds, and then by a final extension of 5 minutes at 72º C. Male founders were crossed with Rosa26R-YFP$^{+/+}$ reporter mice (Srinivas et al., 2001) to determine CreER^{T} induction. Female founders were first crossed to a C57Bl/6 mouse to produce male offspring.

The site of transgene integration was identified as described (Liang et al., 2008). Confirmation of the integration locus was performed by multiplex PCR on genomic DNA from tail tip biopsies, using primers #47wt_For1 5'-GAGGGAGAGATCAGGACCATGC-3', #47pA_For2 5'-CACTGCATTCTAGTTGTGGTTTGTCC-3', and #47wt_Rev 5'-ATCGCCTCACTCCTCCTTTGC-3'. Primers #47wt_For1 and #47wt_Rev produced a product of 478 bp in the wild type region, while primers #47pA_For2 and #47wt_Rev produced a product of 267 bp in the transgenic allele. Amplification conditions were used as previously mentioned, with an annealing temperature of 60º C.

Tamoxifen treatment and embryos

Pregnant females were injected intraperitoneally with 2 mg of tamoxifen in corn oil (from a 10 mg/ml stock solution) per 20 grams of body weight, unless stated otherwise. Embryos were harvested by cesarean section. When the *R26R-YFP* reporter was used, embryos were washed in PBS and observed under a fluorescence stereoscope (SteREO Lumar.V12, Zeiss). Alternatively, when experiments involved the *R26R-β-gal* reporter, embryos were fixed with Mirsky's fixative (National Diagnostics) and stained for *β*-galactosidase activity, as previously described in chapter 2.

III.6 - Acknowledgments

To A. Gossler and B. Herrmann for kindly providing the Tstreak-CreER^{T} construct.

Author contributions: A.D.J. and M.M. designed research; A.D.J. and M.M. performed research; A.N. performed pronuclear microinjection of DNA constructs; A.D.J. and M.M. analyzed data; and A.D.J. and M.M. wrote the paper.

Chapter IV

Compartment-dependent activities of Wnt3a/*β*-catenin signaling during the extension of the mouse body

adapted from

Jurberg AD, Aires R, Nóvoa A, Rowland JE, Aulehla A, Mallo M. Compartment-dependent activities of Wnt3a/*β*-catenin signaling during vertebrate axial extension. *In preparation*

IV.1 - Summary

Axial growth results from the activity of axial progenitors that produce precursors for the different body tissues. A variety of analyses is consistent with the existence of common progenitors for the neural tissue and the paraxial mesoderm, first localized in the epiblast next to the anterior region of the PS and later in the tail bud. We show that Wnt3a/*β*-catenin signaling in the epiblast indeed impacts neural differentiation, but does not promote mesoderm production as expected. High levels of Wnt3a resulted in the accumulation of undifferentiated epiblast progenitors that failed to ingress through the PS, suggesting that Wnt3a in the epiblast is not sufficient to promote the formation of mesoderm. On the contrary, Wnt3a/*β*-catenin signaling in the epiblast is involved in the maintenance of these axial progenitors. In addition, high levels of Wnt3a in the epiblast also impacted somite size and lateral mesoderm production, suggesting that the different effects of Wnt3a/*β*-catenin signaling during posterior extension of the body are context-dependent.

IV.2 - Background

Formation of the vertebrate body requires a combination of well orchestrated cell proliferation and differentiation processes. After initial patterning events that define the embryonic AP axis and trigger gastrulation, most of the embryo is made by sequential addition of new tissue at its posterior end (reviewed in Stern et al., 2006). These tissues are continuously produced from axial progenitors that have been suggested to have stem cell-like properties. In a first phase, these progenitors are localized in the epiblast and respond to the organizing activity of the PS. Later in development, axial progenitors relocate to

the tail bud, which becomes the driver for posterior growth (reviewed in Wilson et al., 2009). Axial progenitors comprise an heterogeneous cell population. They include a population of bipotent N-M cells that are able to originate both neural tube and paraxial mesoderm all along the AP body axis (Tzouanacou et al., 2009; Wilson et al., 2009). These N-M progenitors are first located in the region between the node and the anterior region of the PS, known as the node-streak border (NSB), and later in the chordoneural hinge (CNH) within the tail bud (Wilson et al., 2009). In addition to the N-M progenitors, the epiblast also contains progenitor cells for the lateral and intermediate mesoderm. In association with the endoderm, these mesodermal compartments assembly most of the trunk-related organs (Carlson, 1999). The mechanisms that control coordinated production of all these progenitors are still not well understood, but a variety of molecular and genetic analyses have shown the involvement of many signaling pathways, such as Wnt/*β*-catenin, FGF, RA and BMP (Iulianella et al., 1999; Martin and Kimelman, 2012; Olivera-Martinez et al., 2012; Takemoto et al., 2011; Wilson et al., 2009). However, understanding the specific roles of those signaling systems on axial progenitors is not always straightforward, because they are often involved in more than one process relevant to axial growth, such as somitogenesis and body patterning (Dubrulle and Pourquié, 2004b).

One of the best studied signaling pathways during axial extension is activated upon Wnt3a binding (Petersen and Reddien, 2009). Mutant embryos for *Wnt3a* are truncated posterior to the forelimbs (Takada et al., 1994), which suggests that this factor might be essential for the proper function of axial progenitors. Such truncation is associated with a strong reduction of mesodermal structures and with

the over-production of neural tissues (Takada et al., 1994; Yoshikawa et al., 1997). Recently, it has been suggested that this phenotype resulted from abnormal behavior of the bipotent N-M progenitors, which in the absence of Wnt3a take a neural fate (Martin and Kimelman, 2012). In particular, these authors have shown that progenitors in the tail tip of the zebrafish undergo neural or mesodermal differentiation depending on whether the Wnt3a/*β*-catenin pathway is blocked or stimulated, respectively (Martin and Kimelman, 2012). However, other studies seemed to be somewhat conflicting with this interpretation. Takemoto et al. (2006) have reported that the combined activity of FGF and Wnt/*β*-catenin signaling promote *Sox2* expression in the NSB. Afterwards, Takemoto et al. (2011) have shown that the activation of *Tbx6* in the PS and presomitic mesoderm (PSM) drives them into a mesodermal fate, a process that requires downregulation of *Sox2*. Strikingly, *Tbx6* seemed to block *Sox2* expression not by direct interaction with the relevant enhancer, but rather through the downregulation of *Wnt3a* (Takemoto et al., 2011). According to these findings, these authors have proposed that the ectopic neural tube in *Tbx6* mutant embryos resulted from persistent *Wnt3a* expression in the prospective PSM region, which would keep the activation of *Sox2* in this tissue (Takemoto et al., 2011). However, these observations seem to be at odds with other known activities of Wnt3a/*β*-catenin signaling during embryogenesis (Aulehla and Pourquié, 2010). In particular, Wnt3a and *β*-catenin are present in the PSM as a posterior to anterior gradient, which participates in the maintenance of PSM cells in an undifferentiated state that prevents segmentation (Aulehla et al., 2008; Dunty et al., 2008). More specifically, sustained activation of *β*-catenin in the PS resulted in a

strong inhibition of somitogenesis posterior to the first few somites and an enlarged PSM (Aulehla et al., 2008; Dunty et al., 2008). The ultimate fate of the PSM tissue which failed to produce somites was not further scrutinized. However, it seems unlikely that they acquired a neural fate, as would be expected if the ectopic neural tube of *Tbx6* mutants was a consequence of upregulated *Wnt3a* in the prospective paraxial mesoderm. One possible explanation for these discrepancies is that Wnt3a/*β*-catenin signaling produce distinct effects in progenitors and in prospective mesodermal cells after their ingression through the PS.

Here, we show that activation of Wnt3a or *β*-catenin in different embryonic compartments produces dissimilar effects associated to AP patterning and growth processes. Overexpression of *Wnt3a* in the epiblast prior to cell ingression through the PS resulted in strong malformations posterior to the forelimb buds. Molecular analyses indicate that Wnt3a activation in this region impaired neural development, but still allowed mesodermal differentiation, which kept a considerable degree of patterning. On the other hand, Wnt3a activity in the PSM promoted or stabilized mesodermal fates with no apparent impact on neural fate. In the context of previously published data (Martin and Kimelman, 2012; Takemoto et al., 2006, 2011), our current results suggest different context-dependent roles for Wnt3a/*β*-catenin signaling.

IV.3 - Results

Stabilization of *β*-catenin in mesodermal derivatives results in non-segmented mesoderm and seemingly unaffected neural tube

T-Cre::β-catenin$^{del(ex3)/+}$ embryos have an expanded PSM and a virtual absence of somitogenesis after the first few somites were formed (Aulehla et al., 2008). To evaluate the fate of the PSM tissue that failed to produce somites, we let these embryos develop until embryonic stage (E)10.5. At this stage, *T-Cre::β-catenin*$^{del(ex3)/+}$ embryos presented malformations that correlated with those observed at younger stages (Aulehla et al., 2008). They included the absence of most embryonic structures posterior to the heart region, in addition to a large ectopic mass in the ventral part of the embryo and a recognizable tail bud (Fig. 31).

Molecular analyses indicated that the posterior region of these embryos exhibited an expansion of the *Tbx6* domain and a seemingly well developed neural tube with a kinked morphology along the AP body axis, as evidenced by *Sox2* expression (Fig. 31A-D). These findings suggest that the stabilization of *β*-catenin in mesoderm derivatives leads to the continuous accumulation of non-segmented paraxial mesoderm without greatly impacting neural differentiation. It is possible that the kinked neural tube phenotype is derived from its fitting to the shorter AP length of the body in these embryos.

We also observed an unexpected degree of conservation of basic embryonic patterns, although forelimbs and hindlimbs were not readily evident (Fig. 31). The tail bud in these embryos preserved its organization when compared to wild type littermates, with a dorso-medial *Sox2*-positive neural tube and a *Tbx6*-positive PSM, although

this latter tissue remained unable to form somites (Fig. 31A-D). The AP patterning of the body seemed also relatively unaffected in the *T-Cre::β-catenin*$^{del(ex3)/+}$ embryos. In particular, *Hoxc10* had a clear anterior expression border both in the neural tube and within the *Tbx6*-positive mass (Fig. 31E,F). Its anterior expression border in the neural tube seemed to match the expression in wild type littermates, although the *T-Cre::β-catenin*$^{del(ex3)/+}$ embryos lacked mesodermal hallmarks (*e.g.* somites and hindlimb buds) normally used as morphological reference of the AP level. We also identified *Tbx4*-positive spots in the posterior region of *T-Cre::β-catenin*$^{del(ex3)/+}$ embryos (Fig. 31G,H). A ventral domain of *Tbx4* expression between the posterior border of the enlarged *Tbx6*-positive region and the antero-ventral border of the tail bud was consistent with the presence of ventral lateral mesoderm (Fig. 31G,H), suggesting that the trunk to tail transition occurred normally in *T-Cre::β-catenin*$^{del(ex3)/+}$ embryos. Other more lateral *Tbx4*-positive spots could be remnants of the lateral mesoderm forming the hindlimb (Fig. 31G,H). This suggests that the mechanisms involved in the specification of hindlimb position along the AP axis were activated in these embryos, but hindlimb development was impaired upon the stabilization of *β*-catenin in mesodermal derivatives. The low level of *Tbx4* expression in both domains would indicate that, contrary to the paraxial mesoderm, formation of the lateral mesoderm in these embryos was strongly reduced. Accordingly, expression of the splanchnic lateral mesoderm marker *Wnt2* was also compromised in these embryos, being reduced to thin stripes ventral to the large mass of PSM (Fig. 31I,J).

These results show that persistent activation of the *β*-catenin in mesodermal derivatives does not induce neural differentiation,

indicating that the production of ectopic neural tube in the prospective PSM region of *Tbx6* mutant embryos is either independent of *Wnt3a* expression or requires Wnt3a interaction with additional factors that are missing in the absence of *Tbx6*. Our findings also indicate that activated *β*-catenin in *T-Cre::β-catenin*$^{del(ex3)/+}$ embryos had little effects on the functional characteristics of axial progenitors, as they were able to keep producing neural tissue and undergo trunk to tail transition to generate the tail bud.

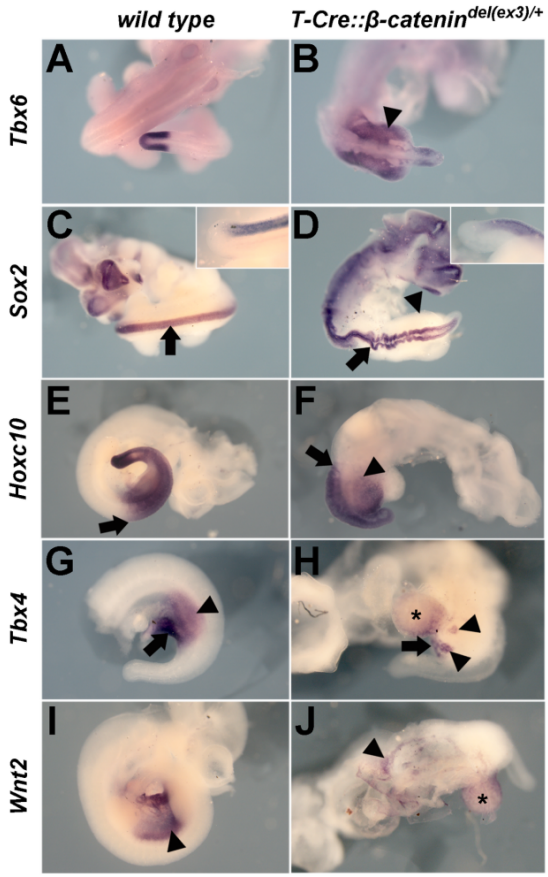

Figure 31. Stabilization of *β*-catenin in mesodermal derivatives results in axial abnormalities. Whole-mount *in situ* hybridization of wild type (A,C,E,G,I) and *T-Cre::β-catenin*$^{del(ex3)/+}$ embryos (B,D,F,H,J) at E10.5. **A,B** Expansion of unsegmented paraxial mesoderm in *T-Cre::β-catenin*$^{del(ex3)/+}$ embryos, as revealed by *Tbx6* expression (*arrowhead*). **C,D** *Sox2* expression evidenced neural tube morphologies (*arrows*). *Arrowhead* indicates unsegmented paraxial mesoderm. **E,F** *Hoxc10* expression. *Arrows* and *arrowheads* mark the anterior border of expression in the neural tube and paraxial mesoderm, respectively. In **E**, these borders are coincident. **G,H** Impairment of hindlimb outgrowth following *β-catenin* stabilization in mesodermal derivatives, as revealed by *Tbx4* expression (*arrowheads*). **I,J** Visceral lateral mesoderm revealed by *Wnt2* expression (*arrowheads*). * marks the ectopic mass of lateral mesoderm.

Overexpression of *Wnt3a* in the epiblast causes severe axial abnormalities

We reasoned that the absence of negative effects on neural tube development in *T-Cre::β-catenin*$^{del(ex3)/+}$ embryos could derive from the absence of activated *β*-catenin in their bipotent N-M progenitors. Consistent with this hypothesis, recombination in the *T-Cre* mouse line used to generate the *T-Cre::β-catenin*$^{del(ex3)/+}$ embryos was essentially detected in the mesodermal compartments with no signs of activity in the neural tube (Perantoni et al., 2005). Therefore, to evaluate the effect of Wnt3a on axial progenitors we generated transgenic embryos in which *Wnt3a* was expressed under the control of an enhancer of the *Cdx2* gene (*Cdx2P-Wnt3a* transgenics). This element has been shown to be active in the posterior epiblast and the PS from early embryonic stages and in a variety of their derivatives (Benahmed et al., 2008; Gaunt et al., 2005). We could only recover a few *Cdx2P-Wnt3a* transgenic embryos at E18.5, which had no obvious abnormalities (not shown). The low proportion of transgenics recovered at this stage suggested early developmental lethality. Consistent with this, most *Cdx2P-Wnt3a* transgenic embryos recovered at E10.5 were strongly malformed and exhibited defective vasculogenesis in the yolk sac, with no evident large blood vessels (Fig. 32A,B). Morphologically, these embryos were grossly normal up to the forelimb bud, but posterior to this level they were much shorter than their wild type littermates (Fig. 32). These malformations were clearly different to those observed in *T-Cre::β-catenin*$^{del(ex3)/+}$ embryos and still contained some recognizable body structures (Figs. 31 and 32). In particular, *Cdx2P-Wnt3a* embryos exhibited lateral protrusions resembling hindlimb buds, as well as small and misshapen paired segmented elements resembling somites. *Cdx2P-*

Wnt3a transgenic embryos failed to rotate, remaining dorsally bent and ventrally open (Fig. 32C-G). These embryos also contained a spherical cellular mass at their caudal end that seemed to be contiguous to other inner embryonic tissues (Fig. 32C-G). This ectopic mass was morphologically similar to the one also observed in *T-Cre::β-catenin*$^{del(ex3)/+}$ embryos (Figs. 31G-J and 32C-G). Globally, the morphological characteristics of *Cdx2P-Wnt3a* transgenic embryos suggested that, despite their strong overall malformations caudal to the forelimbs, they could still preserve a degree of normal patterning.

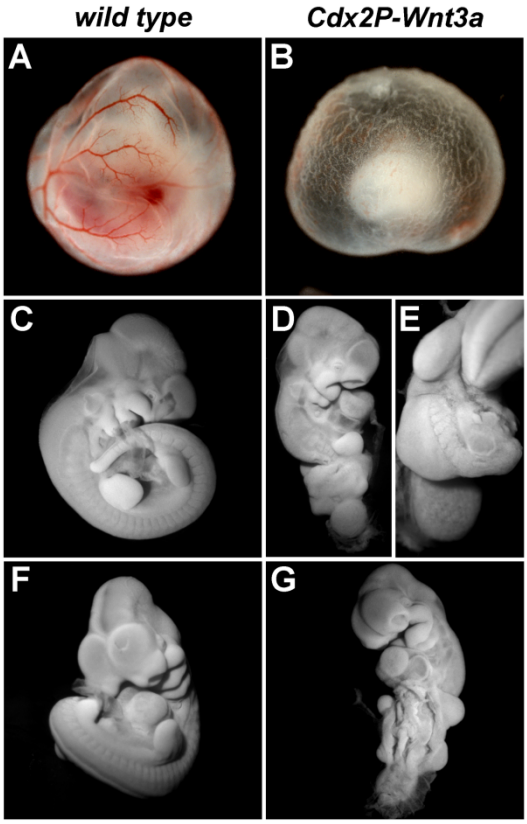

Figure 32. High levels of Wnt3a in the epiblast cause severe abnormalities. A,B Yolk sac morphology of wild type (**A**) and transgenic (**B**) embryos revealed lack of large blood vessels upon high levels of Wnt3a in the epiblast. **C-G** Gross morphology of wild type (**C,F**) and *Cdx2P-Wnt3a* (**D,E,G**) embryos at E10.5. **C,D** Lateral view. **E,F** Dorsal view of the trunk. **G** Ventral view.

High levels of Wnt3a in the epiblast impact axial progenitor behavior and differentiation

To further characterize the nature of the tissues posterior to the forelimb buds in *Cdx2P-Wnt3a* transgenic embryos, we performed an extensive analysis using molecular markers for different embryonic tissues. Expression of the neural primordial marker *Sox2* was strongly downregulated posterior to the forelimbs (Fig. 33A,B), indicating that the contribution of neural tissue to this region was severely compromised. Further analyses of *Cdx2P-Wnt3a* transgenics revealed the presence of all mesodermal compartments in the embryonic tissue posterior to the forelimbs. The identity of the somite-like structures observed in *Cdx2P-Wnt3a* embryos was confirmed by *Uncx4*.1 expression (Fig. 33C-E). In the most posterior somites, this gene was expressed in a striped pattern indicating a relative conservation of AP polarity within these small somites. However, this pattern was lost in more anterior somites within the malformed tissue, suggesting that AP polarity was not maintained in more mature somites (Fig. 33C-E). The compact morphology of the *Cdx2P-Wnt3a* transgenics hampered a proper analysis of the segmentation clock in the PSM. Despite this, the determination front marker *Mesp2* was expressed in single bilateral stripes in the *Cdx2P-Wnt3a* embryos, resembling the pattern observed in wild type littermattes. We observed that *Mesp2* expression pattern, however, was slightly more extended in its AP size in the trasgenics than in wild type embryos (Fig. 33F,G).

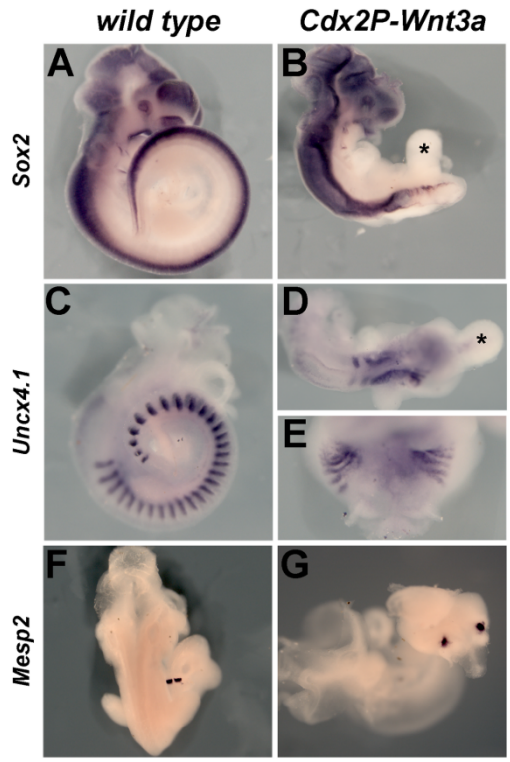

Figure 33. Abnormal neural and mesodermal development upon high levels of Wnt3 in the epiblast. Whole-mount *in situ* hybridization of wild type (A,C,F) and *Cdx2P-Wnt3a* embryos (B,D,E,G) at E10.5. **A,B** Impairment of neural tube development in *Cdx2P-Wnt3a* embryos, as revealed by *Sox2* expression. **C-E** *Uncx4.1* expression reveals abnormal somite morphology in the transgenics. **F,G** *Mesp2* expression reveals the determination front in both wild type and transgenic embryos. * marks the ectopic mass of lateral mesoderm.

In the posterior part of the embryo, the *Uncx4.1* elements surrounded a mass of tissue, which was strongly positive for *Wnt3a*, but negative for the mesodermal markers *T*, *Tbx6* and the *Fgf8* target gene *Spry4* (Fig. 34). This Wnt3a-positive tissue mass exhibited a disorganized morphology and epithelial characteristics (Fig. 34A-B'), suggesting that high levels of Wnt3a in the epiblast have impaired axial progenitor behavior. Conversely, such mesodermal markers were restricted to the most caudal region of the transgenic embryos. It is possible, therefore, that *Wnt3a*-positive cells remained as undifferentiated axial progenitors, while a subset entered the paraxial

mesodermal fate, giving rise to an abnormal PSM still competent to generate somites. When compared to wild type embryos, the PSM of *Cdx2P-Wnt3a* transgenics appeared reduced in its AP length but wider (Fig. 34C-H), which is compatible with their smaller somite size.

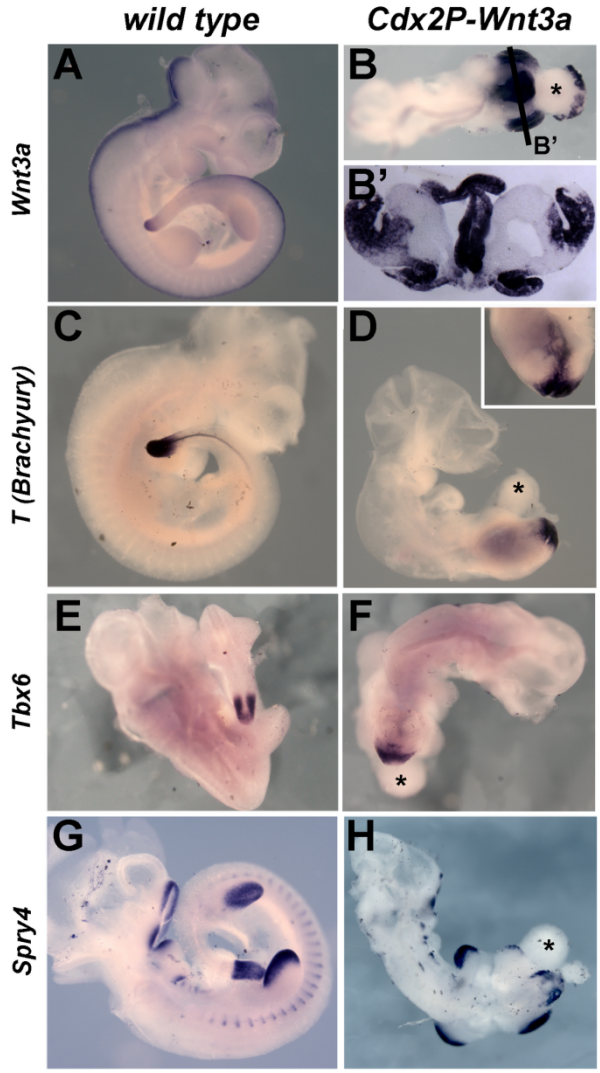

Figure 34. Abnormal paraxial mesoderm morphology in *Cdx2P-Wnt3a* embryos. Whole-mount *in situ* hybridization of wild type (A,C,E,G) and *Cdx2P-Wnt3a* transgenic (B,B',D,F,H) embryos at E10.5. **A-B'** *Wnt3a* expression revealed a posterior region in the *Cdx2P-Wnt3a* transgenics that was negative for other PSM markers (**C-H**) and ectopic expression of *Wnt3a* in the hindlimbs. **B'** Transversal section revealed an epithelial organization of the Wnt3a-positive midline mass. **C,D** Expression of *T*, and **E,F** *Tbx6* expression revealed an abnormal PSM. *Inset* in **D** Ventral view. **G,H** *Spry4* expression identified forelimbs, hindlimbs and the abnormal PSM in *Cdx2P-Wnt3a* transgenics. * marks the ectopic mass of lateral mesoderm.

Altogether, these results indicate that activation of Wnt3a signaling in the epiblast is able to prevent bipotent N-M progenitors from taking a neural fate. This observation is consistent with experiments in the tail bud of the zebrafish (Martin and Kimelman, 2012). However, high levels of *Wnt3a* did not seem sufficient to stimulate the production of paraxial mesoderm from axial progenitors, but seemed to impair their exit from the epiblast. This raises the possibility that additional signals act on these cells to drive the formation of mesoderm. In this context, cells that are able to take a paraxial mesodermal fate produce a relatively functional, but smaller PSM, which preserves to some extent the segmentation program. These observations in *Cdx2P-Wnt3a* embryos are somewhat paradoxical considering the expanded PSM and lack of segmentation observed in *T-Cre::β-catenin*$^{del(ex3)/+}$ embryos (Aulehla et al., 2008). Such discrepancies, therefore, indicate that the corresponding phenotypes might derive from Wnt3a/*β*-catenin activity in different cellular compartments (epiblast and mesodermal derivatives). Alternatively, they may result from the distinct strategies used to activate the Wnt3a/*β*-catenin signaling in the *Cdx2P-Wnt3a* and *T-Cre::β-catenin*$^{del(ex3)/+}$ embryos.

Wnt3a expression in the PSM affects segmentation and somite polarity

To address this issue, we overexpressed *Wnt3a* in the PSM using the msd enhancer of *Dll1* (*Dll1P-Wnt3a* transgenics) (Beckers et al., 2000). High levels of *Wnt3a* in the PSM resulted in much milder phenotypes than those observed in either *T-Cre::β-catenin*$^{del(ex3)/+}$ or *Cdx2P-Wnt3a* embryos (Figs. 31-35). At E10.5, *Dll1P-Wnt3a* embryos extended their

AP axis further than any of the other two types of embryos and preserved many of the normal embryonic characteristics found in wild type littermates. These transgenic embryos contained recognizable somites, although in the most affected cases they were slightly abnormal in shape (Fig. 35A,B). Interestingly, we did not observe the typical stripped pattern of *Uncx4.1* expression in *Dll1P-Wnt3a* embryos (Fig. 35A,B), which indicates compromised somite AP polarity. To analyze the origin of this phenotype, we evaluated *Tbx6* and *Mesp2* expression given their roles in segmentation and in generating AP polarity within the somites (White, 2003). Expression of *Tbx6* in *Dll1P-Wnt3a* transgenics was essentially restricted to the tail bud mesenchyme, but it did not show a sharp anterior border as it typically has in wild type embryos (Fig. 35C,D). Instead, the *Tbx6* domain appeared anteriorly extended, following the expanded expression of *Wnt3a* in these transgenic embryos (Fig. 35E,F). Expression of *Mesp2* extended anteriorly into the somite-containing region of the paraxial mesoderm in *Dll1P-Wnt3a* embryos (Fig. 35G,H), apparently matching the expanded Tbx6 expression domain.

The different phenotypes observed in *Dll1P-Wnt3a* and *T-Cre::β-catenin*$^{del(ex3)/+}$ embryos suggest that excessive Wnt3a signaling in the PSM is still compatible with intersomitic border formation as long as *β*-catenin is susceptible of feedback regulation. However, high levels of Wnt3a in the PSM affected the establishment of proper AP polarity in the somites. Despite these abnormalities, the size of the PSM was apparently unaffected in *Dll1P-Wnt3a* transgenics, suggesting that the reduced PSM observed in the *Cdx2P-Wnt3a* transgenics was most probably derived from Wnt3a activity in the progenitors for the paraxial mesoderm rather than in mesodermal cells themselves.

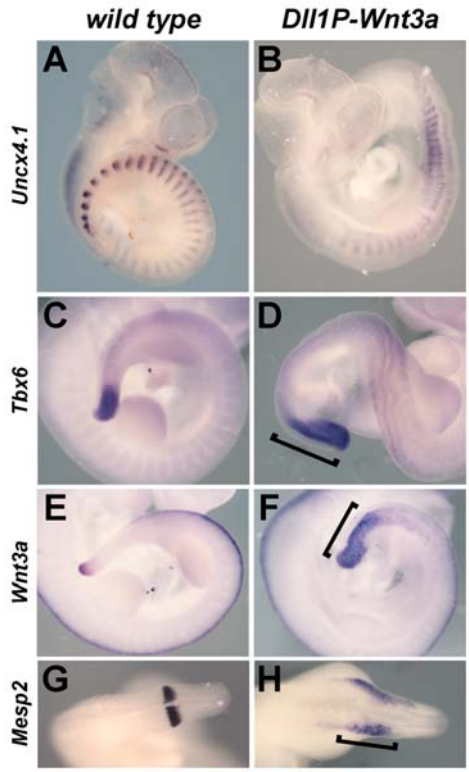

Figure 35. Abnormal segmentation is *Dll1P-Wnt3a* transgenics. Whole-mount *in situ* hybridization of wild type (A,C,E,G) and *Dll1P-Wnt3a* transgenic (B,D,F,H) embryos at E10.5. **A,B** *Uncx4.1* expression revealed loss of AP somite polarity and abnormal somite morphology in the transgenics. **C,D** Expanded PSM in the transgenics, as evidenced by *Tbx6* expression. **E,F** Overexpression of *Wnt3a* in the PSM expanded the Wnt3a gradient in the transgenics. **G,H** Extended domain of *Mesp2* expression in the transgenics. *Brackets* labels extended expression domains.

High levels of Wnt3a in the epiblast impairs axial extension and body organization

We next examined the impact of high levels of *Wnt3a* in the epiblast on trunk-associated tissues other than those derived from N-M progenitors. *Cdx2P-Wnt3a* transgenics contained derivatives of the node and most anterior region of the PS. In particular, expression of *Shh* and *T* revealed a reduced axial mesoderm in length, which apparently split in two longitudinal domains (Figs. 34C,D and 36A,B). We also detected the presence of visceral endoderm as revealed by *Foxa1* expression (Fig. 36C,D). The patterns obtained for this gene were different to

those observed in wild type embryos, most likely reflecting the lack of ventral closure in the transgenics. Interestingly, we observed a strong domain of *Shh* expression at the level of the hindlimb buds (Fig. 36A,B), corresponding to the most posterior limit of *Foxa1* expression (Fig. 36C,D). The location of this *Shh* domain likely identifies the endodermal component of the developing cloaca. However, the strong malformations observed in the *Cdx2P-Wnt3a* transgenics did not allow us to rule out the possibility of an accumulation of axial mesoderm, but the absence of an equivalent concentration of transcripts for *T* seems to argue against it (Fig. 34C,D). If the *Shh*-positive caudal domain indeed corresponds to the cloaca, this would indicate the existence of a degree of AP patterning in the visceral endoderm of *Cdx2P-Wnt3a* transgenics.

Morphological examination of *Cdx2P-Wnt3a* transgenics revealed that, despite their strong malformations, these embryos contained forelimb and hindlimb buds (Fig. 37A-D). We confirmed their presence by expression of several markers, including the *Fgf8* target gene *Spry4*, as well as *Tbx5*, *Tbx4* and *Hand2* (Figs. 34G,H and 37A-F). The restricted expression of *Tbx5* and *Tbx4* to the forelimb and hindlimb buds respectively indicates conservation of at least some regional specific characteristics along the AP axis of the *Cdx2P-Wnt3a* embryos (Fig. 37A-D). In addition to the limb buds, *Cdx2P-Wnt3a* transgenics also contained other components of the lateral mesoderm, as shown by the expression of *Hand2* and *Wnt2* (Fig. 37E-H). Moreover, *Tbx4* expression extended into ventral tissues between the hindlimb buds, suggesting the presence of ventral lateral mesoderm involved in the development of the cloacal structures. This observation supports that the *Shh*-positive domain in this area can indeed represent the endodermal component of the cloaca.

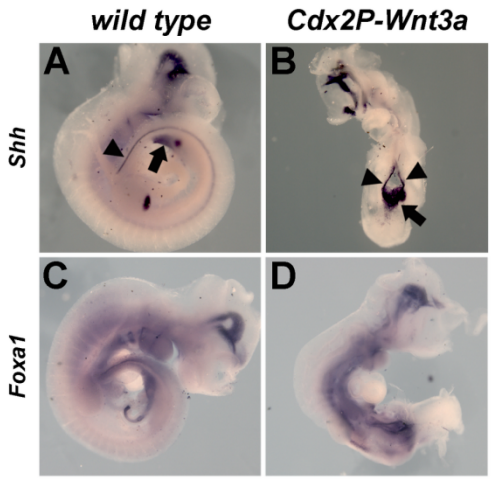

Figure 36. Impaired ventral closure in *Cdx2P-Wnt3a* transgenics. Whole-mount *in situ* hybridization of wild type (A,C) and *Cdx2P-Wnt3a* transgenic (B,D) embryos at E10.5. **A,B** *Shh* expression revealed an apparent split in axial mesoderm of transgenic embryos (*arrowheads*). *Arrows* mark the endodermal component of the developing cloaca. **C,D** Expression of *Foxa1* revealed disorganized visceral endoderm in the transgenics.

Interestingly, the spherical mass of tissue at the caudal end of *Cdx2P-Wnt3a* transgenic embryos was positive for *Wnt2* and *Tbx4* (Fig. 37C,D,G,H), suggesting that it could represent an ectopic outgrowth of lateral mesoderm. Immunostaining with the endothelial marker PECAM-1 revealed that this structure is formed by a complex vascular plexus (Fig. 37I). These characteristics indicate that this mass represents an ectopic accumulation of lateral mesoderm-derived tissue. A similar *Wnt2* and *Tbx4*-positive mass was also observed in *T-Cre::β-catenin*$^{del(ex3)/+}$ embryos (Fig. 31G-J), suggesting that stabilization of *β*-catenin in mesodermal derivatives causes improper production of lateral mesoderm. Lastly, the presence of intermediate mesoderm in *Cdx2P-Wnt3a* transgenic embryos was indicated by the stripe of *Pax2* expression lateral to the somites (Fig. 37J,K).

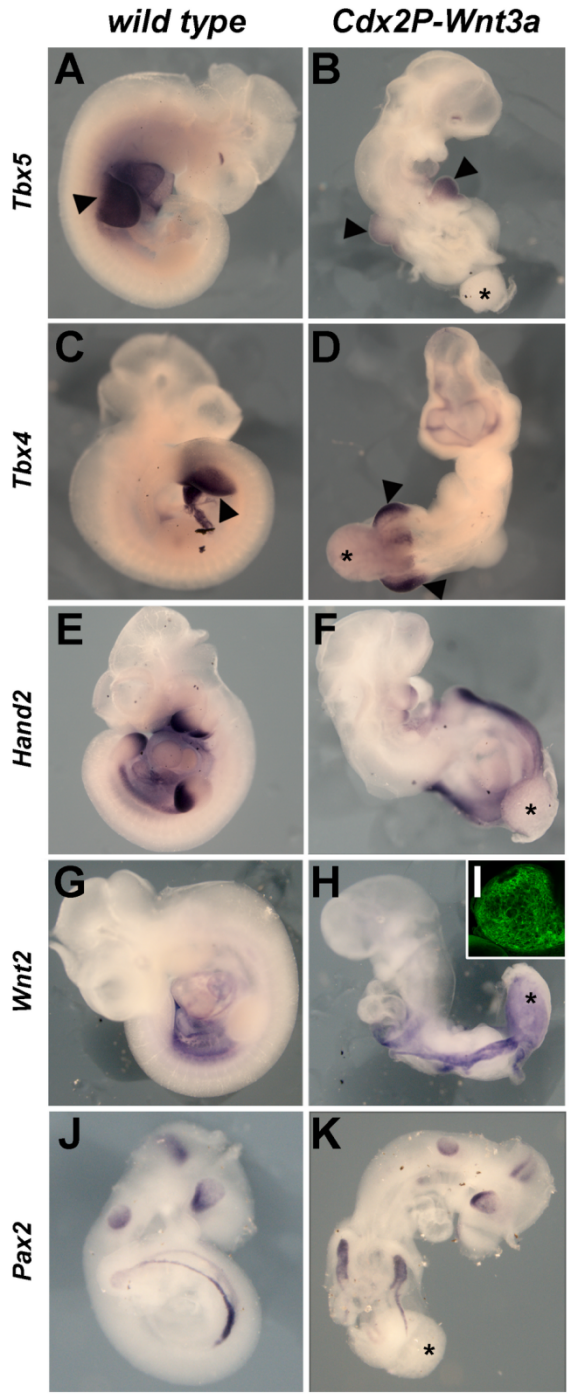

Figure 37. Abnormal mesoderm formation upon high levels of Wnt3a in the epiblast. Whole-mount *in situ* hybridization of wild type (A,C,E,G,J) and *Cdx2P-Wnt3a* embryos (B,D,F,H,I,K) at E10.5. **A,B** Forelimb identification by *Tbx5* expression. **C,D** Hindlimb identification by *Tbx4* expression. **E-H** Lateral mesoderm evidenced by *Hand2* (**E,F**) and *Wnt2* (**G,H**) expression. The ectopic mass of caudal tissue (*asterisk*) also expresses these two genes. **I** PECAM-1 immunostaning revealed a complex vasculature network in this ectopic mass. **J,K** Intermediate mesoderm identification by *Pax2* expression.

Wnt3a induces posterior Hox genes in the mouse

The compressed morphology of *Cdx2P-Wnt3a* embryos suggests that posterior differentiation programs are precociously activated upon high levels of Wnt3a in the epiblast. Despite their severe phenotypes, embryonic structures seemed to be formed in a proper AP sequence, raising the possibility that Wnt3a causes a global posteriorization of the body in these transgenics. We then examined the expression of trunk and tail Hox genes to evaluate the impact of increased Wnt3a levels on the AP patterning of the body, focusing on posterior Hox genes as they label posterior body structures.

Expression of *Hoxa9* in *Cdx2P-Wnt3a* transgenics followed a pattern that resembled the one observed in wild type embryos. In particular, it was detected in the forelimb bud and extended over the interlimb lateral mesoderm at lower levels to become stronger again at the level of the hindlimb bud (Fig. 38A,B). In more medial structures, *Hoxa9* expression was observed at very high levels in the tissue posterior to the forelimb bud in *Cdx2P-Wnt3a* transgenics (Fig. 38A,B). *Hoxc10* expression was also expressed in midline structures at very high levels in the area that corresponds to the *Wnt3a*-positive mass of *Cdx2P-Wnt3a* transgenic embryos (Fig. 38C,D). Interestingly, when compared to *Hoxa9* expression, the anterior border of *Hoxc10* expression was located at a more posterior axial level than the one observed for *Hoxa9*, similar to what was observed in wild type embryos (Fig. 38A-D). In addition, the anterior expression border of *Hoxc10* expression in midline structures of *Cdx2P-Wnt3a* transgenic embryos coincided with the anterior expression border in more lateral structures, which could represent the paraxial and lateral mesoderm (Fig. 38C,D). In this latter structure, *Hoxc10* expression coincides with

the hindlimb bud, thus also reproducing the expression patterns observed in wild type embryos (Fig. 38C,D). These observations indicate that despite the strong morphological alterations observed in *Cdx2P-Wnt3a* transgenics, Hox gene expression still preserved some of its normal characteristics, including their collinear activation and their relationship to specific morphological landmarks. In addition, it is clear that the overall position of the anterior borders of *Hoxa9* and *Hoxc10* expression was more anteriorly located in *Cdx2P-Wnt3a* transgenics than in wild type embryos, which could indicate a global posteriorization of the embryo caudal to the forelimb bud.

We have recently shown that Gdf11 signaling is a major coordinator of the trunk to tail transition, also acting in the axial progenitors (chapter 2). We therefore reasoned that if *Cdx2P-Wnt3a* transgenic embryos are posteriorized, the activity of Wnt3a could be mediated by Gdf11 signaling. *Gdf11* was expressed in the area of the *Cdx2P-Wnt3a* transgenics roughly corresponding to the PSM at levels that were not very different from those observed in wild type embryos (Fig. 38E,F). This indicates that at least the accumulation of *Gdf11* transcripts is not affected by the overexpression of *Wnt3a*. To further test this hypothesis, we compared the levels of phosphorylated Smad2/Smad3 in the posterior region of *Cdx2P-Wnt3a* and wild type littermates. Western blot analysis indicated that phosphorylated Smad2/Smad3 levels in *Cdx2P-Wnt3a* embryos were actually significantly lower than in the wild type embryos (Fig. 38G). Together, these findings indicate that if Wnt3a activity posteriorizes the embryo caudal to the forelimb bud, it does it most probably through a mechanism that does not involve activation of Gdf11/Alk5 signaling.

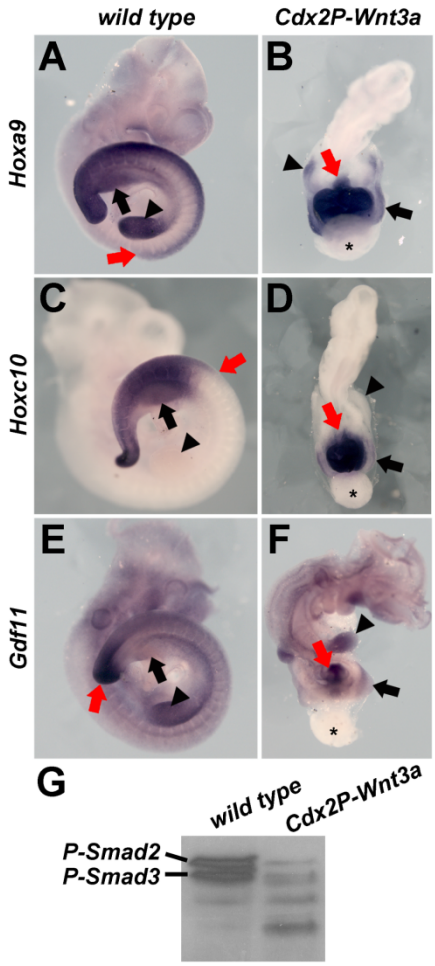

Figure 38. Wnt3a affects AP patterning of the body without perturbing *Gdf11* expression. Whole-mount *in situ* hybridization of wild type (A,C,E) and *Cdx2P-Wnt3a* embryos (B,D,F) at E10.5. **A,B** *Hoxa9* expression. **C,D** *Hoxc10* expression. *Red arrows* mark the anterior boundary of Hox expression in the neural tube. **E,F** Expression of *Gdf11* is unaffected upon high levels of Wnt3a in the epiblast. *Red arrows* mark the PSM-like structure. *Arrowheads* mark forelimb position. *Arrows* mark the hindlimbs. **G** Western blot analysis of P-Smad2/3 levels in the posterior embryonic region upon overexpression of Wnt3a in the epiblast.

IV.4 - Discussion

Wnt3a levels influence distinct cell fate decisions during axial extension

Our findings indicate that the tissues posterior to the forelimb bud of *Cdx2P-Wnt3a* embryos are mostly composed of mesodermal and

endodermal derivatives, at the expense of neural tissue. These observations are consistent with previous findings in zebrafish (Martin and Kimelman, 2012). Although overtly malformed, affected tissues still preserved a high degree of organization both in the AP and medial-lateral axes, producing a structure that could be regarded as a compressed version of the equivalent area of a wild type embryo. We were able to identify all mesodermal compartments in *Cdx2P-Wnt3a* transgenics, indicating that Wnt3a activity is not incompatible with mesodermal production. Conversely, a strong Wnt3a-positive tissue in the medio-posterior region of these embryos was clearly negative for all tested mesodermal markers, suggesting that this tissue comprise undifferentiated epiblast progenitors that fail to ingress through the PS. In this case, it is possible that Wnt3a activity on its own is not sufficient to promote the formation of mesoderm from these progenitors, but might require the concerted activity of other factors. These findings also indicate that the Wnt3a-mediated inhibition of neural fates does not require activation of the mesodermal program.

Genetic studies in the mouse indicate that activation of *Tbx6* is essential for bipotent N-M progenitors to give rise to paraxial mesoderm. While the activation of *Tbx6* seems to require Wnt3a activity (Dunty et al., 2008; Hofmann et al., 2004; Yamaguchi et al., 1999), *Tbx6* expression is only weakly detected in the epiblast, regardless of the presence of *Wnt3a* in this structure (Takemoto et al., 2011). Only after cells ingress through the PS, *Tbx6* expression become strong (Takemoto et al., 2011). Therefore, the factors that collaborate with Wnt3a to produce paraxial mesoderm might be connected to the transit of prospective mesodermal cells through the PS. In the case of the *Cdx2P-Wnt3a* transgenics, even with the concomitant blocking in

the formation of neural tissue, the absence of extra paraxial mesoderm might reflect an impairment in cell ingression through the PS. As a consequence, those cells would stay in an epithelial-like structure directly derived from the epiblast where the progenitors are originally localized.

Does Wnt3a signaling in the epiblast lead to global body posteriorization?

The compressed structure of the *Cdx2P-Wnt3a* embryos posterior to their forelimb buds, with the maintenance of a considerable degree of normal AP and dorso-ventral (medio-lateral in this case) patterns, raises the possibility that this phenotype resulted from a global posteriorization caudal to the forelimbs. The relative position of hindlimb buds in these embryos is compatible with this hypothesis, since they were located closer to the forelimbs than in wild type embryos. Similarly, the anterior expression borders of *Hoxa9* and *Hoxc10* also looked anteriorly displaced when compared to wild type littermates, also fitting the interpretation of global posteriorization. This could mean that Wnt3a signaling produces a precocious activation of Hox gene expression, which would be in accordance to previous reports showing that Hox gene expression can indeed be stimulated by Wnt signaling (Klapholz-Brown et al., 2007; Lengerke et al., 2008).

However, it should be noted that the same phenotypic characteristics could be explained according to an alternative hypothesis. In particular, it is clear that formation of the tissues more relevant to AP axis extension, such as the neural tube and the paraxial mesoderm, were compromised to a large extent in *Cdx2P-Wnt3a* transgenics. In addition, the progenitors seemed to accumulate in a

folded epithelial structure that did not undergo extensive posterior extension. Under these conditions, progressive establishment of "normal patterns" (like Hox gene activation) in the tissues derived from axial progenitors would not unfold properly along the AP axis, but would rather become trapped within the abnormal epithelial folds, giving a false impression of posteriorization. The production of lateral mesoderm seemed somewhat less compromised in these embryos, which resulted in the formation of recognizable structures, most particularly the hindlimbs. Under the conditions imposed to the progenitor derivatives, the absolute position of the hindlimb buds would then also be closer to the forelimb buds, but just as a result of physical constraints rather than to their more anterior induction. Differentiation between these possibilities is not simple, as it is not the design of experimental approaches that would allow to definitely solve this issue.

Intrinsic cell properties may determine Wnt3a/*β*-catenin activity in the epiblast and the paraxial mesoderm

The effect that we observed for Wnt3a in the epiblast contrasts with its ability to promote *Tbx6* expression when present in the PSM. This indicates that after cells had already taken a paraxial mesodermal fate, Wnt3a/*β*-catenin signaling is able to promote and/or maintain the mesodermal program. Interestingly, however, during normal development, *Wnt3a* transcripts are downregulated as newly produced cells leave the PS (Takemoto et al., 2011). Such downregulation is most likely mediated by Tbx6 activity, as it does not occur in *Tbx6* mutants (Takemoto et al., 2011). It is possible that the transcriptional block of *Wnt3a* in the cells as they enter the PSM is in the origin of the

posterior to anterior gradient of Wnt3a/*β*-catenin activity through the PSM (Aulehla et al., 2008). In this case, this would follows a mechanism similar to that described for Fgf8 (Dubrulle and Pourquié, 2004a).

Altogether, these results indicate a sequential activity of Wnt3a-mediated signals during the production of the paraxial mesoderm. In a first step, Wnt3a might be required to balance the decision of bipotent N-M progenitors to produce nervous tissue or mesoderm. In this case, those cells exposed to higher Wnt3a levels would be prevented from taking a neural fate and would become competent to respond paraxial mesoderm-inducing signals when in contact with the PS. This is consistent with the phenotype of the *Wnt3a* mutant embryos, which contain an excess of neural tissue at the expense of paraxial mesoderm (Takada et al., 1994; Yoshikawa et al., 1997). Thus, the known role of Wnt3a/*β*-catenin signaling in participating in the determination front during somitogenesis would only become activated after cells entered the PSM (Pourquié, 2011).

It has been described that *Wnt3a* is expressed in the prospective PSM area of *Tbx6* mutants, although this region differentiates into neural tissue (Takemoto et al., 2011). From this phenotype, it is patent that Tbx6 is required for repressing neural fates in this tissue. However, the role that Wnt3a plays in this process is still obscure. The coexistence of neural tissue with Wnt3a expression suggests that, contrary to what happens in the axial progenitors, Wnt3a might not be able to block neural programs in cells after ingression through the PS. It is not clear if this is the consequence of the requirement of Tbx6 for such inhibition or if it derives from intrinsic properties of the cells after they transit through the PS. Although it is not possible to properly

evaluate these possibilities on the basis of currently available data, our observation that Wnt3a blocks neural differentiation without activation of *Tbx6* in *Cdx2P-Wnt3a* transgenics gives some support to the second possibility.

An important characteristic of the *Cdx2P-Wnt3a* transgenics is that their phenotype is mostly restricted to the embryonic area posterior to the forelimb bud. This could be the consequence of the activity of the *Cdx2P* enhancer. However, this regulatory element has been reported to be already active in the mouse posterior epiblast as early as E7.5 (Benahmed et al., 2008; Gaunt et al., 2005). Alternatively, it might reflect intrinsic properties of axial progenitors populating the epiblast before or after the axial level of the forelimb. This explanation is consistent with the phenotype of the *Wnt3a* mutant embryos, which also affects embryonic tissues posterior to the forelimb bud (Takada et al., 1994). If this is the case, it would suggest the existence of a major switch in tissue competence at this axial level. Interestingly, there are several other mutant phenotypes that share this characteristic with *Wnt3a* mutants and *Cdx2P-Wnt3a* transgenic embryos. For instance, in the absence of genes like *Raldh2*, *T, Tbx6* or in compound *Cdx* mutants, development proceeds up to the level of the first few somites, but gets arrested posterior to this level (Chapman and Papaioannou, 1998; Herrmann et al., 1990; Mic et al., 2002; Niederreither et al., 1999; van Rooijen et al., 2012). These observations indicate that axial extension through the forelimb bud level might be accompanied by relevant changes in functional properties of the new tissue. This view is also supported by the differential mode of notochord production during axis elongation (Yamanaka et al., 2007). In this context, *Raldh2* mutants have special relevance, because their phenotype can be rescued to a

large extent when exogenous administration of RA is provided at the precise embryonic stage in which their development becomes arrested (Mic et al., 2002; Niederreither et al., 1999, 2000, 2001). Therefore, it is possible that RA activity might be required for eliciting the transition in cell competence at this axial level. Experiments are currently in progress to address this hypothesis.

IV.5 - Material and Methods

Transgenic constructs, mice and embryos

T-Cre::β-catenin$^{del(ex3)/+}$ embryos were generated as previously described (Aulehla et al., 2008). Transgenic constructs were generated by cloning the mouse *Wnt3a* cDNA (NM_009522) downstream of the 9.5 kb fragment enhancer of the *Cdx2* gene (Benahmed et al., 2008) or the msd enhancer of *Dll1* (Beckers et al., 2000) using standard molecular biology techniques. Constructs were released from plasmid sequences, gel purified and used to generate transgenic embryos by pronuclear microinjection. Embryos were collected by cesarean section, fixed in 4% PFA and analyzed by whole mount *in situ* hybridization as previously described (Kanzler et al., 1998). See *in situ* probe information in chapter 2 (page 129). Morphological examination using the carmine staining technique was performed as previously described (chapter 2). Genotyping was performed as described in chapter 2, using primers summarized in Table 4.

Table 4. Primer information for genotyping.

Gene	Forward	Reverse
Wnt3a	GAGGAATGGTCTCTCGGGAG	CTTGAAGTACGTGTAACGTGGC
Ctnnb1	TAGCTGCAGGGGTCCTCTGTG	GGCACCAATGTCCAGTCCAAG

Whole-mount immunostaining

For whole-mount PECAM-1 immunostaining, PFA-fixed embryos were washed in PBS, dehydrated and rehydrated in methanol/PBT series, and washed twice in PBT. Embryos were blocked overnight in a 1% BSA+0.5% Tween-20 solution in PBS at 4º C, under agitation. They were then washed three times in PBT and incubated overnight in the primary antibody solution (1/100 PECAM-1/CD31 diluted in 0.5%BSA+0.25% Tween-20 in PBS) at 4º C, under agitation. Embryos were then washed thoroughly in PBS at room temperature and incubated overnight in the secondary antibody solution (1/100 goat anti-rat Alexa488 diluted in 0.5%BSA+0.25% Tween-20 in PBS) at 4º C, under agitation and protected from the light. They were washed thoroughly in PBS at room temperature, in the dark, and dehydrated in a methanol/PBT series. Then, embryos were cleared in a methyl salicylate/methanol series and imaged by laser scanning confocal microscopy (Zeiss LSM-510 Meta).

IV.6 - Acknowledgments

We would like to thank José Belo, Jacqueline Deschamps, Denis Duboule, Achim Gossler, Bernhard Herrmann, Andreas Kispert, Malcolm Logan, Andrew McMahon and Erik Olson for sending plasmids containing regulatory elements and probes for *in situ* hybridization. This work was supported by grants PTDC/BIA-BCM/110638/2009 and PTDC/SAU-BID/110640/2009 to M.M. and by PhD fellowships SFRH/BD/33562/2008 to A.D.J. and SFRH/BD/51876/2012 to R.A.

Author contributions: A.D.J. and M.M. designed research; A.D.J., R.A., J.E.R., A.A. and M.M. performed research; A.N. performed pronuclear microinjection of DNA constructs; A.D.J. and M.M. analyzed data; and A.D.J. and M.M. wrote the paper.

Chapter V – Final considerations

"El conocimiento es como navegar en un océano de incertidumbre entre archipiélagos de certeza"

Edgar Morin

Final considerations

The posterior extension of the vertebrate AP axis is a complex process, involving the generation of different tissue derivatives with specific patterning information (AP, DV and LR). At the same time, a pool of progenitor cells must remain undifferentiated to sustain further tissue production. Any imbalance between these two processes may lead to embryo lethality usually due to circulatory abnormalities or the precocious termination of the AP axis. The work presented in this thesis aimed at investigating mechanisms controlling the formation of the posterior vertebrate body. More specifically, three main processes were focused during the course of this research: 1) mesoderm production, 2) regional patterning of the body, and 3) behavior of axial progenitors.

V.1 - Mesoderm production

Mesoderm arises initially from the ingression of epiblast cells through the PS and then from the activity of the tail bud (Wilson et al., 2009). Our results suggest that high levels of Wnt3a in the epiblast impair axial progenitor differentiation into neural tissue. Surprisingly, although mesoderm production was not impaired, overexpression of Wnt3a did not induce large amounts of mesoderm from these epiblast cells. The effects were somewhat different in the various mesodermal compartments. Paraxial mesoderm seemed to be the most affected as these embryos only had a small PSM and small somites. Globally, formation of lateral mesoderm seemed less affected by Wnt3a overexpression, since most of the typical structures derived from this compartment were identifiable, such as the hindlimb buds and the ventral lateral mesoderm. These observations are compatible with the

fate-mapping of the PS, in which more posterior regions (exposed to higher Wnt3a levels) give rise to lateral mesoderm and more anterior regions (exposed to lower Wnt3a levels) contribute to paraxial mesoderm (Fig. 39) (Lawson et al., 1991; Tam and Beddington, 1987; Wilson and Beddington, 1996). It is possible, therefore, that lateral mesoderm is less susceptible to higher Wnt3a levels. Interestingly, we found evidence that part of the lateral mesoderm also became delocalized in the *Cdx2P-Wnt3a* transgenics. This conclusion was based on the presence of a caudal accumulation of vascularized tissue with lateral mesoderm characteristics (*e.g.* expression of *Wnt2*, *Hand2* and *Tbx4*) in these embryos. If this is indeed the case, this impact on the lateral mesoderm could have resulted from the inability of cells to properly migrate away to more anterior regions. In agreement with this, Sweetman et al. (2008) have described that Wnt3a inhibits cell migration from the posterior PS in the chicken. Alternatively, this ectopic mass could have also derived from the accommodation of an excess of lateral mesoderm into a smaller region in the *Cdx2P-Wnt3a* transgenics. Recently, Martin and Kimelman (2012) have shown that committed mesoderm differentiates into blood endothelium in the absence of Wnt3a. As the ectopic aggregate is no longer exposed to Wnt3a, a similar mechanism could be in the origin of the increased formation of blood vessels in this tissue.

The observation that Wnt3a alone cannot induce mesoderm from epiblast cells suggests that specification of mesoderm requires the concomitant activity of other signaling pathways. It is also possible that the *Cdx2P-Wnt3a* phenotype results from the inability of induced mesoderm to ingress through the PS. A likely candidate to act in synergy with the Wt3a/*β*-catenin pathway is the FGF signaling, because

inactivation of *Fgf8* or *Fgfr1* results in the arrest of embryo development at the gastrulation stage due to the accumulation of cells in the epiblast (Ciruna and Rossant, 2001; Ciruna et al., 1997; Deng et al., 1994; Guo and Li, 2007; Sun et al., 1999; Yamaguchi et al., 1994). In addition, *Fgf8* is able to induce the expression of the nascent mesoderm marker *T* (Fletcher et al., 2006; Guo and Li, 2007). Further experiments need to be carried out to examine the impact of FGF signaling or other pathways in conjunction with Wnt3a/*β*-catenin signaling during mesoderm formation.

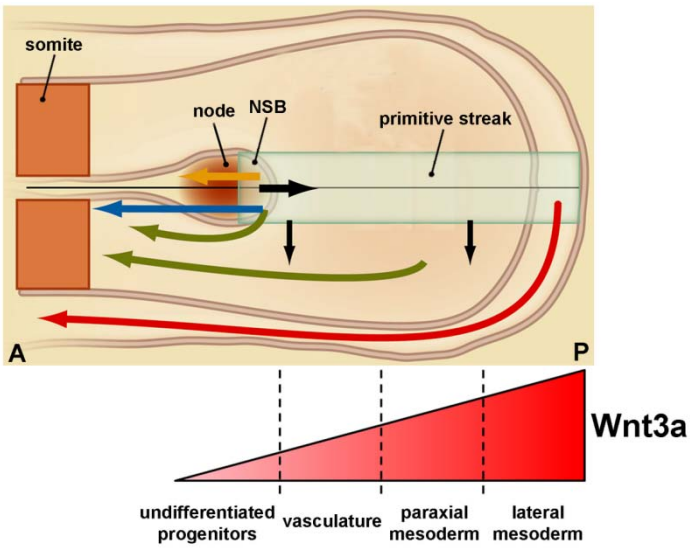

Figure 39. A model for Wnt3a activity in the primitive streak. A posterior (P) to anterior (A) gradient of Wnt3a results in the differentiation of distinct compartments during early axial extension. The switch in the mode of tissue production during trunk to tail transition may lead to a different requirement of Wnt3a activity to sustain undifferentiated axial progenitors. See Figure 40 and text for further information. Vasculature differentiation occurs as specified lateral mesoderm leave regions under the influence of high levels of Wnt3a (adapted from Ramkumar and Anderson, 2011).

The inability of Wnt3a to produce paraxial mesodermal upon overexpression in the epiblast seems contradictory with the observation that zebrafish tailbud cells take a mesodermal fate upon activation of the Wnt/*β*-catenin pathway (Martin and Kimelman, 2012). A possible

explanation for these distinct observations is the difference in target tissues. In the *Cdx2P-Wnt3a* transgenics, the target tissue encompasses progenitors in the epiblast, which exhibit epithelial characteristics (Fig. 39). In turn, the zebrafish tail bud harbors mesenchymal progenitor cells. Therefore, the switch in the mode of tissue production during the trunk to tail transition might influence the response of axial progenitors to Wnt3a levels. In particular, axial progenitors in the epiblast are initially exposed to different levels of Wnt3a, whereas bipotent N-M progenitors occupy a region (the NSB) with low levels of Wnt3a (Fig. 39). After the trunk to tail transition, N-M progenitors are reallocated to a region (the CNH) with high levels of Wnt3a (Fig. 40). Whether this is the case, it remains to be experimentally evaluated.

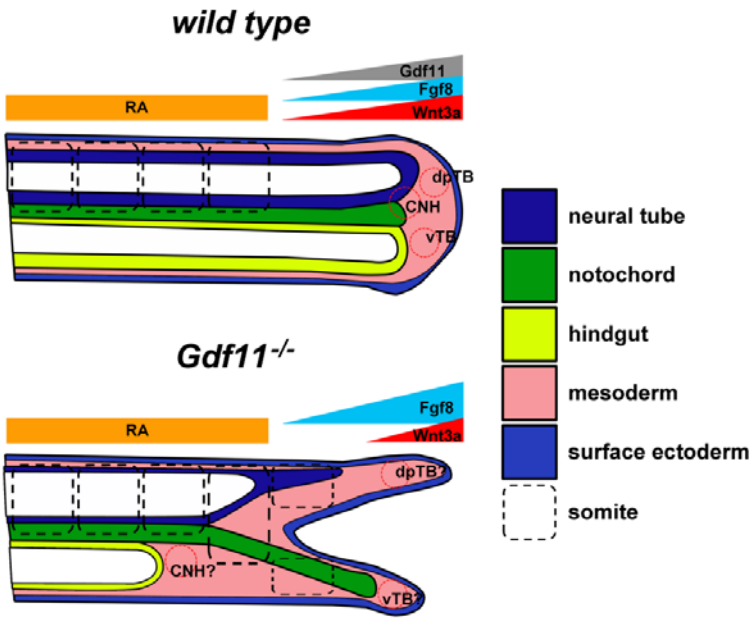

Figure 40. A model for tail bud organization in the mouse. Schematic representation of wild type (*top*) and *Gdf11* mutant split (*bottom*) tails. Loss of *Gdf11* (*gray triangle*) leads to the segregation of tail bud cells and abnormal formation of neural tube (*dark blue*), notochord (*green*) and hindgut (*yellow*), in addition to an increase in *Fgf8* expression (*light blue triangles*) and decrease in *Wnt3a* expression (*red triangles*). *CNH* cordoneural hinge, *dpTB* dorso-posterior tail bud, *vTB* ventral tail bud.

We found that high levels of Wnt3a in the epiblast impacts somitogenesis, reducing somite size. This could be due to a reduction in the production of paraxial mesoderm from the epiblast or to an impact in the length of gene oscillations in the PSM. In this context, Gibb et al. (2009) have reported that Wnt/*β*-catenin signaling controls the periodicity of the segmentation clock in chick and mouse. In particular, downregulation of the Wnt/*β*-catenin pathway by using a pharmacological inhibitor of the casein kinase 1 resulted in an increase in the oscillatory period of *Lfng* expression. In the complementary experiment, however, they showed that exogenous Wnt3a only accelerated *Lfng* oscillations in very few cases (Gibb et al. 2009). Although we have not assessed *Lfng* expression in our *Cdx2P-Wnt3a* transgenics due to their strong axial phenotype, it is possible that the reduced level of Wnt3a in the PSM of *Cdx2P-Wnt3a* transgenics caused a reduction in the cycling period of *Lfng* and resulted in smaller somites. Alternatively, the small somites of *Cdx2P-Wnt3a* transgenics could have also resulted from the smaller PSM, which would affect the gradients (*e.g.* FGF) involved in somitogenesis and impact the number of cells contributing for every new somite. Further experiments are being performed to examine these possibilities.

Our findings also revealed the involvement of Wnt3a signaling in producing somites with proper AP polarity. Interestingly, both intersomitic border formation and somite AP polarity have been previously shown to depend on similar mechanisms involving Notch signaling, *Tbx6* and *Mesp2* (Morimoto et al., 2005, 2006; Oates et al., 2005; Oginuma et al., 2008, 2010; Rodrigues et al., 2006; Saga, 2007). However, how they specifically affect each process is less clear.

The different phenotypes observed in *Dll1P-Wnt3a* and *T-Cre::β-catenin*$^{del(ex3)/+}$ embryos suggest that intersomitic border formation requires that *β*-catenin proteins are susceptible for feedback regulation. Interestingly, our embryos overexpressing *Wnt3a* in the epiblast (*Cdx2P-Wnt3a* transgenics) or a constitutive active form of *β*-catenin in distinct mesodermal compartments (*T-Cre::β-catenin*$^{del(ex3)/+}$ embryos) exhibited some similar abnormalities, such as shortening of the AP axis and an ectopic mass of lateral mesoderm tissue. These observations led us to the conclusion that most of the abnormalities found in *Cdx2P-Wnt3a* embryos resulted from the stabilization of *β*-catenin in mesodermal derivatives.

V.2 - Axial extension and regionalization of the body

The observation that vertebrates bearing extended trunks frequently exhibit loss of the hindlimbs lead us to investigate a common mechanism controlling the transition from trunk to tail and the specification of hindlimb position. Based on our results, we speculate that the positioning of the limbs along the body marks the switch in the mode of tissue generation during AP axis extension. According to our findings, the emergence of hindlimbs and cloaca results from the terminal differentiation of lateral mesoderm progenitors associated with the transition from trunk to tail (Fig. 41). Intriguingly, production of the forelimbs is somehow connected with the induction of the heart field from the lateral mesoderm, roughly coinciding with the neck to trunk transition (see Waxman et al., 2008; Zhao et al., 2009). Together, these observations raise the intriguing possibility that limb induction may mark the switch in the mode of tissue production during vertebrate axial extension, dividing body formation in three phases. The first

phase would comprise the production of the head and the neck, whereas the second and third phases regard the formation of the trunk and the tail, respectively. Thus, the forelimbs would mark the onset of lateral mesoderm production and the head-neck to trunk transition, whereas the hindlimbs would mark the termination of lateral mesoderm formation and the switch from trunk to the production of tail tissues.

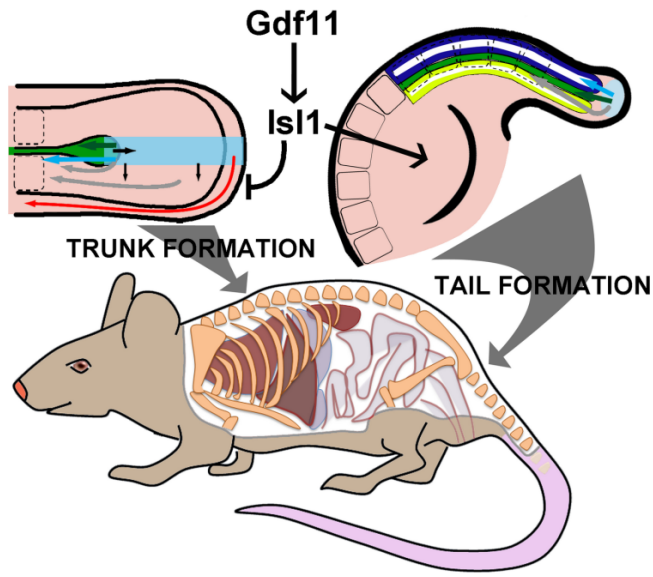

Figure 41. A model for trunk to tail transition in the mouse. Schematic representation of the activity of Gdf11 in activating *Isl1* expression in axial progenitors during the switch in the mode of tissue production from the primitive streak (*light blue rectangle* in the left) to the tail bud (*light blue ellipse* in the right). *Isl1* leads to the terminal differentiation of lateral mesoderm progenitors (*red arrow* in the left) and the induction of hindlimbs and cloaca (in the right). *light blue arrow* indicates neural tube production (in *dark blue* in the right), *dark green arrow* indicates notochord formation (in *green*), *light gray arrows* indicate somites (*dashed and solid boxes*). *Top left* Dorsal view of the posterior region of an E8.5 embryo. *Top right* Lateral view of the posterior region of an E10.5 embryo. *Bottom* Scheme of an adult mouse, highlighting the skeleton system and trunk-associated organs.

Such scenario implies that production of the body is regionally different along the AP axis. This idea is compatible with a number of observations. For instance, head development includes the participation of neural crest cells, which are responsible for making a large part of the head skeleton (Cordero et al., 2011; Le Douarin and Dupin, 2012;

Helms and Schneider, 2003). Accordingly, the head mesoderm and the first seven-eight somites, which give rise to the occipital and cervical areas, are produced in a variety of mouse mutants, such as *T*, *Wnt3a*, *Tbx6* and *Raldh2* or *Cdx* compound mutants, whereas their subsequent axial development is blocked (Chapman and Papaioannou, 1998; Herrmann et al., 1990; Mic et al., 2002; Niederreither et al., 1999; van Rooijen et al., 2012; Takada et al., 1994; Wilson and Beddington, 1997; Yoshikawa et al., 1997). Likewise, the regionalized mode of notochord morphogenesis also fits this hypothesis (Yamanaka et al., 2007). The results presented in this thesis can be also interpreted according to this model, as our transgenics typically failed to show evident abnormalities anterior to the forelimbs. However, this characteristic could have resulted from a tissue-restricted activity of the *Cdx2* enhancer used in our studies, although previous characterization of this promoter seems to argue against this possibility (Benahmed et al., 2008; Gaunt et al., 2005). Additionally, we cannot exclude the possibility that tissues anterior to the forelimbs are not competent to respond to the genes used in our experiments. This would imply a change in tissue competence at the level of the forelimb bud, which matches the transition from neck to trunk. In this respect, it should be also noted that we never found *Cdx2P-Isl1* transgenics with hindlimbs closer than 6 somites to the forelimb buds or with axial truncations anterior to the 8th thoracic segment. This may indicate the existence of a change in competence at this axial level. On the other hand, using the same experimental conditions, we were able to induce hindlimb buds closer to the forelimbs by overexpressing $Alk5^{CA}$. Considering that Gdf11 signaling participates in the induction of *Isl1*, this raises the possibility that tissue competence to respond to *Isl1* is provided by

Gdf11. Whether this is the case as well as the mechanisms mediating this gain of competence were not addressed in this thesis.

The diversity of vertebrate body plans could be explained on the basis of this three phase hypothesis. For instance, the long necks of birds would have arisen from an extended first phase, whereas their short tails would have resulted from a reduced third phase. Snakes, on the other hand, would have a very restricted first phase, an extended second phase and a short third phase. In turn, lizards would have fairly regular first and second phases, but an increased third phase. Hence, the modularity in the production of these anatomical regions could provide the grounds for the evolution of morphological diversity within the vertebrates by simply affecting the length of each phase during axial extension.

Our results indicate that the Gdf11-Alk5-Smad-Isl1 pathway might be within the functional core determining the position of the trunk to tail transition in the mouse (Fig. 41). However, the observation that inactivation of *Gdf11* resulted in an extended trunk to some degree, but did not block completely such transition suggest the existence of redundant mechanisms. The stronger phenotype of *Gdf11* and *Gdf8* double mutants (McPherron et al., 2009) indicates that *Gdf8* could be indeed part of this mechanism. Another key question to understand this process relies in the identification of the mechanisms that activate Gdf11 signaling at a particular axial level. Moreover, whether a similar Gdf11-Isl1 network is conserved in other vertebrate species awaits to be determined.

To support our three phase hypothesis, it is also important to characterize the mechanisms that regulate the transition from the head-neck to the trunk region. A good candidate for such role is the RA

signaling. In particular, *Raldh2* mutant embryos, which cannot synthesize RA, fail to produce forelimb buds and extend further this axial level (Niederreither et al., 1999). However, this phenotype can be rescued to a large extent by an exogenous dose of RA at the time when the forelimb bud is being formed (Mic et al., 2003; Niederreither et al., 1999), suggesting that RA signaling could be involved in the change of cell competence associated to this transition.

On the other hand, the phenotype of the *Cdx2P-Wnt3a* transgenics could be interpreted as a global posteriorization of the body. In this case, Wnt/*β*-catenin signaling may also impact the trunk to tail transition. Interestingly, bioinformatics analysis have identified a putative binding site for Lef1 in the CR2 enhancer element of *Isl1*, suggesting that this transcription factor could be also downstream of Wnt/*β*-catenin signaling. Experiments are being currently performed to test this possibility. In addition, our results showed that both the inactivation of *Gdf11* and the overexpression of $Alk5^{CA}$ in the epiblast resulted in the misexpression or downregulation of *Wnt3a*, respectively. However, it is not clear if this was a direct or an indirect effect. Conversely, expression of *Gdf11* in *Cdx2P-Wnt3a* transgenics did not seem to be perturbed. Analysis of phosphorylated Smad2/3 levels in the caudal region of *Cdx2P-Wnt3a* embryos also did not reveal any direct crosstalk between these two pathways, suggesting that, if *Wnt3a* is involved in setting the position of the trunk to tail transition, its mechanism most probably does not involve the regulation of Gdf11 signaling. Alternatively, the phenotype of *Cdx2P-Wnt3a* embryos could be interpreted as an indirect consequence of a global shortening of the embryonic structures derived from the effects of Wnt3a on the axial progenitors of the epiblast.

Surprisingly, our results indicate that Hox genes do not play a major role in determining the position of the trunk to tail transition. In particular, overexpression of trunk Hox genes in the epiblast or in mesodermal compartments (PSM and LPM) had very mild or no visible effects on this process. Indeed, only *Cdx2P-Hoxb9* transgenic mice exhibited a consistent anterior displacement of the hindlimbs, most of the times by one segmental unit. This phenotype is in agreement with the inactivation of all *Hox9* members, which produces a slight extended lumbar region, with the sacrum and the hindlimbs located two vertebral elements more caudally (McIntyre et al., 2007). Interestingly, it has been shown that expression of *Hoxa5* and *Hoxb8* in the epiblast can rescue the posterior axial truncation in a *Cdx2/4* mutant background, revealing that trunk Hox genes play a role in axial extension to some extent (Young et al., 2009). Likewise, *Hox13* genes have been shown to produce the opposite effect, inducing the premature termination of the AP axis (Young et al., 2009). Our findings indicate that *Hox11* genes might also play a role in the regulation of tail growth. In particular, both the increased size of tail structures observed in *Gdf11* mutants and the tail reduction of *Cdx2P-Alk5*^{CA} transgenics correlate with delayed and precocious *Hoxd11* activation, respectively. Interestingly, the tail phenotype of the *Gdf11* mutants recapitulates several phenotypic characteristics of *Hox11* mutants (Wellik and Capecchi, 2003), which further supports the connection between *Hox11* genes and the size of tail structures. Therefore, several observations support a role for Hox genes in the control of axial extension. However, it should be noted that those effects seemed restricted to the axial skeleton with no apparent influence on the relative AP position of derivatives of the lateral mesoderm progenitors. This suggests that, although coordinated, the

mechanisms controlling the extension of the different parts of the vertebrate body are regulated by independent mechanisms.

V.3 - Axial progenitors

Progenitors for the different tissues are produced as the vertebrate body gradually elongates, initially from the epiblast and the PS, and are subsequently relocated to the CNH within the tail bud. Our results indicate that Gdf11 signaling has two effects on these cells, acting in their relocation from the NSB to the CNH, as well as on their functional properties once they have reached the tail bud. They showed that, although coordinated, these two activities are based on different mechanisms.

The role of Gdf11 in the relocation of the progenitors seems to involve the modulation of RA signaling, as cell distribution in the tail bud of *Gdf11* mutants can be rescued by blocking RA receptors. Accordingly, mutants for the RARγ are insensitive to exogenous administration of RA and exhibit normal tails (Iulianella et al., 1999). However, Gdf11 does not seem to regulate RARγ expression. Instead, our results indicate that the modulation of RA signaling by Gdf11 is mediated by the control of *Cyp26a1* levels. In particular, the levels of this enzyme varied in the absence of *Gdf11*, being downregulated during the trunk to tail transition and upregulated at later stages. The observation that *Cyp26a1* expression was reduced but still present in *Gdf11* mutants during the trunk to tail transition may explain why the tail phenotype of *Gdf11* mutants is not as strong as the *Cyp26a1* mutant phenotype (Abu-Abed et al., 2001, 2003; Sakai et al., 2001). In this case, progenitors located closer to the tail tip would still be protected from RA by enough *Cyp26a1* and only more rostral progenitors would

be exposed to RA due to the reduced levels of *Cyp26a1* expression. The observation that RA-exposed and RA-non exposed progenitors in *Gdf11* mutants seem to segregate from each other also suggests that RA activity might affect the regulation of specific characteristics (*e.g.* adhesive properties?) that would be important to target these cells to the CNH. Possible candidates include components of the extracellular matrix (*e.g.* integrins and cadherins?). Current experiments are being performed to explore these possibilities.

The regionalization of the wild type tail bud mesenchyme could also explain the split phenotype in *Gdf11* mutants (Fig. 40). In this context, loss of *Gdf11* would impair the maintenance of the tail bud organization, resulting in the segregation of the progenitor population. The group of *T*-positive cells that lags behind and eventually locates close to the hindlimbs gives rise to an ectopic ventral mass of nervous tissue. The formation of nervous tissue from this population suggests that these cells comprise bipotent N-M progenitors of the CNH which fail to persist within the tail bud upon loss of Gdf11. Under this new environment, these progenitors further differentiate into neural tissue due to the absence of Wnt3a stimulus (Martin and Kimelman, 2012). In turn, the remaining *T*-positive domain(s) at the tail tip(s) of *Gdf11* mutants would comprise the dorsal posterior and the ventral tail bud populations found in wild type embryos. These cells exhibit restricted ability to produce paraxial mesoderm in wild type embryos (McGrew et al., 2008). Thus, the disruption of tail bud organization in *Gdf11* mutants would lead to the production of somites in both the ventral and dorsal parts of the split tail. From this perspective, we speculate that these both dpTB and vTB populations consist of lineage intermediates with transit-amplifying behavior (Fig. 40). The concept of "transit-

amplifying cells" was described in many adult tissues and refers to cells restricted in fate that have the ability at some extent of self-replication (*e.g.* Lander et al., 2009; Sancho et al., 2004; Zhao et al., 2011). Indeed, McGrew et al. (2008) have reported that the CNH in wild type mice and chicken contributes cells to the dpTB region. However, the relationship between the other regions of the tail bud remains to be examined.

To evaluate the "transit-amplifying cells" hypothesis, we took advantage of transgenic mouse lines that we have previously generated (see chapter 3). These lines express a tamoxifen-inducible form of Cre recombinase ($CreER^T$) driven by a *T* regulatory element. Using mouse reporter lines, we observed recombined cells in both neural and mesodermal compartments of the transgenic embryos, confirming *T* as a marker for axial progenitors. However, we could not use one of the lines to track cell relationships in the absence of *Gdf11* because we were unable to recover *Gdf11*$^{-/-}$*;R26R-β-gal*$^{+/0}$*;T-streak-CreER*$^{T+/0}$ embryos. This finding raises the possibility that the *T-streak-CreER*^{T} transgene in the mouse line #47 had disrupted an important component that interacts functionally with the Gdf11 pathway. Thus, transgenic alleles do not affect mouse development when Gdf11 is present, but are critical when Gdf11 is absent. We are currently analyzing this genetic interaction.

Alternatively, we also tried to determine specific markers for the identification of bipotent N-M progenitors in the tail bud. Due to the Gdf11 tail phenotype, we reasoned to identify Gdf11 receptors in the tail bud of wild type embryos (Alk4, Alk5 and Alk7), but none of our many attempts were successful. Except for RARγ, all other gene candidates resulted in non-exclusive labeling patterns. For instance, we

and others have shown that *T*, *Wnt3a*, *Cdx2*, *Sox2*, *Foxa2*, *Fgf8* and *Noto* all localize to the CNH region of the mouse tail, but are also present in nearby regions (Abdelkhalek et al., 2004; Cambray and Wilson, 2007; Ukita et al., 2009). This has hampered the proper characterization of these progenitors. Using a similar strategy of tamoxifen administration as previously described, we are currently performing experiments aiming at isolating these cells by cell sorting of *T-streak-CreER*$^{T+/0}$*;Rosa26R-YFP* $^{+/0}$ embryos.

The second role that we identified for Gdf11 signaling involves the progressive termination of the main embryonic body axis. Whereas wild type skeletons exhibit gradually smaller vertebrae and no neural tube posterior to the fourth or fifth caudal vertebra, skeletons of untreated and RA-inhibitor-treated *Gdf11* mutants showed an expansion in the size of these vertebrae and of the neural tube. These observations can be interpreted on the basis of the previously described chalone activity of *Gdf11* (Gamer et al., 2003; Gokoffski et al., 2011; Wu et al., 2003). This would indicate that progenitors incorporated into the tail bud of *Gdf11* mutants keep producing more tissue than they normally generate in wild type embryos. In this case, Gdf11 could be negatively regulating the rate of progenitor production, thus controlling the progressive termination of the axis. Some preliminary results seem to suggest an increase in cell proliferation in the tail bud of E10.5 *Gdf11* mutants (not shown), but a quantitative analysis needs to be done. Consistent with this scenario, hyper-activation of Gdf11 signaling in the epiblast resulted in the truncation of the AP axis (strong phenotype of *Cdx2P-Alk5*^{CA} transgenics). We are currently testing this hypothesis, although the lack of specific markers for the axial progenitors complicates this analysis.

Lastly, tail truncation in *Gdf11* mutants could be a secondary effect of the segregation of axial progenitors. We observed an abnormal accumulation of blood vessels in the ventral region close to the tail, whereas dorsal regions became gradually deprived of blood vessels as the mutant grew older. It is very probable that the lack of nutrients and oxygenation that would result from the absence of vascularization in the tail bud of *Gdf11* mutants is the origin of the increased apoptosis we observed at the tail tip(s) from E11.5 onwards. This could also explain the precocious termination of axial extension in these mutants.

V.4 - A model for axial extension

To integrate the results described in this thesis with the available body of literature, we propose the following model of axial extension. The first cell fate decision in the axial progenitors occurs between the formation of neural and mesodermal tissue. At this moment, Wnt3a would be involved in blocking the production of neural tissue from these progenitors. Thus, only those cells exposed to lower Wnt3a levels would be able to enter the neural lineage. Progenitor cells exposed to higher Wnt3a levels would be available for interacting with other mesoderm-inducing factors to generate the different mesodermal compartments. There, the levels of Wnt3a signaling can also be involved in the production of different cell lineages. Those exposed to higher Wnt3a levels (located towards the most posterior part of the PS) would be able to differentiate into lateral mesoderm upon interaction with other proper signals. Cells exposed to lower Wnt3a levels (but still high enough to block neural differentiation) would interact with mesodermal-inducing factors to produce paraxial mesoderm. In these cells, mesodermal differentiation require the activation of Tbx6, which

blocks neural fates by downregulating *Sox2* (Takemoto et al., 2011). The onset of Gdf11 activity marks the transition from trunk to tail, which results in the terminal differentiation of lateral mesoderm progenitors (Fig. 41). Gdf11 signaling induces *Isl1* expression, which modulates *β*-catenin activation to initiate hindlimb growth (Kawakami et al., 2011). The levels of *β*-catenin, however, need to be further downregulated to allow hindlimb morphogenesis. Gdf11 also participates in the relocation of bipotent N-M progenitors to the CNH by protecting them from RA. Transit-amplifying cells in the dpTB and vTB generate paraxial mesoderm. Gdf11 signaling ultimately exert negative control on the production of progenitors in the tail bud, acting on multiple signaling pathways, such as FGF, RA and Wnt/*β*-catenin. In this new environment (the tail bud), Wnt3a protects resident bipotent N-M progenitors from precocious differentiation, whereas Gdf11 signaling leads to the progressive and regulated termination of tail growth (Fig. 40).

Final remarks

In conclusion, our knowledge on axial extension is now meeting the molecular mechanisms that control the behavior of axial progenitors, but much of our understanding regarding these cells is still incipient. This work sheds light into many aspects of mesoderm production, posterior regionalization of the body and regulation of axial progenitors. The hypotheses raised from our results are being currently scrutinized. Lastly, our proposed model provides an extension of current models that explain other aspects of axial growth, including somitogenesis and patterning of the axial skeleton (Mallo et al., 2010; Pourquié, 2011).

Chapter V – References

Abdelkhalek, H. Ben, Beckers, A., Schuster-Gossler, K., Pavlova, M.N., Burkhardt, H., Lickert, H., Rossant, J., Reinhardt, R., Schalkwyk, L.C., Müller, I., et al. (2004). The mouse homeobox gene Not is required for caudal notochord development and affected by the truncate mutation. Genes & Development *18*, 1725–1736.

Abu-Abed, S., Dollé, P., Metzger, D., Beckett, B., Chambon, P., and Petkovich, M. (2001). The retinoic acid-metabolizing enzyme, CYP26A1, is essential for normal hindbrain patterning, vertebral identity, and development of posterior structures. Genes & Development *15*, 226–240.

Abu-Abed, S., Dollé, P., Metzger, D., Wood, C., MacLean, G., Chambon, P., and Petkovich, M. (2003). Developing with lethal RA levels: genetic ablation of Rarg can restore the viability of mice lacking Cyp26a1. Development (Cambridge, England) *130*, 1449–1459.

Abu-Issa, R., and Kirby, M.L. (2007). Heart field: from mesoderm to heart tube. Annual Review of Cell and Developmental Biology *23*, 45–68.

Acampora, D., Mazan, S., Lallemand, Y., Avantaggiato, V., Maury, M., Simeone, a, and Brûlet, P. (1995). Forebrain and midbrain regions are deleted in Otx2-/- mutants due to a defective anterior neuroectoderm specification during gastrulation. Development (Cambridge, England) *121*, 3279–3290.

Acampora, D., Di Giovannantonio, L.G., Di Salvio, M., Mancuso, P., and Simeone, A. (2009). Selective inactivation of Otx2 mRNA isoforms reveals isoform-specific requirement for visceral endoderm anteriorization and head morphogenesis and highlights cell diversity in the visceral endoderm. Mechanisms of Development *126*, 882–897.

Acloque, H., Ocaña, O.H., Matheu, A., Rizzoti, K., Wise, C., Lovell-Badge, R., and Nieto, M.A. (2011). Reciprocal Repression between Sox3 and

Snail Transcription Factors Defines Embryonic Territories at Gastrulation. Developmental Cell *21*, 546–558.

Agarwal, P., Wylie, J.N., Galceran, J., Arkhitko, O., Li, C., Deng, C., Grosschedl, R., and Bruneau, B.G. (2003). Tbx5 is essential for forelimb bud initiation following patterning of the limb field in the mouse embryo. Development (Cambridge, England) *130*, 623–633.

Van den Akker, E., Fromental-Ramain, C., De Graaff, W., Le Mouellic, H., Brûlet, P., Chambon, P., and Deschamps, J. (2001). Axial skeletal patterning in mice lacking all paralogous group 8 Hox genes. Development (Cambridge, England) *128*, 1911–1921.

Van den Akker, E., Forlani, S., Chawengsaksophak, K., De Graaff, W., Beck, F., Meyer, B.I., and Deschamps, J. (2002). Cdx1 and Cdx2 have overlapping functions in anteroposterior patterning and posterior axis elongation. Development (Cambridge, England) *129*, 2181–2193.

Alev, C., Wu, Y., Kasukawa, T., Jakt, L.M., Ueda, H.R., and Sheng, G. (2010). Transcriptomic landscape of the primitive streak. Development (Cambridge, England) *2874*, 2863–2874.

Alexander, T., Nolte, C., and Krumlauf, R. (2009). Hox genes and segmentation of the hindbrain and axial skeleton. Annual Review of Cell and Developmental Biology *25*, 431–456.

Alles, A.J., and Sulik, K.K. (1990). Retinoic acid-induced spina bifida: evidence for a pathogenetic mechanism. Development (Cambridge, England) *108*, 73–81.

Andersson, O., Reissmann, E., and Ibáñez, C.F. (2006). Growth differentiation factor 11 signals through the transforming growth factor-beta receptor ALK5 to regionalize the anterior-posterior axis. EMBO Reports *7*, 831–837.

Arman, E., Haffner-Krausz, R., Chen, Y., Heath, J.K., and Lonai, P. (1998). Targeted disruption of fibroblast growth factor (FGF) receptor 2 suggests a role for FGF signaling in pregastrulation mammalian development. Proceedings of the National Academy of Sciences of the United States of America *95*, 5082–5087.

Arnold, S.J., and Robertson, E.J. (2009). Making a commitment: cell lineage allocation and axis patterning in the early mouse embryo. Nature Reviews. Molecular Cell Biology *10*, 91–103.

Arnold, S.J., Stappert, J., Bauer, A., Kispert, A., Herrmann, B.G., and Kemler, R. (2000). Brachyury is a target gene of the Wnt/beta-catenin signaling pathway. Mechanisms of Development *91*, 249–258.

Artus, J., Douvaras, P., Piliszek, A., Isern, J., Baron, M.H., and Hadjantonakis, A.-K. (2012). BMP4 signaling directs primitive endoderm-derived XEN cells to an extraembryonic visceral endoderm identity. Developmental Biology *361*, 245–262.

Asrar, Z., Haq, F., and Abbasi, A.A. (2012). Fourfold paralogy regions on human HOX-bearing chromosomes: Role of ancient segmental duplications in the evolution of vertebrate genome. Molecular Phylogenetics and Evolution.

Aulehla, A., and Pourquié, O. (2010). Signaling gradients during paraxial mesoderm development. Cold Spring Harbor Perspectives in Biology *2*, a000869.

Aulehla, A., Wehrle, C., Brand-Saberi, B., Kemler, R., Gossler, A., Kanzler, B., and Herrmann, B.G. (2003). Wnt3a plays a major role in the segmentation clock controlling somitogenesis. Developmental Cell *4*, 395–406.

Aulehla, A., Wiegraebe, W., Baubet, V., Wahl, M.B., Deng, C., Taketo, M., Lewandoski, M., and Pourquié, O. (2008). A beta-catenin gradient links

the clock and wavefront systems in mouse embryo segmentation. Nature Cell Biology *10*, 186–193.

Bachiller, D., Macías, A., Duboule, D., and Morata, G. (1994). Conservation of a functional hierarchy between mammalian and insect Hox/HOM genes. The EMBO Journal *13*, 1930–1941.

Bailey, W.J., Kim, J., Wagner, G.P., and Ruddle, F.H. (1997). Phylogenetic reconstruction of vertebrate Hox cluster duplications. Molecular Biology and Evolution *14*, 843–853.

Barrow, J.R., Howell, W.D., Rule, M., Hayashi, S., Thomas, K.R., Capecchi, M.R., and McMahon, A.P. (2007). Wnt3 signaling in the epiblast is required for proper orientation of the anteroposterior axis. Developmental Biology *312*, 312–320.

Batlle, E., Sancho, E., Francí, C., Domínguez, D., Monfar, M., Baulida, J., and García De Herreros, a (2000). The transcription factor snail is a repressor of E-cadherin gene expression in epithelial tumour cells. Nature Cell Biology *2*, 84–89.

Beck, S., Le Good, J.A., Guzman, M., Ben Haim, N., Roy, K., Beermann, F., and Constam, D.B. (2002). Extraembryonic proteases regulate Nodal signalling during gastrulation. Nature Cell Biology *4*, 981–985.

Becker, D., Jiang, Z., Knödler, P., Deinard, A.S., Eid, R., Kidd, K.K., Shashikant, C.S., Ruddle, F.H., and Schughart, K. (1996). Conserved regulatory element involved in the early onset of Hoxb6 gene expression. Developmental Dynamics : an Official Publication of the American Association of Anatomists *205*, 73–81.

Beckers, J., Schlautmann, N., and Gossler, A. (2000). The mouse rib-vertebrae mutation disrupts anterior-posterior somite patterning and genetically interacts with a Delta1 null allele. Mechanisms of Development *95*, 35–46.

Beddington, R.S. (1982). An autoradiographic analysis of tissue potency in different regions of the embryonic ectoderm during gastrulation in the mouse. Journal of Embryology and Experimental Morphology *69*, 265–285.

Beddington, R.S. (1994). Induction of a second neural axis by the mouse node. Development (Cambridge, England) *120*, 613–620.

Beddington, S.P. (1981). An autoradiographic analysis of the potency of embryonic ectoderm in the 8th day postimplantation mouse embryo. Journal of Embryology and Experimental Morphology *64*, 87–104.

Beddington, R.S., and Robertson, E.J. (1999). Axis development and early asymmetry in mammals. Cell *96*, 195–209.

Bei, L., Shah, C., Wang, H., Huang, W., Roy, R., and Eklund, E. a (2012). β-Catenin Activates the HOXA10 and CDX4 Genes in Myeloid Progenitor Cells. The Journal of Biological Chemistry *287*, 39589–39601.

Bejder, L., and Hall, B.K. (2002). Limbs in whales and limblessness in other vertebrates: mechanisms of evolutionary and developmental transformation and loss. Evolution & Development *4*, 445–458.

Belo, J.A., Bouwmeester, T., Leyns, L., Kertesz, N., Gallo, M., Follettie, M., and De Robertis, E.M. (1997). Cerberus-like is a secreted factor with neutralizing activity expressed in the anterior primitive endoderm of the mouse gastrula. Mechanisms of Development *68*, 45–57.

Benahmed, F., Gross, I., Gaunt, S.J., Beck, F., Jehan, F., Domon-Dell, C., Martin, E., Kedinger, M., Freund, J.-N., and Duluc, I. (2008). Multiple regulatory regions control the complex expression pattern of the mouse Cdx2 homeobox gene. Gastroenterology *135*, 1238–1247, 1247.e1–3.

Bénazet, J.-D., and Zeller, R. (2009). Vertebrate limb development: moving from classical morphogen gradients to an integrated 4-dimensional

patterning system. Cold Spring Harbor Perspectives in Biology *1*, a001339.

Bendel-Stenzel, M., Anderson, R., Heasman, J., and Wylie, C. (1998). The origin and migration of primordial germ cells in the mouse. Seminars in Cell & Developmental Biology *9*, 393–400.

Ben-Haim, N., Lu, C., Guzman-Ayala, M., Pescatore, L., Mesnard, D., Bischofberger, M., Naef, F., Robertson, E.J., and Constam, D.B. (2006). The nodal precursor acting via activin receptors induces mesoderm by maintaining a source of its convertases and BMP4. Developmental Cell *11*, 313–323.

Bialecka, M., Wilson, V., and Deschamps, J. (2010). Cdx mutant axial progenitor cells are rescued by grafting to a wild type environment. Developmental Biology *347*, 228–234.

Boehm, B., Westerberg, H., Lesnicar-Pucko, G., Raja, S., Rautschka, M., Cotterell, J., Swoger, J., and Sharpe, J. (2010). The role of spatially controlled cell proliferation in limb bud morphogenesis. PLoS Biology *8*, e1000420.

Boehm, B., Rautschka, M., Quintana, L., Raspopovic, J., Jan, Z., and Sharpe, J. (2011). A landmark-free morphometric staging system for the mouse limb bud. Development (Cambridge, England) *1234*, 1227–1234.

Boulet, A.M., and Capecchi, M.R. (2012). Signaling by FGF4 and FGF8 is required for axial elongation of the mouse embryo. Developmental Biology *371*, 235–245.

Bowles, J., and Koopman, P. (2013). Precious cargo: regulation of sex-specific germ cell development in mice. Sexual Development : Genetics, Molecular Biology, Evolution, Endocrinology, Embryology, and Pathology of Sex Determination and Differentiation *7*, 46–60.

Brennan, J., Lu, C.C., Norris, D.P., Rodriguez, T.A., Beddington, R.S., and Robertson, E.J. (2001). Nodal signalling in the epiblast patterns the early mouse embryo. Nature *411*, 965–969.

Brent, A.E., and Tabin, C.J. (2002). Developmental regulation of somite derivatives: muscle, cartilage and tendon. Current Opinion in Genetics & Development *12*, 548–557.

Burdsal, C.A., Damsky, C.H., and Pedersen, R.A. (1993). The role of E-cadherin and integrins in mesoderm differentiation and migration at the mammalian primitive streak. Development (Cambridge, England) *118*, 829–844.

Burke, A.C., Nelson, C.E., Morgan, B.A., and Tabin, C. (1995). Hox genes and the evolution of vertebrate axial morphology. Development (Cambridge, England) *121*, 333–346.

Burn, S.F., Boot, M.J., De Angelis, C., Doohan, R., Arques, C.G., Torres, M., and Hill, R.E. (2008). The dynamics of spleen morphogenesis. Developmental Biology *318*, 303–311.

Cai, K.Q., Capo-Chichi, C.D., Rula, M.E., Yang, D.-H., and Xu, X.-X. (2008). Dynamic GATA6 expression in primitive endoderm formation and maturation in early mouse embryogenesis. Developmental Dynamics : an Official Publication of the American Association of Anatomists *237*, 2820–2829.

Cambray, N., and Wilson, V. (2002). Axial progenitors with extensive potency are localised to the mouse chordoneural hinge. Development (Cambridge, England) *129*, 4855–4866.

Cambray, N., and Wilson, V. (2007). Two distinct sources for a population of maturing axial progenitors. Development (Cambridge, England) *134*, 2829–2840.

Cano, A., Pérez-Moreno, M.A., Rodrigo, I., Locascio, A., Blanco, M.J., Del Barrio, M.G., Portillo, F., and Nieto, M.A. (2000). The transcription factor snail controls epithelial-mesenchymal transitions by repressing E-cadherin expression. Nature Cell Biology *2*, 76–83.

Capdevila, J., and Izpisúa Belmonte, J.C. (2001). Patterning mechanisms controlling vertebrate limb development. Annual Review of Cell and Developmental Biology *17*, 87–132.

Carapuço, M., Nóvoa, A., Bobola, N., and Mallo, M. (2005). Hox genes specify vertebral types in the presomitic mesoderm. Genes & Development *19*, 2116–2121.

Carey, F.J., Linney, E.A., and Pedersen, R.A. (1995). Allocation of epiblast cells to germ layer derivatives during mouse gastrulation as studied with a retroviral vector. Developmental Genetics *17*, 29–37.

Carlson, B.M. (1999). Human embryology and developmental biology (St. Louis: Mosby Inc.).

Carvajal, J.J., Cox, D., Summerbell, D., and Rigby, P.W. (2001). A BAC transgenic analysis of the Mrf4/Myf5 locus reveals interdigitated elements that control activation and maintenance of gene expression during muscle development. Development (Cambridge, England) *128*, 1857–1868.

Carver, E.A., Jiang, R., Lan, Y., Oram, K.F., and Gridley, T. (2001). The mouse snail gene encodes a key regulator of the epithelial-mesenchymal transition. Molecular and Cellular Biology *21*, 8184–8188.

Chalamalasetty, R.B., Dunty, W.C., Biris, K.K., Ajima, R., Iacovino, M., Beisaw, A., Feigenbaum, L., Chapman, D.L., Yoon, J.K., Kyba, M., et al. (2011). The Wnt3a/β-catenin target gene Mesogenin1 controls the

segmentation clock by activating a Notch signalling program. Nature Communications *2*, 390.

Chambers, I., Colby, D., Robertson, M., Nichols, J., Lee, S., Tweedie, S., and Smith, A. (2003). Functional expression cloning of Nanog, a pluripotency sustaining factor in embryonic stem cells. Cell *113*, 643–655.

Chapman, D.L., and Papaioannou, V.E. (1998). Three neural tubes in mouse embryos with mutations in the T-box gene Tbx6. Nature *391*, 695–697.

Chapman, D.L., Agulnik, I., Hancock, S., Silver, L.M., and Papaioannou, V.E. (1996). Tbx6, a mouse T-Box gene implicated in paraxial mesoderm formation at gastrulation. Developmental Biology *180*, 534–542.

Charng, M.J., Kinnunen, P., Hawker, J., Brand, T., and Schneider, M.D. (1996). FKBP-12 recognition is dispensable for signal generation by type I transforming growth factor-beta receptors. The Journal of Biological Chemistry *271*, 22941–22944.

Chawengsaksophak, K., James, R., Hammond, V.E., Köntgen, F., and Beck, F. (1997). Homeosis and intestinal tumours in Cdx2 mutant mice. Nature *386*, 84–87.

Chawengsaksophak, K., De Graaff, W., Rossant, J., Deschamps, J., and Beck, F. (2004). Cdx2 is essential for axial elongation in mouse development. Proceedings of the National Academy of Sciences of the United States of America *101*, 7641–7645.

Chazaud, C., and Rossant, J. (2006). Disruption of early proximodistal patterning and AVE formation in Apc mutants. Development (Cambridge, England) *133*, 3379–3387.

Chazaud, C., Yamanaka, Y., Pawson, T., and Rossant, J. (2006). Early lineage segregation between epiblast and primitive endoderm in mouse blastocysts through the Grb2-MAPK pathway. Developmental Cell *10*, 615–624.

Chen, F., Greer, J., and Capecchi, M.R. (1998). Analysis of Hoxa7/Hoxb7 mutants suggests periodicity in the generation of the different sets of vertebrae. Mechanisms of Development *77*, 49–57.

Chen, L., Wang, D., Wu, Z., Ma, L., and Daley, G.Q. (2010). Molecular basis of the first cell fate determination in mouse embryogenesis. Cell Research *20*, 982–993.

Cheng, A.M., Saxton, T.M., Sakai, R., Kulkarni, S., Mbamalu, G., Vogel, W., Tortorice, C.G., Cardiff, R.D., Cross, J.C., Muller, W.J., et al. (1998). Mammalian Grb2 Regulates Multiple Steps in Embryonic Development and Malignant Transformation University of California at Davis. *95*, 793–803.

Chesley, P. (1935). Development of the short-tailed mutant in the house mouse. Journal of Experimental Zoology *70*, 429–459.

Cho, K.W., and De Robertis, E.M. (1990). Differential activation of Xenopus homeo box genes by mesoderm-inducing growth factors and retinoic acid. Genes & Development *4*, 1910–1916.

Christ, B., Huang, R., and Wilting, J. (2000). The development of the avian vertebral column. Anatomy and Embryology *202*, 179–194.

Christ, B., Huang, R., and Scaal, M. (2007). Amniote somite derivatives. Developmental Dynamics : an Official Publication of the American Association of Anatomists *236*, 2382–2396.

Chu, J., and Shen, M.M. (2010). Functional redundancy of EGF-CFC genes in epiblast and extraembryonic patterning during early mouse embryogenesis. Developmental Biology *342*, 63–73.

Ciruna, B., and Rossant, J. (2001). FGF signaling regulates mesoderm cell fate specification and morphogenetic movement at the primitive streak. Developmental Cell *1*, 37–49.

Ciruna, B.G., Schwartz, L., Harpal, K., Yamaguchi, T.P., and Rossant, J. (1997). Chimeric analysis of fibroblast growth factor receptor-1 (Fgfr1) function: a role for FGFR1 in morphogenetic movement through the primitive streak. Development (Cambridge, England) *124*, 2829–2841.

Clements, D., Taylor, H.C., Herrmann, B.G., and Stott, D. (1996). Distinct regulatory control of the Brachyury gene in axial and non-axial mesoderm suggests separation of mesoderm lineages early in mouse gastrulation. Mechanisms of Development *56*, 139–149.

Cohn, M.J., and Bright, P.E. (1999). Molecular control of vertebrate limb development, evolution and congenital malformations. Cell and Tissue Research *296*, 3–17.

Cohn, M.J., and Tickle, C. (1999). Developmental basis of limblessness and axial patterning in snakes. Nature *399*, 474–479.

Conaway, R.C., and Conaway, J.W. (1988). ATP activates transcription initiation from promoters by RNA polymerase II in a reversible step prior to RNA synthesis. The Journal of Biological Chemistry *263*, 2962–2968.

Condie, B.G., and Capecchi, M.R. (1993). Mice homozygous for a targeted disruption of Hoxd-3 (Hox-4.1) exhibit anterior transformations of the first and second cervical vertebrae, the atlas and the axis. Development (Cambridge, England) *119*, 579–595.

Condie, B.G., and Capecchi, M.R. (1994). Mice with targeted disruptions in the paralogous genes hoxa-3 and hoxd-3 reveal synergistic interactions. Nature *370*, 304–307.

Conlon, F.L., Lyons, K.M., Takaesu, N., Barth, K.S., Kispert, A., Herrmann, B., and Robertson, E.J. (1994). A primary requirement for nodal in the formation and maintenance of the primitive streak in the mouse. Development (Cambridge, England) *120*, 1919–1928.

Conlon, R.A., Reaume, A.G., and Rossant, J. (1995). Notch1 is required for the coordinate segmentation of somites. Development (Cambridge, England) *121*, 1533–1545.

Cordero, D.R., Brugmann, S., Chu, Y., Bajpai, R., Jame, M., and Helms, J. a (2011). Cranial neural crest cells on the move: their roles in craniofacial development. American Journal of Medical Genetics. Part A *155A*, 270–279.

Costantini, F., and Kopan, R. (2010). Patterning a complex organ: branching morphogenesis and nephron segmentation in kidney development. Developmental Cell *18*, 698–712.

Cox, W.G., and Hemmati-Brivanlou, A. (1995). Caudalization of neural fate by tissue recombination and bFGF. Development (Cambridge, England) *121*, 4349–4358.

Crickmore, M.A., and Mann, R.S. (2006). Hox control of organ size by regulation of morphogen production and mobility. Science (New York, N.Y.) *313*, 63–68.

Dale, J.K., Malapert, P., Chal, J., Vilhais-Neto, G., Maroto, M., Johnson, T., Jayasinghe, S., Trainor, P., Herrmann, B., and Pourquié, O. (2006). Oscillations of the snail genes in the presomitic mesoderm coordinate segmental patterning and morphogenesis in vertebrate somitogenesis. Developmental Cell *10*, 355–366.

Deng, C.X., Wynshaw-Boris, A., Shen, M.M., Daugherty, C., Ornitz, D.M., and Leder, P. (1994). Murine FGFR-1 is required for early

postimplantation growth and axial organization. Genes & Development *8*, 3045–3057.

Dequéant, M.-L., Glynn, E., Gaudenz, K., Wahl, M., Chen, J., Mushegian, A., and Pourquié, O. (2006). A complex oscillating network of signaling genes underlies the mouse segmentation clock. Science (New York, N.Y.) *314*, 1595–1598.

Dequéant, M.-L., Ahnert, S., Edelsbrunner, H., Fink, T.M. a, Glynn, E.F., Hattem, G., Kudlicki, A., Mileyko, Y., Morton, J., Mushegian, A.R., et al. (2008). Comparison of pattern detection methods in microarray time series of the segmentation clock. PloS One *3*, e2856.

Diez del Corral, R., Olivera-Martinez, I., Goriely, A., Gale, E., Maden, M., and Storey, K. (2003). Opposing FGF and retinoid pathways control ventral neural pattern, neuronal differentiation, and segmentation during body axis extension. Neuron *40*, 65–79.

Di-Poï, N., Montoya-Burgos, J.I., Miller, H., Pourquié, O., Milinkovitch, M.C., and Duboule, D. (2010). Changes in Hox genes' structure and function during the evolution of the squamate body plan. Nature *464*, 99–103.

Dollé, P., Izpisúa-Belmonte, J.C., Falkenstein, H., Renucci, A., and Duboule, D. (1989). Coordinate expression of the murine Hox-5 complex homoeobox-containing genes during limb pattern formation. Nature *342*, 767–772.

Le Douarin, N.M., and Dupin, E. (2012). The neural crest in vertebrate evolution. Current Opinion in Genetics & Development *22*, 381–389.

Dressler, G.R. (2009). Advances in early kidney specification, development and patterning. Development (Cambridge, England) *136*, 3863–3874.

Duboule, D. (1991). Patterning in the vertebrate limb. Current Opinion in Genetics & Development *1*, 211–216.

Duboule, D., and Dollé, P. (1989). The structural and functional organization of the murine HOX gene family resembles that of Drosophila homeotic genes. The EMBO Journal *8*, 1497–1505.

Duboule, D., and Morata, G. (1994). Colinearity and functional hierarchy among genes of the homeotic complexes. Trends in Genetics : TIG *10*, 358–364.

Dubrulle, J., and Pourquié, O. (2004a). fgf8 mRNA decay establishes a gradient that couples axial elongation to patterning in the vertebrate embryo. Nature *427*, 419–422.

Dubrulle, J., and Pourquié, O. (2004b). Coupling segmentation to axis formation. Development (Cambridge, England) *131*, 5783–5793.

Dubrulle, J., McGrew, M.J., and Pourquié, O. (2001). FGF signaling controls somite boundary position and regulates segmentation clock control of spatiotemporal Hox gene activation. Cell *106*, 219–232.

Duester, G. (2008). Retinoic acid synthesis and signaling during early organogenesis. Cell *134*, 921–931.

Dunty, W.C., Biris, K.K., Chalamalasetty, R.B., Taketo, M.M., Lewandoski, M., and Yamaguchi, T.P. (2008). Wnt3a/beta-catenin signaling controls posterior body development by coordinating mesoderm formation and segmentation. Development (Cambridge, England) *135*, 85–94.

Dupé, V., Davenne, M., Brocard, J., Dollé, P., Mark, M., Dierich, A., Chambon, P., and Rijli, F.M. (1997). In vivo functional analysis of the Hoxa-1 3’ retinoic acid response element (3'RARE). Development (Cambridge, England) *124*, 399–410.

Esquela, A.F., and Lee, S.-J. (2003). Regulation of metanephric kidney development by growth/differentiation factor 11. Developmental Biology *257*, 356–370.

Essalmani, R., Zaid, A., Marcinkiewicz, J., Chamberland, A., Pasquato, A., Seidah, N.G., and Prat, A. (2008). In vivo functions of the proprotein convertase PC5/6 during mouse development: Gdf11 is a likely substrate. Proceedings of the National Academy of Sciences of the United States of America *105*, 5750–5755.

Evans, A.L., Faial, T., Gilchrist, M.J., Down, T., Vallier, L., Pedersen, R.A., Wardle, F.C., and Smith, J.C. (2012). Genomic targets of Brachyury (T) in differentiating mouse embryonic stem cells. PloS One *7*, e33346.

Evrard, Y.A., Lun, Y., Aulehla, A., Gan, L., and Johnson, R.L. (1998). lunatic fringe is an essential mediator of somite segmentation and patterning. Nature *394*, 377–381.

Favier, B., Rijli, F.M., Fromental-Ramain, C., Fraulob, V., Chambon, P., and Dollé, P. (1996). Functional cooperation between the non-paralogous genes Hoxa-10 and Hoxd-11 in the developing forelimb and axial skeleton. Development (Cambridge, England) *122*, 449–460.

Feldman, B., Poueymirou, W., Papaioannou, V.E., DeChiara, T.M., and Goldfarb, M. (1995). Requirement of FGF-4 for postimplantation mouse development. Science (New York, N.Y.) *267*, 246–249.

Feller, J., Schneider, A., Schuster-Gossler, K., and Gossler, A. (2008). Noncyclic Notch activity in the presomitic mesoderm demonstrates uncoupling of somite compartmentalization and boundary formation. Genes & Development *22*, 2166–2171.

Fernandez-Teran, M., and Ros, M.A. (2008). The Apical Ectodermal Ridge: morphological aspects and signaling pathways. The International Journal of Developmental Biology *52*, 857–871.

Finley, K.R., Tennessen, J., and Shawlot, W. (2003). The mouse secreted frizzled-related protein 5 gene is expressed in the anterior visceral

endoderm and foregut endoderm during early post-implantation development. Gene Expression Patterns : GEP *3*, 681–684.

Fletcher, R.B., Baker, J.C., and Harland, R.M. (2006). FGF8 spliceforms mediate early mesoderm and posterior neural tissue formation in Xenopus. Development (Cambridge, England) *133*, 1703–1714.

Fomenou, M.D., Scaal, M., Stockdale, F.E., Christ, B., and Huang, R. (2005). Cells of all somitic compartments are determined with respect to segmental identity. Developmental Dynamics : an Official Publication of the American Association of Anatomists *233*, 1386–1393.

Forlani, S. (2003). Acquisition of Hox codes during gastrulation and axial elongation in the mouse embryo. Development *130*, 3807–3819.

Frankenberg, S., Gerbe, F., Bessonnard, S., Belville, C., Pouchin, P., Bardot, O., and Chazaud, C. (2011). Primitive endoderm differentiates via a three-step mechanism involving Nanog and RTK signaling. Developmental Cell *21*, 1005–1013.

Fujikura, J., Yamato, E., Yonemura, S., Hosoda, K., Masui, S., Nakao, K., Miyazaki, J., and Niwa, H. (2002). Differentiation of embryonic stem cells is induced by GATA factors. 784–789.

Gajović, S., and Kostović-Knezević, L. (1995). Ventral ectodermal ridge and ventral ectodermal groove: two distinct morphological features in the developing rat embryo tail. Anatomy and Embryology *192*, 181–187.

Galceran, J., Fariñas, I., Depew, M.J., Clevers, H., and Grosschedl, R. (1999). Wnt3a-/--like phenotype and limb deficiency in Lef1(-/-)Tcf1(-/-) mice. Genes & Development *13*, 709–717.

Galceran, J., Hsu, S.C., and Grosschedl, R. (2001). Rescue of a Wnt mutation by an activated form of LEF-1: regulation of maintenance but

not initiation of Brachyury expression. Proceedings of the National Academy of Sciences of the United States of America *98*, 8668–8673.

Gamer, L.W., Nove, J., and Rosen, V. (2003). Return of the chalones. Developmental Cell *4*, 143–144.

Garcia-Fernàndez, J. (2005). The genesis and evolution of homeobox gene clusters. Nature Reviews. Genetics *6*, 881–892.

Gaunt, S.J., and Strachan, L. (1996). Temporal colinearity in expression of anterior Hox genes in developing chick embryos. Developmental Dynamics : an Official Publication of the American Association of Anatomists *207*, 270–280.

Gaunt, S., Sharpe, P., and Duboule, D. (1988). Spatially restricted domains of homeo-gene transcripts in mouse embryos: relation to a segmented body plan. Development *104*, 169–179.

Gaunt, S.J., Drage, D., and Trubshaw, R.C. (2005). cdx4/lacZ and cdx2/lacZ protein gradients formed by decay during gastrulation in the mouse. The International Journal of Developmental Biology *49*, 901–908.

Gehring, W.J. (1987). Homeo boxes in the study of development. Science (New York, N.Y.) *236*, 1245–1252.

Gerbe, F., Cox, B., Rossant, J., and Chazaud, C. (2008). Dynamic expression of Lrp2 pathway members reveals progressive epithelial differentiation of primitive endoderm in mouse blastocyst. Developmental Biology *313*, 594–602.

Gibb, S., Zagorska, A., Melton, K., Tenin, G., Vacca, I., Trainor, P., Maroto, M., and Dale, J.K. (2009). Interfering with Wnt signalling alters the periodicity of the segmentation clock. Developmental Biology *330*, 21–31.

Gibson-Brown, J.J., Agulnik, S.I., Chapman, D.L., Alexiou, M., Garvey, N., Silver, L.M., and Papaioannou, V.E. (1996). Evidence of a role for T-box genes in the evolution of limb morphogenesis and the specification of forelimb/hindlimb identity. Mechanisms of Development *56*, 93–101.

Gilbert, S.F. (2003). Developmental Biology (Sunderland: Sinauer Associates Inc.).

Ginsburg, M., Snow, M.H., and McLaren, A. (1990). Primordial germ cells in the mouse embryo during gastrulation. Development (Cambridge, England) *110*, 521–528.

Gittes, G.K. (2009). Developmental biology of the pancreas: a comprehensive review. Developmental Biology *326*, 4–35.

Gofflot, F., Hall, M., and Morriss-Kay, G.M. (1997). Genetic patterning of the developing mouse tail at the time of posterior neuropore closure. Developmental Dynamics : an Official Publication of the American Association of Anatomists *210*, 431–445.

Gofflot, F., Hall, M., and Morriss-Kay, G.M. (1998). Genetic patterning of the posterior neuropore region of curly tail mouse embryos: deficiency of Wnt5a expression. The International Journal of Developmental Biology *42*, 637–644.

Gokoffski, K.K., Wu, H.-H., Beites, C.L., Kim, J., Kim, E.J., Matzuk, M.M., Johnson, J.E., Lander, A.D., and Calof, A.L. (2011). Activin and GDF11 collaborate in feedback control of neuroepithelial stem cell proliferation and fate. Development (Cambridge, England) *4142*, 4131–4142.

Goldin, S.N., and Papaioannou, V.E. (2003). Paracrine action of FGF4 during periimplantation development maintains trophectoderm and primitive endoderm. Genesis (New York, N.Y. : 2000) *36*, 40–47.

Goldman, D.C., Martin, G.R., and Tam, P.P. (2000). Fate and function of the ventral ectodermal ridge during mouse tail development. Development (Cambridge, England) *127*, 2113–2123.

González-Reyes, A., and Morata, G. (1990). The developmental effect of overexpressing a Ubx product in Drosophila embryos is dependent on its interactions with other homeotic products. Cell *61*, 515–522.

Gordon, J., and Manley, N.R. (2011). Mechanisms of thymus organogenesis and morphogenesis. Development (Cambridge, England) *138*, 3865–3878.

Gould, A., Itasaki, N., and Krumlauf, R. (1998). Initiation of rhombomeric Hoxb4 expression requires induction by somites and a retinoid pathway. Neuron *21*, 39–51.

Graham, A., Papalopulu, N., and Krumlauf, R. (1989). The murine and Drosophila homeobox gene complexes have common features of organization and expression. Cell *57*, 367–378.

Grandel, H., and Brand, M. (2011). Zebrafish limb development is triggered by a retinoic acid signal during gastrulation. Developmental Dynamics : an Official Publication of the American Association of Anatomists *240*, 1116–1126.

Granier, C., Gurchenkov, V., Perea-Gomez, A., Camus, A., Ott, S., Papanayotou, C., Iranzo, J., Moreau, A., Reid, J., Koentges, G., et al. (2011). Nodal cis-regulatory elements reveal epiblast and primitive endoderm heterogeneity in the peri-implantation mouse embryo. Developmental Biology *349*, 350–362.

Greene, H.W., and Cundall, D. (2000). Perspectives: evolutionary biology. Limbless tetrapods and snakes with legs. Science (New York, N.Y.) *287*, 1939–1941.

Gruneberg, H. (1958). Genetical studies on the skeleton of the mouse. XXIII. The development of brachyury and anury. Journal of Embryology and Experimental Morphology *6*, 424–443.

Gu, Z., Nomura, M., Simpson, B.B., Lei, H., Feijen, A., Van den Eijnden-van Raaij, J., Donahoe, P.K., and Li, E. (1998). The type I activin receptor ActRIB is required for egg cylinder organization and gastrulation in the mouse. Genes & Development *12*, 844–857.

Guo, Q., and Li, J.Y.H. (2007). Distinct functions of the major Fgf8 spliceform, Fgf8b, before and during mouse gastrulation. Development (Cambridge, England) *134*, 2251–2260.

Guo, G., Huss, M., Tong, G.Q., Wang, C., Li Sun, L., Clarke, N.D., and Robson, P. (2010). Resolution of cell fate decisions revealed by single-cell gene expression analysis from zygote to blastocyst. Developmental Cell *18*, 675–685.

Haegel, H., Larue, L., Ohsugi, M., Fedorov, L., Herrenknecht, K., and Kemler, R. (1995). Lack of beta-catenin affects mouse development at gastrulation. Development (Cambridge, England) *121*, 3529–3537.

Handrigan, G.R. (2003). Concordia discors: duality in the origin of the vertebrate tail. Journal of Anatomy *202*, 255–267.

Haraguchi, R., Suzuki, K., Murakami, R., Sakai, M., Kamikawa, M., Kengaku, M., Sekine, K., Kawano, H., Kato, S., Ueno, N., et al. (2000). Molecular analysis of external genitalia formation: the role of fibroblast growth factor (Fgf) genes during genital tubercle formation. Development (Cambridge, England) *127*, 2471–2479.

Hart, C.P., Fainsod, A., and Ruddle, F.H. (1987). Sequence analysis of the murine Hox-2.2, -2.3, and -2.4 homeo boxes: evolutionary and structural comparisons. Genomics *1*, 182–195.

Hashimoto, K., Fujimoto, H., and Nakatsuji, N. (1987). An ECM substratum allows mouse mesodermal cells isolated from the primitive streak to exhibit motility similar to that inside the embryo and reveals a deficiency in the T/T mutant cells. Development (Cambridge, England) *100*, 587–598.

Hayashi, S., and McMahon, A.P. (2002). Efficient recombination in diverse tissues by a tamoxifen-inducible form of Cre: a tool for temporally regulated gene activation/inactivation in the mouse. Developmental Biology *244*, 305–318.

Helms, J.A., and Schneider, R.A. (2003). Cranial skeletal biology. Nature *423*, 326–331.

Hermesz, E., Mackem, S., and Mahon, K.A. (1996). Rpx : a novel anterior-restricted homeobox gene progressively activated in the prechordal plate , anterior neural plate and Rathke ' s pouch of the mouse embryo. *52*, 41–52.

Herrmann, B.G. (1991). Expression pattern of the Brachyury gene in whole-mount TWis/TWis mutant embryos. Development (Cambridge, England) *113*, 913–917.

Herrmann, B.G., Labeit, S., Poustka, A., King, T.R., and Lehrach, H. (1990). Cloning of the T gene required in mesoderm formation in the mouse. Nature *343*, 617–622.

Hierholzer, A., and Kemler, R. (2010). Beta-catenin-mediated signaling and cell adhesion in postgastrulation mouse embryos. Developmental Dynamics : an Official Publication of the American Association of Anatomists *239*, 191–199.

Ho, D.M., Yeo, C.-Y., and Whitman, M. (2010). The role and regulation of GDF11 in Smad2 activation during tailbud formation in the Xenopus embryo. Mechanisms of Development *127*, 485–495.

Van der Hoeven, F., Zákány, J., and Duboule, D. (1996). Gene transpositions in the HoxD complex reveal a hierarchy of regulatory controls. Cell *85*, 1025–1035.

Hofmann, M., Schuster-Gossler, K., Watabe-Rudolph, M., Aulehla, A., Herrmann, B.G., and Gossler, A. (2004). WNT signaling, in synergy with T/TBX6, controls Notch signaling by regulating Dll1 expression in the presomitic mesoderm of mouse embryos. Genes & Development *18*, 2712–2717.

Hogan, B., Beddington, R., Constantini, F., and Lacy, E. (1994). Manipulating The Mouse Embryo: A Laboratory Manual (Cold Spring Harbor, New York: Cold Spring Harbor Laboratory Press).

Holland, P.W., Garcia-Fernàndez, J., Williams, N.A., and Sidow, A. (1994). Gene duplications and the origins of vertebrate development. Development (Cambridge, England). Supplement *1994*, 125–133.

Horan, G.S., Wu, K., Wolgemuth, D.J., and Behringer, R.R. (1994). Homeotic transformation of cervical vertebrae in Hoxa-4 mutant mice. Proceedings of the National Academy of Sciences of the United States of America *91*, 12644–12648.

Horan, G.S., Ramirez-Solis, R., Featherstone, M.S., Wolgemuth, D.J., Bradley, a, and Behringer, R.R. (1995). Compound mutants for the paralogous hoxa-4, hoxb-4, and hoxd-4 genes show more complete homeotic transformations and a dose-dependent increase in the number of vertebrae transformed. Genes & Development *9*, 1667–1677.

Hrabě de Angelis, M., McIntyre, J., and Gossler, A. (1997). Maintenance of somite borders in mice requires the Delta homologue DII1. Nature *386*, 717–721.

Huelsken, J., Vogel, R., Brinkmann, V., Erdmann, B., Birchmeier, C., and Birchmeier, W. (2000). Requirement for beta-catenin in anterior-

posterior axis formation in mice. The Journal of Cell Biology *148*, 567–578.

Iimura, T., and Pourquié, O. (2006). Collinear activation of Hoxb genes during gastrulation is linked to mesoderm cell ingression. Nature *442*, 568–571.

Ikenouchi, J., Matsuda, M., Furuse, M., and Tsukita, S. (2003). Regulation of tight junctions during the epithelium-mesenchyme transition: direct repression of the gene expression of claudins/occludin by Snail. Journal of Cell Science *116*, 1959–1967.

Ikeya, M., and Takada, S. (2001). Wnt-3a is required for somite specification along the anteroposterior axis of the mouse embryo and for regulation of cdx-1 expression. Mechanisms of Development *103*, 27–33.

Itou, J., Kawakami, H., Quach, T., Osterwalder, M., Evans, S.M., Zeller, R., and Kawakami, Y. (2012). Islet1 regulates establishment of the posterior hindlimb field upstream of the Hand2-Shh morphoregulatory gene network in mouse embryos. Development (Cambridge, England) *1629*, 1620–1629.

Iulianella, A., Beckett, B., Petkovich, M., and Lohnes, D. (1999). A molecular basis for retinoic acid-induced axial truncation. Developmental Biology *205*, 33–48.

Izpisúa-Belmonte, J.C., Falkenstein, H., Dollé, P., Renucci, A., and Duboule, D. (1991). Murine genes related to the Drosophila AbdB homeotic genes are sequentially expressed during development of the posterior part of the body. The EMBO Journal *10*, 2279–2289.

Jeannotte, L., Lemieux, M., Charron, J., Poirier, F., and Robertson, E.J. (1993). Specification of axial identity in the mouse: role of the Hoxa-5 (Hox1.3) gene. Genes & Development *7*, 2085–2096.

Kang, J., Nathan, E., Xu, S.-M., Tzahor, E., and Black, B.L. (2009). Isl1 is a direct transcriptional target of Forkhead transcription factors in second-heart-field-derived mesoderm. Developmental Biology *334*, 513–522.

Kanki, J.P., and Ho, R.K. (1997). The development of the posterior body in zebrafish. Development (Cambridge, England) *124*, 881–893.

Kant, R., and Goldstein, R.S. (1999). Plasticity of axial identity among somites: cranial somites can generate vertebrae without expressing Hox genes appropriate to the trunk. Developmental Biology *216*, 507–520.

Kanzler, B., Kuschert, S.J., Liu, Y.H., and Mallo, M. (1998). Hoxa-2 restricts the chondrogenic domain and inhibits bone formation during development of the branchial area. Development (Cambridge, England) *125*, 2587–2597.

Kappen, C., Schughart, K., and Ruddle, F.H. (1989). Two steps in the evolution of Antennapedia-class vertebrate homeobox genes. Proceedings of the National Academy of Sciences of the United States of America *86*, 5459–5463.

Kaufman, M.H. (1992). The Atlas of Mouse Development (Academic Press).

Kawakami, Y., Marti, M., Kawakami, H., Itou, J., Quach, T., Johnson, A., Sahara, S., O'Leary, D.D.M., Nakagawa, Y., Lewandoski, M., et al. (2011). Islet1-mediated activation of the β-catenin pathway is necessary for hindlimb initiation in mice. Development (Cambridge, England) *138*, 4465–4473.

Kelly, O.G., Pinson, K.I., and Skarnes, W.C. (2004). The Wnt co-receptors Lrp5 and Lrp6 are essential for gastrulation in mice. Development (Cambridge, England) *131*, 2803–2815.

Kemp, C., Willems, E., Abdo, S., Lambiv, L., and Leyns, L. (2005). Expression of all Wnt genes and their secreted antagonists during

mouse blastocyst and postimplantation development. Developmental Dynamics : an Official Publication of the American Association of Anatomists *233*, 1064–1075.

Kessel, M. (1992). Respecification of vertebral identities by retinoic acid. Development (Cambridge, England) *115*, 487–501.

Kessel, M., and Gruss, P. (1991). Homeotic transformations of murine vertebrae and concomitant alteration of Hox codes induced by retinoic acid. Cell *67*, 89–104.

Kieny, M., Mauger, A., and Sengel, P. (1972). Early regionalization of somitic mesoderm as studied by the development of axial skeleton of the chick embryo. Developmental Biology *28*, 142–161.

Kimura, C., Yoshinaga, K., Tian, E., Suzuki, M., Aizawa, S., and Matsuo, I. (2000). Visceral endoderm mediates forebrain development by suppressing posteriorizing signals. Developmental Biology *225*, 304–321.

Kimura, C., Shen, M.M., Takeda, N., Aizawa, S., and Matsuo, I. (2001). Complementary functions of Otx2 and Cripto in initial patterning of mouse epiblast. Developmental Biology *235*, 12–32.

Kimura-Yoshida, C., Nakano, H., Okamura, D., Nakao, K., Yonemura, S., Belo, J.A., Aizawa, S., Matsui, Y., and Matsuo, I. (2005). Canonical Wnt signaling and its antagonist regulate anterior-posterior axis polarization by guiding cell migration in mouse visceral endoderm. Developmental Cell *9*, 639–650.

Kinder, S.J., Tsang, T.E., Quinlan, G.A., Hadjantonakis, A.K., Nagy, A., and Tam, P.P. (1999). The orderly allocation of mesodermal cells to the extraembryonic structures and the anteroposterior axis during gastrulation of the mouse embryo. Development (Cambridge, England) *126*, 4691–4701.

Kinder, S.J., Tsang, T.E., Wakamiya, M., Sasaki, H., Behringer, R.R., Nagy, A., and Tam, P.P. (2001). The organizer of the mouse gastrula is composed of a dynamic population of progenitor cells for the axial mesoderm. Development (Cambridge, England) *128*, 3623–3634.

Kissinger, C.R., Liu, B.S., Martin-Blanco, E., Kornberg, T.B., and Pabo, C.O. (1990). Crystal structure of an engrailed homeodomain-DNA complex at 2.8 A resolution: a framework for understanding homeodomain-DNA interactions. Cell *63*, 579–590.

Klapholz-Brown, Z., Walmsley, G.G., Nusse, Y.M., Nusse, R., and Brown, P.O. (2007). Transcriptional program induced by Wnt protein in human fibroblasts suggests mechanisms for cell cooperativity in defining tissue microenvironments. PloS One *2*, e945.

Kolm, P.J., and Sive, H.L. (1995). Regulation of the Xenopus labial homeodomain genes, HoxA1 and HoxD1: activation by retinoids and peptide growth factors. Developmental Biology *167*, 34–49.

Kondo, T., and Duboule, D. (1999). Breaking colinearity in the mouse HoxD complex. Cell *97*, 407–417.

Kondoh, H., and Takemoto, T. (2012). Axial stem cells deriving both posterior neural and mesodermal tissues during gastrulation. Current Opinion in Genetics & Development 1–7.

Krol, A.J., Roellig, D., Dequéant, M.-L., Tassy, O., Glynn, E., Hattem, G., Mushegian, A., Oates, A.C., and Pourquié, O. (2011). Evolutionary plasticity of segmentation clock networks. Development (Cambridge, England) *138*, 2783–2792.

Krumlauf, R. (1994). Hox genes in vertebrate development. Cell *78*, 191–201.

Kurimoto, K., Yabuta, Y., Ohinata, Y., Ono, Y., Uno, K.D., Yamada, R.G., Ueda, H.R., and Saitou, M. (2006). An improved single-cell cDNA

amplification method for efficient high-density oligonucleotide microarray analysis. Nucleic Acids Research *34*, e42.

Kutejova, E., Engist, B., Self, M., Oliver, G., Kirilenko, P., and Bobola, N. (2008). Six2 functions redundantly immediately downstream of Hoxa2. Development (Cambridge, England) *135*, 1463–1470.

Kwon, G.S., Viotti, M., and Hadjantonakis, A.-K. (2008). The endoderm of the mouse embryo arises by dynamic widespread intercalation of embryonic and extraembryonic lineages. Developmental Cell *15*, 509–520.

Lamb, T.M., and Harland, R.M. (1995). Fibroblast growth factor is a direct neural inducer, which combined with noggin generates anterior-posterior neural pattern. Development (Cambridge, England) *121*, 3627–3636.

Lander, A.D., Gokoffski, K.K., Wan, F.Y.M., Nie, Q., and Calof, A.L. (2009). Cell lineages and the logic of proliferative control. PLoS Biology *7*, e15.

Langston, A.W., and Gudas, L.J. (1992). Identification of a retinoic acid responsive enhancer 3' of the murine homeobox gene Hox-1.6. Mechanisms of Development *38*, 217–227.

Langston, A.W., Thompson, J.R., and Gudas, L.J. (1997). Retinoic acid-responsive enhancers located 3' of the Hox A and Hox B homeobox gene clusters. Functional analysis. The Journal of Biological Chemistry *272*, 2167–2175.

Larue, L., Ohsugi, M., Hirchenhain, J., and Kemler, R. (1994). E-cadherin null mutant embryos fail to form a trophectoderm epithelium. Proceedings of the National Academy of Sciences of the United States of America *91*, 8263–8267.

Lawson, K.A., and Pedersen, R.A. (1987). Cell fate, morphogenetic movement and population kinetics of embryonic endoderm at the time of germ layer formation in the mouse. Development (Cambridge, England) *101*, 627–652.

Lawson, K.A., and Pedersen, R.A. (1992). Clonal analysis of cell fate during gastrulation and early neurulation in the mouse. Ciba Foundation Symposium *165*, 3–21.

Lawson, K.A., Meneses, J.J., and Pedersen, R.A. (1986). Cell fate and cell lineage in the endoderm of the presomite mouse embryo, studied with an intracellular tracer. Developmental Biology *115*, 325–339.

Lawson, K.A., Meneses, J.J., and Pedersen, R.A. (1991). Clonal analysis of epiblast fate during germ layer formation in the mouse embryo. Development (Cambridge, England) *113*, 891–911.

Lee, J.D., and Anderson, K. V (2008). Morphogenesis of the node and notochord: the cellular basis for the establishment and maintenance of left-right asymmetry in the mouse. Developmental Dynamics : an Official Publication of the American Association of Anatomists *237*, 3464–3476.

Lee, Y.J., McPherron, A., Choe, S., Sakai, Y., Chandraratna, R.A., Lee, S.-J., and Oh, S.P. (2010). Growth differentiation factor 11 signaling controls retinoic acid activity for axial vertebral development. Developmental Biology *347*, 195–203.

Lengerke, C., and Daley, G.Q. (2012). Caudal genes in blood development and leukemia. Annals of the New York Academy of Sciences *1266*, 47–54.

Lengerke, C., Schmitt, S., Bowman, T. V, Jang, I.H., Maouche-Chretien, L., McKinney-Freeman, S., Davidson, A.J., Hammerschmidt, M., Rentzsch, F., Green, J.B.A., et al. (2008). BMP and Wnt specify

hematopoietic fate by activation of the Cdx-Hox pathway. Cell Stem Cell *2*, 72–82.

Lewandoski, M. (2001). Conditional control of gene expression in the mouse. Nature Reviews. Genetics *2*, 743–755.

Lewis, E.B. (1978). A gene complex controlling segmentation in Drosophila. Nature *276*, 565–570.

Lewis, S.L., and Tam, P.P.L. (2006). Definitive endoderm of the mouse embryo: formation, cell fates, and morphogenetic function. Developmental Dynamics : an Official Publication of the American Association of Anatomists *235*, 2315–2329.

Liang, Z., Breman, A.M., Grimes, B.R., and Rosen, E.D. (2008). Identifying and genotyping transgene integration loci. Transgenic Research *17*, 979–983.

Lin, C.-J., Lin, C.-Y., Chen, C.-H., Zhou, B., and Chang, C.-P. (2012). Partitioning the heart: mechanisms of cardiac septation and valve development. Development *139*, 3277–3299.

Liu, J.-P. (2006). The function of growth/differentiation factor 11 (Gdf11) in rostrocaudal patterning of the developing spinal cord. Development (Cambridge, England) *133*, 2865–2874.

Liu, J.P., Laufer, E., and Jessell, T.M. (2001). Assigning the positional identity of spinal motor neurons: rostrocaudal patterning of Hox-c expression by FGFs, Gdf11, and retinoids. Neuron *32*, 997–1012.

Liu, P., Wakamiya, M., Shea, M.J., Albrecht, U., Behringer, R.R., and Bradley, A. (1999). Requirement for Wnt3 in vertebrate axis formation. Nature Genetics *22*, 361–365.

Lohnes, D., Mark, M., Mendelsohn, C., Dollé, P., Dierich, A., Gorry, P., Gansmuller, A., and Chambon, P. (1994). Function of the retinoic acid receptors (RARs) during development (I). Craniofacial and skeletal

abnormalities in RAR double mutants. Development (Cambridge, England) *120*, 2723–2748.

Lu, C.C., Brennan, J., and Robertson, E.J. (2001). From fertilization to gastrulation: axis formation in the mouse embryo. Current Opinion in Genetics & Development *11*, 384–392.

Machado-Silva, J.R., Pelajo-Machado, M., Lenzi, H.L., and Gomes, D.C. (1998). Morphological study of adult male worms of Schistosoma mansoni Sambon, 1907 by confocal laser scanning microscopy. Memórias Do Instituto Oswaldo Cruz *93 Suppl 1*, 303–307.

MacMurray, A., and Shin, H.S. (1988). The antimorphic nature of the Tc allele at the mouse T locus. Genetics *120*, 545–550.

Madabhushi, M., and Lacy, E. (2011). Anterior visceral endoderm directs ventral morphogenesis and placement of head and heart via BMP2 expression. Developmental Cell *21*, 907–919.

Mahlapuu, M., Ormestad, M., Enerbäck, S., and Carlsson, P. (2001). The forkhead transcription factor Foxf1 is required for differentiation of extra-embryonic and lateral plate mesoderm. Development (Cambridge, England) *128*, 155–166.

Mahomed, N., and Naidoo, J. (2009). Spinal segmental dysgenesis. South African Journal of Radiology 29–32.

Mallo, M., and Brändlin, I. (1997). Segmental identity can change independently in the hindbrain and rhombencephalic neural crest. Developmental Dynamics : an Official Publication of the American Association of Anatomists *210*, 146–156.

Mallo, M., Vinagre, T., and Carapuço, M. (2009). The road to the vertebral formula. The International Journal of Developmental Biology *53*, 1469–1481.

Mallo, M., Wellik, D.M., and Deschamps, J. (2010). Hox genes and regional patterning of the vertebrate body plan. Developmental Biology.

Manley, N.R., and Capecchi, M.R. (1997). Hox group 3 paralogous genes act synergistically in the formation of somitic and neural crest-derived structures. Developmental Biology *192*, 274–288.

Martin, B.L., and Kimelman, D. (2008). Regulation of canonical Wnt signaling by Brachyury is essential for posterior mesoderm formation. Developmental Cell *15*, 121–133.

Martin, B.L., and Kimelman, D. (2012). Canonical Wnt Signaling Dynamically Controls Multiple Stem Cell Fate Decisions during Vertebrate Body Formation. Developmental Cell *22*, 223–232.

Mathis, L., and Nicolas, J.F. (2000a). Clonal organization in the postnatal mouse central nervous system is prefigured in the embryonic neuroepithelium. Developmental Dynamics : an Official Publication of the American Association of Anatomists *219*, 277–281.

Mathis, L., and Nicolas, J.F. (2000b). Different clonal dispersion in the rostral and caudal mouse central nervous system. Development (Cambridge, England) *127*, 1277–1290.

Matsuo, I., Kuratani, S., Kimura, C., Takeda, N., and Aizawa, S. (1995). Mouse Otx2 functions in the formation and patterning of rostral head. Genes & Development *9*, 2646–2658.

McGinnis, W., Hart, C.P., Gehring, W.J., and Ruddle, F.H. (1984). Molecular cloning and chromosome mapping of a mouse DNA sequence homologous to homeotic genes of Drosophila. Cell *38*, 675–680.

McGrew, M.J., Sherman, A., Lillico, S.G., Ellard, F.M., Radcliffe, P.A., Gilhooley, H.J., Mitrophanous, K.A., Cambray, N., Wilson, V., and

Sang, H. (2008). Localised axial progenitor cell populations in the avian tail bud are not committed to a posterior Hox identity. Development (Cambridge, England) *135*, 2289–2299.

McIntyre, D.C., Rakshit, S., Yallowitz, A.R., Loken, L., Jeannotte, L., Capecchi, M.R., and Wellik, D.M. (2007). Hox patterning of the vertebrate rib cage. Development (Cambridge, England) *134*, 2981–2989.

McPherron, A.C., Lawler, A.M., and Lee, S.J. (1997). Regulation of skeletal muscle mass in mice by a new TGF-beta superfamily member. Nature *387*, 83–90.

McPherron, A.C., Lawler, A.M., and Lee, S.J. (1999). Regulation of anterior/posterior patterning of the axial skeleton by growth/differentiation factor 11. Nature Genetics *22*, 260–264.

McPherron, A.C., Huynh, T. V, and Lee, S.-J. (2009). Redundancy of myostatin and growth/differentiation factor 11 function. BMC Developmental Biology *9*, 24.

Medvinsky, A., Rybtsov, S., and Taoudi, S. (2011). Embryonic origin of the adult hematopoietic system: advances and questions. Development (Cambridge, England) *138*, 1017–1031.

Meno, C., Gritsman, K., Ohishi, S., Ohfuji, Y., Heckscher, E., Mochida, K., Shimono, a, Kondoh, H., Talbot, W.S., Robertson, E.J., et al. (1999). Mouse Lefty2 and zebrafish antivin are feedback inhibitors of nodal signaling during vertebrate gastrulation. Molecular Cell *4*, 287–298.

Mesnard, D., Filipe, M., Belo, J.A., and Zernicka-Goetz, M. (2004). The anterior-posterior axis emerges respecting the morphology of the mouse embryo that changes and aligns with the uterus before gastrulation. Current Biology : CB *14*, 184–196.

Mic, F.A., Haselbeck, R.J., Cuenca, A.E., and Duester, G. (2002). Novel retinoic acid generating activities in the neural tube and heart identified by conditional rescue of Raldh2 null mutant mice. Development (Cambridge, England) *129*, 2271–2282.

Mic, F.A., Molotkov, A., Benbrook, D.M., and Duester, G. (2003). Retinoid activation of retinoic acid receptor but not retinoid X receptor is sufficient to rescue lethal defect in retinoic acid synthesis. Proceedings of the National Academy of Sciences of the United States of America *100*, 7135–7140.

Mic, F.A., Sirbu, I.O., and Duester, G. (2004). Retinoic acid synthesis controlled by Raldh2 is required early for limb bud initiation and then later as a proximodistal signal during apical ectodermal ridge formation. The Journal of Biological Chemistry *279*, 26698–26706.

Mikawa, T., Poh, A.M., Kelly, K.A., Ishii, Y., and Reese, D.E. (2004). Induction and patterning of the primitive streak, an organizing center of gastrulation in the amniote. Developmental Dynamics: An Official Publication of the American Association of Anatomists *229*, 422–432.

Minguillon, C., Nishimoto, S., Wood, S., Vendrell, E., Gibson-Brown, J.J., and Logan, M.P.O. (2012). Hox genes regulate the onset of Tbx5 expression in the forelimb. Development *139*, 3180–3188.

Mitsui, K., Tokuzawa, Y., Itoh, H., Segawa, K., Murakami, M., Takahashi, K., Maruyama, M., Maeda, M., and Yamanaka, S. (2003). The homeoprotein Nanog is required for maintenance of pluripotency in mouse epiblast and ES cells. Cell *113*, 631–642.

Miura, S., Singh, A.P., and Mishina, Y. (2010). Bmpr1a is required for proper migration of the AVE through regulation of Dkk1 expression in the pre-streak mouse embryo. Developmental Biology *341*, 246–254.

Mo, R., Kim, J.H., Zhang, J., Chiang, C., Hui, C.C., and Kim, P.C. (2001). Anorectal malformations caused by defects in sonic hedgehog signaling. The American Journal of Pathology *159*, 765–774.

Molyneaux, K., and Wylie, C. (2004). Primordial germ cell migration. The International Journal of Developmental Biology *48*, 537–544.

Moreno, T.A., and Kintner, C. (2004). Regulation of segmental patterning by retinoic acid signaling during Xenopus somitogenesis. Developmental Cell *6*, 205–218.

Morimoto, M., Takahashi, Y., Endo, M., and Saga, Y. (2005). The Mesp2 transcription factor establishes segmental borders by suppressing Notch activity. Nature *435*, 354–359.

Morimoto, M., Kiso, M., Sasaki, N., and Saga, Y. (2006). Cooperative Mesp activity is required for normal somitogenesis along the anterior-posterior axis. Developmental Biology *300*, 687–698.

Morkel, M., Huelsken, J., Wakamiya, M., Ding, J., Van de Wetering, M., Clevers, H., Taketo, M.M., Behringer, R.R., Shen, M.M., and Birchmeier, W. (2003). Beta-catenin regulates Cripto- and Wnt3-dependent gene expression programs in mouse axis and mesoderm formation. Development (Cambridge, England) *130*, 6283–6294.

Morrisey, E.E., and Hogan, B.L.M. (2010). Preparing for the first breath: genetic and cellular mechanisms in lung development. Developmental Cell *18*, 8–23.

Mukhopadhyay, M., Shtrom, S., Rodriguez-Esteban, C., Chen, L., Tsukui, T., Gomer, L., Dorward, D.W., Glinka, A., Grinberg, A., Huang, S.P., et al. (2001). Dickkopf1 is required for embryonic head induction and limb morphogenesis in the mouse. Developmental Cell *1*, 423–434.

Murray, S.A., and Gridley, T. (2006). Snail family genes are required for left-right asymmetry determination, but not neural crest formation, in

mice. Proceedings of the National Academy of Sciences of the United States of America *103*, 10300–10304.

Nagy, A., Gertsenstein, M., Vintersten, K., and Behringer, R. (2003). Manipulating the mouse embryo: a laboratory manual (Cold Spring Harbor, New York: Cold Spring Harbor Laboratory Press).

Naiche, L.A., and Papaioannou, V.E. (2003). Loss of Tbx4 blocks hindlimb development and affects vascularization and fusion of the allantois. Development (Cambridge, England) *130*, 2681–2693.

Naiche, L.A., and Papaioannou, V.E. (2007). Tbx4 is not required for hindlimb identity or post-bud hindlimb outgrowth. Development (Cambridge, England) *134*, 93–103.

Naiche, L.A., Holder, N., and Lewandoski, M. (2011). FGF4 and FGF8 comprise the wavefront activity that controls somitogenesis. PNAS *2011*.

Van Nes, J., De Graaff, W., Lebrin, F., Gerhard, M., Beck, F., and Deschamps, J. (2006). The Cdx4 mutation affects axial development and reveals an essential role of Cdx genes in the ontogenesis of the placental labyrinth in mice. Development (Cambridge, England) *133*, 419–428.

Ng, J.K., Kawakami, Y., Büscher, D., Raya, A., Itoh, T., Koth, C.M., Rodríguez Esteban, C., Rodríguez-León, J., Garrity, D.M., Fishman, M.C., et al. (2002). The limb identity gene Tbx5 promotes limb initiation by interacting with Wnt2b and Fgf10. Development (Cambridge, England) *129*, 5161–5170.

Nicolas, J.F., Mathis, L., Bonnerot, C., and Saurin, W. (1996). Evidence in the mouse for self-renewing stem cells in the formation of a segmented longitudinal structure, the myotome. Development (Cambridge, England) *122*, 2933–2946.

Niederreither, K., Subbarayan, V., Dollé, P., and Chambon, P. (1999). Embryonic retinoic acid synthesis is essential for early mouse post-implantation development. Nature Genetics *21*, 444–448.

Niederreither, K., Vermot, J., Schuhbaur, B., Chambon, P., and Dollé, P. (2000). Retinoic acid synthesis and hindbrain patterning in the mouse embryo. Development (Cambridge, England) *127*, 75–85.

Niederreither, K., Vermot, J., Messaddeq, N., Schuhbaur, B., Chambon, P., and Dollé, P. (2001). Embryonic retinoic acid synthesis is essential for heart morphogenesis in the mouse. Development (Cambridge, England) *128*, 1019–1031.

Niederreither, K., Vermot, J., Schuhbaur, B., Chambon, P., and Dollé, P. (2002). Embryonic retinoic acid synthesis is required for forelimb growth and anteroposterior patterning in the mouse. Development (Cambridge, England) *129*, 3563–3574.

Nievelstein, R.A., Hartwig, N.G., Vermeij-Keers, C., and Valk, J. (1993). Embryonic development of the mammalian caudal neural tube. Teratology *48*, 21–31.

Niswander, L., and Martin, G.R. (1992). Fgf-4 expression during gastrulation, myogenesis, limb and tooth development in the mouse. Development (Cambridge, England) *114*, 755–768.

Niwa, Y., Masamizu, Y., Liu, T., Nakayama, R., Deng, C.-X., and Kageyama, R. (2007). The initiation and propagation of Hes7 oscillation are cooperatively regulated by Fgf and notch signaling in the somite segmentation clock. Developmental Cell *13*, 298–304.

Norris, D.P., and Robertson, E.J. (1999). Asymmetric and node-specific nodal expression patterns are controlled by two distinct cis-acting regulatory elements. Genes & Development *13*, 1575–1588.

Nowicki, J.L., and Burke, A.C. (2000). Hox genes and morphological identity: axial versus lateral patterning in the vertebrate mesoderm. Development (Cambridge, England) *127*, 4265–4275.

Nowotschin, S., and Hadjantonakis, A.-K. (2010). Cellular dynamics in the early mouse embryo: from axis formation to gastrulation. Current Opinion in Genetics & Development *20*, 420–427.

Oates, A.C., Rohde, L. a, and Ho, R.K. (2005). Generation of segment polarity in the paraxial mesoderm of the zebrafish through a T-box-dependent inductive event. Developmental Biology *283*, 204–214.

Oginuma, M., Niwa, Y., Chapman, D.L., and Saga, Y. (2008). Mesp2 and Tbx6 cooperatively create periodic patterns coupled with the clock machinery during mouse somitogenesis. Development (Cambridge, England) *135*, 2555–2562.

Oginuma, M., Takahashi, Y., Kitajima, S., Kiso, M., Kanno, J., Kimura, A., and Saga, Y. (2010). The oscillation of Notch activation, but not its boundary, is required for somite border formation and rostral-caudal patterning within a somite. Development (Cambridge, England) *137*, 1515–1522.

Oh, S.P., and Li, E. (1997). The signaling pathway mediated by the type IIB activin receptor controls axial patterning and lateral asymmetry in the mouse. 1812–1826.

Oh, S.P., Yeo, C.-Y., Lee, Y., Schrewe, H., Whitman, M., and Li, E. (2002). Activin type IIA and IIB receptors mediate Gdf11 signaling in axial vertebral patterning. Genes & Development *16*, 2749–2754.

Ohta, S., Suzuki, K., Tachibana, K., Tanaka, H., and Yamada, G. (2007). Cessation of gastrulation is mediated by suppression of epithelial-mesenchymal transition at the ventral ectodermal ridge. Development (Cambridge, England) *134*, 4315–4324.

Ohuchi, H., Nakagawa, T., Yamamoto, A., Araga, A., Ohata, T., Ishimaru, Y., Yoshioka, H., Kuwana, T., Nohno, T., Yamasaki, M., et al. (1997). The mesenchymal factor, FGF10, initiates and maintains the outgrowth of the chick limb bud through interaction with FGF8, an apical ectodermal factor. Development (Cambridge, England) *124*, 2235–2244.

Olivera-Martinez, I., Harada, H., Halley, P.A., and Storey, K.G. (2012). Loss of FGF-dependent mesoderm identity and rise of endogenous retinoid signalling determine cessation of body axis elongation. PLoS Biology *10*, e1001415.

Oliver-Krasinski, J.M., and Stoffers, D. a (2008). On the origin of the beta cell. Genes & Development *22*, 1998–2021.

Oosterveen, T., Van Vliet, P., Deschamps, J., and Meijlink, F. (2003a). The direct context of a hox retinoic acid response element is crucial for its activity. The Journal of Biological Chemistry *278*, 24103–24107.

Oosterveen, T., Niederreither, K., Dollé, P., Chambon, P., Meijlink, F., and Deschamps, J. (2003b). Retinoids regulate the anterior expression boundaries of 5' Hoxb genes in posterior hindbrain. The EMBO Journal *22*, 262–269.

Otting, G., Qian, Y.Q., Billeter, M., Müller, M., Affolter, M., Gehring, W.J., and Wüthrich, K. (1990). Protein--DNA contacts in the structure of a homeodomain--DNA complex determined by nuclear magnetic resonance spectroscopy in solution. The EMBO Journal *9*, 3085–3092.

Oulad-Abdelghani, M., Chazaud, C., Bouillet, P., Mattei, M.G., Dollé, P., and Chambon, P. (1998). Stra3/lefty, a retinoic acid-inducible novel member of the transforming growth factor-beta superfamily. The International Journal of Developmental Biology *42*, 23–32.

Palmeirim, I., Henrique, D., Ish-Horowicz, D., and Pourquié, O. (1997). Avian hairy gene expression identifies a molecular clock linked to vertebrate segmentation and somitogenesis. Cell *91*, 639–648.

Parameswaran, M., and Tam, P.P. (1995). Regionalisation of cell fate and morphogenetic movement of the mesoderm during mouse gastrulation. Developmental Genetics *17*, 16–28.

Partanen, J., Schwartz, L., and Rossant, J. (1998). Opposite phenotypes of hypomorphic and Y766 phosphorylation site mutations reveal a function for Fgfr1 in anteroposterior patterning of mouse embryos. Genes & Development *12*, 2332–2344.

Pasteels, J. (1942). New observations concerning the maps of presumptive areas of the young amphibian gastrula. (Amblystoma and Discoglossus). Journal of Experimental Zoology *89*, 255–281.

Pasteels, J.J. (1939). La formation de la queue chez les Vertebres. Annales De La Société Royale Zoologique De Belgique *70*, 33–51.

Pasteels, J.J. (1943). Prolifé rations et croissance dans la gastrulation et la formation de la queue de vert ébré s. Arch Biol (Liege) *54*, 1–51.

Pearson, J.C., Lemons, D., and McGinnis, W. (2005). Modulating Hox gene functions during animal body patterning. Nature Reviews. Genetics *6*, 893–904.

Perantoni, A.O., Timofeeva, O., Naillat, F., Richman, C., Pajni-Underwood, S., Wilson, C., Vainio, S., Dove, L.F., and Lewandoski, M. (2005). Inactivation of FGF8 in early mesoderm reveals an essential role in kidney development. Development (Cambridge, England) *132*, 3859–3871.

Perea-Gomez, A., Rhinn, M., and Ang, S.L. (2001). Role of the anterior visceral endoderm in restricting posterior signals in the mouse embryo. The International Journal of Developmental Biology *45*, 311–320.

Perea-Gomez, A., Vella, F.D.J., Shawlot, W., Oulad-Abdelghani, M., Chazaud, C., Meno, C., Pfister, V., Chen, L., Robertson, E., Hamada, H., et al. (2002). Nodal antagonists in the anterior visceral endoderm prevent the formation of multiple primitive streaks. Developmental Cell *3*, 745–756.

Perea-Gomez, A., Camus, A., Moreau, A., Grieve, K., Moneron, G., Dubois, A., Cibert, C., and Collignon, J. (2004). Initiation of gastrulation in the mouse embryo is preceded by an apparent shift in the orientation of the anterior-posterior axis. Current Biology : CB *14*, 197–207.

Pereira, P.N.G., Dobreva, M.P., Maas, E., Cornelis, F.M., Moya, I.M., Umans, L., Verfaillie, C.M., Camus, A., De Sousa Lopes, S.M.C., Huylebroeck, D., et al. (2012). Antagonism of Nodal signaling by BMP/Smad5 prevents ectopic primitive streak formation in the mouse amnion. Development (Cambridge, England) *139*, 3343–3354.

Perriton, C.L., Powles, N., Chiang, C., Maconochie, M.K., and Cohn, M.J. (2002). Sonic hedgehog signaling from the urethral epithelium controls external genital development. Developmental Biology *247*, 26–46.

Petersen, C.P., and Reddien, P.W. (2009). Wnt signaling and the polarity of the primary body axis. Cell *139*, 1056–1068.

Piccolo, S., Agius, E., Leyns, L., Bhattacharyya, S., Grunz, H., Bouwmeester, T., and De Robertis, E.M. (1999). The head inducer Cerberus is a multifunctional antagonist of Nodal, BMP and Wnt signals. Nature *397*, 707–710.

Plusa, B., Hadjantonakis, A.-K., Gray, D., Piotrowska-Nitsche, K., Jedrusik, A., Papaioannou, V.E., Glover, D.M., and Zernicka-Goetz, M. (2005). The first cleavage of the mouse zygote predicts the blastocyst axis. Nature *434*, 391–395.

Plusa, B., Piliszek, A., Frankenberg, S., Artus, J., and Hadjantonakis, A.-K. (2008). Distinct sequential cell behaviours direct primitive endoderm formation in the mouse blastocyst. Development (Cambridge, England) *135*, 3081–3091.

Pöpperl, H., and Featherstone, M.S. (1993). Identification of a retinoic acid response element upstream of the murine Hox-4.2 gene. Molecular and Cellular Biology *13*, 257–265.

Pourquié, O. (2011). Vertebrate segmentation: from cyclic gene networks to scoliosis. Cell *145*, 650–663.

Pownall, M.E., Tucker, A.S., Slack, J.M., and Isaacs, H. V (1996). eFGF, Xcad3 and Hox genes form a molecular pathway that establishes the anteroposterior axis in Xenopus. Development (Cambridge, England) *122*, 3881–3892.

Psychoyos, D., and Stern, C.D. (1996). Fates and migratory routes of primitive streak cells in the chick embryo. Development (Cambridge, England) *122*, 1523–1534.

Puri, S., and Hebrok, M. (2010). Cellular plasticity within the pancreas--lessons learned from development. Developmental Cell *18*, 342–356.

Quaggin, S.E., and Kreidberg, J.A. (2008). Development of the renal glomerulus: good neighbors and good fences. Development (Cambridge, England) *135*, 609–620.

Quinlan, G.A., Williams, E.A., Tan, S.S., and Tam, P.P. (1995). Neuroectodermal fate of epiblast cells in the distal region of the mouse egg cylinder: implication for body plan organization during early embryogenesis. Development (Cambridge, England) *121*, 87–98.

Rabinowitz, A.H., and Vokes, S.A. (2012). Integration of the transcriptional networks regulating limb morphogenesis. Developmental Biology *368*, 165–180.

Ramírez-Solis, R., Zheng, H., Whiting, J., Krumlauf, R., and Bradley, A. (1993). Hoxb-4 (Hox-2.6) mutant mice show homeotic transformation of a cervical vertebra and defects in the closure of the sternal rudiments. Cell *73*, 279–294.

Ramkumar, N., and Anderson, K. V (2011). SnapShot: Mouse Primitive Streak. Cell *146*, 488–488.e2.

Rancourt, D.E., Tsuzuki, T., and Capecchi, M.R. (1995). Genetic interaction between hoxb-5 and hoxb-6 is revealed by nonallelic noncomplementation. Genes & Development *9*, 108–122.

Richardson, M.K., Allen, S.P., Wright, G.M., Raynaud, A., and Hanken, J. (1998). Somite number and vertebrate evolution. Development (Cambridge, England) *125*, 151–160.

Rivera-Pérez, J.A., and Magnuson, T. (2005). Primitive streak formation in mice is preceded by localized activation of Brachyury and Wnt3. Developmental Biology *288*, 363–371.

Rodrigues, S., Santos, J., and Palmeirim, I. (2006). Molecular characterization of the rostral-most somites in early somitic stages of the chick embryo. Gene Expression Patterns : GEP *6*, 673–677.

Van Rooijen, C., Simmini, S., Bialecka, M., Neijts, R., Van de Ven, C., Beck, F., and Deschamps, J. (2012). Evolutionarily conserved requirement of Cdx for post-occipital tissue emergence. Development (Cambridge, England) *2583*, 2576–2583.

Rossant, J., and Cross, J.C. (2001). Placental development: lessons from mouse mutants. Nature Reviews. Genetics *2*, 538–548.

Rossant, J., and Tam, P.P.L. (2009). Blastocyst lineage formation, early embryonic asymmetries and axis patterning in the mouse. Development (Cambridge, England) *136*, 701–713.

Rossant, J., Chazaud, C., and Yamanaka, Y. (2003). Lineage allocation and asymmetries in the early mouse embryo. Philosophical Transactions of the Royal Society of London. Series B, Biological Sciences *358*, 1341–8; discussion 1349.

Saga, Y. (2007). Segmental border is defined by the key transcription factor Mesp2, by means of the suppression of Notch activity. Developmental Dynamics : an Official Publication of the American Association of Anatomists *236*, 1450–1455.

Sakai, Y., Meno, C., Fujii, H., Nishino, J., Shiratori, H., Saijoh, Y., Rossant, J., and Hamada, H. (2001). The retinoic acid-inactivating enzyme CYP26 is essential for establishing an uneven distribution of retinoic acid along the anterio-posterior axis within the mouse embryo. Genes & Development *15*, 213–225.

Sancho, E., Batlle, E., and Clevers, H. (2004). Signaling pathways in intestinal development and cancer. Annual Review of Cell and Developmental Biology *20*, 695–723.

Sasaki, N., Kiso, M., Kitagawa, M., and Saga, Y. (2011). The repression of Notch signaling occurs via the destabilization of mastermind-like 1 by Mesp2 and is essential for somitogenesis. Development (Cambridge, England) *138*, 55–64.

Sausedo, R.A., and Schoenwolf, G.C. (1993). Cell behaviors underlying notochord formation and extension in avian embryos: quantitative and immunocytochemical studies. The Anatomical Record *237*, 58–70.

Sausedo, R.A., and Schoenwolf, G.C. (1994). Quantitative analyses of cell behaviors underlying notochord formation and extension in mouse embryos. The Anatomical Record *239*, 103–112.

Savory, J.G.A., Bouchard, N., Pierre, V., Rijli, F.M., De Repentigny, Y., Kothary, R., and Lohnes, D. (2009). Cdx2 regulation of posterior

development through non-Hox targets. Development (Cambridge, England) *136*, 4099–4110.

Sawada, A., Shinya, M., Jiang, Y.J., Kawakami, A., Kuroiwa, A., and Takeda, H. (2001). Fgf/MAPK signalling is a crucial positional cue in somite boundary formation. Development (Cambridge, England) *128*, 4873–4880.

Schlueter, J., and Brand, T. (2009). A right-sided pathway involving FGF8/Snai1 controls asymmetric development of the proepicardium in the chick embryo. Proceedings of the National Academy of Sciences of the United States of America *106*, 7485–7490.

Schoenwolf, G.C. (1977). Tail (end) bud contributions to the posterior region of the chick embryo. Journal of Experimental Zoology *201*, 227–245.

Schoenwolf, G.C. (1984). Histological and ultrastructural studies of secondary neurulation in mouse embryos. The American Journal of Anatomy *169*, 361–376.

Schughart, K., Kappen, C., and Ruddle, F.H. (1989). Duplication of large genomic regions during the evolution of vertebrate homeobox genes. Proceedings of the National Academy of Sciences of the United States of America *86*, 7067–7071.

Schultheiss, T.M., Burch, J.B., and Lassar, A.B. (1997). A role for bone morphogenetic proteins in the induction of cardiac myogenesis. Genes & Development *11*, 451–462.

Scott, M.P., and Weinert, A.M.Y.J. (1984). Antennapedia, Ultrabithorax,. *81*, 4115–4119.

Seifert, A.W., Harfe, B.D., and Cohn, M.J. (2008). Cell lineage analysis demonstrates an endodermal origin of the distal urethra and perineum. Developmental Biology *318*, 143–152.

Selleck, M.A., and Stern, C.D. (1991). Fate mapping and cell lineage analysis of Hensen's node in the chick embryo. Development (Cambridge, England) *112*, 615–626.

Shah, M.M., Sampogna, R. V, Sakurai, H., Bush, K.T., and Nigam, S.K. (2004). Branching morphogenesis and kidney disease. Development (Cambridge, England) *131*, 1449–1462.

Shenefelt, R.E. (1972). Morphogenesis of malformations in hamsters caused by retinoic acid: relation to dose and stage at treatment. Teratology *5*, 103–118.

Shum, A.S., Poon, L.L., Tang, W.W., Koide, T., Chan, B.W., Leung, Y.C., Shiroishi, T., and Copp, A.J. (1999). Retinoic acid induces down-regulation of Wnt-3a, apoptosis and diversion of tail bud cells to a neural fate in the mouse embryo. Mechanisms of Development *84*, 17–30.

Siepel, A., Bejerano, G., Pedersen, J.S., Hinrichs, A.S., Hou, M., Rosenbloom, K., Clawson, H., Spieth, J., Hillier, L.W., Richards, S., et al. (2005). Evolutionarily conserved elements in vertebrate, insect, worm, and yeast genomes. Genome Research *15*, 1034–1050.

Simeone, A., Acampora, D., Arcioni, L., Andrews, P.W., Boncinelli, E., and Mavilio, F. (1990). Sequential activation of HOX2 homeobox genes by retinoic acid in human embryonal carcinoma cells. Nature *346*, 763–766.

Singh, A.M., Reynolds, D., Cliff, T., Ohtsuka, S., Mattheyses, A.L., Sun, Y., Menendez, L., Kulik, M., and Dalton, S. (2012). Signaling network crosstalk in human pluripotent cells: a Smad2/3-regulated switch that controls the balance between self-renewal and differentiation. Cell Stem Cell *10*, 312–326.

Sirbu, I.O., and Duester, G. (2006). Retinoic-acid signalling in node ectoderm and posterior neural plate directs left-right patterning of somitic mesoderm. Nature Cell Biology *8*, 271–277.

Si-Tayeb, K., Lemaigre, F.P., and Duncan, S.A. (2010). Organogenesis and development of the liver. Developmental Cell *18*, 175–189.

Smith, J.L., Gesteland, K.M., and Schoenwolf, G.C. (1994). Prospective fate map of the mouse primitive streak at 7.5 days of gestation. Developmental Dynamics *201*, 279–289.

Snow, M.H. (1981). Autonomous development of parts isolated from primitive-streak-stage mouse embryos. Is development clonal? Journal of Embryology and Experimental Morphology *65 Suppl*, 269–287.

Soriano, P. (1999). Generalized lacZ expression with the ROSA26 Cre reporter strain. Nature Genetics *21*, 70–71.

Srinivas, S., Watanabe, T., Lin, C.S., William, C.M., Tanabe, Y., Jessell, T.M., and Costantini, F. (2001). Cre reporter strains produced by targeted insertion of EYFP and ECFP into the ROSA26 locus. BMC Developmental Biology *1*, 4.

Srivastava, D. (2006). Making or breaking the heart: from lineage determination to morphogenesis. Cell *126*, 1037–1048.

Stennard, F.A., and Harvey, R.P. (2005). T-box transcription factors and their roles in regulatory hierarchies in the developing heart. Development (Cambridge, England) *132*, 4897–4910.

Stern, C.D., Charité, J., Deschamps, J., Duboule, D., Durston, A.J., Kmita, M., Nicolas, J.-F., Palmeirim, I., Smith, J.C., and Wolpert, L. (2006). Head-tail patterning of the vertebrate embryo: one, two or many unresolved problems? The International Journal of Developmental Biology *50*, 3–15.

Stott, D., Kispert, A., and Herrmann, B.G. (1993). Rescue of the tail defect of Brachyury mice. Genes & Development *7*, 197–203.

Studer, M., Gavalas, A., Marshall, H., Ariza-McNaughton, L., Rijli, F.M., Chambon, P., and Krumlauf, R. (1998). Genetic interactions between Hoxa1 and Hoxb1 reveal new roles in regulation of early hindbrain patterning. Development (Cambridge, England) *125*, 1025–1036.

Subramanian, V., Meyer, B.I., and Gruss, P. (1995). Disruption of the murine homeobox gene Cdx1 affects axial skeletal identities by altering the mesodermal expression domains of Hox genes. Cell *83*, 641–653.

Sulik, K., Dehart, D.B., Iangaki, T., Carson, J.L., Vrablic, T., Gesteland, K., and Schoenwolf, G.C. (1994). Morphogenesis of the murine node and notochordal plate. Developmental Dynamics : an Official Publication of the American Association of Anatomists *201*, 260–278.

Sun, X., Meyers, E.N., Lewandoski, M., and Martin, G.R. (1999). Targeted disruption of Fgf8 causes failure of cell migration in the gastrulating mouse embryo. Genes & Development *13*, 1834–1846.

Suzuki, K., Economides, A., Yanagita, M., Graf, D., and Yamada, G. (2009). New horizons at the caudal embryos: coordinated urogenital/reproductive organ formation by growth factor signaling. Current Opinion in Genetics & Development *19*, 491–496.

Sweetman, D., Wagstaff, L., Cooper, O., Weijer, C., and Münsterberg, A. (2008). The migration of paraxial and lateral plate mesoderm cells emerging from the late primitive streak is controlled by different Wnt signals. BMC Developmental Biology *8*, 63.

Szumska, D., Pieles, G., Essalmani, R., Bilski, M., Mesnard, D., Kaur, K., Franklyn, A., El Omari, K., Jefferis, J., Bentham, J., et al. (2008). VACTERL/caudal regression/Currarino syndrome-like malformations

in mice with mutation in the proprotein convertase Pcsk5. Genes & Development *22*, 1465–1477.

Takada, S., Stark, K.L., Shea, M.J., Vassileva, G., McMahon, J.A., and McMahon, A.P. (1994). Wnt-3a regulates somite and tailbud formation in the mouse embryo. Genes & Development *8*, 174–189.

Takaoka, K., Yamamoto, M., Shiratori, H., Meno, C., Rossant, J., Saijoh, Y., and Hamada, H. (2006). The mouse embryo autonomously acquires anterior-posterior polarity at implantation. Developmental Cell *10*, 451–459.

Takaoka, K., Yamamoto, M., and Hamada, H. (2011). Origin and role of distal visceral endoderm, a group of cells that determines anterior-posterior polarity of the mouse embryo. Nature Cell Biology *13*, 743–752.

Takemoto, T., Uchikawa, M., Kamachi, Y., and Kondoh, H. (2006). Convergence of Wnt and FGF signals in the genesis of posterior neural plate through activation of the Sox2 enhancer N-1. Development (Cambridge, England) *133*, 297–306.

Takemoto, T., Uchikawa, M., Yoshida, M., Bell, D.M., Lovell-Badge, R., Papaioannou, V.E., and Kondoh, H. (2011). Tbx6-dependent Sox2 regulation determines neural or mesodermal fate in axial stem cells. Nature *470*, 394–398.

Tam, P.P. (1981). The control of somitogenesis in mouse embryos. Journal of Embryology and Experimental Morphology *65 Suppl*, 103–128.

Tam, P.P. (1989). Regionalisation of the mouse embryonic ectoderm: allocation of prospective ectodermal tissues during gastrulation. Development (Cambridge, England) *107*, 55–67.

Tam, P.P., and Beddington, R.S. (1987). The formation of mesodermal tissues in the mouse embryo during gastrulation and early organogenesis. Development (Cambridge, England) *99*, 109–126.

Tam, P.P., and Behringer, R.R. (1997). Mouse gastrulation: the formation of a mammalian body plan. Mechanisms of Development *68*, 3–25.

Tam, P.P., and Steiner, K.A. (1999). Anterior patterning by synergistic activity of the early gastrula organizer and the anterior germ layer tissues of the mouse embryo. Development (Cambridge, England) *126*, 5171–5179.

Tam, P.P., and Tan, S.S. (1992). The somitogenetic potential of cells in the primitive streak and the tail bud of the organogenesis-stage mouse embryo. Development (Cambridge, England) *115*, 703–715.

Tam, P.P.L., and Loebel, D.A.F. (2007). Gene function in mouse embryogenesis: get set for gastrulation. Nature Reviews. Genetics *8*, 368–381.

Tam, P.P., Parameswaran, M., Kinder, S.J., and Weinberger, R.P. (1997). The allocation of epiblast cells to the embryonic heart and other mesodermal lineages: the role of ingression and tissue movement during gastrulation. Development (Cambridge, England) *124*, 1631–1642.

Tam, P.P., Gad, J.M., Kinder, S.J., Tsang, T.E., and Behringer, R.R. (2001). Morphogenetic tissue movement and the establishment of body plan during development from blastocyst to gastrula in the mouse. BioEssays : News and Reviews in Molecular, Cellular and Developmental Biology *23*, 508–517.

Thewissen, J.G.M., Cohn, M.J., Stevens, L.S., Bajpai, S., Heyning, J., and Horton, W.E. (2006). Developmental basis for hind-limb loss in dolphins and origin of the cetacean bodyplan. Proceedings of the

National Academy of Sciences of the United States of America *103*, 8414–8418.

Thomas, P., and Beddington, R. (1996). Anterior primitive endoderm may be responsible for patterning the anterior neural plate in the mouse embryo. Current Biology : CB *6*, 1487–1496.

Thomas, P.Q., Brown, A., and Beddington, R.S. (1998). Hex: a homeobox gene revealing peri-implantation asymmetry in the mouse embryo and an early transient marker of endothelial cell precursors. Development (Cambridge, England) *125*, 85–94.

Torres-Padilla, M.-E., Richardson, L., Kolasinska, P., Meilhac, S.M., Luetke-Eversloh, M.V., and Zernicka-Goetz, M. (2007). The anterior visceral endoderm of the mouse embryo is established from both preimplantation precursor cells and by de novo gene expression after implantation. Developmental Biology *309*, 97–112.

Tortelote, G.G., Manuel Hernández-Hernández, J., Quaresma, A.J.C., Nickerson, J. a, Imbalzano, A.N., and Rivera-Pérez, J. a (2012). Wnt3 function in the epiblast is required for the maintenance but not the initiation of gastrulation in mice. Developmental Biology 1–10.

Tremblay, K.D. (2011). Inducing the liver: understanding the signals that promote murine liver budding. Journal of Cellular Physiology *226*, 1727–1731.

Tzouanacou, E., Wegener, A., Wymeersch, F.J., Wilson, V., and Nicolas, J.-F. (2009). Redefining the progression of lineage segregations during mammalian embryogenesis by clonal analysis. Developmental Cell *17*, 365–376.

Ukita, K., Hirahara, S., Oshima, N., Imuta, Y., Yoshimoto, A., Jang, C.-W., Oginuma, M., Saga, Y., Behringer, R.R., Kondoh, H., et al. (2009). Wnt signaling maintains the notochord fate for progenitor cells and

supports the posterior extension of the notochord. Mechanisms of Development *126*, 791–803.

Varlet, I., Collignon, J., and Robertson, E.J. (1997). Nodal Expression in the Primitive Endoderm Is Required for Specification of the Anterior Axis During Mouse Gastrulation. Development (Cambridge, England) *124*, 1033–1044.

Van de Ven, C., Bialecka, M., Neijts, R., Young, T., Rowland, E.J., Stringer, E.J., Van Rooijen, C., Meijlink, F., Nóvoa, A., Freund, J.-N., et al. (2011). Concerted involvement of Cdx/Hox genes and Wnt signaling in morphogenesis of the caudal neural tube and cloacal derivatives from the posterior growth zone. Development (Cambridge, England) *3462*, 3451–3462.

Vermot, J., and Pourquié, O. (2005). Retinoic acid coordinates somitogenesis and left-right patterning in vertebrate embryos. Nature *435*, 215–220.

Vermot, J., Schuhbaur, B., Le Mouellic, H., McCaffery, P., Garnier, J.-M., Hentsch, D., Brûlet, P., Niederreither, K., Chambon, P., Dollé, P., et al. (2005). Retinaldehyde dehydrogenase 2 and Hoxc8 are required in the murine brachial spinal cord for the specification of Lim1+ motoneurons and the correct distribution of Islet1+ motoneurons. Development (Cambridge, England) *132*, 1611–1621.

Vinagre, T., Moncaut, N., Carapuço, M., Nóvoa, A., Bom, J., and Mallo, M. (2010). Evidence for a Myotomal Hox/Myf Cascade Governing Nonautonomous Control of Rib Specification within Global Vertebral Domains. Developmental Cell *18*, 655–661.

Vincent, S.D., Dunn, N.R., Hayashi, S., Norris, D.P., and Robertson, E.J. (2003). Cell fate decisions within the mouse organizer are governed by graded Nodal signals. Genes & Development *17*, 1646–1662.

Voiculescu, O., Bertocchini, F., Wolpert, L., Keller, R.E., and Stern, C.D. (2007). The amniote primitive streak is defined by epithelial cell intercalation before gastrulation. Nature *449*, 1049–1052.

Wahl, M.B., Deng, C., Lewandoski, M., and Pourquié, O. (2007). FGF signaling acts upstream of the NOTCH and WNT signaling pathways to control segmentation clock oscillations in mouse somitogenesis. Development (Cambridge, England) *134*, 4033–4041.

Watson, C.M., and Tam, P.P. (2001). Cell lineage determination in the mouse. Cell Structure and Function *26*, 123–129.

Waxman, J.S., Keegan, B.R., Roberts, R.W., Poss, K.D., and Yelon, D. (2008). Hoxb5b acts downstream of retinoic acid signaling in the forelimb field to restrict heart field potential in zebrafish. Developmental Cell *15*, 923–934.

Wellik, D.M. (2007). Hox patterning of the vertebrate axial skeleton. Developmental Dynamics : an Official Publication of the American Association of Anatomists *236*, 2454–2463.

Wellik, D.M., and Capecchi, M.R. (2003). Hox10 and Hox11 genes are required to globally pattern the mammalian skeleton. Science (New York, N.Y.) *301*, 363–367.

White, P.H. (2003). Defective somite patterning in mouse embryos with reduced levels of Tbx6. Development *130*, 1681–1690.

White, J.A., Guo, Y.D., Baetz, K., Beckett-Jones, B., Bonasoro, J., Hsu, K.E., Dilworth, F.J., Jones, G., and Petkovich, M. (1996). Identification of the retinoic acid-inducible all-trans-retinoic acid 4-hydroxylase. The Journal of Biological Chemistry *271*, 29922–29927.

White, P.H., Farkas, D.R., and Chapman, D.L. (2005). Regulation of Tbx6 expression by Notch signaling. Genesis (New York, N.Y. : 2000) *42*, 61–70.

Wiens, J.J., and Slingluff, J.L. (2001). How lizards turn into snakes: a phylogenetic analysis of body-form evolution in anguid lizards. Evolution; International Journal of Organic Evolution *55*, 2303–2318.

Wieser, R., Wrana, J.L., and Massagué, J. (1995). GS domain mutations that constitutively activate T beta R-I, the downstream signaling component in the TGF-beta receptor complex. The EMBO Journal *14*, 2199–2208.

Wilder, P.J., Kelly, D., Brigman, K., Peterson, C.L., Nowling, T., Gao, Q.S., McComb, R.D., Capecchi, M.R., and Rizzino, a (1997). Inactivation of the FGF-4 gene in embryonic stem cells alters the growth and/or the survival of their early differentiated progeny. Developmental Biology *192*, 614–629.

Wilkinson, D.G., Bhatt, S., and Herrmann, B.G. (1990). Expression pattern of the mouse T gene and its role in mesoderm formation. Nature *343*, 657–659.

Williams, M., Burdsal, C., Periasamy, A., Lewandoski, M., and Sutherland, A. (2012). Mouse primitive streak forms *in situ* by initiation of epithelial to mesenchymal transition without migration of a cell population. Developmental Dynamics : an Official Publication of the American Association of Anatomists *241*, 270–283.

Wilson, V., and Beddington, R. (1997). Expression of T protein in the primitive streak is necessary and sufficient for posterior mesoderm movement and somite differentiation. Developmental Biology *192*, 45–58.

Wilson, V., and Beddington, R.S. (1996). Cell fate and morphogenetic movement in the late mouse primitive streak. Mechanisms of Development *55*, 79–89.

Wilson, V., Rashbass, P., and Beddington, R.S. (1993). Chimeric analysis of T (Brachyury) gene function. Development (Cambridge, England) *117*, 1321–1331.

Wilson, V., Manson, L., Skarnes, W.C., and Beddington, R.S. (1995). The T gene is necessary for normal mesodermal morphogenetic cell movements during gastrulation. Development (Cambridge, England) *121*, 877–886.

Wilson, V., Olivera-Martinez, I., and Storey, K.G. (2009). Stem cells, signals and vertebrate body axis extension. Development (Cambridge, England) *136*, 2133–2133.

Woltering, J.M. (2012). From lizard to snake; behind the evolution of an extreme body plan. Current Genomics *13*, 289–299.

Woltering, J.M., Vonk, F.J., Müller, H., Bardine, N., Tuduce, I.L., De Bakker, M.A.G., Knöchel, W., Sirbu, I.O., Durston, A.J., and Richardson, M.K. (2009). Axial patterning in snakes and caecilians: evidence for an alternative interpretation of the Hox code. Developmental Biology *332*, 82–89.

Wu, H.-H., Ivkovic, S., Murray, R.C., Jaramillo, S., Lyons, K.M., Johnson, J.E., and Calof, A.L. (2003). Autoregulation of neurogenesis by GDF11. Neuron *37*, 197–207.

Xu, B., and Wellik, D.M. (2011). Axial Hox9 activity establishes the posterior field in the developing forelimb. 1–5.

Yamada, G., Suzuki, K., Haraguchi, R., Miyagawa, S., Satoh, Y., Kamimura, M., Nakagata, N., Kataoka, H., Kuroiwa, A., and Chen, Y. (2006). Molecular genetic cascades for external genitalia formation: an emerging organogenesis program. Developmental Dynamics : an Official Publication of the American Association of Anatomists *235*, 1738–1752.

Yamaguchi, T.P., Harpal, K., Henkemeyer, M., and Rossant, J. (1994). Fgfr-1 Is Required for Embryonic Growth and Mesodermal Patterning During Mouse Gastrulation. Genes & Development *8*, 3032–3044.

Yamaguchi, T.P., Takada, S., Yoshikawa, Y., Wu, N., and McMahon, A.P. (1999). T (Brachyury) is a direct target of Wnt3a during paraxial mesoderm specification. Genes & Development *13*, 3185–3190.

Yamamoto, M., Beppu, H., Takaoka, K., Meno, C., Li, E., Miyazono, K., and Hamada, H. (2009). Antagonism between Smad1 and Smad2 signaling determines the site of distal visceral endoderm formation in the mouse embryo. The Journal of Cell Biology *184*, 323–334.

Yamanaka, Y., Tamplin, O.J., Beckers, A., Gossler, A., and Rossant, J. (2007). Live imaging and genetic analysis of mouse notochord formation reveals regional morphogenetic mechanisms. Developmental Cell *13*, 884–896.

Yanagisawa, K.O. (1990). Does the T gene determine the anteroposterior axis of a mouse embryo? Idengaku Zasshi *65*, 287–297.

Yanagisawa, K.O., Fujimoto, H., and Urushihara, H. (1981). Effects of the brachyury (T) mutation on morphogenetic movement in the mouse embryo. Developmental Biology *87*, 242–248.

Yang, L., Cai, C.-L., Lin, L., Qyang, Y., Chung, C., Monteiro, R.M., Mummery, C.L., Fishman, G.I., Cogen, A., and Evans, S. (2006). Isl1Cre reveals a common Bmp pathway in heart and limb development. Development (Cambridge, England) *133*, 1575–1585.

Yasuhiko, Y., Haraguchi, S., Kitajima, S., Takahashi, Y., Kanno, J., and Saga, Y. (2006). Tbx6-mediated Notch signaling controls somite-specific Mesp2 expression. Proceedings of the National Academy of Sciences of the United States of America *103*, 3651–3656.

Yasuhiko, Y., Kitajima, S., Takahashi, Y., Oginuma, M., Kagiwada, H., Kanno, J., and Saga, Y. (2008). Functional importance of evolutionally conserved Tbx6 binding sites in the presomitic mesoderm-specific enhancer of Mesp2. Development (Cambridge, England) *135*, 3511–3519.

Yoshikawa, Y., Fujimori, T., McMahon, A.P., and Takada, S. (1997). Evidence that absence of Wnt-3a signaling promotes neuralization instead of paraxial mesoderm development in the mouse. Developmental Biology *183*, 234–242.

Young, T., Rowland, J.E., Van de Ven, C., Bialecka, M., Novoa, A., Carapuco, M., Van Nes, J., De Graaff, W., Duluc, I., Freund, J.-N., et al. (2009). Cdx and Hox genes differentially regulate posterior axial growth in mammalian embryos. Developmental Cell *17*, 516–526.

Zakin, L., Reversade, B., Virlon, B., Rusniok, C., Glaser, P., Elalouf, J.M., and Brulet, P. (2000). Gene expression profiles in normal and Otx2-/- early gastrulating mouse embryos. Proceedings of the National Academy of Sciences of the United States of America *97*, 14388–14393.

Zeller, R., López-Ríos, J., and Zuniga, A. (2009). Vertebrate limb bud development: moving towards integrative analysis of organogenesis. Nature Reviews. Genetics *10*, 845–858.

Zhang, F., Pöpperl, H., Morrison, A., Kovàcs, E.N., Prideaux, V., Schwarz, L., Krumlauf, R., Rossant, J., and Featherstone, M.S. (1997). Elements both 5’ and 3' to the murine Hoxd4 gene establish anterior borders of expression in mesoderm and neurectoderm. Mechanisms of Development *67*, 49–58.

Zhao, H., Li, S., Han, D., Kaartinen, V., and Chai, Y. (2011). Alk5-mediated transforming growth factor β signaling acts upstream of

fibroblast growth factor 10 to regulate the proliferation and maintenance of dental epithelial stem cells. Molecular and Cellular Biology *31*, 2079–2089.

Zhao, X., Sirbu, I.O., Mic, F.A., Molotkova, N., Molotkov, A., Kumar, S., and Duester, G. (2009). Retinoic acid promotes limb induction through effects on body axis extension but is unnecessary for limb patterning. Current Biology : CB *19*, 1050–1057.

Zohn, I.E., Li, Y., Skolnik, E.Y., Anderson, K. V, Han, J., and Niswander, L. (2006). p38 and a p38-interacting protein are critical for downregulation of E-cadherin during mouse gastrulation. Cell *125*, 957–969.

Zorn, A.M., and Wells, J.M. (2009). Vertebrate endoderm development and organ formation. Annual Review of Cell and Developmental Biology *25*, 221–251.

ITQB-UNL | Av. da República, 2780-157 Oeiras, Portugal
Tel (+351) 214 469 100
Fax (+351) 214 411 277

www.itqb.unl.pt